Lentes gravitacionales en astrofísica y cosmología

Martín Makler
CBPF & ICAS/IFICI/CONICET-UNSAM

Estructura general de la materia

Parte III: lensing a nivel cosmológico y tópicos avanzados

- Efecto débil de lentes (fundamentos de *weak lensing*, regímenes y métodos)
- Mas allá del plano único: lentes y estructura en gran escala
- *Lensing* de la radiación cósmica de fondo
- Lentes en gravedad modificada
- Lentes en la óptica ondulatória
- *Lensing* de ondas gravitacionales

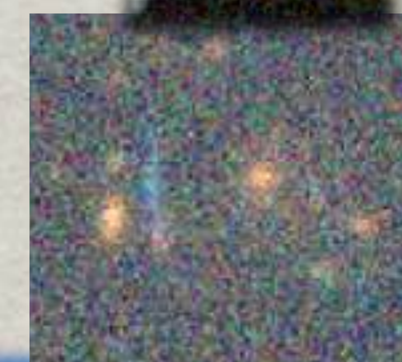

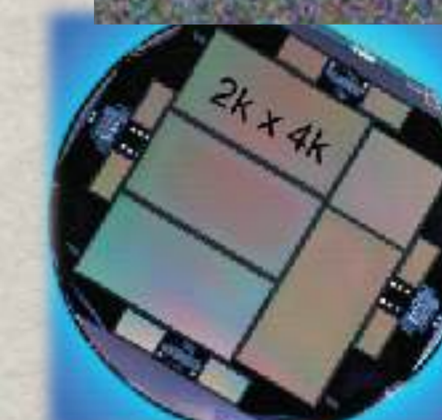

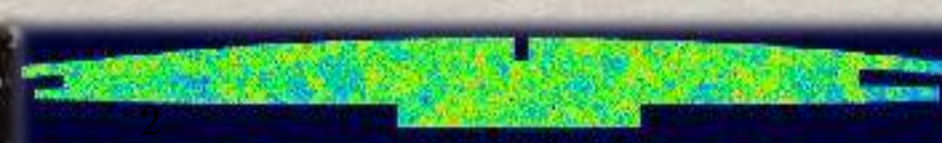

Lentes gravitacionales

Hipótesis/condiciones/regímenes

- Lente fina
- Relatividad general
- Campo débil (gravedad linear)
- Óptica geométrica
- Ondas electromagnéticas

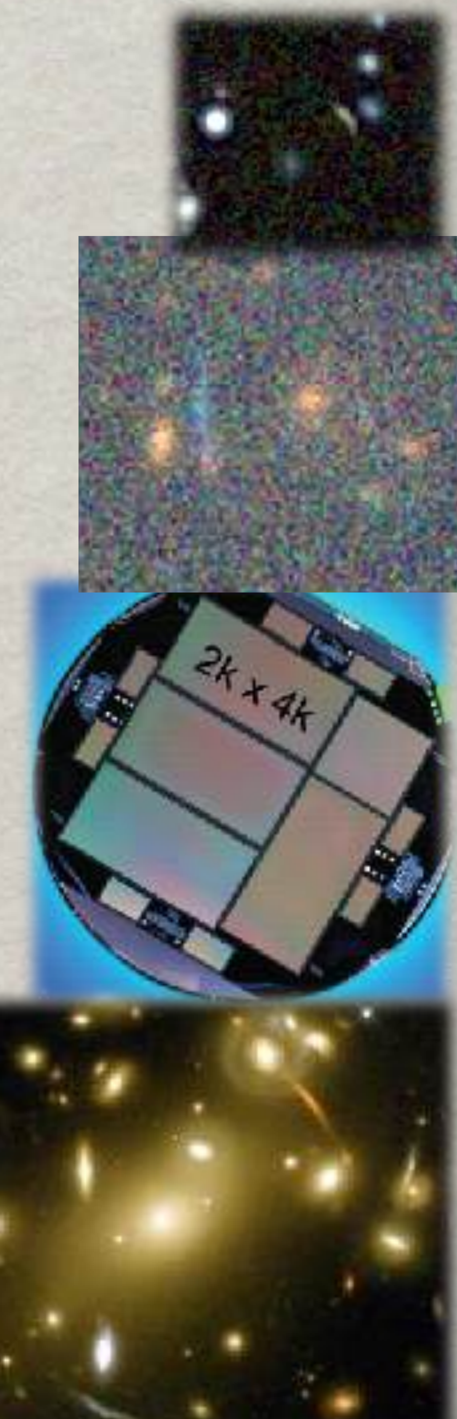

Efecto Débil de lente gravitacional

Efecto débil y fuerte de lente

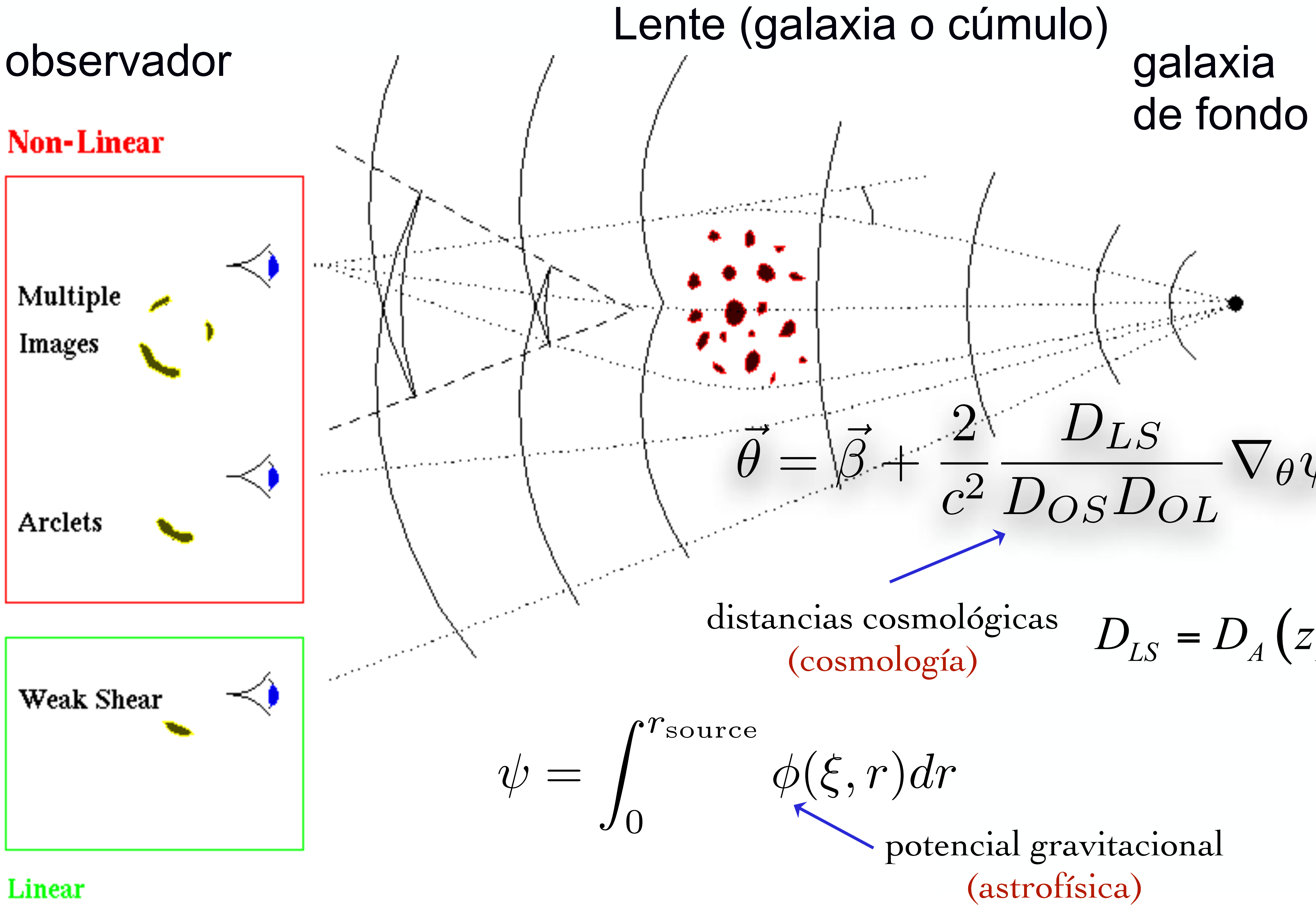

$$\vec{\theta} = \vec{\beta} + \frac{2}{c^2} \frac{D_{LS}}{D_{OS} D_{OL}} \nabla_\theta \psi \left(\vec{\theta} \right)$$

distancias cosmológicas
(cosmología)

$$D_{LS} = D_A \left(z_L , z_S \right) \ldots$$

$$\psi = \int_0^{r_{\mathrm{source}}} \phi(\xi, r) dr$$

potencial gravitacional
(astrofísica)

Efecto fuerte: el domínio de las cáusticas y curvas críticas

- mapeo imagem → fuente

$$\frac{\partial \beta_i}{\partial \theta_j} = \delta_{ij} - \frac{\partial^2 \Psi(\vec{\theta})}{\partial \theta_i \partial \theta_j}$$

- autovalores:

$$\mu_1 = \frac{1}{1-\kappa+\gamma}, \mu_2 = \frac{1}{1-\kappa-\gamma}$$

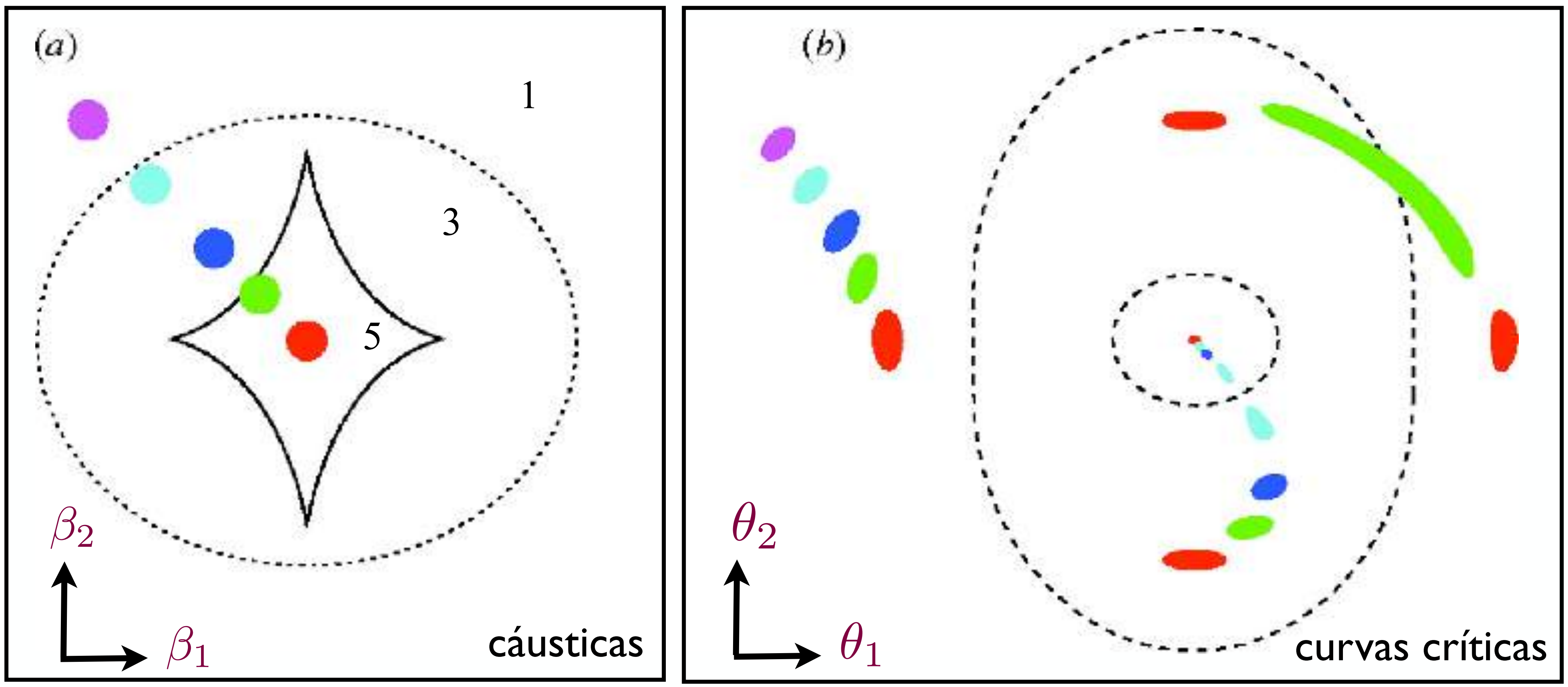

Plano de las fuentes

Lente/imágenes

Los números en el plano de las fuentes indicam la multiplicidad de las imágenes

Jacobiana de la transformación

$$\vec{\beta} = \vec{\theta} - \vec{\nabla}_\theta \Psi\left(\vec{\theta}\right)$$

$$J_{ij} = \left(\frac{\partial \vec{\beta}}{\partial \vec{\theta}}\right)_{ij} = \delta_{ij} - \frac{\partial^2 \Psi}{\partial \theta_i \partial \theta_j},$$ definiendo $\Psi_{ij} = \frac{\partial^2 \Psi}{\partial \theta_i \partial \theta_j}$

tenemos $\mathbf{J} = \begin{pmatrix} 1 - \Psi_{11} & -\Psi_{12} \\ -\Psi_{21} & 1 - \Psi_{22} \end{pmatrix}$

como $\nabla_\theta^2 \Psi = \Psi_{11} + \Psi_{22} = 2\kappa$

$$\mathbf{J} = (1-\kappa)\mathbf{I} - \begin{pmatrix} \frac{1}{2}\left(\Psi_{11} - \Psi_{22}\right) & \Psi_{12} \\ \Psi_{21} & -\frac{1}{2}\left(\Psi_{11} - \Psi_{22}\right) \end{pmatrix}$$

Jacobiana de la transformación

$$\mathbf{J} = (1-\kappa)\mathbf{I} - \begin{pmatrix} \frac{1}{2}\left(\Psi_{11} - \Psi_{22}\right) & \Psi_{12} \\ \Psi_{21} & -\frac{1}{2}\left(\Psi_{11} - \Psi_{22}\right) \end{pmatrix}$$

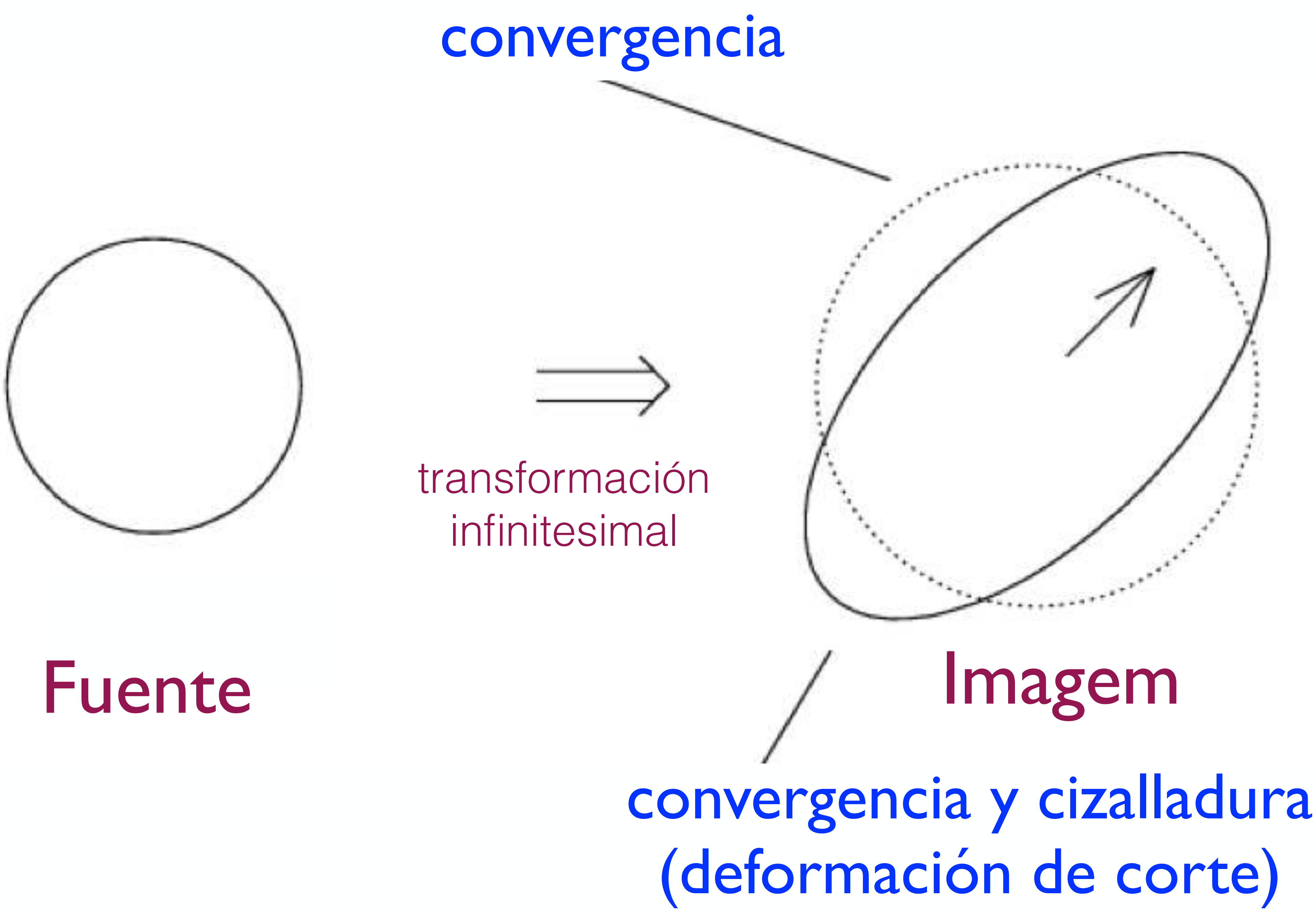

Convergencia

Ecuación de Poisson

$$\nabla^2_\theta \Psi = \frac{2}{c^2} \frac{D_{\mathrm{LS}}}{D_{\mathrm{OS}} D_{\mathrm{OL}}} D^2_{\mathrm{OL}} 4\pi G \, \Sigma\left(\vec{\theta}\right) = 2 \frac{\Sigma\left(\vec{\theta}\right)}{\Sigma_{\mathrm{crit}}}$$

Densidad superficial crítica

$$\boxed{\Sigma_{\mathrm{crit}} = \frac{c^2}{4\pi G} \frac{D_{\mathrm{OS}}}{D_{\mathrm{OL}} D_{\mathrm{LS}}}}$$

Convergencia

$$\kappa\left(\vec{\theta}\right) = \frac{\Sigma\left(\vec{\theta}\right)}{\Sigma_{\mathrm{crit}}}$$

Ecuación de Poisson $\boxed{\nabla^2_\theta \Psi = 2\kappa\left(\vec{\theta}\right)}$

Cizalladura

$$\mathbf{J} = (1-\kappa)\mathbf{I} - \begin{pmatrix} \frac{1}{2}\left(\Psi_{11}-\Psi_{22}\right) & \Psi_{12} \\ \Psi_{21} & -\frac{1}{2}\left(\Psi_{11}-\Psi_{22}\right) \end{pmatrix}$$

Cizalladura:

$$\gamma_1(\vec{\theta}) = \frac{1}{2}(\Psi_{11} - \Psi_{22})$$

$$\gamma_2(\vec{\theta}) = \Psi_{12} = \Psi_{21}$$

$$\gamma = \sqrt{\gamma_1^2 + \gamma_2^2}$$

Em términos de la cizalladura y la convergencia tenemos

$$\mathbf{J} = (1-\kappa)\mathbf{I} + \begin{pmatrix} -\gamma_1 & -\gamma_2 \\ -\gamma_2 & \gamma_1 \end{pmatrix}$$

Autovalores de $\mathbf{J}^{-1}$

$$\mu_1 = \frac{1}{1-\kappa-\gamma}, \quad \mu_2 = \frac{1}{1-\kappa+\gamma}$$

Mapeo Lineal

Fuente circular

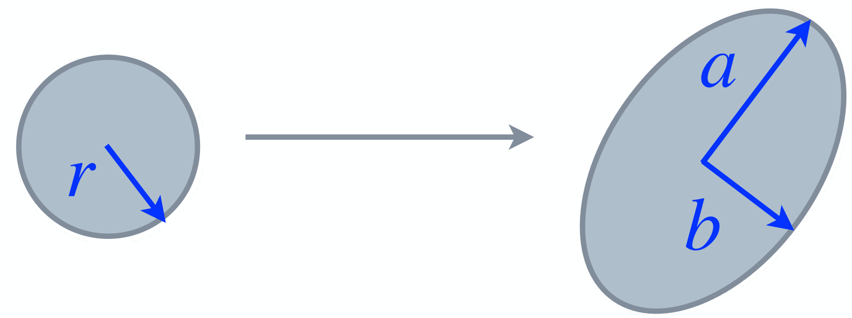

$$a = \left(\frac{1}{1-\kappa-\gamma}\right) r$$

$$b = \left(\frac{1}{1-\kappa+\gamma}\right) r$$

- Magnificación

$$\mu = \frac{A_{\text{imagem}}}{A_{\text{fonte}}} = \left[(1-\kappa)^2 - \gamma^2\right]^{-1}$$

- Elipticidad

$$\boxed{\epsilon := \frac{a-b}{a+b} = \frac{\gamma}{1-\kappa} =: g}$$

¿Qué es la elipticidad para una fuente real?

Real sources

- Center of the object (image)

$$\bar{\theta}_i = \frac{\int \mathrm{d}^2\theta q_I \left[I\left(\theta\right)\right]\theta_i}{\int \mathrm{d}^2\theta q_I \left[I\left(\theta\right)\right]}$$

- Second order momenta

$$Q_{ij} = \frac{\int d^2\theta q_I[I(\theta)](\theta_i - \bar{\theta}_i)(\theta_j - \bar{\theta}_j)}{\int d^2\theta q_I[I(\theta)]}$$

- Area

$$\Omega = \left(Q_{11}Q_{22} - Q_{12}^2\right)^{1/2}$$

- Ellipticity

$$\epsilon := \frac{Q_{11} - Q_{22} + 2\,i\,Q_{12}}{Q_{11} + Q_{22} + 2\left(Q_{11}Q_{22} - Q_{12}^2\right)^{1/2}}$$

Mapeo LineaL

- Efectos:
  - Distorsión (más usual): variación en la orientación
  - Magnificación: cambio en el área y en la densidad de objetos
  - Análogamente a la cizalladura γ, la elipticidad tiene 2 componentes: matriz, pseudo-vector o número complejo

$$\epsilon = \epsilon_1 + i\epsilon_2 = |\epsilon| e^{2i\varphi}$$

  - La cizalladura también se suele escribir como un número complejo

$$\gamma = \gamma_1 + i\gamma_2$$

  - En *weak lensing*, tenemos $\kappa \ll 1$ y $|\gamma| \ll 1$

Real sources

- Second order momenta

$$Q_{ij} = \frac{\int d^2\theta q_I[I(\theta)](\theta_i - \bar{\theta}_i)(\theta_j - \bar{\theta}_j)}{\int d^2\theta q_I[I(\theta)]}$$

- Area

$$\Omega = \left(Q_{11}Q_{22} - Q_{12}^2\right)^{1/2}$$

- Ellipticity

$$\epsilon := \frac{Q_{11} - Q_{22} + 2\,i\,Q_{12}}{Q_{11} + Q_{22} + 2\,(Q_{11}Q_{22} - Q_{12}^2)^{1/2}}$$

- Linear distortion

$$\epsilon_S = \frac{\epsilon_I - g}{1 - g^*\epsilon_I} \qquad g_i := \frac{\gamma_i(\theta)}{1 - \kappa(\theta)} \qquad |g| \leq 1$$

reduced shear o cizalladura o distorción reducida

Weak Lensing

- Slight shear in background galaxies (change in axis + size)
- Weak lensing regime

$$\epsilon = \epsilon_I = \epsilon_S + g$$

- "weak lensing fundamental theorem":

$$\boxed{\langle \epsilon \rangle = g}$$

- but

$$|g| \ll |\varepsilon|$$

- observational, instrumental, computational and theoretical challenges!

Technical challenges

Sarah Bridle

- Model the PSF distortion (many sources)
  - measure a large number of stars in the field

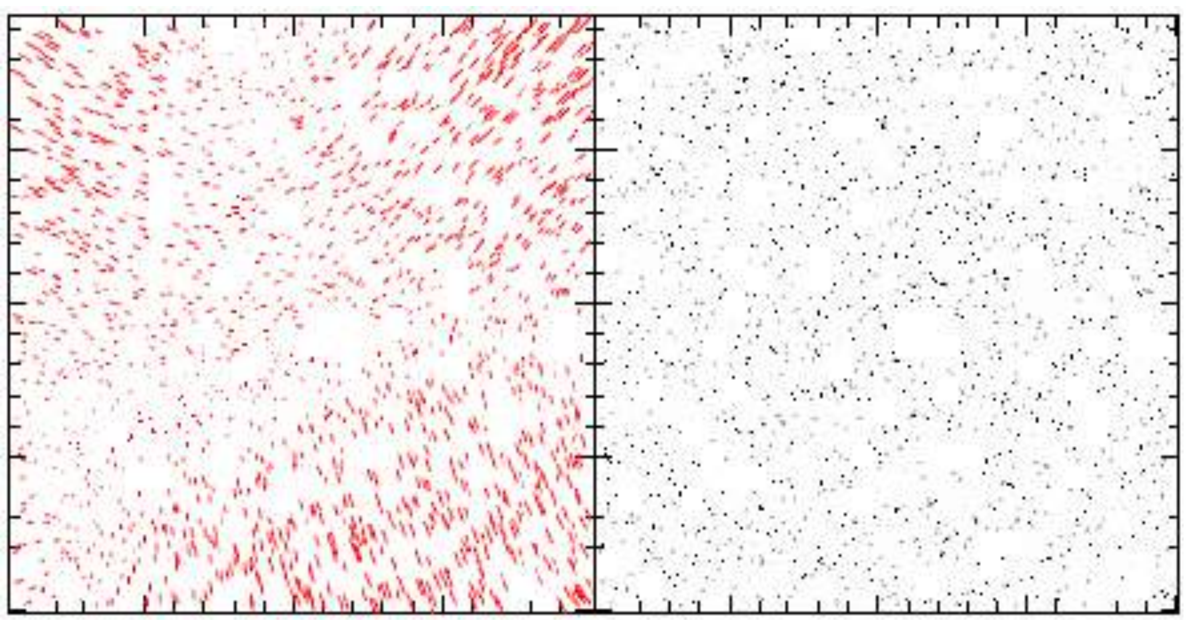

CFHTLS Deep 1
Gavazzi, Soucail 2006

- Difficulties: saturated stars, charge transfer efficiency, halos, tracking...

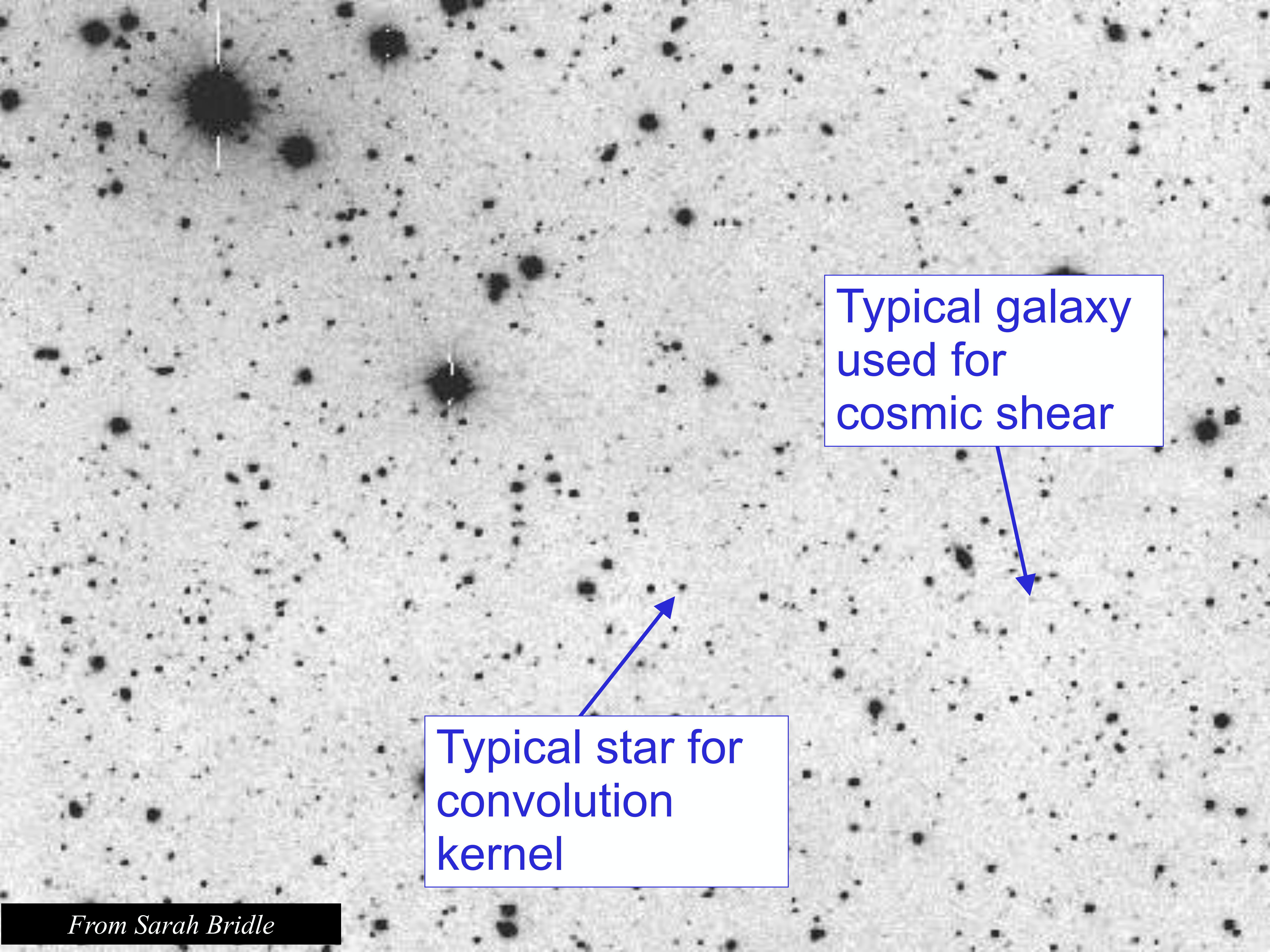
Typical galaxy used for cosmic shear
Typical star for convolution kernel
From Sarah Bridle

Measuring weak lensing

- Signal $\langle \varepsilon_I \rangle = \gamma$ $\quad (\varepsilon_I = \varepsilon_S + \gamma)$
- Noise $\sigma_\varepsilon = \langle |\varepsilon_S{}^2| \rangle^{1/2} \sim 0.3 \gg \gamma$
- Win over the noise by averaging over a large number of galaxies

Regime	γ	$\gamma/\sigma_\varepsilon$	N_{gal} for S/N~ 1
weak lensing by clusters	0.03	0.1	10^2
galaxy-galaxy lensing	0.003	0.01	10^4
cosmic shear	0.001	0.003	10^5

Much more galaxies for precision measurements needed.

(de Kilbinger)

El camino…

1) Obtener las medidas de forma de las galaxias

- Modelar las distorsiones de la PSF (muchas fuentes)
- Medir la forma de las galaxi…
- Aplicar la PSF a las … a de las galaxias
- Seleccionar … /magnitud, etc.)

2) Realizar las me… es relevantes

- Una miríada de … y de estimadores estadísticos
- Obtener estimadores óptimos, teniendo en cuenta efectos instrumentales y observacionales
- Determinar las incertidumbres

El dominio de la estadística

Ejemplo: separación estrella-galaxia

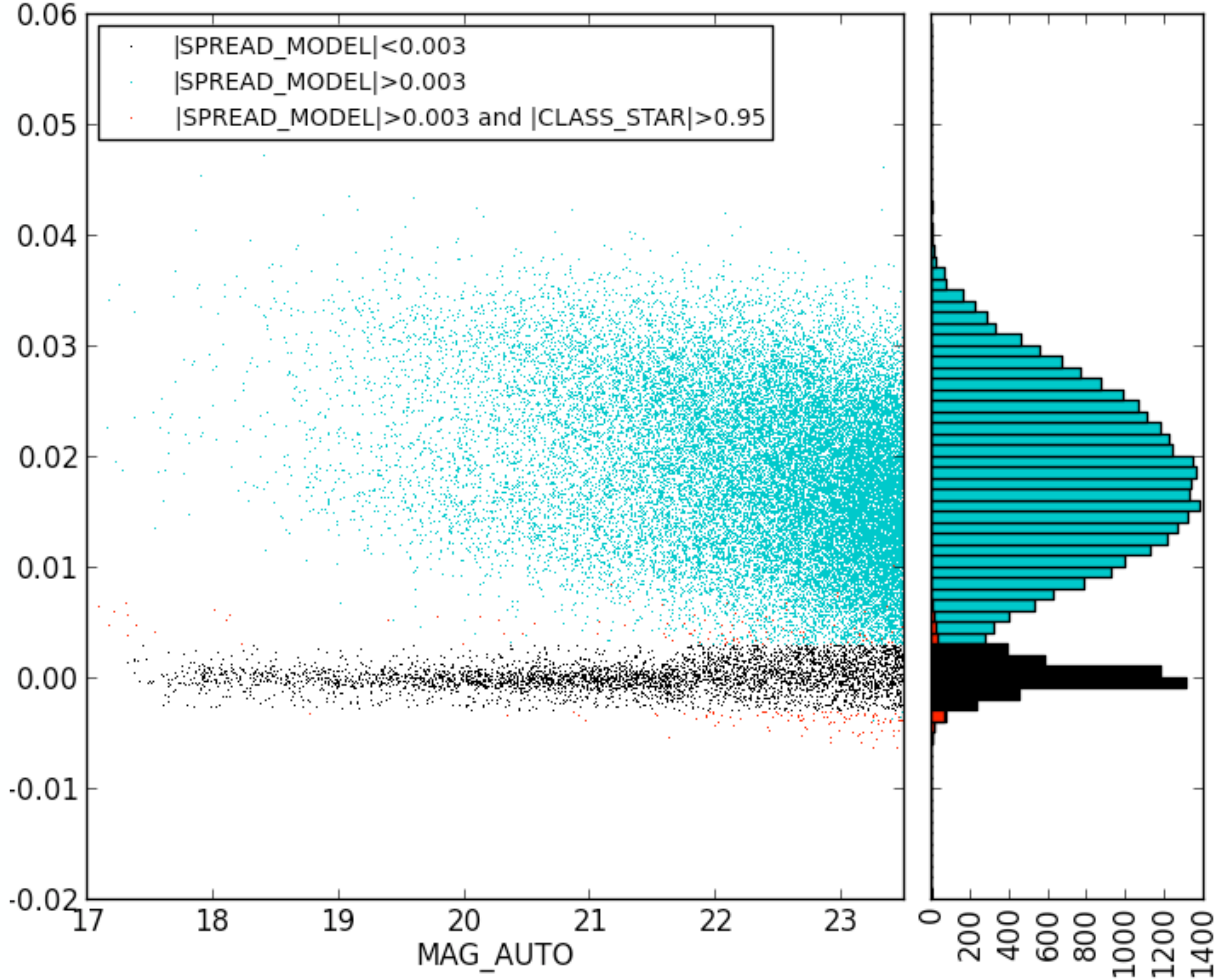

Corrimientos al rojo fotométricos

- Características marcantes del espectro

(quiebra de 4000 A)

- Diferencia en el flujo en los distintos filtros cuando la galaxia tiene su espectro corrido al rojo

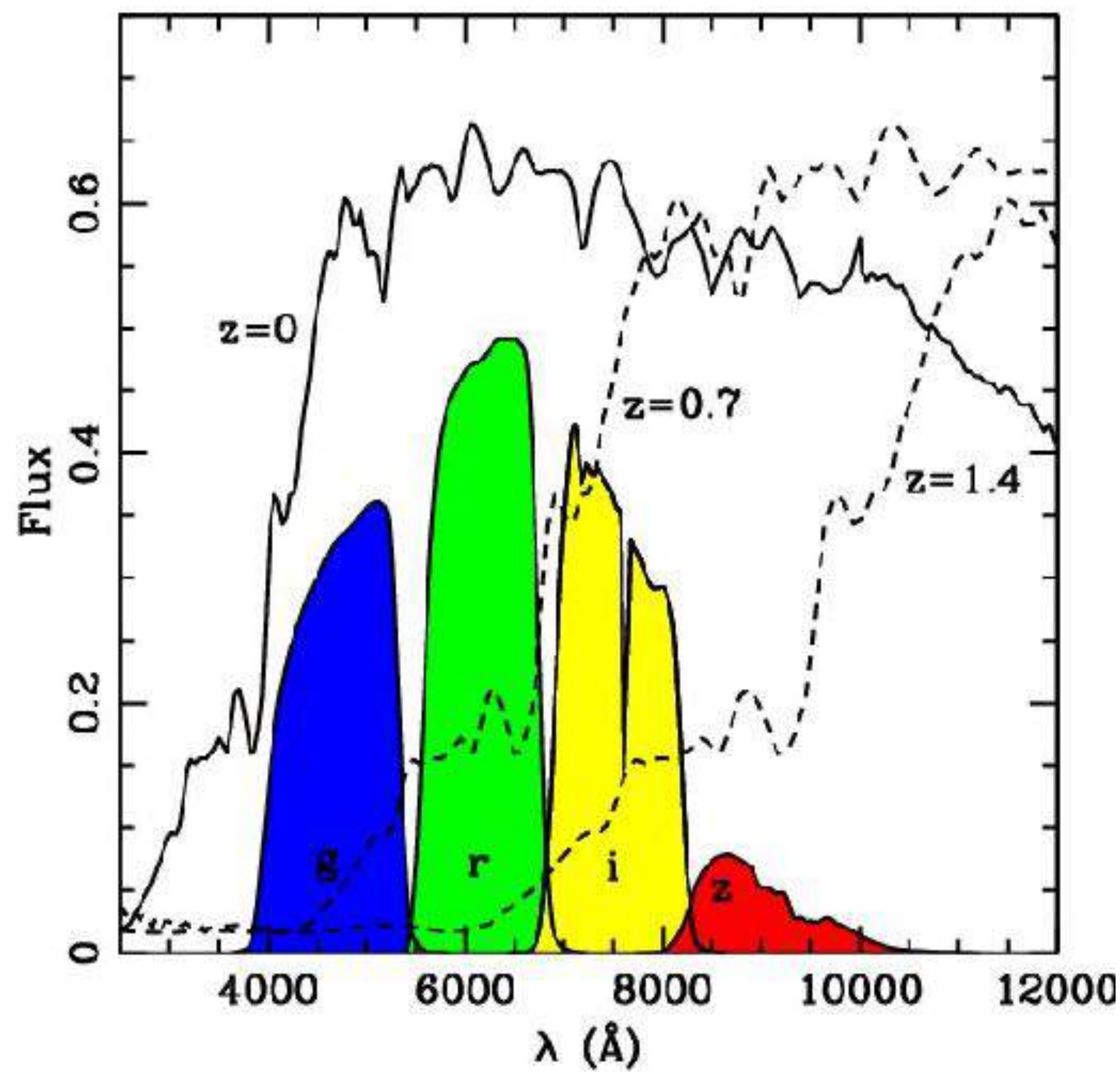

2 Regimes and Methods

Lensing by galaxies and clusters

- Larger signal
- Center of reference
- Model/profile fitting
- Individual objects or *Stacking* of the signal

Large-scale structure

- Convergence maps (also in clusters)
- Correlations:
  - power spectrum, correlation function
  - among different probes, z-bins, CMB, etc.

Lensing by galaxies and clusters

- Larger signal
- Center of reference
- Model/profile fitting
- Individual objects or Stacking of the signal

Applications

- Mass calibration for cosmology
- Radial profiles x models
- stellar mass/total mass relation
- etc.

Components of the Shear

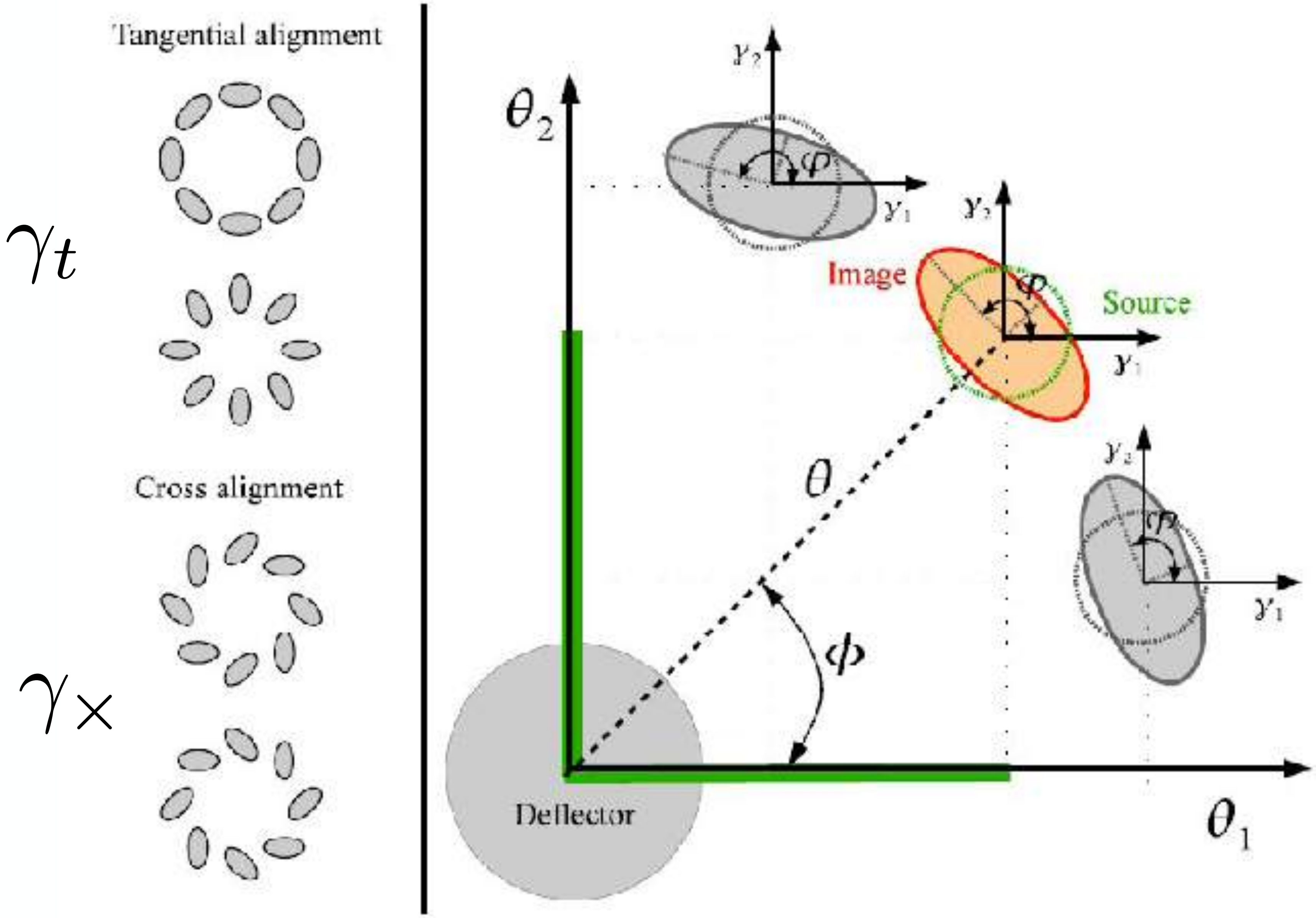

Figueiró 2011

Mean shear in circles

$$< \gamma_t(\theta) >= \bar{\kappa}(\theta) - < k(\theta) >$$

Mean shear and radial profiles

It is possible to show that

$$< \gamma_t(\theta) >= \bar{\kappa}(\theta) - < k(\theta) >$$

mean along a circle of the tangential component of the shear

mean within a disk of radius θ

mean on the circle

In practice: mean on annuli (radial bins)

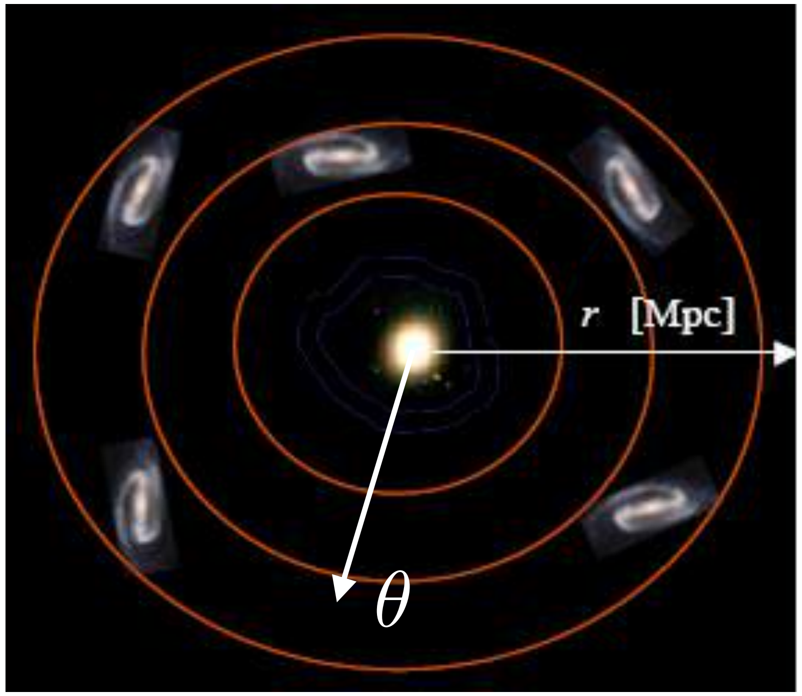

Also: $< \gamma_\times >= 0$ ← test for systematics!

Stacking of the signal

Need (and possibility) to increase the S/*N*

Combine data on many galaxies or clusters: mean signal

Physical signal and models: $\Sigma(r) \longrightarrow$ multiply by $\Sigma_{\rm crit}$

$$\Sigma_{\rm crit} \times < \gamma_t(\theta) > = \Big(\bar{\kappa}(\theta) - < k(\theta) > \Big) \times \Sigma_{\rm crit}$$

$$\boxed{\Sigma_{\rm crit} \times < \gamma_t(r) > = \bar{\Sigma}(r) - < \Sigma(r) > := \Delta\Sigma(r)}$$

redshifts

shapes

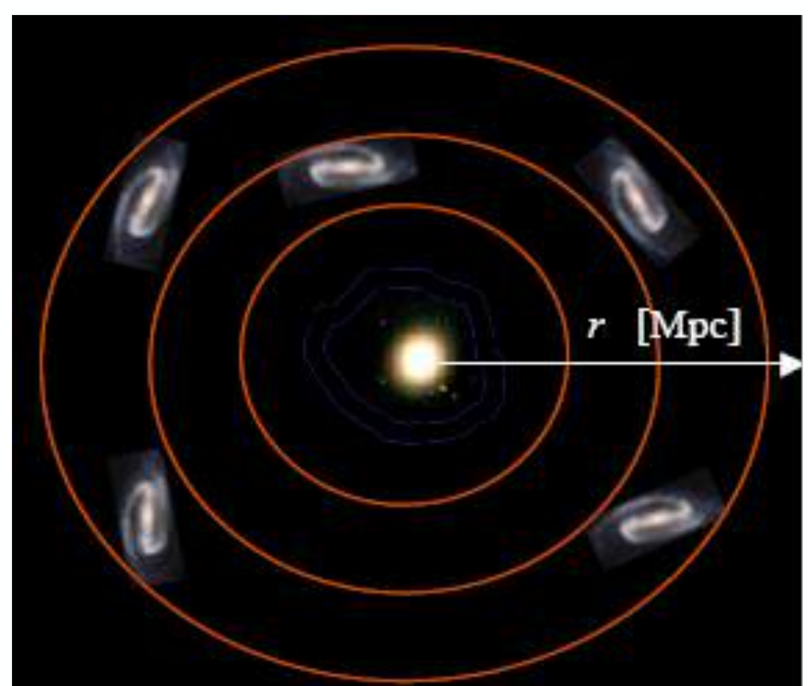

model

$$\Delta\Sigma_{\times} = \Sigma_{\rm crit} < \gamma_{\times} >$$

test for systematics!

Mass reconstruction in clusters (radial profile)

- Measure the tangential shear to get $\Delta\Sigma$

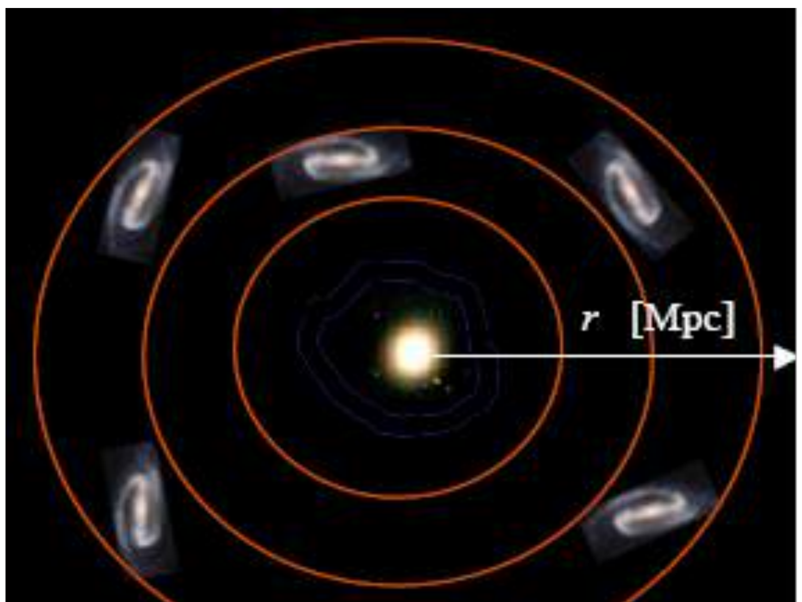

$$\Delta\Sigma(r) \equiv \bar{\Sigma}(<r) - \bar{\Sigma}(r) = \Sigma_{crit} \times \gamma_t(r)$$

$$\Sigma_{crit} = \frac{c^2}{4\pi G}\frac{D_{OS}}{D_{OL}D_{LS}}$$

- Masses:

$$\bar{M}_{NFW} = (1.0 \pm 0.2)10^{14}h^{-1}M_\odot$$

$$\frac{\Delta M_{200}}{M_{200}} \simeq 2.5\%$$

Makler 2002

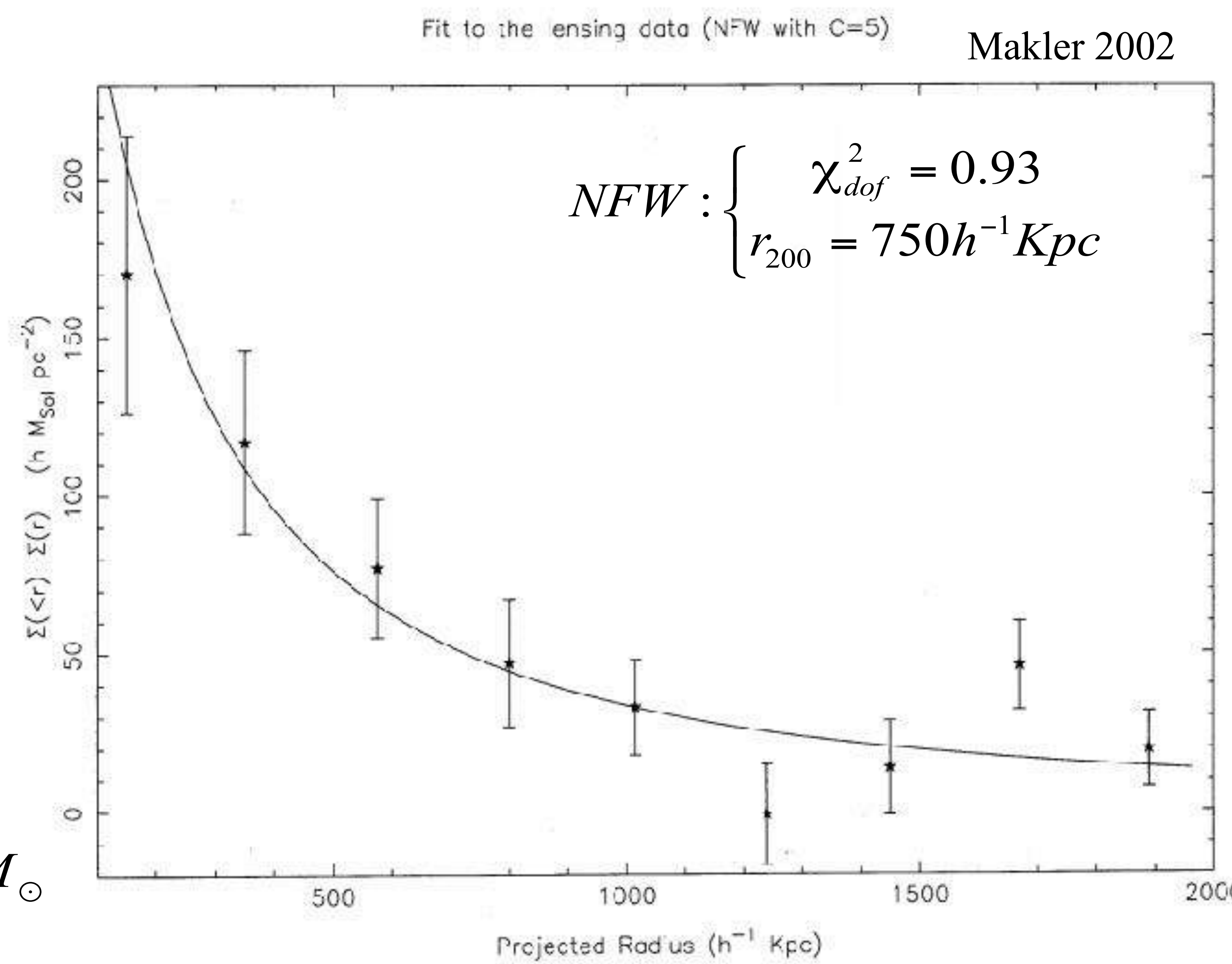

$$NFW : \begin{cases} \chi^2_{dof} = 0.93 \\ r_{200} = 750h^{-1}Kpc \end{cases}$$

42 clusters (RASS/SDSS), Sheldon, et al., ApJ 554, 88 (2001)

Ajustes de perfiles

- Se pueden hacer en un amplio rango de masas y tipos de lentes, desde galaxias individuales hasta cúmulos de galaxias
- Requieren “solo”:
- Estadística suficiente de galaxias de fondo
- Un centro bien definido (incluso con *voids*!)
- ejemplo: grupos compactos
- Uso de la componente cruzada para control de los sistemáticos

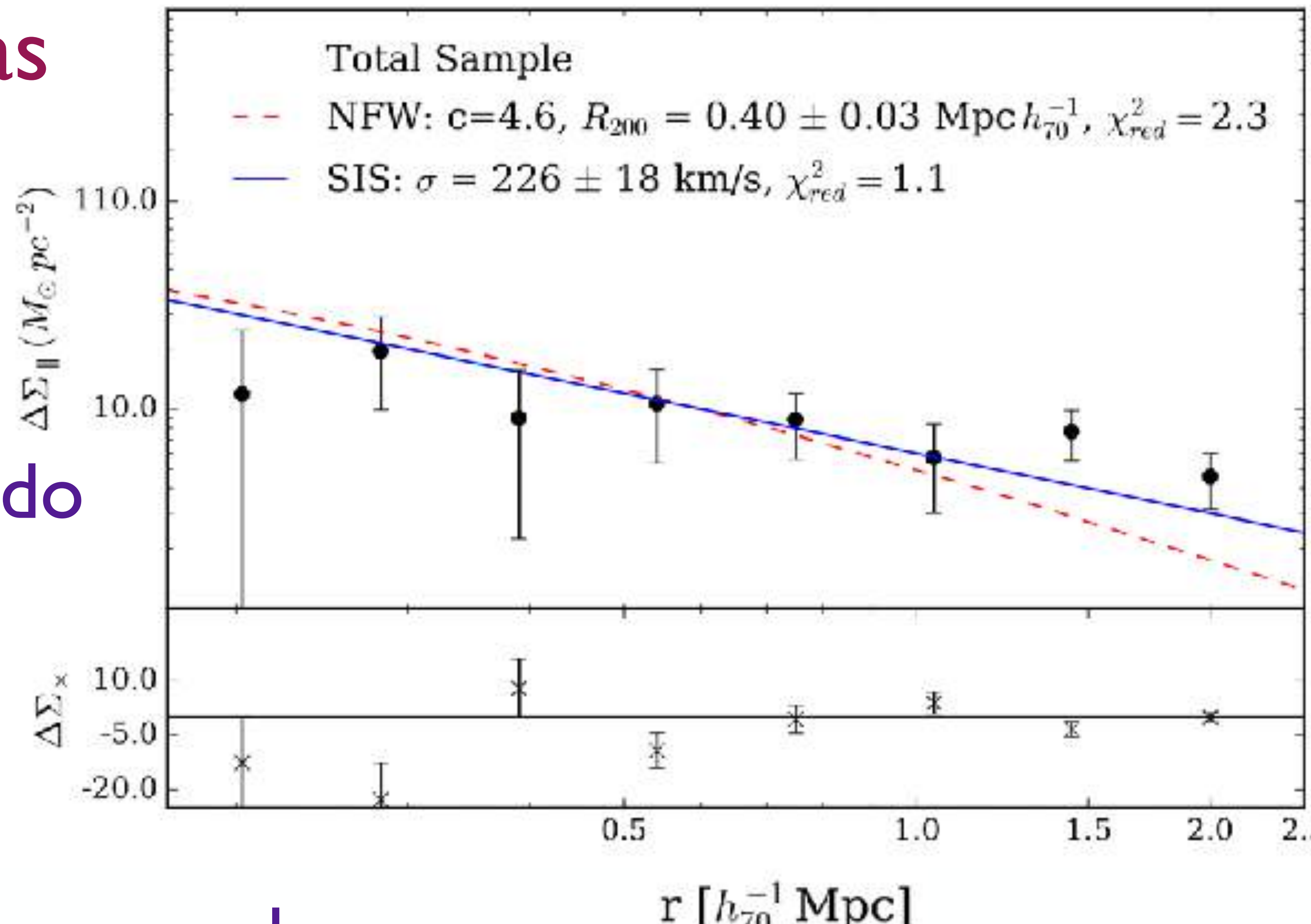

Chalela et al., MNRAS 479, 1170 (2018)

Ajustes de perfiles

- Se pueden hacer en un amplio rango de masas y tipos de lentes, desde galaxias individuales hasta cúmulos de galaxias
- Requieren "solo":
- Estadística suficiente de galaxias de fondo
- Un centro bien definido (incluso con *voids*!)
- ejemplo: pares de galaxias
- Uso de la componente cruzada para control de los sistemáticos

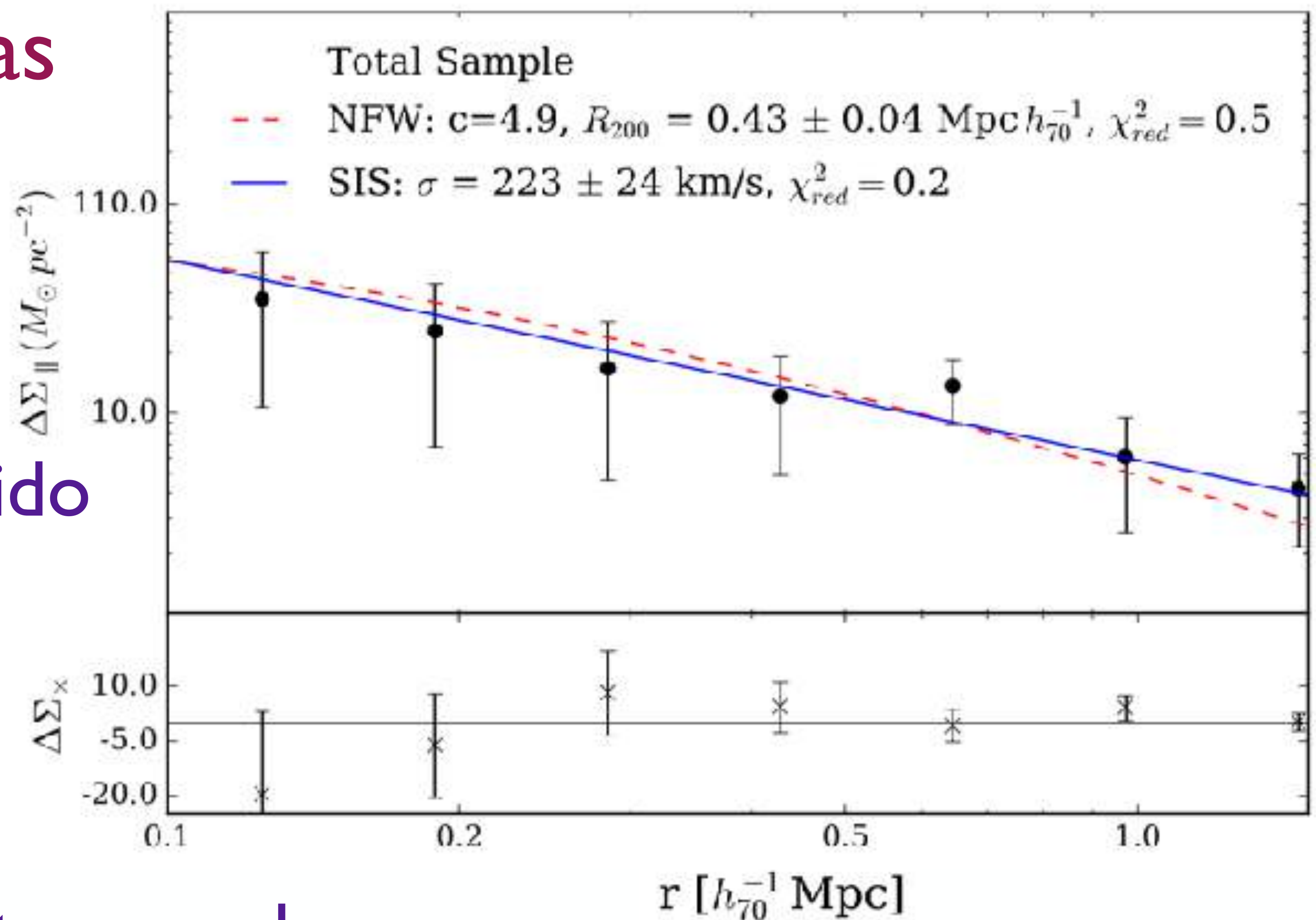

Gonzalez et al., A& 62, A90 (2019)

Modeling the mass profile

Interpretation with the halo model: halos x galaxies correlation

- ☑ 1-halo term: matter density in the halo

Exemple: NFW $\rho(r) = \dfrac{\rho_0}{(r/r_s)\,(1+r/r_s)^2}$ compute $\Sigma(r)$

- ☑ 2-halo term: correlation with other halos (large scale structure) $\rho(r) = b\bar{\rho}_m\xi(r)$ where

$$\xi(r) = \frac{1}{2\pi^2}\int dk\,k^2 P(k)\frac{\sin(kr)}{kr} \qquad b(\nu) = 1 - A\frac{\nu^a}{\nu^a + \delta_c^a} + B\nu^b + C\nu^c$$

$$\nu = \delta_c/\sigma(M) = 1.686/\sigma(M) \qquad \sigma(R) = \frac{1}{2\pi^2}\int dk\,k^2 P(k,z)\hat{W}^2(k,R)$$

$$R = (3M/4\pi\bar{\rho}_m)^{1/3}$$ (mass function, peak-background split)

- ☑ Term for the *offset* of the profile with respect to other center
- ☑ Central potential (central galaxy, e.g. SIS)

Example: Cluster mass calibration

Shan et al. 2015 (CS82)

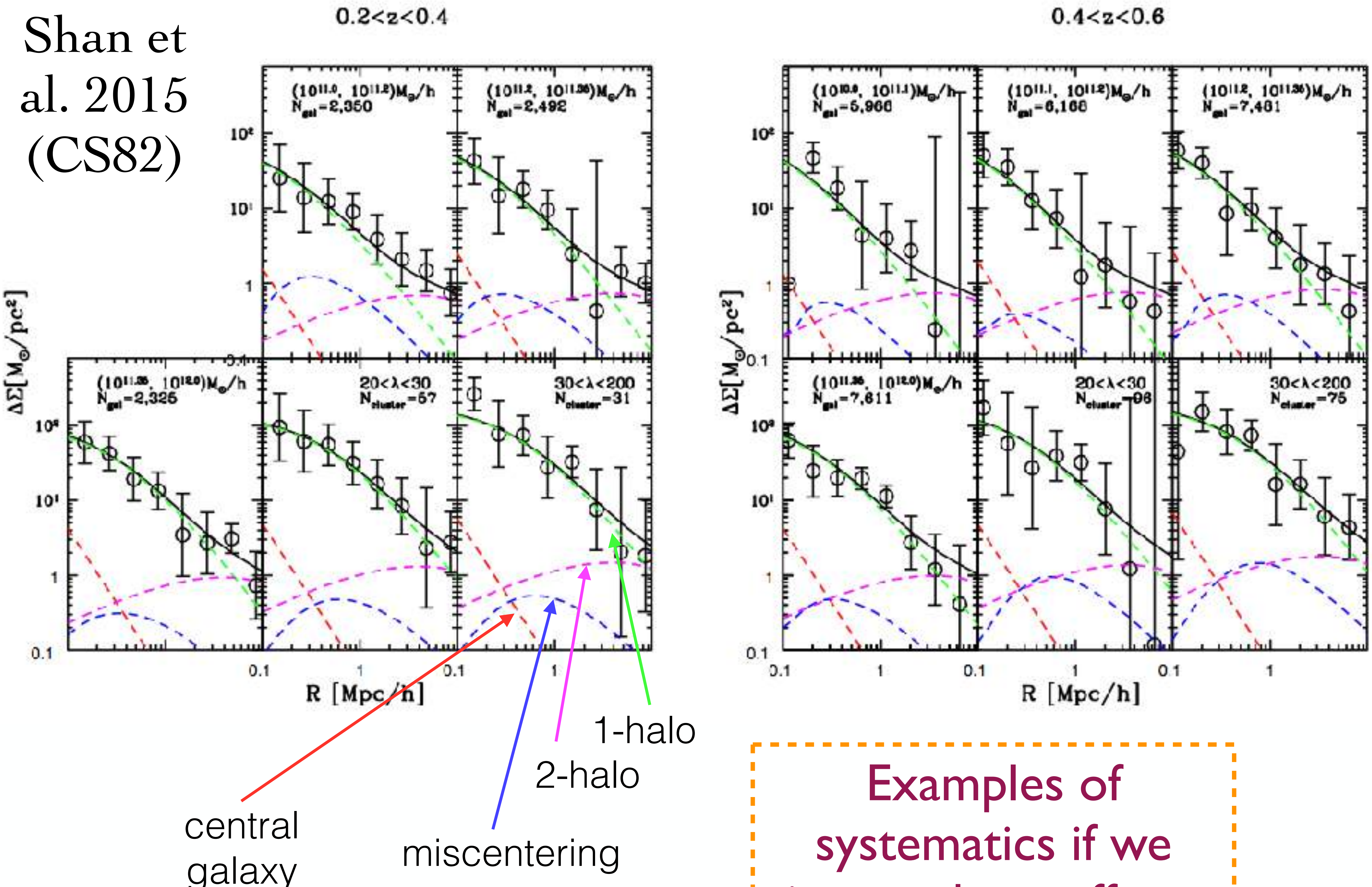

Examples of systematics if we ignore these effects

Mass calibration

Shan et al. 2015 (CS82)

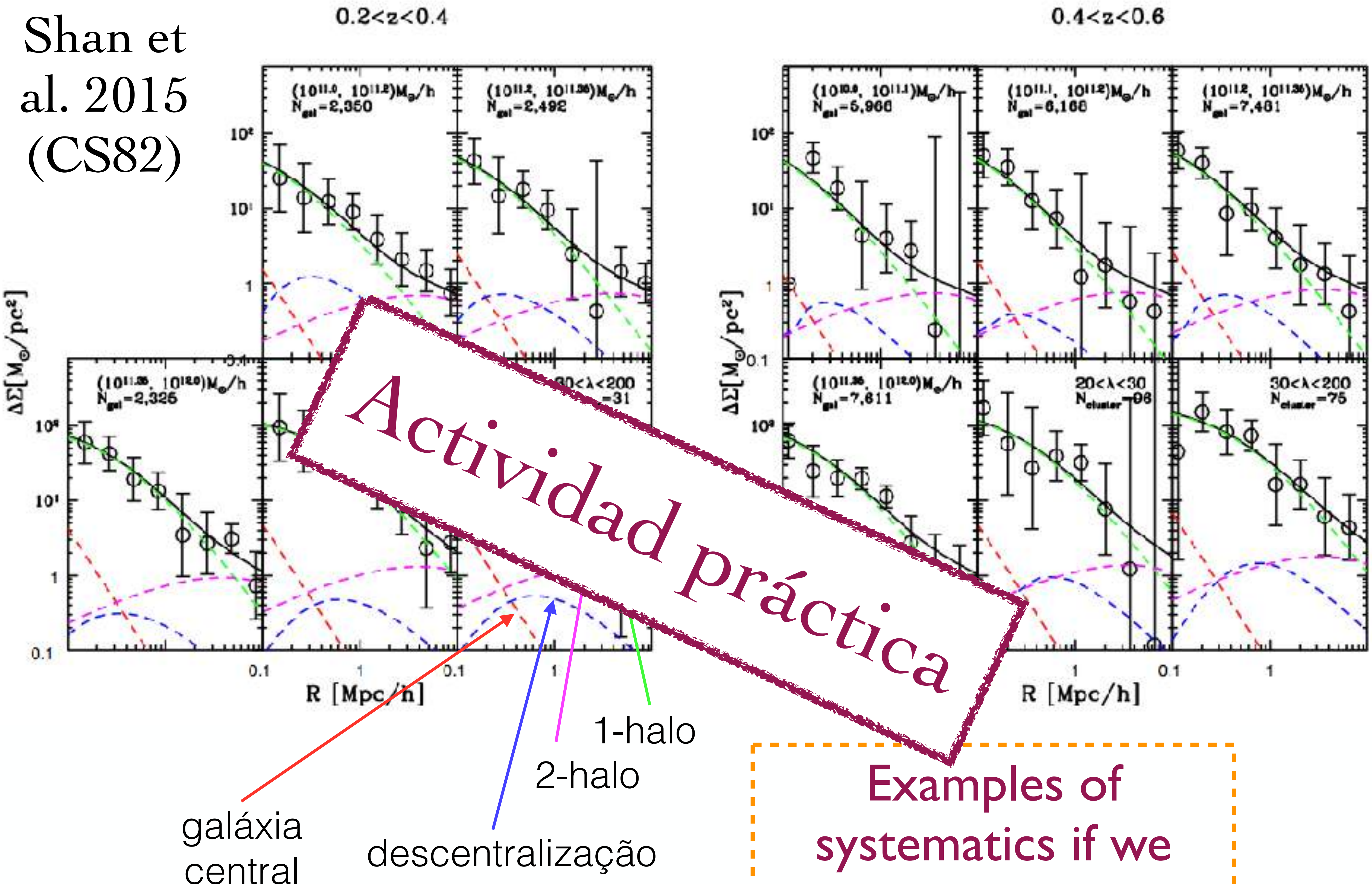

Actividad práctica

Examples of systematics if we ignore these effects

2D Mass reconstruction

Projected potential

$$\psi\left(\vec{\xi}\right) = 2G \int d^2\xi' \Sigma\left(\vec{\xi'}\right) \ln|\xi - \xi'|$$

Lensing potential $\Psi \equiv \frac{2}{c^2} \frac{D_{\mathrm{LS}}}{D_{\mathrm{OS}} D_{\mathrm{OL}}} \psi$

Critical surface density $\Sigma_{\mathrm{crit}} = \frac{c^2}{4\pi G} \frac{D_{\mathrm{OS}}}{D_{\mathrm{OL}} D_{\mathrm{LS}}}$

Convergence $\kappa\left(\vec{\theta}\right) = \frac{\Sigma\left(\vec{\theta}\right)}{\Sigma_{\mathrm{crit}}}$

$$\boxed{\Psi\left(\vec{\theta}\right) = \frac{1}{\pi} \int d^2\theta' \kappa\left(\vec{\theta'}\right) \ln\left|\left(\vec{\theta} - \vec{\theta'}\right)\right|}$$

2D Mass reconstruction

Lens potential

$$\Psi\left(\vec{\theta}\right) = \frac{1}{\pi}\int d^2\theta' \kappa\left(\vec{\theta'}\right) \ln\left|\left(\vec{\theta} - \vec{\theta'}\right)\right|$$

Shear

$$\gamma_1(\vec{\theta}) = \frac{1}{2}(\Psi_{11} - \Psi_{22})$$

$$\gamma_2(\vec{\theta}) = \Psi_{12} = \Psi_{21}$$

$$\Gamma := \gamma_1 + i\gamma_2 = \left(\frac{\partial_1^2 - \partial_2^2}{2} + i\partial_1\partial_2\right)\Psi$$

$$\Gamma = \frac{1}{\pi}\left(\frac{\partial_1^2 - \partial_2^2}{2} + i\partial_1\partial_2\right)\int d^2\theta' \kappa\left(\vec{\theta'}\right) \ln\left|\left(\vec{\theta} - \vec{\theta'}\right)\right|$$

2D Mass reconstruction

Convolution of convergence

$$\Gamma(\vec{\theta}) = \frac{1}{\pi}\left(\frac{\partial_1^2 - \partial_2^2}{2} + i\partial_1\partial_2\right)\int d^2\theta' \kappa(\vec{\theta}') \ln|\vec{\theta} - \vec{\theta}'|$$
$$= \frac{1}{\pi}\int d^2\theta' \kappa(\vec{\theta}') D(\vec{\theta} - \vec{\theta}').$$

Kernel

$$D(\vec{\theta}) \equiv \left(\frac{\partial_1^2 - \partial_2^2}{2} + i\partial_1\partial_2\right) \ln|\vec{\theta}| = \frac{-1}{(\theta_1 - i\theta_2)^2}.$$

Fourier space

$$D(\vec{\ell}) \equiv \int d^2\theta D(\vec{\theta}) e^{i\vec{\theta}\cdot\vec{\ell}} = \pi \frac{\ell_1^2 - \ell_2^2 + 2i\ell_1\ell_2}{|\vec{\ell}|^2}.$$

Since $D(\vec{\ell})D^*(\vec{\ell}) = \pi^2$ as $\Gamma(\vec{\ell}) = D(\vec{\ell})\kappa(\vec{\ell})/\pi$

we have $\kappa(\vec{\ell}) = D^*(\vec{\ell})\Gamma(\vec{\ell})/\pi$

$$\boxed{\kappa(\vec{\theta}) = \kappa_0 + \frac{1}{\pi}\int d^2\theta' D^*(\vec{\theta} - \vec{\theta}')\Gamma(\vec{\theta}').}$$

Mass reconstruction in clusters

E. S. Cypriano, et al., astro-ph/0504036

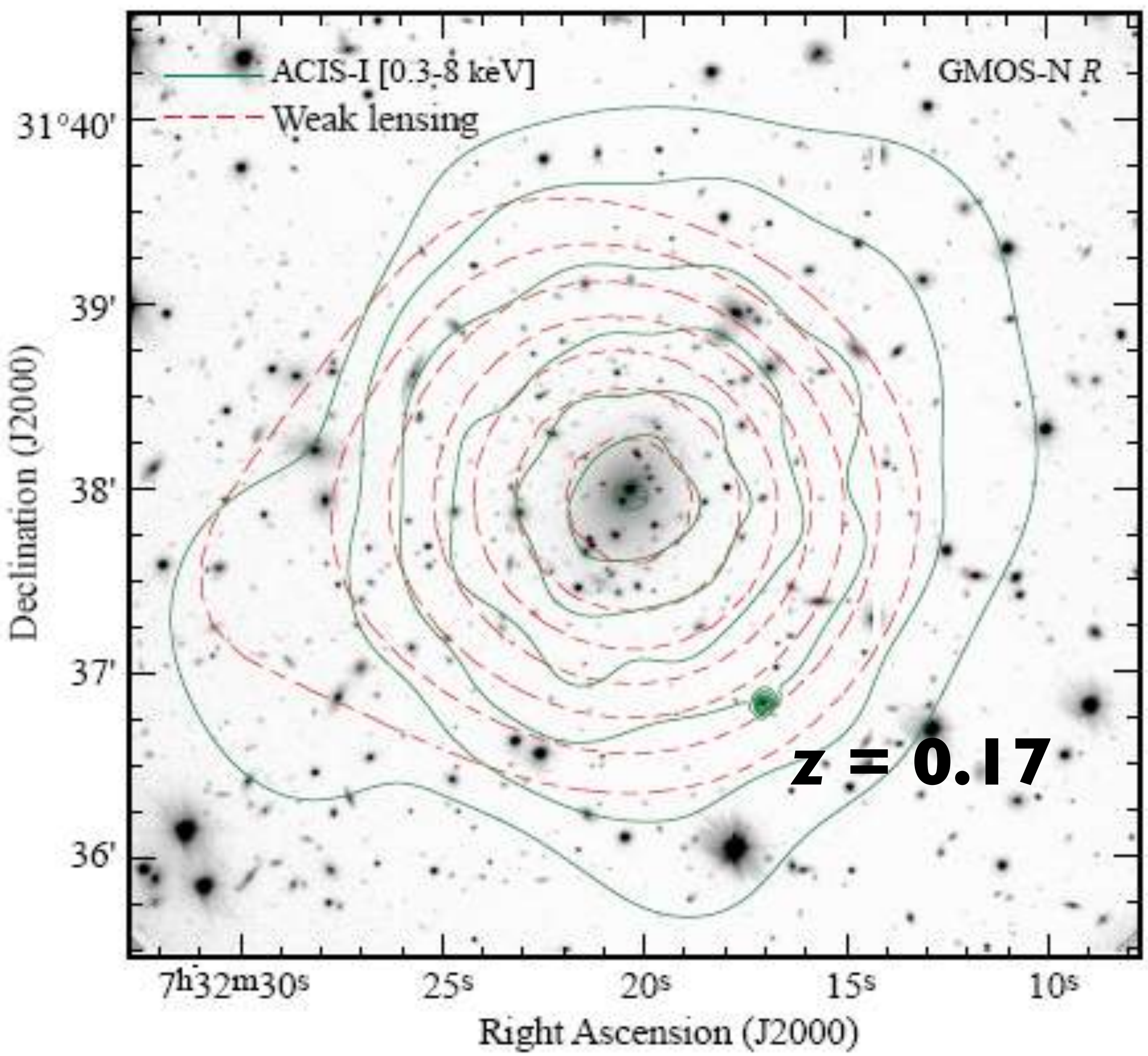

Mass distribution

- Weak Lensing
- x-ray emission
- Velocity dispersion

20% agreement
(in general, for relaxed clusters)

Dark Matter dominates

Evidencia "directa" de la materia oscura

- Aglomerado de la bala (1E0657-558)

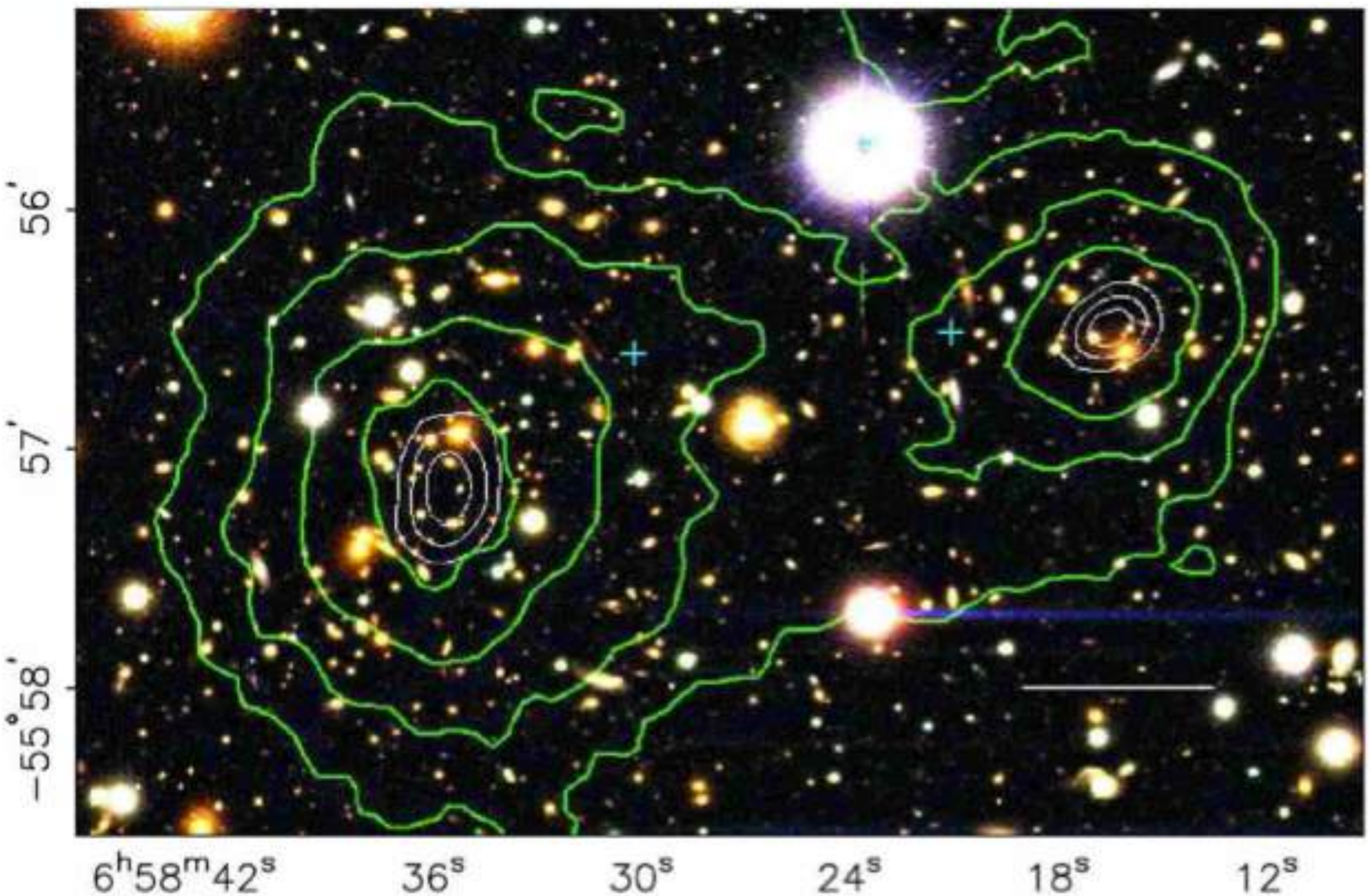

astro-ph/0608407

Reconstrucción de la masa por el efecto débil de lente gravitacional

Evidencia “directa” de la materia oscura

- Distribuição del gás

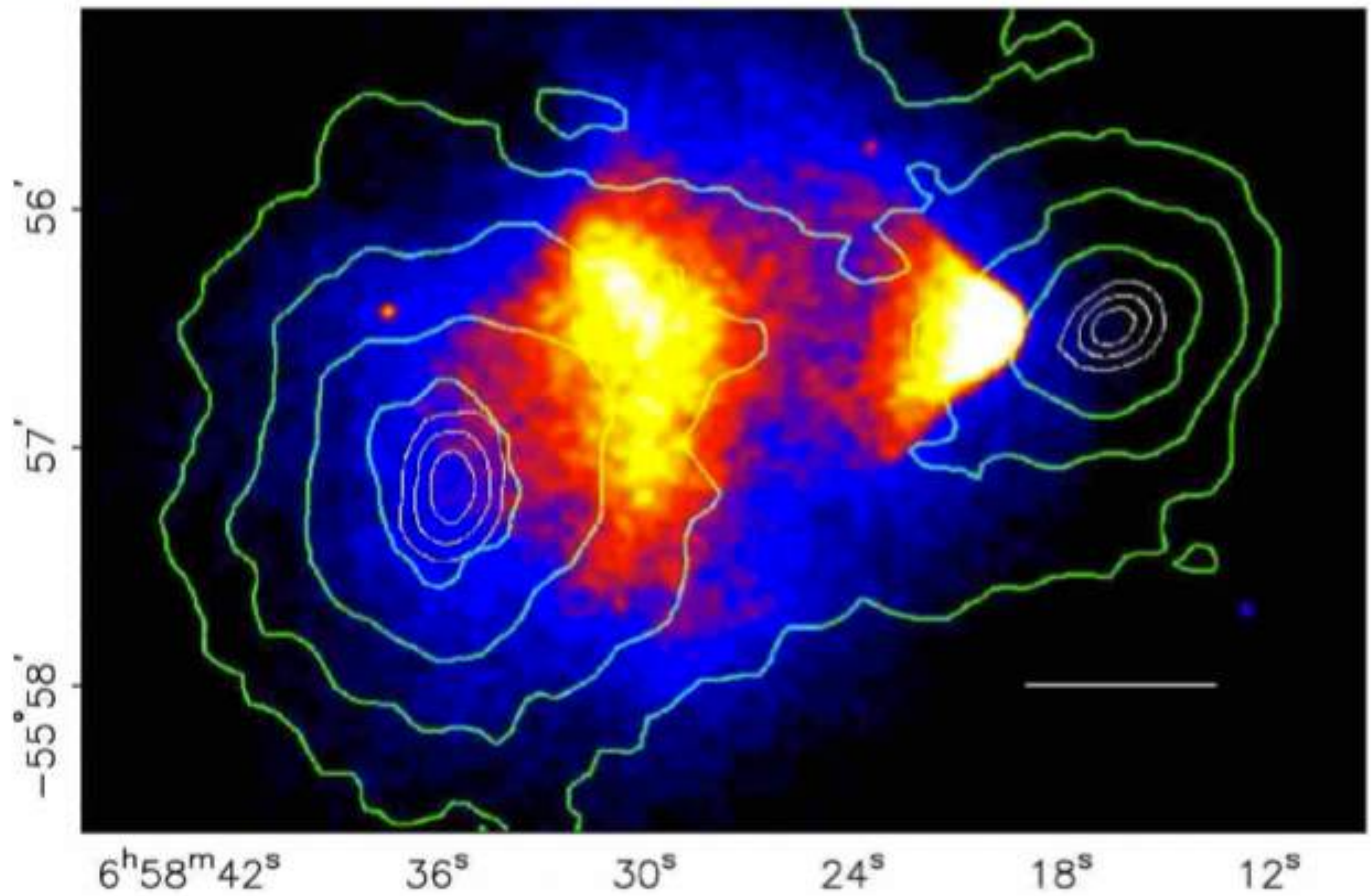

astro-ph/0608407

Desviación de 8σ en los centros de masa!

Convergence Maps

Invertendo para obter $\kappa\left(\vec{\theta}\right)$

- CS82
  - *i*' seeing: 0.65"
  - Area: 173 deg²
  - Maior mapa contíguo
- Picos ➔aglomerados?
  - Arcos em "picos escuros"
  - Correlação com outros catálogos/comprimentos de onda
- Estatística de picos

CS82

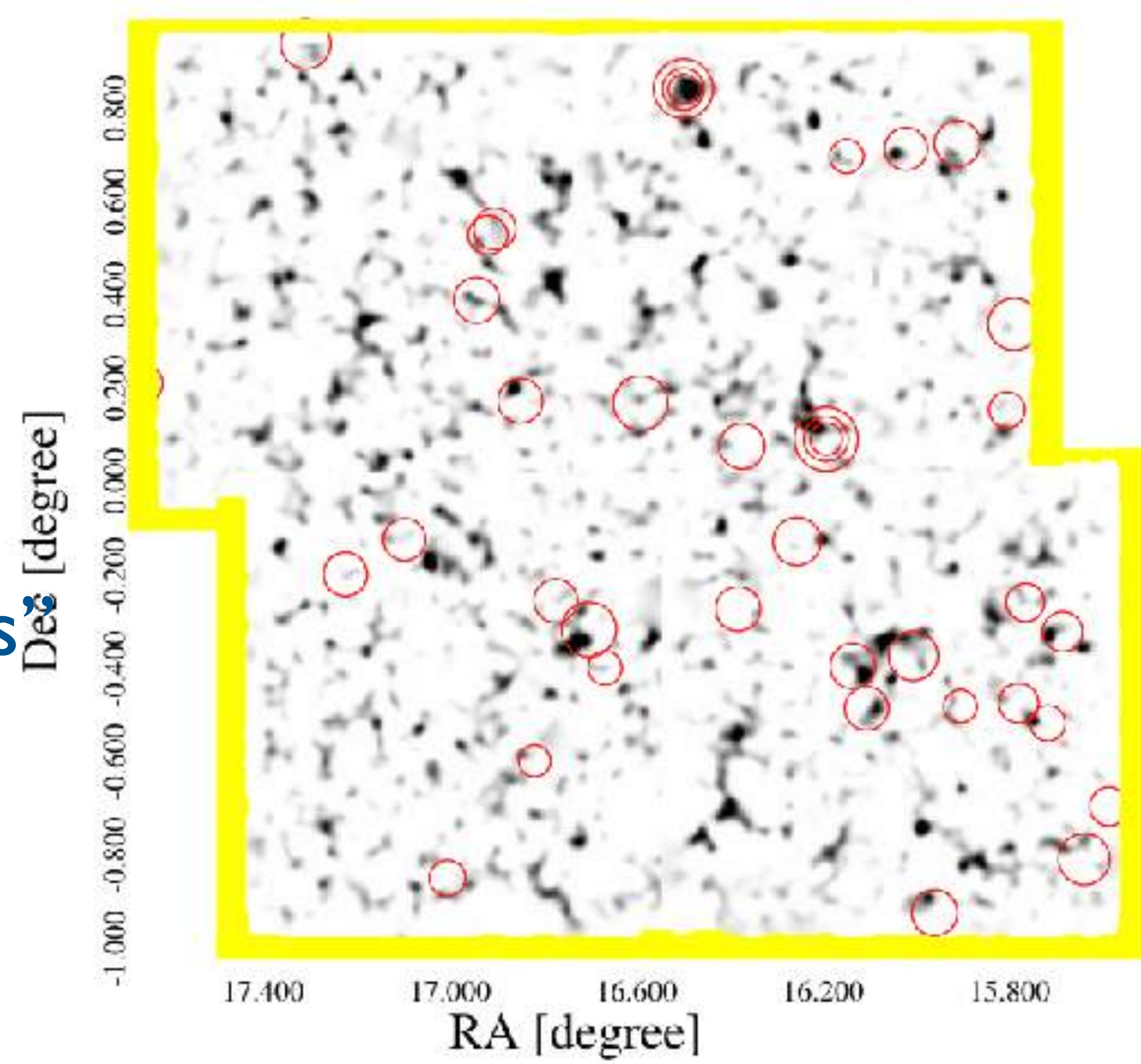

Huan Yuan Shen, et al. 2014
arXiv:1311.1319

Grupo faz mapeamento detalhado da matéria escura no Universo

Novo levantamento revelou pontos de concentração em algumas áreas inesperadas do Cosmos

Invisível, matéria escura é um dos maiores mistérios da astronomia e precisa de 'truque' para ser identificada

SALVADOR NOGUEIRA
COLABORAÇÃO PARA A FOLHA

Um grupo internacional de cientistas acaba de concluir um mapeamento detalhado da distribuição da misteriosa matéria escura no Universo.

Ninguém sabe exatamente do que ela é feita, o que se torna ainda mais constrangedor diante do fato de que ela responde por cerca de 80% de toda a matéria do Cosmos.

Os novos resultados parecem apoiar o modelo mais popular entre os cientistas, segundo o qual a matéria escura é composta por partículas que se movem a velocidades muito inferiores às da luz e que, apesar de terem massa, interagem muito fracamente com a matéria convencional.

Contudo, o estudo ainda está longe de ser capaz de discriminar de forma definitiva entre os diversos modelos cosmológicos possíveis.

"Ainda há muitas alternativas que se encaixam", disse à **Folha** Martín Makler, do Centro Brasileiro de Pesquisas Físicas (CBPF) e que participou do trabalho, publicado "Monthly Notices of the Royal Astronomical Society".

Não é trivial fazer um mapeamento de uma forma de matéria que não emite luz e que, portanto, é invisível. É preciso recorrer ao único efeito detectável produzido pela matéria escura: a gravidade que ela exerce sobre objetos visíveis. Em particular, o grupo, que tem pesquisadores da Suíça, da França, do Canadá, da Alemanha e do Brasil, explorou um fenômeno que foi primeiro previsto pela teoria da relatividade geral, de Einstein: as lentes gravitacionais.

É a ideia de que um corpo celeste mais próximo, que esteja entre nós e outro objeto mais distante, faz com que os raios de luz do objeto afastado se curvem suavemente, do mesmo jeito que a refração de uma lente convencional faz.

Como a matéria escura representa muito mais massa do que a convencional, seu efeito nas lentes gravitacionais é pronunciado. Ao detectar as distorções nos caminhos da luz, é possível estimar a quantidade de matéria escura até o objeto.

O resultado do esforço, feito com o Telescópio Canadá-França-Havaí, é um mapa bidimensional —sem profundidade— da distribuição da matéria escura, que cobre uma faixa do céu com 170 graus quadrados de área.

Uma das novidades importantes do estudo é a inclusão de concentrações não muito grandes de matéria escura.

O trabalho também traz novos mistérios. Os pesquisadores encontraram alguns picos que não correspondem a grupos e aglomerados de galáxias. Ou seja, os "objetos" que teriam curvado os raios de luz seriam 100% escuros, sem matéria convencional. Os cientistas agora estão concentrados em confirmar que esses picos são reais.

MACIÇA E INTOCÁVEL
Matéria escura é um dos grandes mistérios da ciência

O QUE É MATÉRIA ESCURA

> A matéria escura é invisível

> Astrônomos sabem que ela existe porque ela mantém galáxias coesas: galáxias giram tão rápido que, sem a gravidade da matéria escura, jogaria estrelas para fora

> A matéria escura deve ser feita de partículas diferentes, que não interagem com átomos da maneira usual (por meio da força eletromagnética); experimentos especias tentam capturá-la

Estadística de Picos y Cosmologia en CS82

Xiangkun Liu, et al. 2015

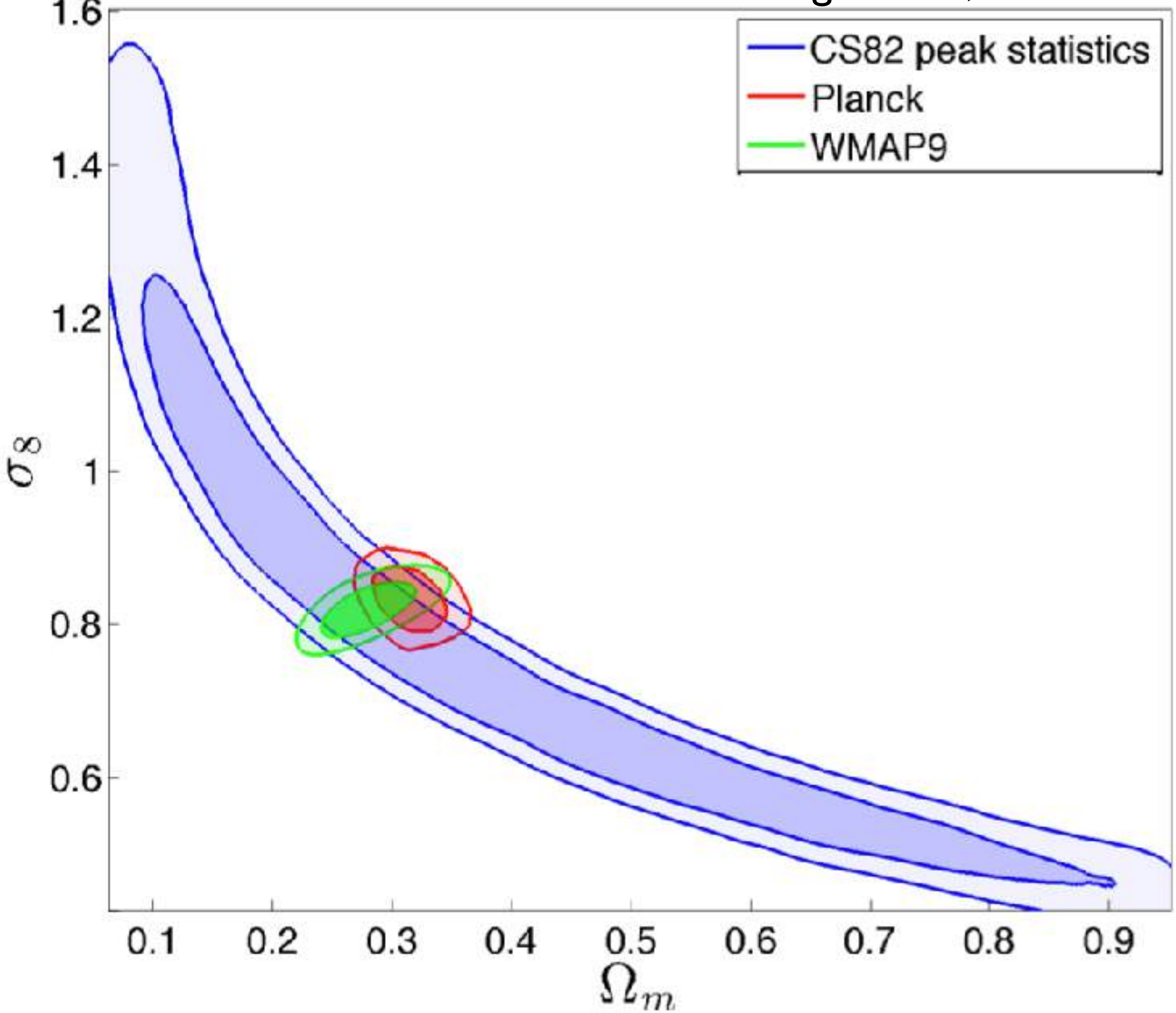

Lensing por la estructura en gran escala

Estrutura en Grandes Escalas: El domínio de la estadística

- No solo a nivel de la cantidad de datos y de la medida estadística de las formas
- Observables típicamente estadísticos:
  - estimadores conectados a correlaciones
- Función de correlación:
  - espacio real, más directamente relacionado con las observaciones
    (aunque espacio de redshift, distorsiones, etc).
- Espacio de Fourier:
  - relacionado al espectro primordial (modelos/teoría)
  - desacople entre modos

¿Cómo se formaron las estructuras?

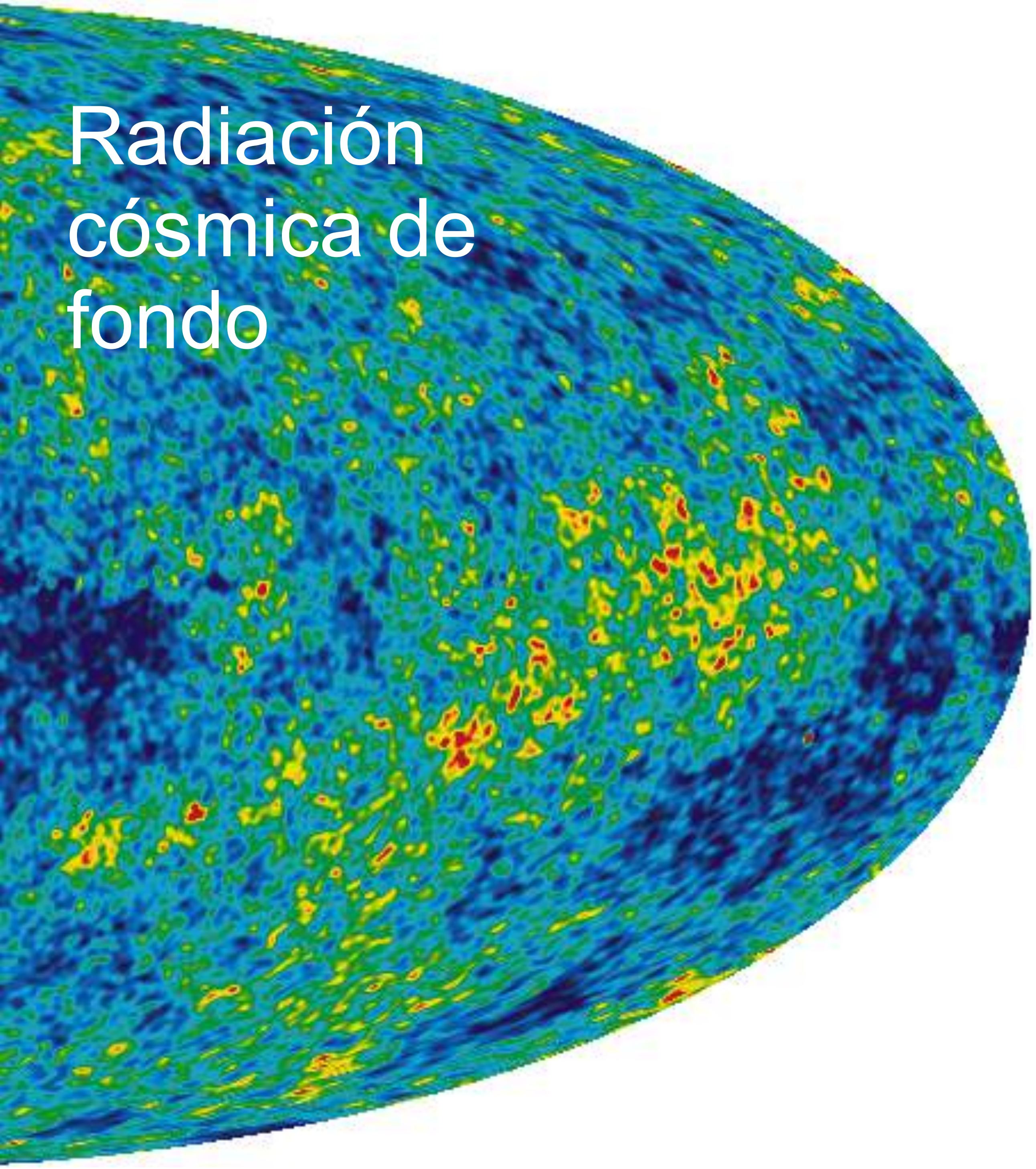

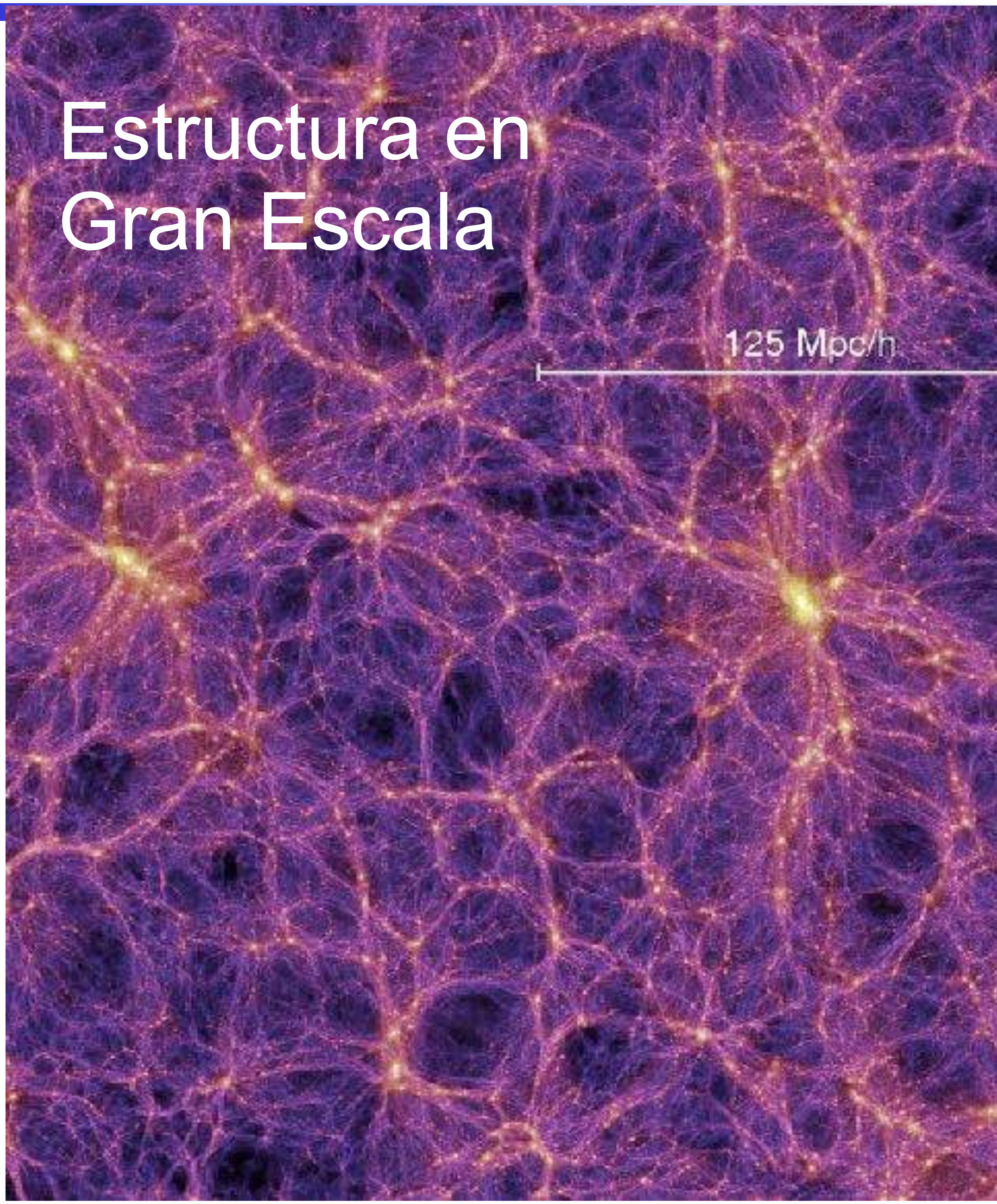

Fluctuaciones ~ 10^{-4}

Fluctuaciones ~ 10^{3}

Límite newtoniano y teoria de perturbación relativista

- Teoria de perturbación cosmológica: métrica de Robertson-Walker perturbada

$$
\begin{aligned}
ds^2 &= \left[g^{(0)}_{\mu\nu} + g^{(1)}_{\mu\nu}\right] dx^\mu dx^\nu \\
&= a^2(\tau)\left[-d\tau^2 + \gamma_{ij}(\vec{x})dx^i dx^j + h_{\mu\nu}(\vec{x},\tau)dx^\mu dx^\nu\right] \quad ,
\end{aligned}
$$

- Modos tensoriales, vectoriales y escalares
- Desacople entre los modos en el regimen lineal
- Perturbaciones escalares están asociadas a fluctuaciones de densidad:

$$\boxed{ds^2 = a^2(\tau)\left[-(1+2\Psi)d\tau^2 + (1-2\phi)\gamma_{ij}\, dx^i dx^j\right]}$$

(para um fluido perfecto $\Phi = \Psi$)

- Nuevamente, límite newtoniano para $\dfrac{\phi}{c^2} \ll 1 \quad \left(\dfrac{v}{c}\right)^2 \ll 1$
- Fluctuaciones de densidad:

$$\rho(\vec{x},\tau) = \bar{\rho}(\tau) + \delta\rho(\vec{x},\tau)$$

Back to weak lensing
2 Regimes and Methods

Lensing by galaxies and clusters

- Larger signal
- Center of reference
- Model/profile fitting
- Individual objects or *Stacking* of the signal

Large-scale structure

- Convergence maps (also in clusters)
- Correlations:
  - power spectrum, correlation function
  - among different probes, z-bins, CMB, etc.

Cosmic shear

- Large-scale structure of the Universe
- Tomography

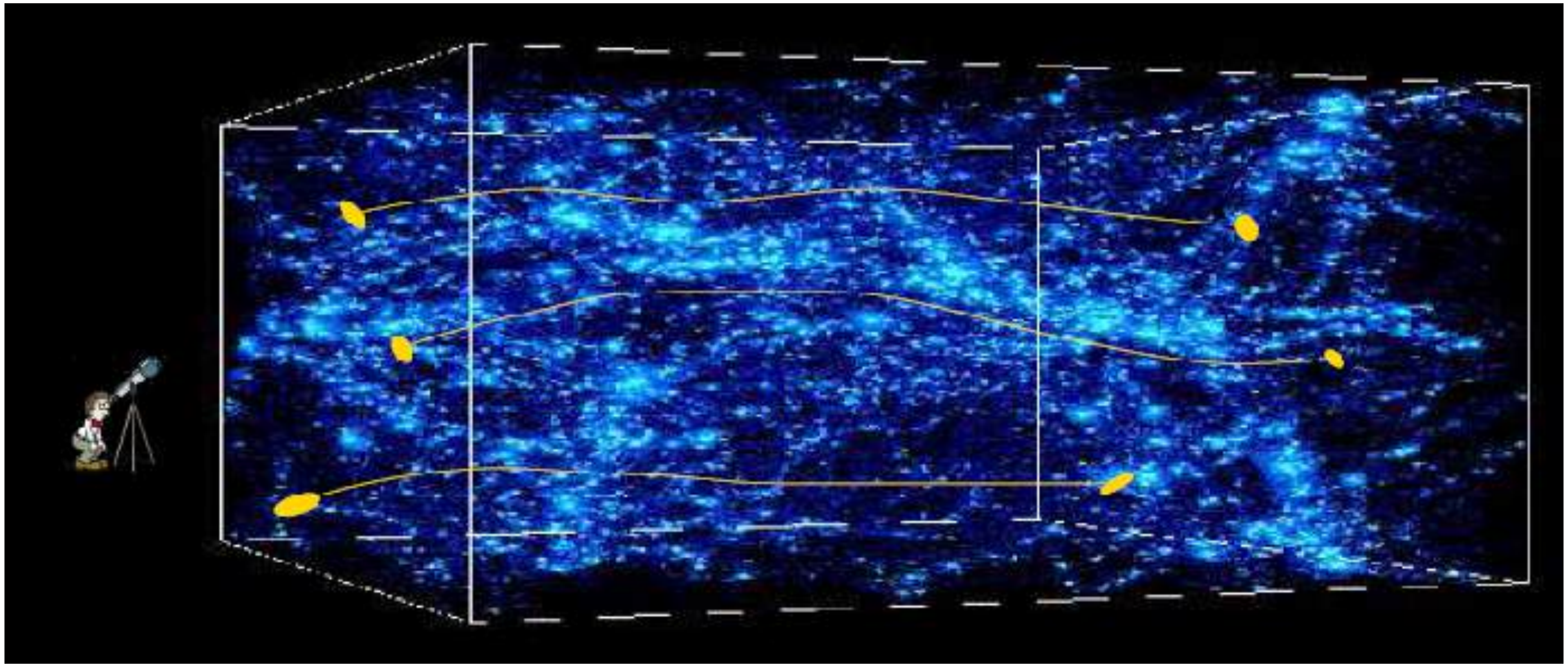

Martin Kilbinger, Institut d'Astrophysique de Paris

Otros sistemas de coordenadas

- Forma "usual" de la métrica de FLRW

$$ds^2 = dt^2 - a^2(t)\left(\frac{1}{1-Kr^2}dr^2 + r^2 d\theta^2 + r^2 sen^2\theta\, d\phi^2\right)$$

- Forma más usada en lentes y otros contextos cosmológicos

$$ds^2 = -dt^2 + a^2(t)\left(d\chi^2 + F(\chi)(d\theta^2 + sen^2\theta\, d\phi^2)\right)$$

Recapitulando

Metrica de Friedmann con perturbación escalar

$$ds^2 = a^2(\tau)\left\{(1+2\frac{\varphi}{c^2})d\tau^2 - (1-2\frac{\varphi}{c^2})\left[d\chi^2 + r^2(\chi)(d\theta^2 + \sin^2\theta d\phi^2)\right]\right\}$$

geometria del fondo (FLRW)

Propagación de la luz en el fondo homogéneo

$$\chi = \tau_0 - \tau$$

Lensing por la estructura en gran escala: mas allá de la aproximación de lente fina

Metrica de Friedmann con perturbación escalar

$$ds^2 = a^2(\tau)\left\{(1+2\frac{\varphi}{c^2})d\tau^2 - (1-2\frac{\varphi}{c^2})\left[d\chi^2 + r^2(\chi)(d\theta^2 + \sin^2\theta d\phi^2)\right]\right\}$$

Ecuación de la geodésica

$$\frac{d^2x^i}{d\lambda^2} = -g^{ik}\left(\frac{\partial g_{kl}}{\partial x^m} - \frac{1}{2}\frac{\partial g_{lm}}{\partial x^k}\right)\frac{dx^m}{d\lambda}\frac{dx^l}{d\lambda}$$

Ángulo de desvio

fuente

lente

$$\theta_\sigma(\chi) = \theta_\sigma^0 - \frac{2}{c^2}\int_0^{\chi}\frac{d\chi'}{r^2(\chi')}\int_0^{\chi'} d\chi''\varphi_{,\sigma}(\vec{\theta}r(\chi''),\chi'')$$

Funciones de lente

Angulo de desvio

$$\theta_\sigma(\chi) = \theta_\sigma^0 - \frac{2}{c^2}\int_0^\chi \frac{\mathrm{d}\chi'}{r^2(\chi')}\int_0^{\chi'} \mathrm{d}\chi'' \varphi_{,\sigma}(\vec{\theta} r(\chi''), \chi'')$$

Se reduce a una integral a lo largo de la trayectoria del fotón

fuente lente

$$\theta_\sigma(\chi) = \theta_\sigma^0 - \frac{2}{c^2}\int_0^\chi \mathrm{d}\chi' \varphi_{,\sigma}(\vec{\theta} r(\chi'), \chi') \frac{r(\chi - \chi')}{r(\chi) r(\chi')}$$

Potencial de lente

$$\Psi = \frac{2}{c^2 r(\chi)}\int_0^\chi \mathrm{d}\chi' \varphi(\vec{\theta} r(\chi'), \chi') \frac{r(\chi - \chi')}{r(\chi')}$$

Convergencia

$$\kappa(\vec{\theta}) = \frac{1}{2}\nabla_\theta^2 \Psi = \frac{1}{c^2}\int_0^\chi \mathrm{d}\chi' \nabla_\perp^2 \varphi(\vec{x}_\perp, \chi') \frac{r(\chi - \chi') r(\chi')}{r(\chi)}$$

Convergencia

Usando la ecuación de Poisson para las perturbaciones

$$\nabla^2 \varphi(\vec{x}, \tau) = \frac{3H_0^2\Omega_m}{2a(\tau)} \delta(\vec{x}, \tau)$$

Y promediando para una distribución no uniforme de fuentes

$$n(\chi) = N_{tot}^{-1}(\mathrm{d}N/\mathrm{d}\chi)$$

La convergencia se escribe como

$$\kappa(\vec{\theta}) = \frac{3H_0^2\Omega_m}{2c^2} \int_0^{\chi_H} \mathrm{d}\chi \delta(\vec{x}_\perp, \chi) \frac{g(\chi)}{a(\chi)}$$

Función ventana
eficiencia de lentes

donde

$$g(\chi) = r(\chi) \int_\chi^{\chi_H} \mathrm{d}\chi' \frac{r(\chi - \chi')n(\chi')}{r(\chi')}$$

Correlaciones

$$\kappa(\vec{\theta}) = \frac{3H_0^2\Omega_m}{2c^2}\int_0^{\chi_H} \mathrm{d}\chi\delta(\vec{x}_\perp,\chi)\frac{g(\chi)}{a(\chi)}$$

En el espacio de Fourier

$$\boldsymbol{\kappa}(\vec{\ell}) = \int \mathrm{d}^2\theta\ \boldsymbol{\kappa}(\vec{\theta})e^{i\vec{\ell}\cdot\vec{\theta}}$$

tenemos

$$\langle\kappa(\vec{\ell})\kappa(\vec{\ell}')\rangle = (2\pi)^2\delta^{(2)}(\vec{\ell}-\vec{\ell}')P_\kappa(\ell)$$

Espectro de potencias
de la estructura en gran escala:
dependencia cosmológica!

el espectro de potencias es dado por

$$P_\kappa(\ell) = \frac{9H_0^4\Omega_m^2}{4c^4}\int_0^{\chi_H} \mathrm{d}\chi\frac{g^2(\chi)}{a^2(\chi)}P_\delta\left(\frac{\ell}{r(\chi)},\chi\right)$$

Correlaciones

$$P_\kappa(\ell) = \frac{9H_0^4\Omega_m^2}{4c^4}\int_0^{\chi_H} \mathrm{d}\chi \frac{g^2(\chi)}{a^2(\chi)} P_\delta\left(\frac{\ell}{r(\chi)}, \chi\right)$$

Espectro de potencias
de la estructura en gran escala:
dependencia cosmológica!

Espectro de potencias

$$\begin{aligned} P_\delta(k,\tau) &= D_+(k,\tau)P_k^{\mathrm{lin}} \\ &= D_+(k,\tau)T(k)P_k \\ &= D_+(k,\tau)T(k)A_0k^{n_s-1} \end{aligned}$$

Angular x espacial en el espacio k

$$k_\sigma = \ell_\sigma / r(\chi)$$

Tiempo conforme

$$\chi = \tau_0 - \tau$$

Cosmic Shear

- Separating into redshift bins
- Weak lensing (statistical)

Sensitive to dark energy (geometry + growth factor)

Less sensitive to baryonic physics

- large separations: linear
- Example: cosmic shear power spectrum on three photo-z slices (tomography)

•DES:

- unique combination of area, seeing and depth
- shapes of ~ 300 million galaxies with ⟨z⟩ = 0.7

$$C_\ell^{x_a x_b} = \int dz \frac{H(z)}{D_A^2(z)} W_a(z) W_b(z) P^{s_a s_b}(k=\ell/D_A; z)$$

$$\Delta C_\ell = \sqrt{\frac{2}{(2\ell-1) f_{sky}}}\left(C_\ell + \frac{\sigma^2(\gamma_i)}{n_{eff}}\right)$$

10-20 galáxias/arcmin²

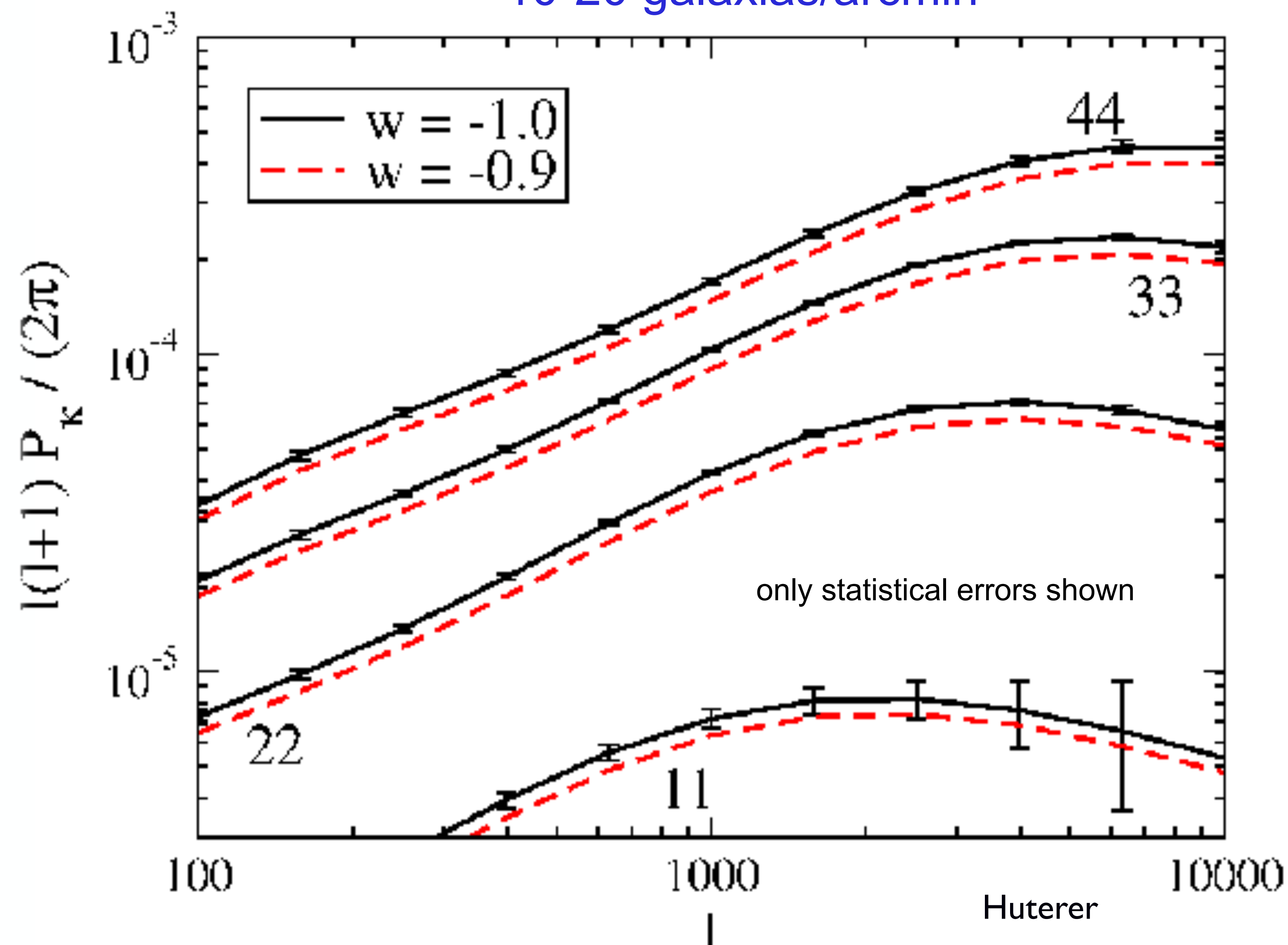

Example: DES Y1 Results

- Data
  - 1321 deg^2 of g,r,i,z imaging data
  - 26 million source galaxies
  - 650,000 luminous red galaxies (redMaGIC)
- Combined analysis of 3 two-point function
  - the cosmic shear correlation function in four redshift bins
  - the galaxy angular autocorrelation function of LRGs in five redshift bins
  - the galaxy-shear cross-correlation of LRG positions and source galaxy
  - shears.
- Dark Energy Survey Year 1 Results: Cosmological Constraints from Galaxy Clustering and Weak Lensing
  - 10 "supporting papers" jointly submitted
  - Careful analysis of systematics
  - Joint likelihoods

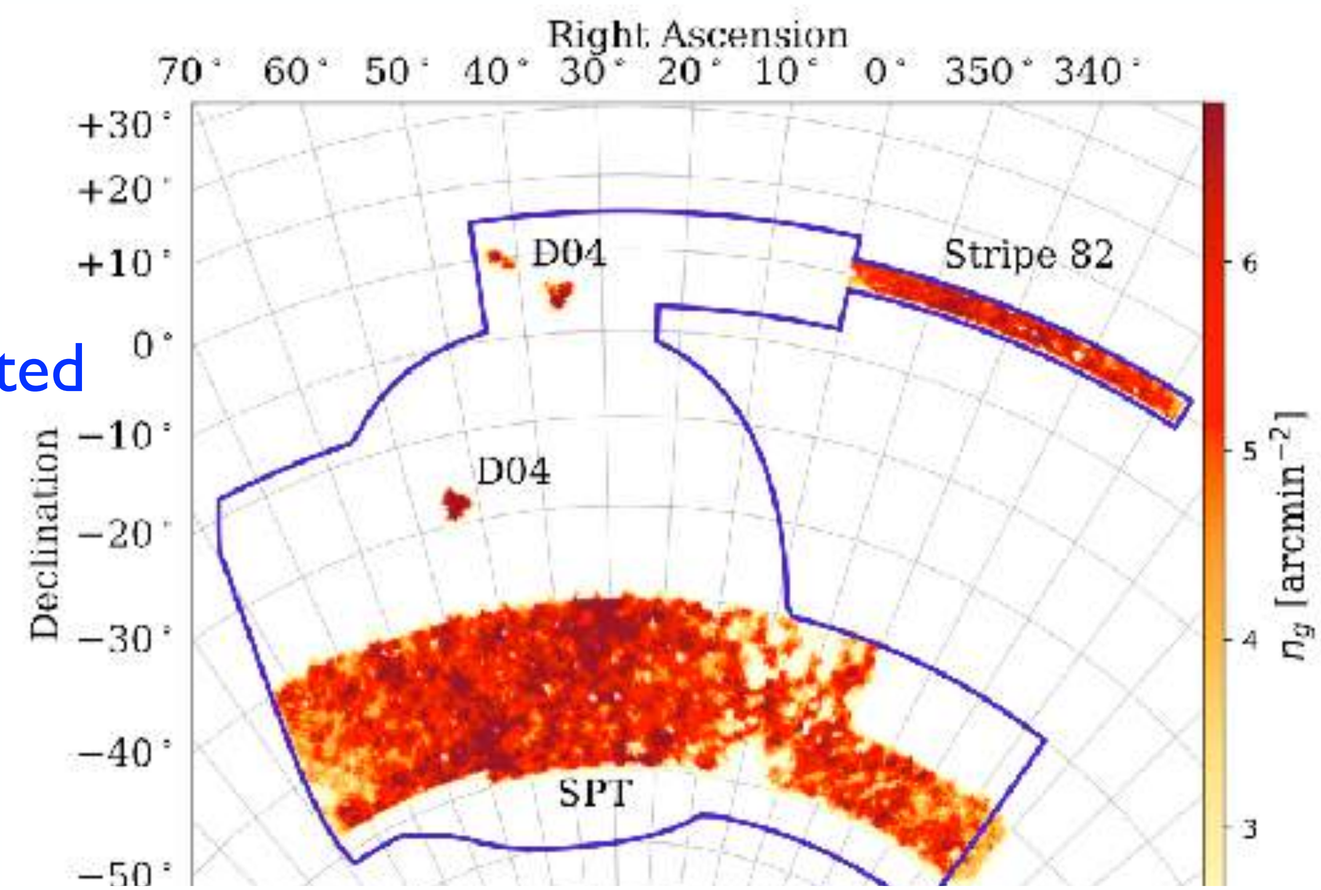

http://www.darkenergysurvey.org/des-year-1-cosmology-results-papers/

Cosmic Shear Measurements

Dark Matter Map 2.0

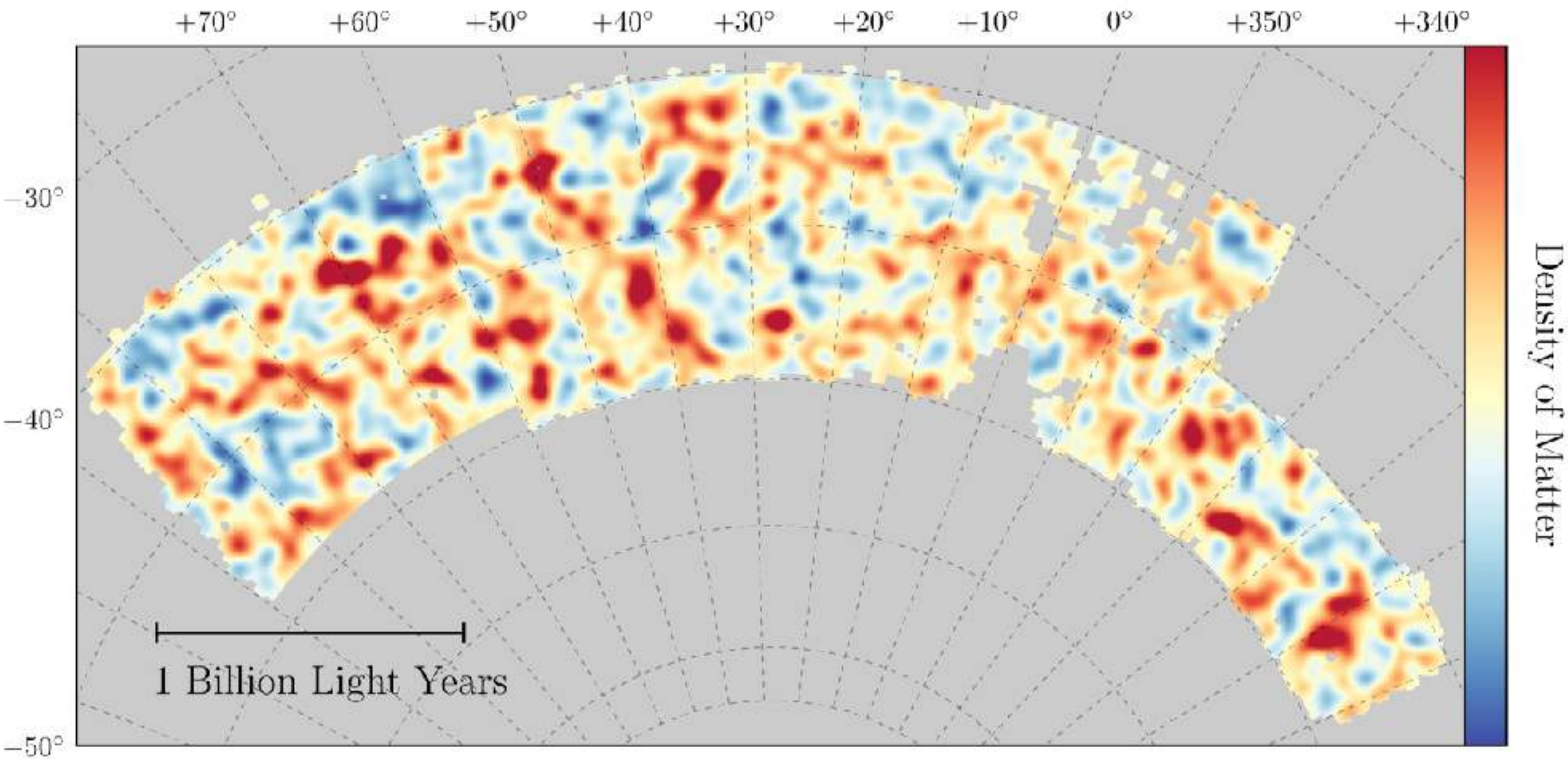

DARK ENERGY SURVEY

- **Led by Fermilab**
- **DECam**: The 570 Megapixel camera for the Blanco 4m telescope in Chile.
- Survey Observations 2013-2019 ("Y3" means 2013-16).
- **Wide field:** 5000 sq. deg. in 5 bands. ~23 magnitude depth.
- 27 sq. deg. 5-yr SNIa survey

N. Jeffrey: Dark Energy Survey Collaboration

Dark Matter map from DES observations

DES Year 3: pixels to cosmology

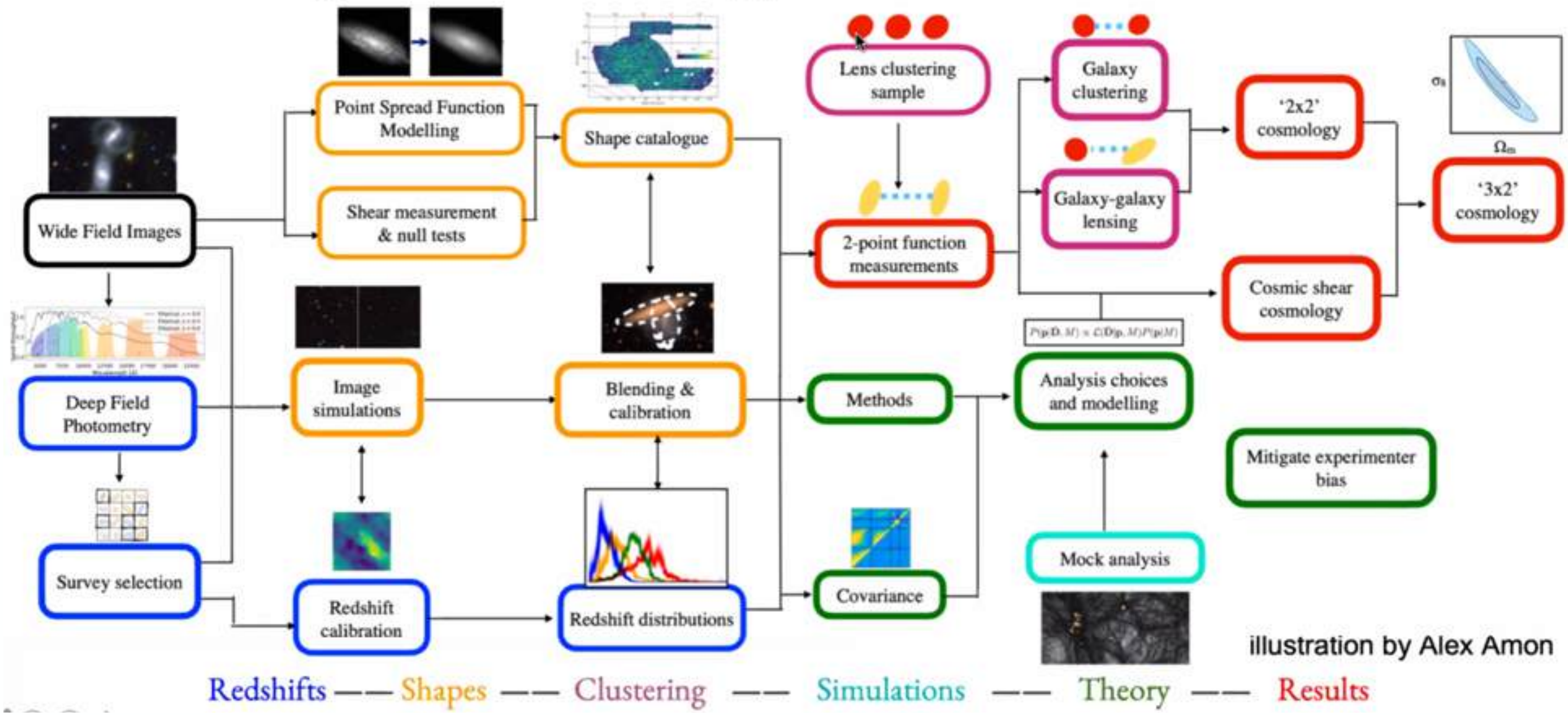

Estimadores estadísticos

Dark Energy Survey Year 1 Results: Cosmological Constraints from Galaxy Clustering and Weak Lensing

Galaxy–galaxy lensing: $\gamma_t(\theta)$

Cosmic shear: $\xi_\pm(\theta)$

$$\xi^{ij}_{+/-}(\theta) = (1+m^i)(1+m^j)\int \frac{dl\,l}{2\pi} J_{0/4}(l\theta) \int d\chi \frac{q^i_\kappa(\chi) q^j_\kappa(\chi)}{\chi^2} P_{\rm NL}\left(\frac{l+1/2}{\chi}, z(\chi)\right)$$

$$q^i_\kappa(\chi) = \frac{3H_0^2\Omega_m}{2c^2}\frac{\chi}{a(\chi)}\int_\chi^{\chi_h} d\chi' \frac{n^i_\kappa(z(\chi'))dz/d\chi'}{\bar{n}^i_\kappa}\frac{\chi'-\chi}{\chi'}, \tag{IV.3}$$

Galaxy Clustering: $w(\theta)$

$$w^i(\theta) = \int \frac{dl\,l}{2\pi} J_0(l\theta) \int d\chi \frac{q^i_{\delta_g}\left(\frac{l+1/2}{\chi}, \chi\right) q^j_{\delta_g}\left(\frac{l+1/2}{\chi}, \chi\right)}{\chi^2} \times P_{\rm NL}\left(\frac{l+1/2}{\chi}, z(\chi)\right) \tag{IV.4}$$

Weak Lensing Tomography

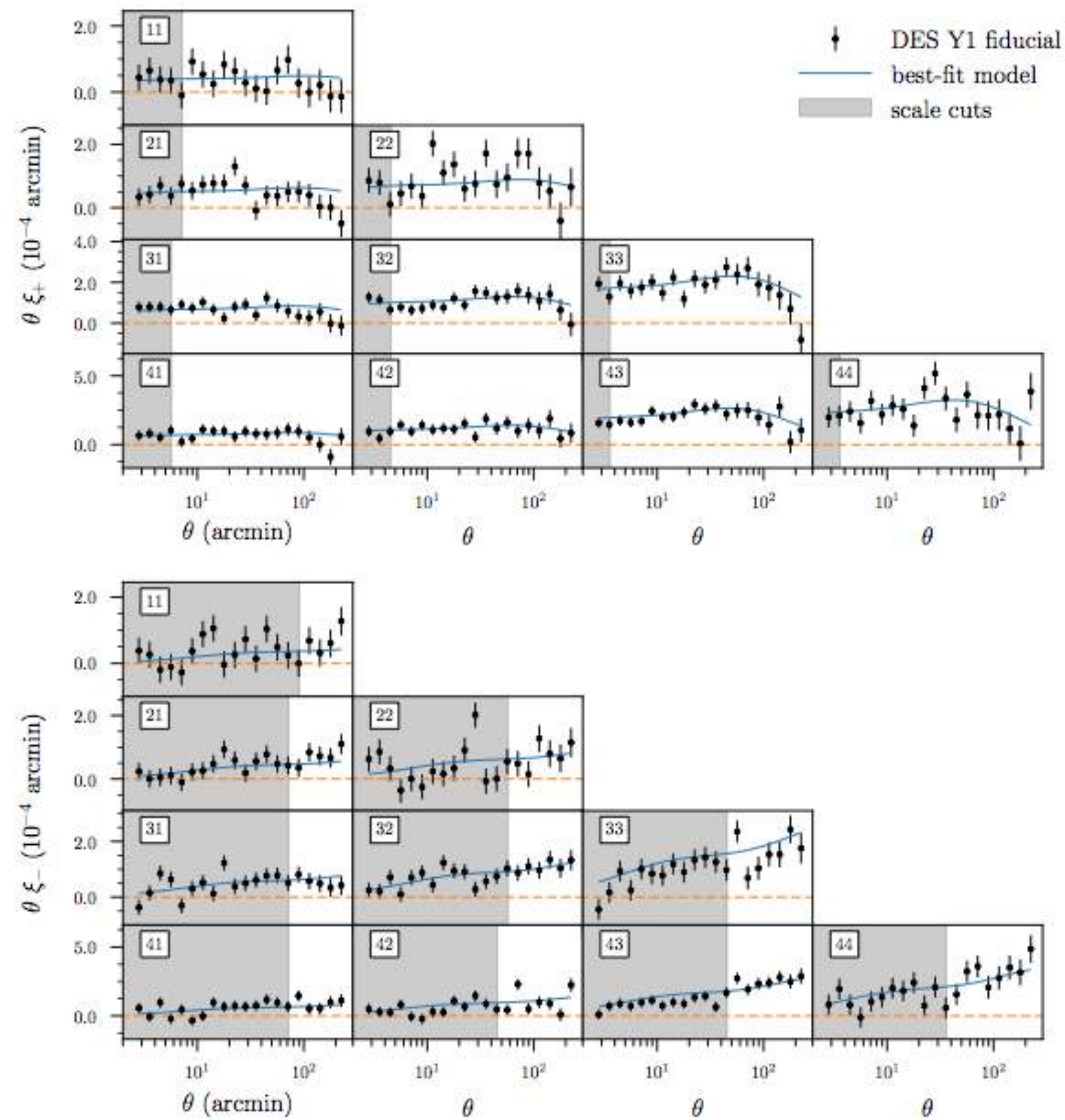

galaxy-shear correlation

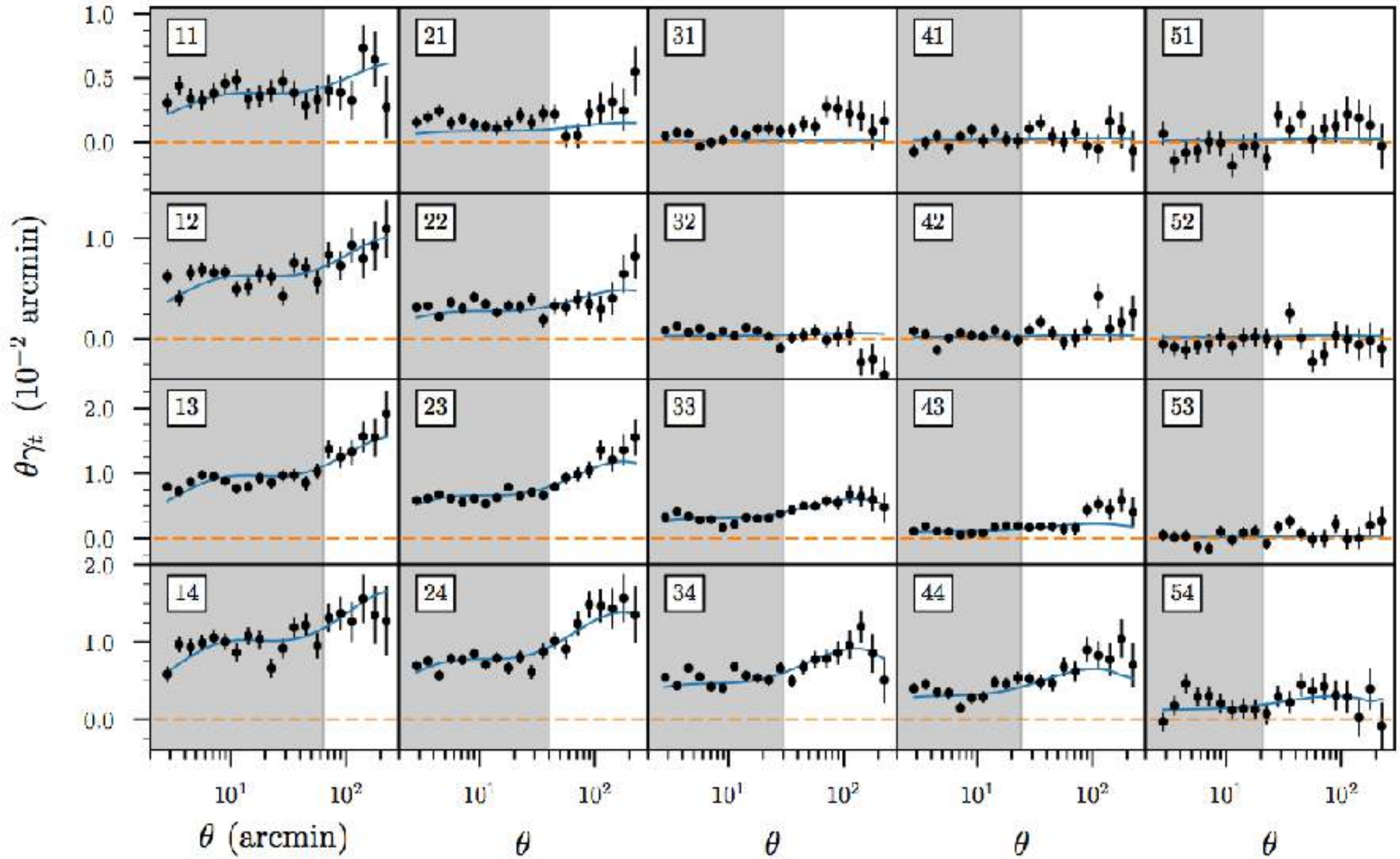

Angular Correlation Function

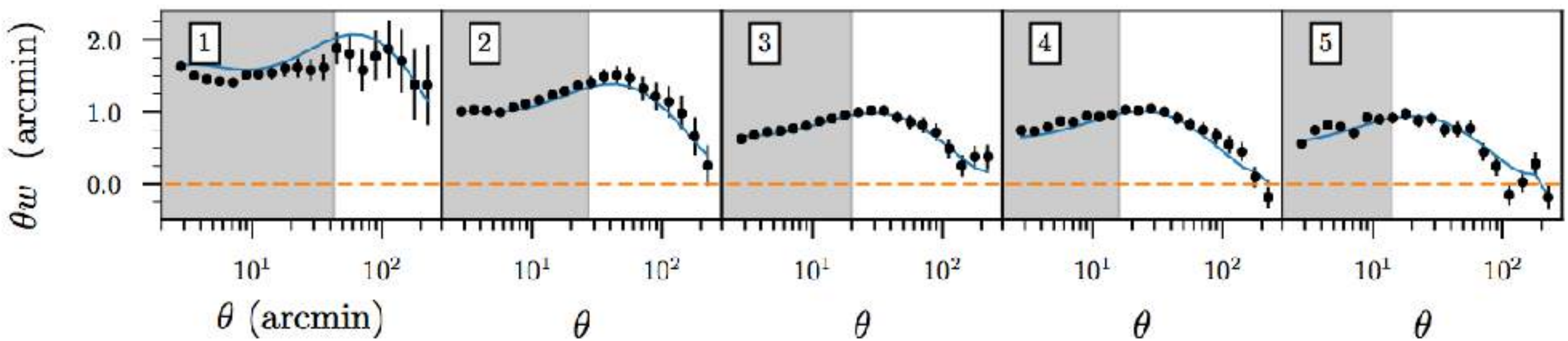

Scaled angular correlation function, θw(θ), of redMaGiC galaxies in five redshift bins

Consistency of the Probes

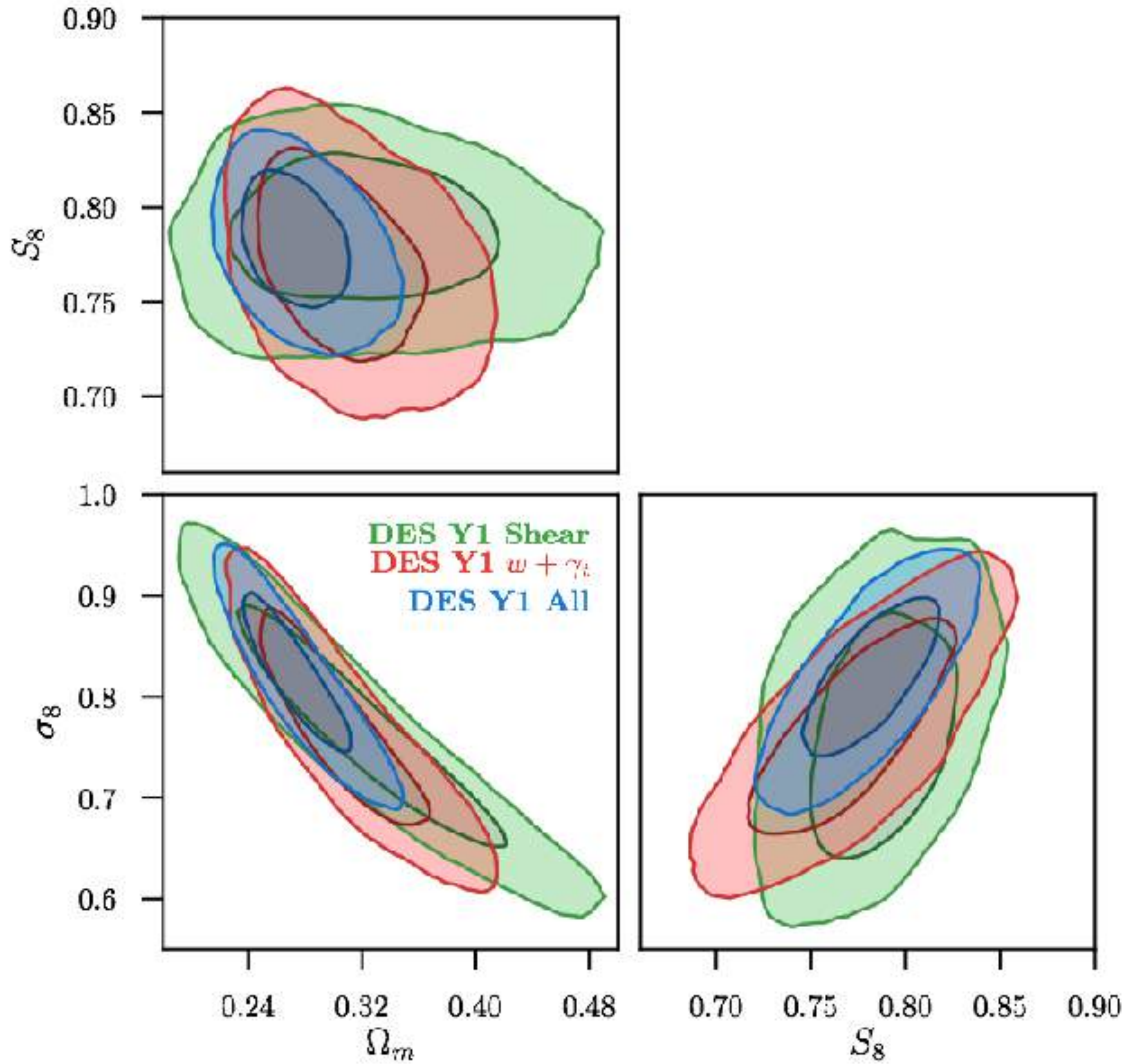

Combined Analysis

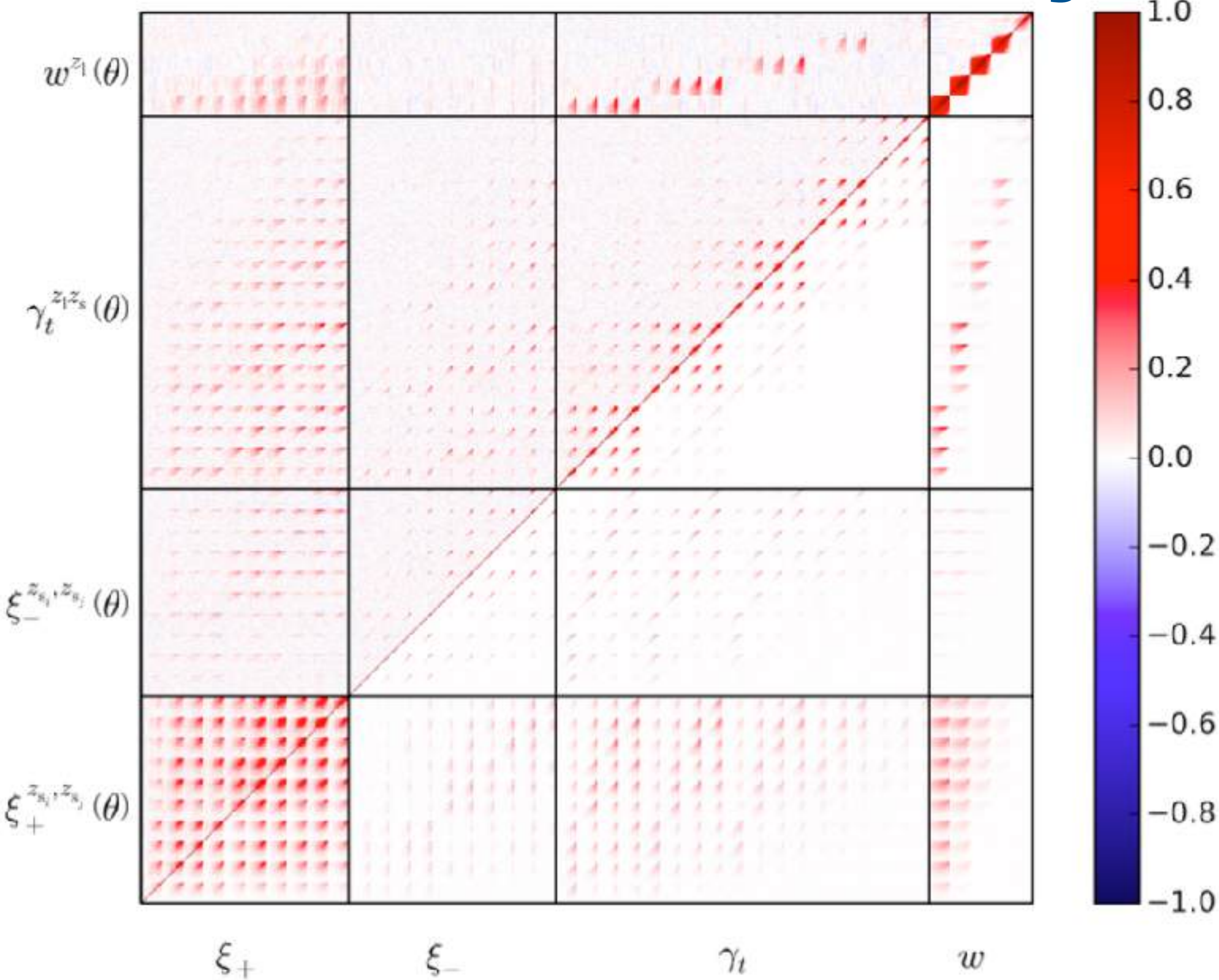

457 × 457 element covariance matrix!

20 “nuisance parameters” + 6/7 cosmological

Kilo Degree Survey

KiDS: 1000 sq-deg

http://kids.strw.leidenuniv.nl/KiDS-1000_preprints.php

Cosmological parameter constraints from tomographic weak gravitational lensing

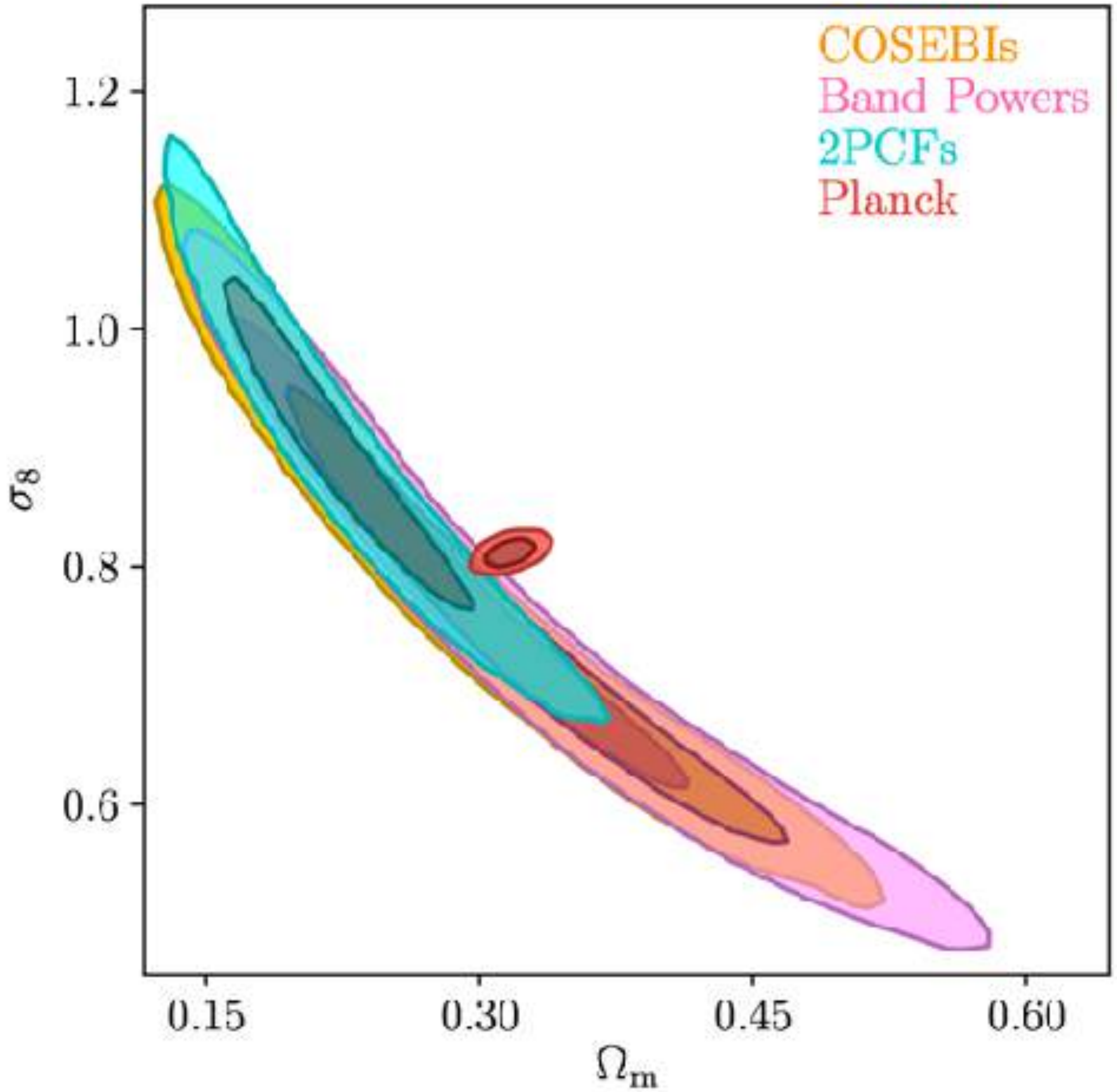

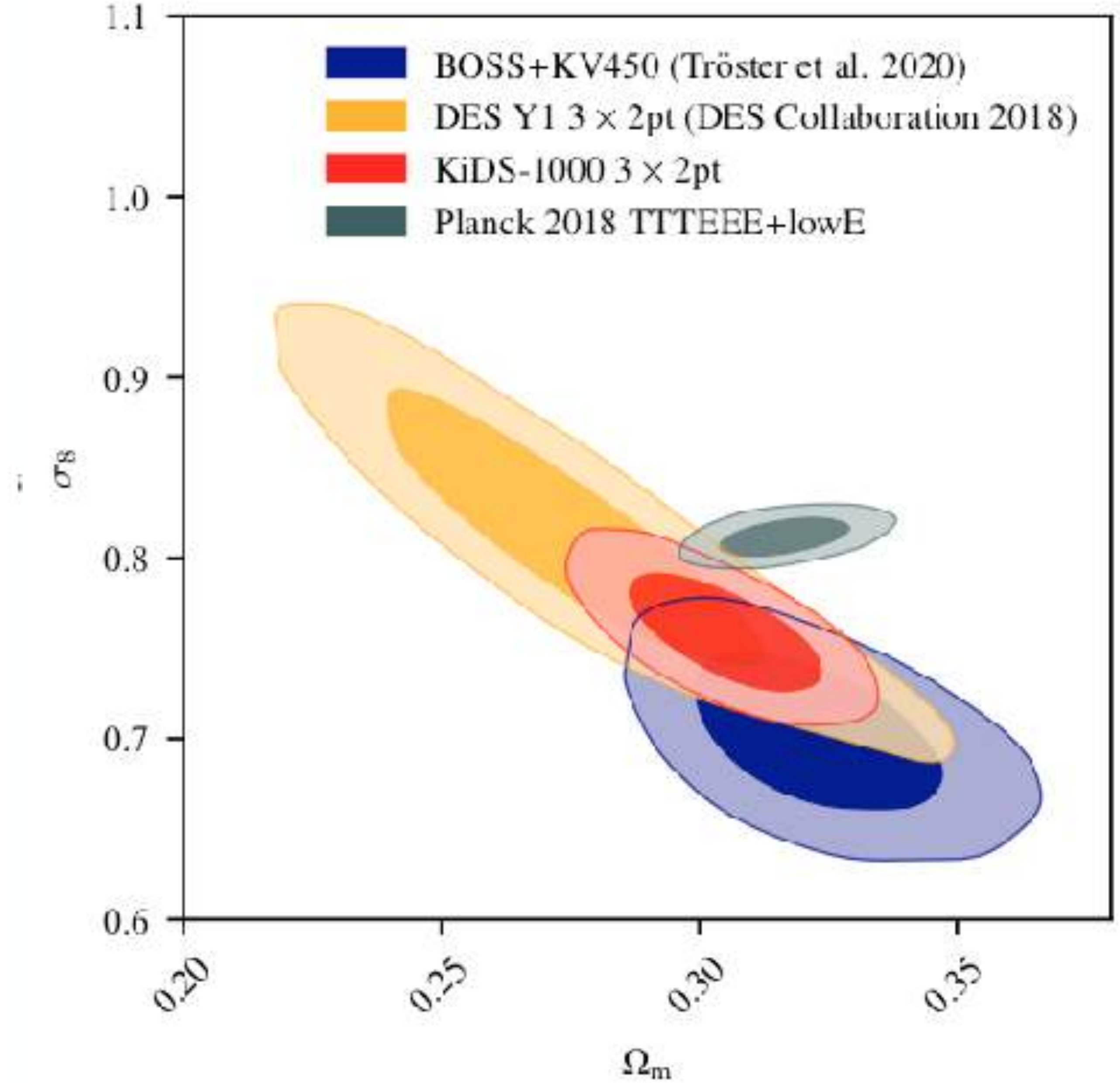

Cosmic shear cosmological constraints

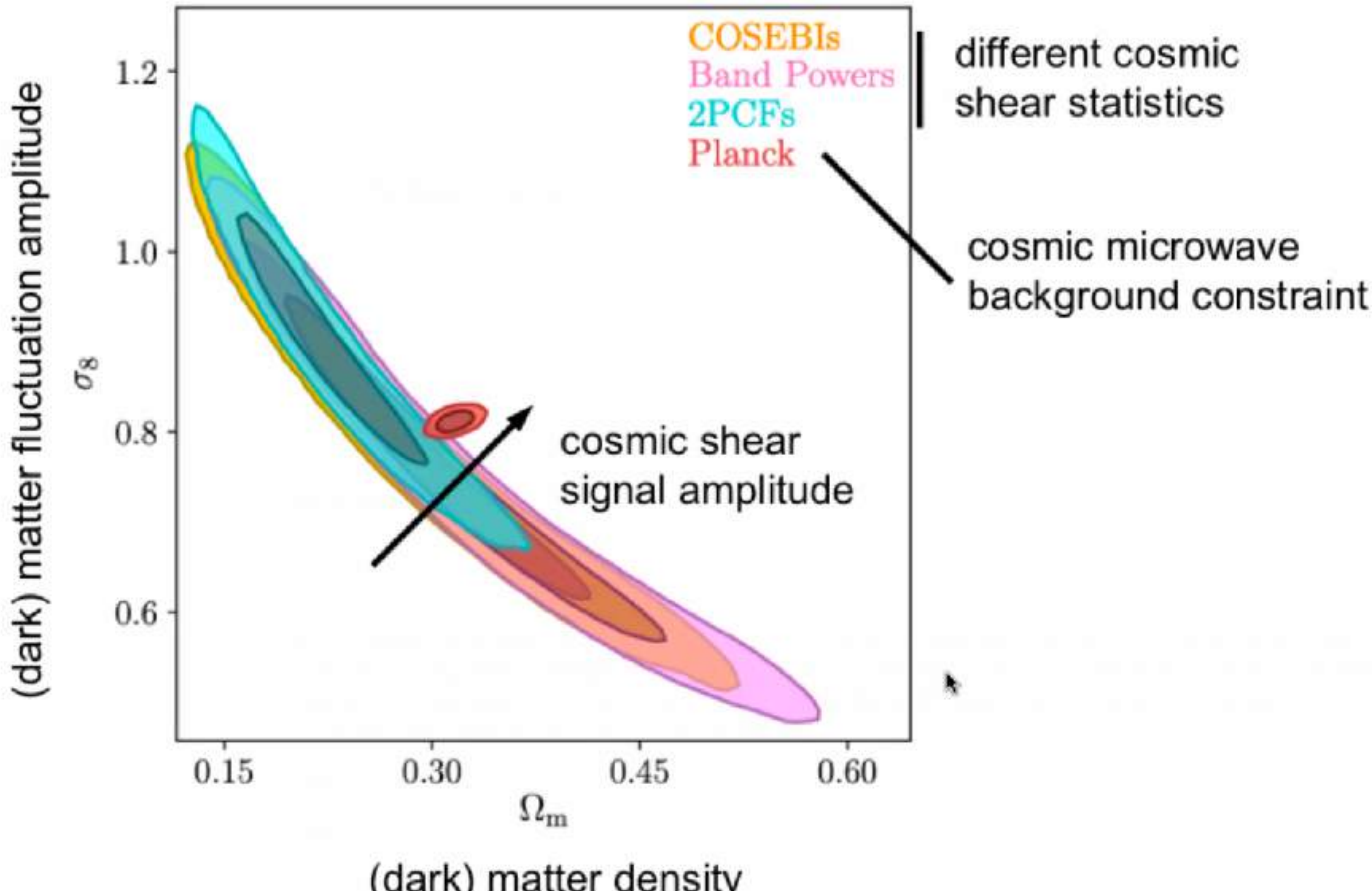

Asgari, Lin, Joachimi+ (2021)

Consistency with DES

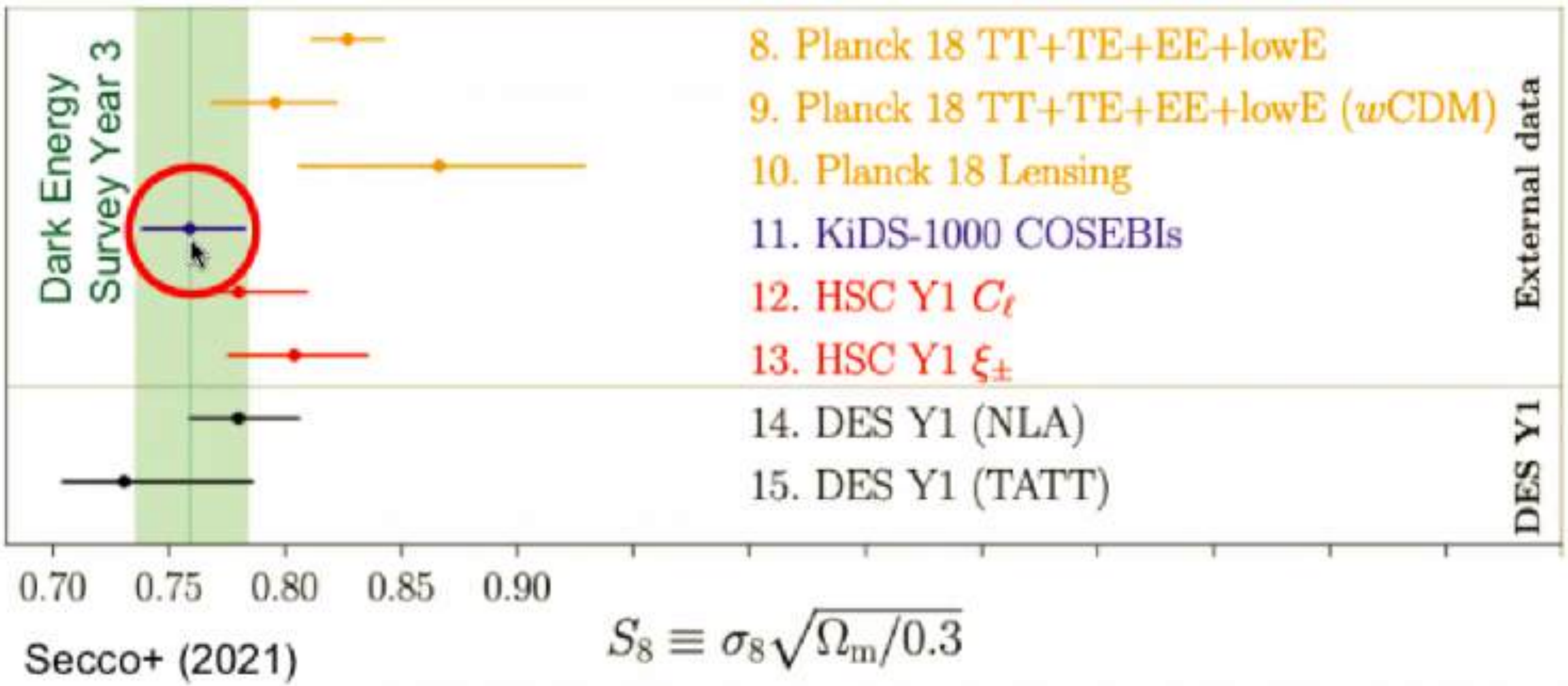

Cosmic shear agreement with nearly independent DES Year 3 results is excellent.

Problema con S_8 que se fue intensificando con el tiempo!

Cosmic Microwave Background Power Spectrum

$T_2(\theta_2, \phi_2)$

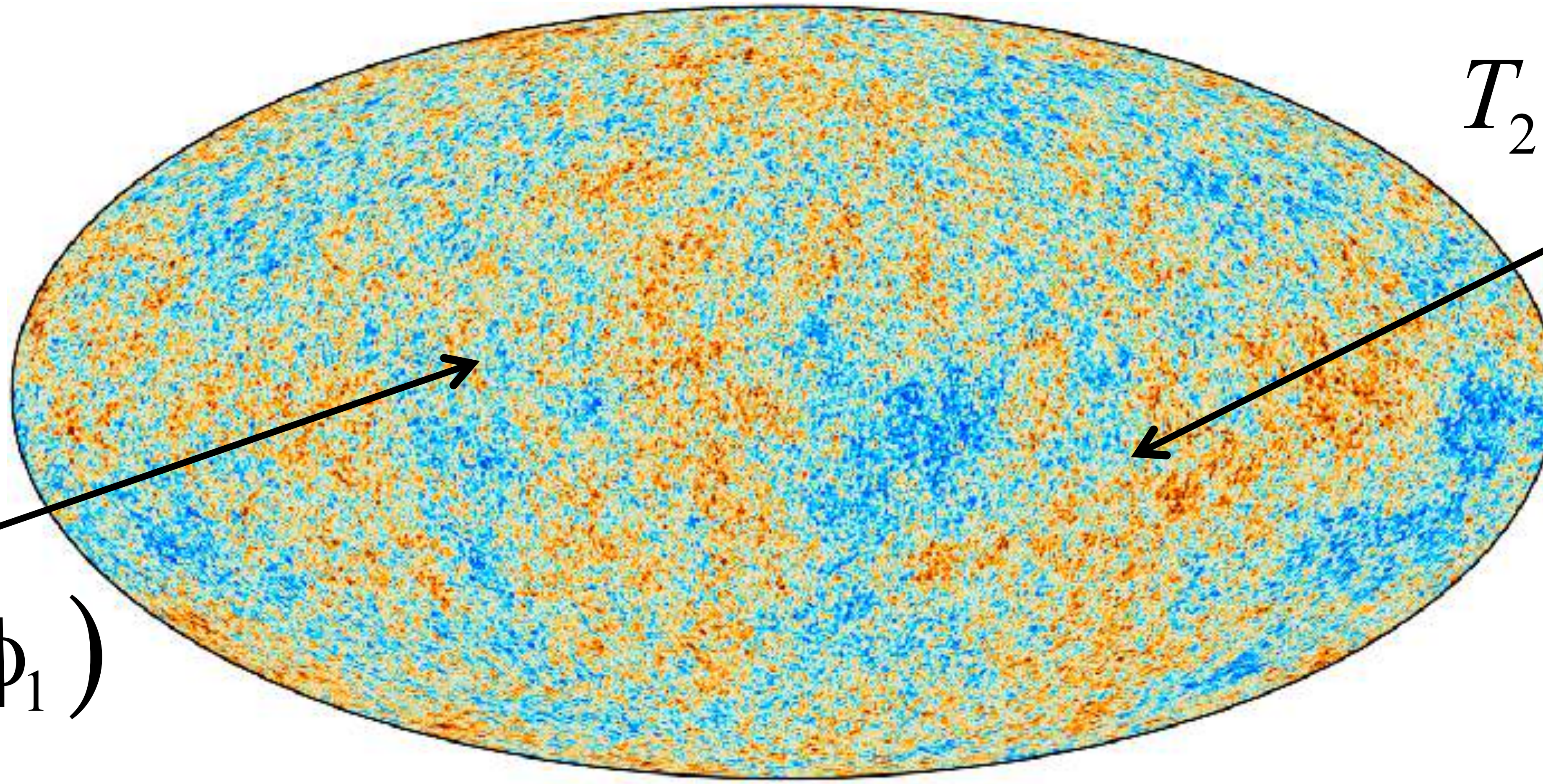

$T_1(\theta_1, \phi_1)$

$$\langle T_1 T_2 \rangle = \sum a_{lm} Y_{lm}(\theta, \phi)$$

$$\left\langle |a_{lm}|^2 \right\rangle^{1/2} \equiv C_l$$

Planck 2015

Relativistic perturbation theory

- The starting point is the perturbed Robertson-Walker metric

$$
\begin{aligned}
ds^2 &= \left[g^{(0)}_{\mu\nu} + g^{(1)}_{\mu\nu}\right] dx^\mu dx^\nu \\
&= a^2(\tau)\left[-d\tau^2 + \gamma_{ij}(\vec{x}\,)dx^i dx^j + h_{\mu\nu}(\vec{x},\tau)dx^\mu dx^\nu\right] \;,
\end{aligned}
$$

- At the linear level modes decouple
- Scalar perturbations:

$$\boxed{ds^2 = a^2(\tau)\left[-(1+2\Psi)d\tau^2 + (1-2\phi)\gamma_{ij}\, dx^i dx^j\right]}$$

(for a perfect fluid $\Phi = \Psi$)

Angular Power Spectrum

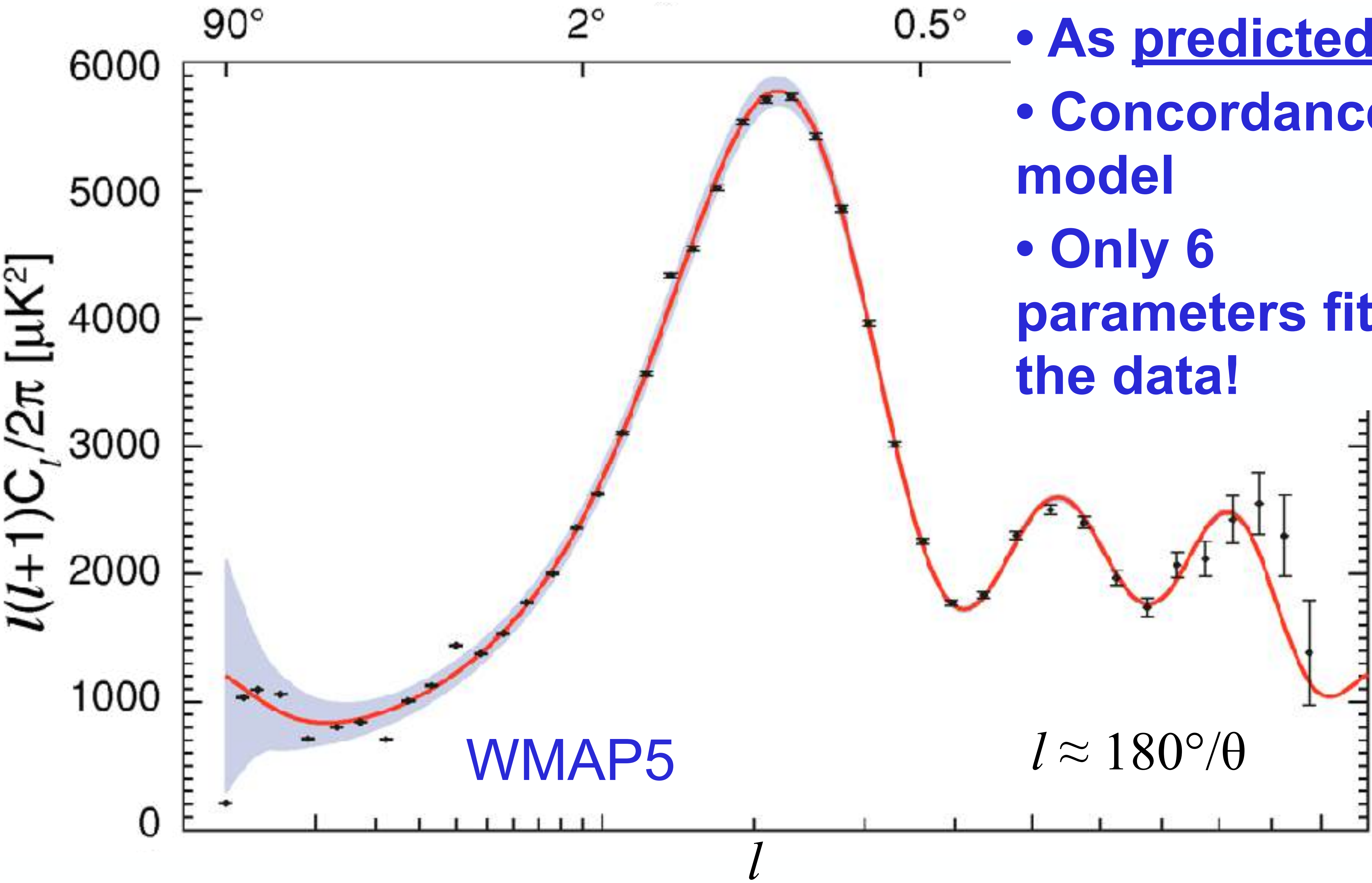

- As predicted
- Concordance model
- Only 6 parameters fit the data!

The holy grail of Cosmology

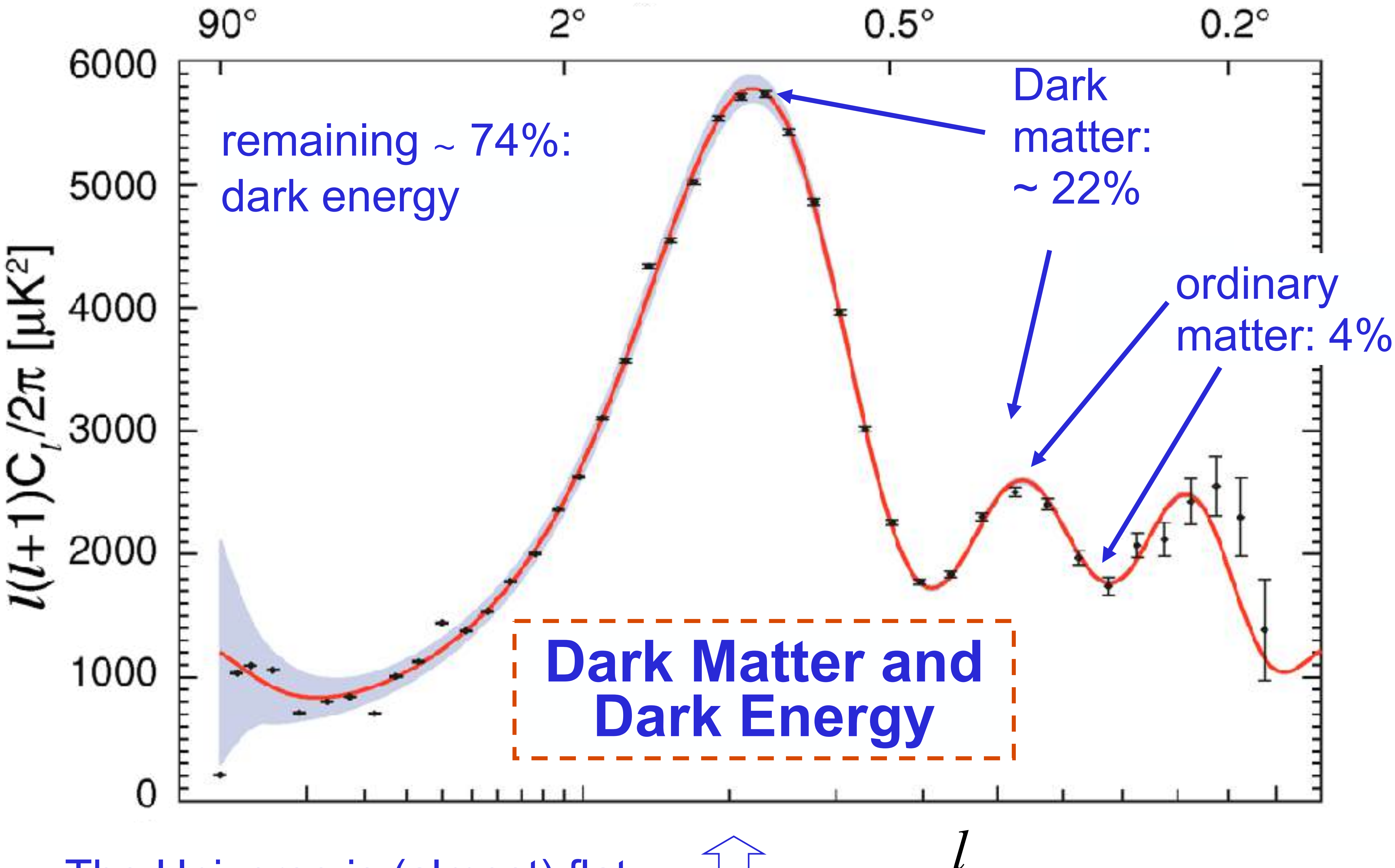

The Universe is (almost) flat

Planck 2015 power spectrum

Planck collaboration, 2016, A&A 594, A11 (2016)

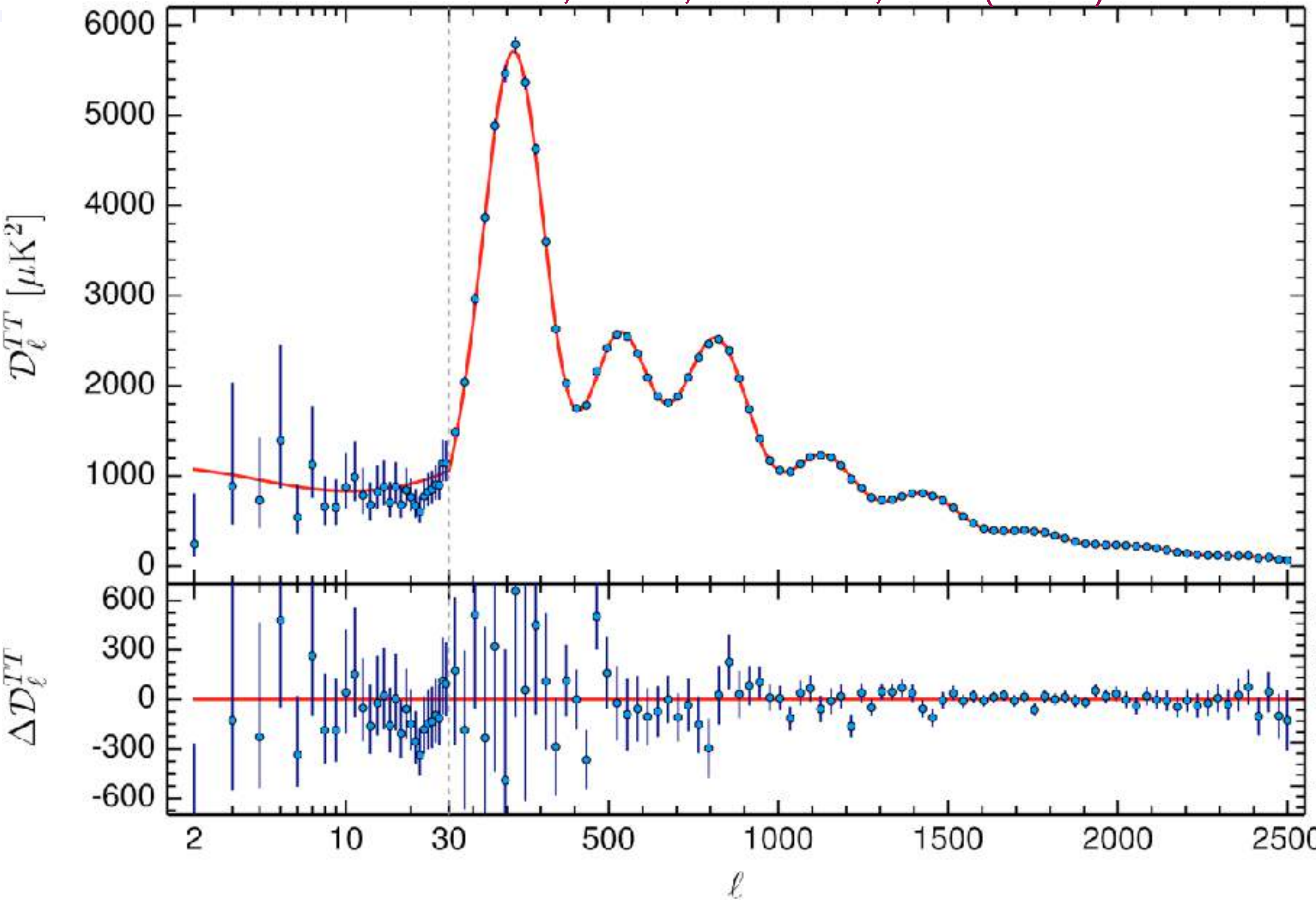

Secondary Anisotropies

- Integrated Sachs-Wolfe effect
- Gravitational Lensing
- Rees-Sciama effect
- Gravitational waves
- Scattering: reionization and Sunyaev Zel'dovich

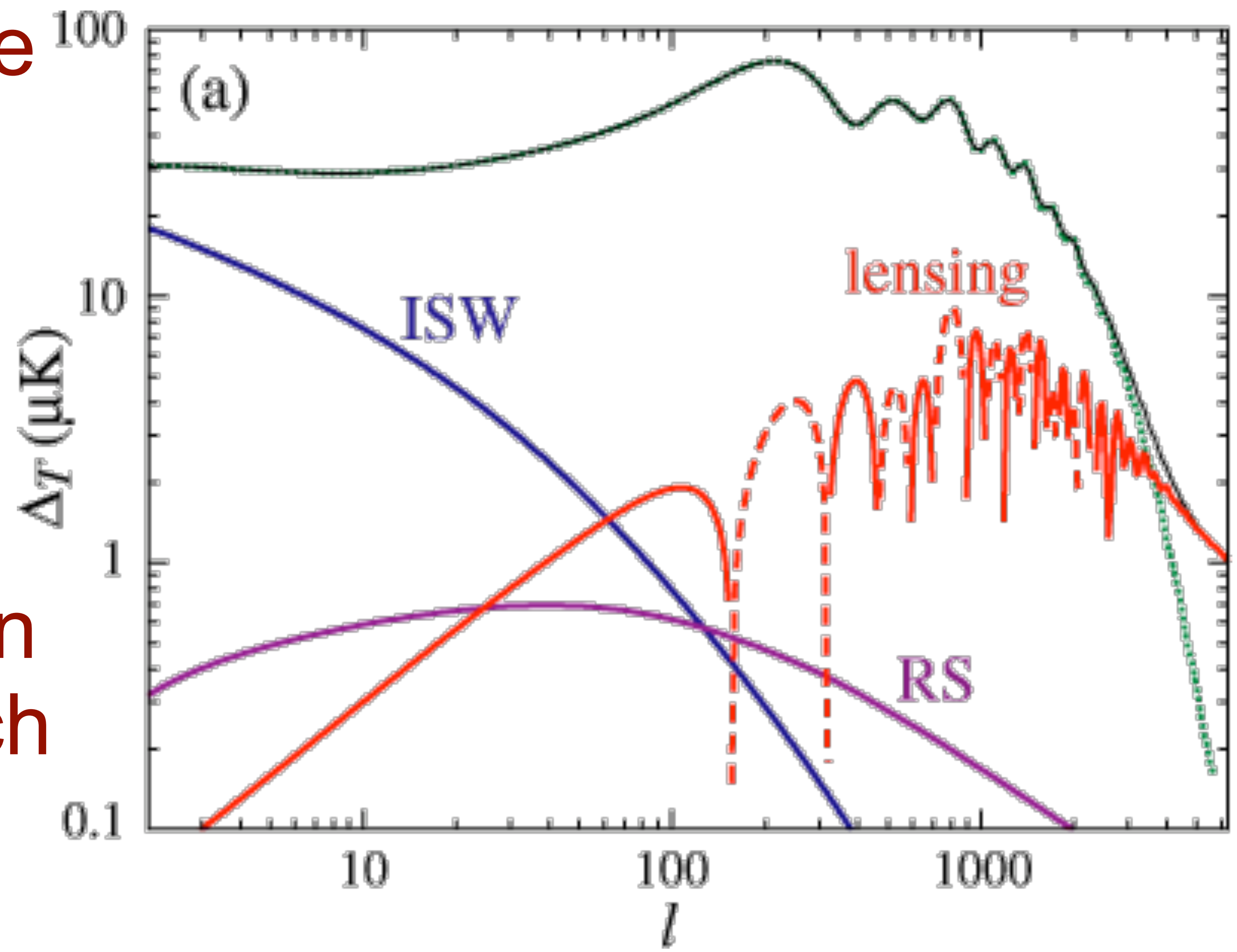

CMB Polarization

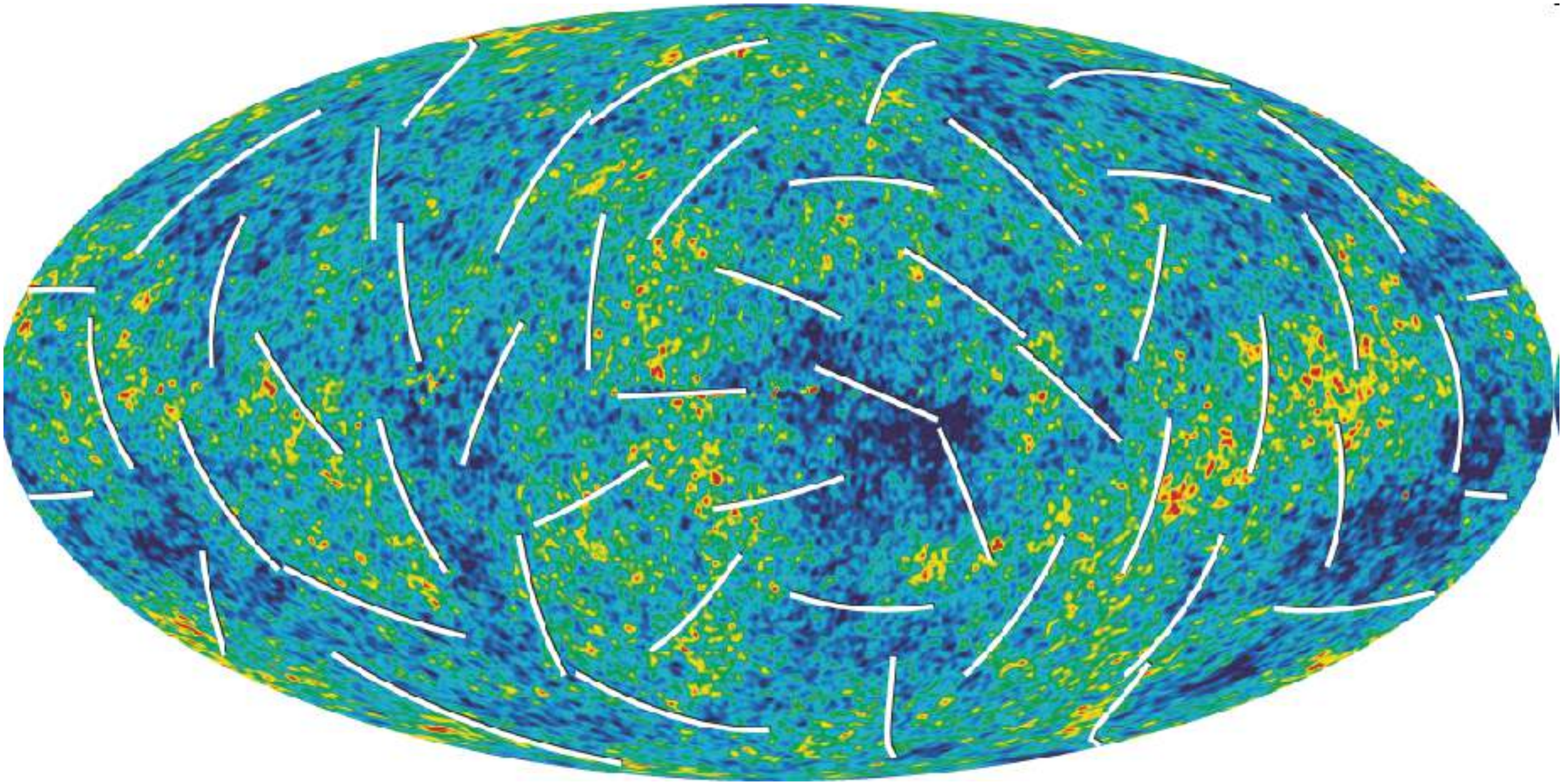

Planck Polarization Map

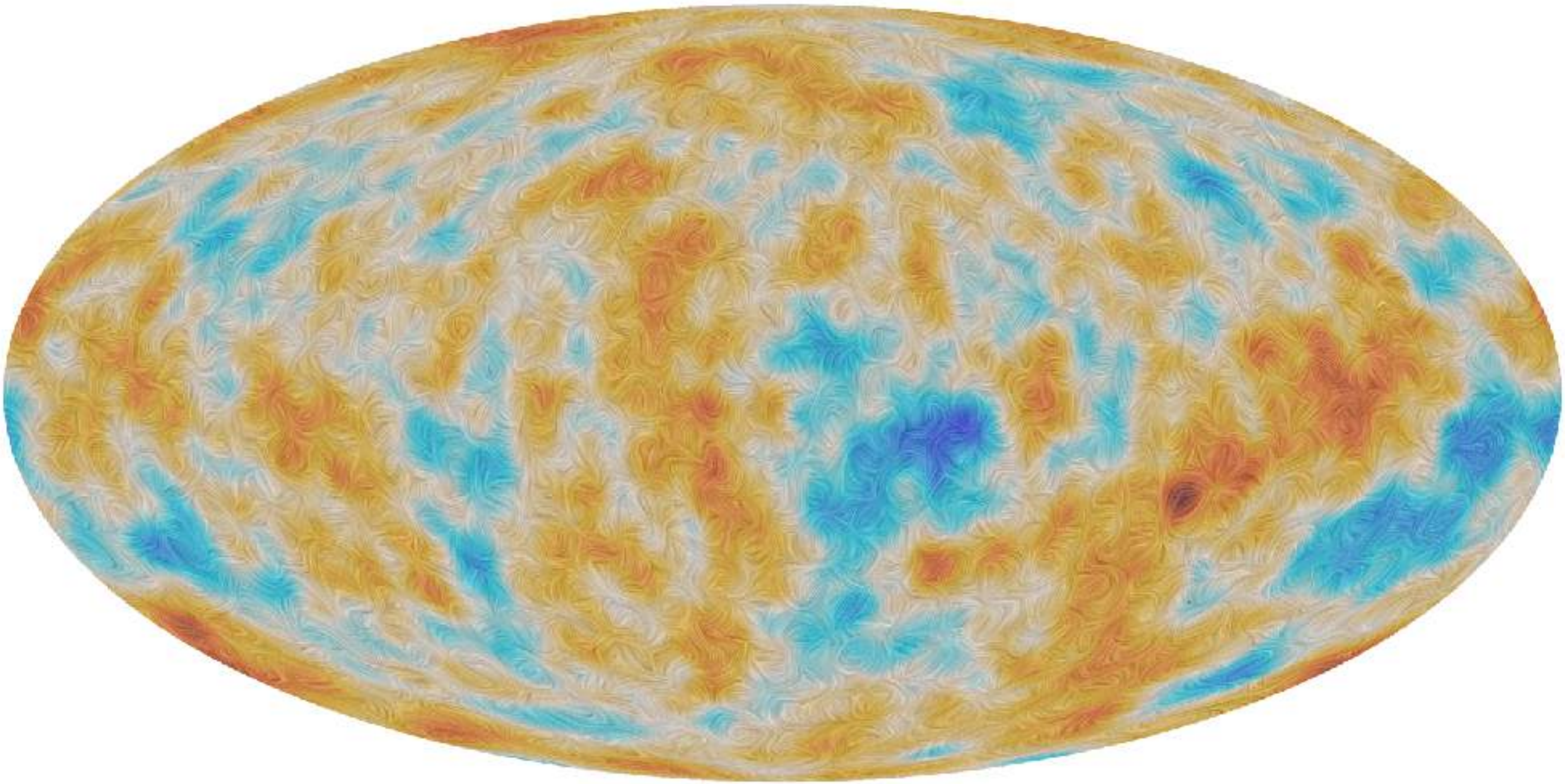

Espectro da Polarização

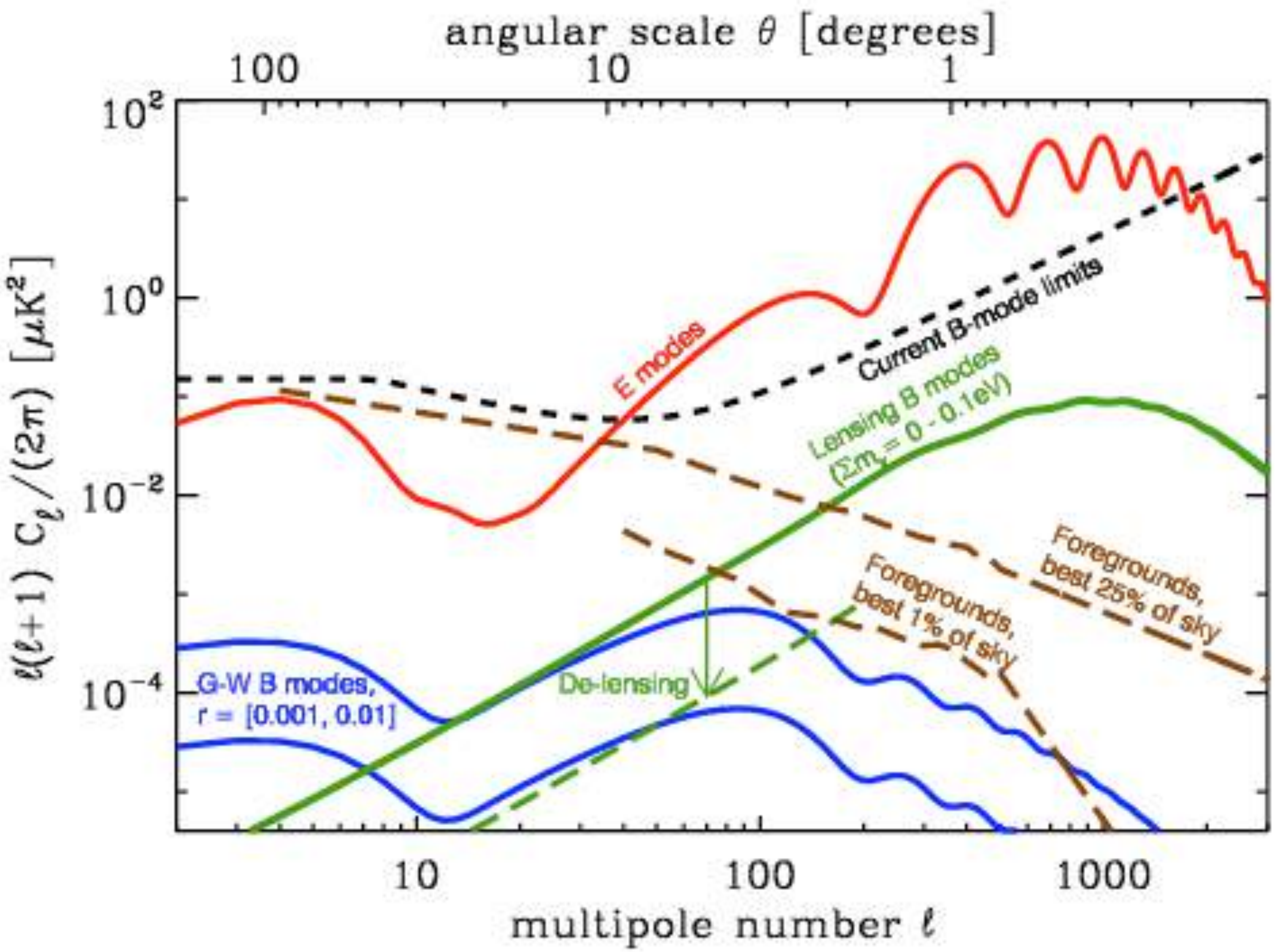

- Componentes TE e EE
- Componente BB:
- Efeito de lente + Ondas gravitacionais
- Futuro?

Polarization Spectrum

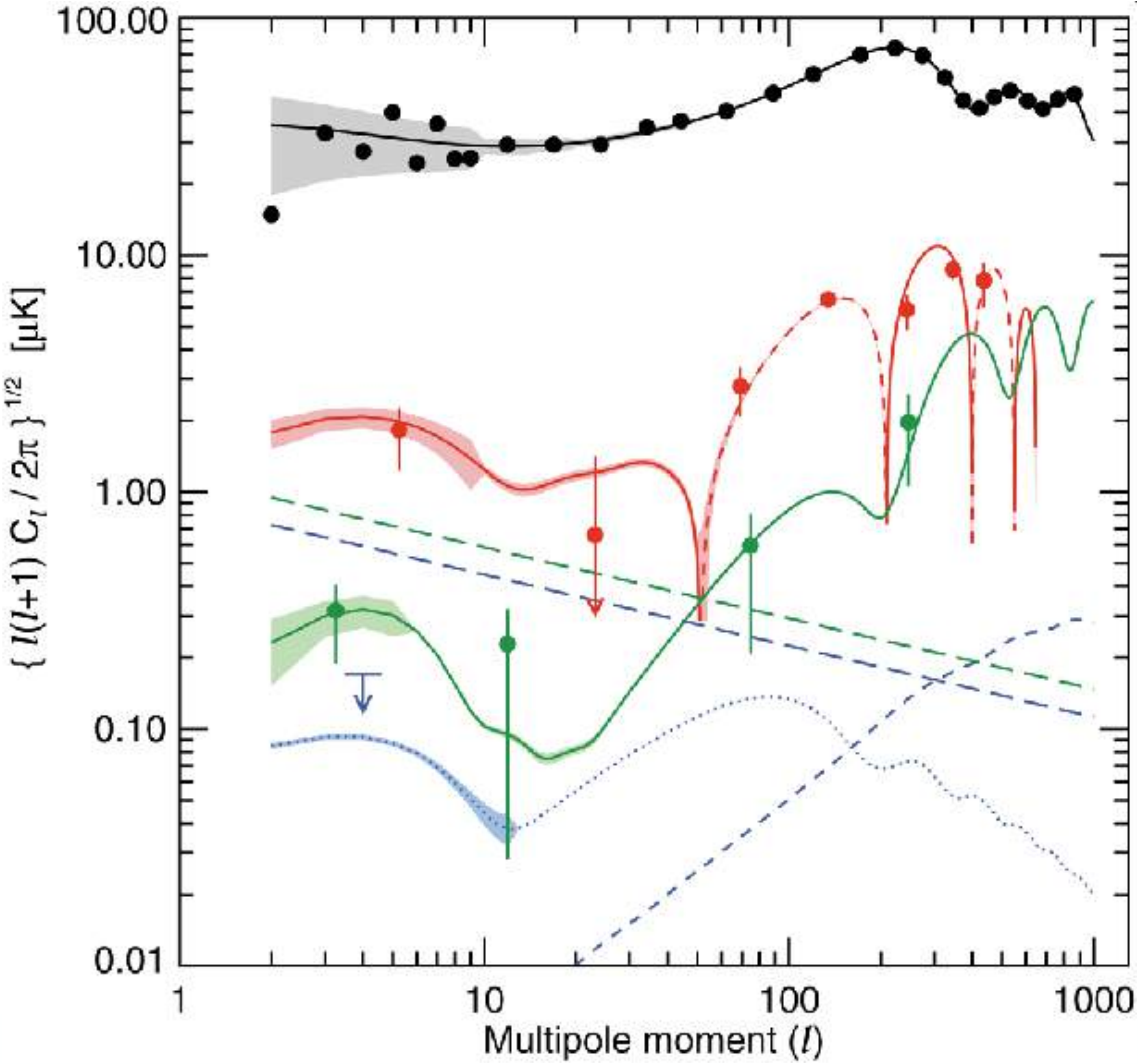

- TE and EE components
- BB component
- Gravitational waves

Polarization Power Spectra

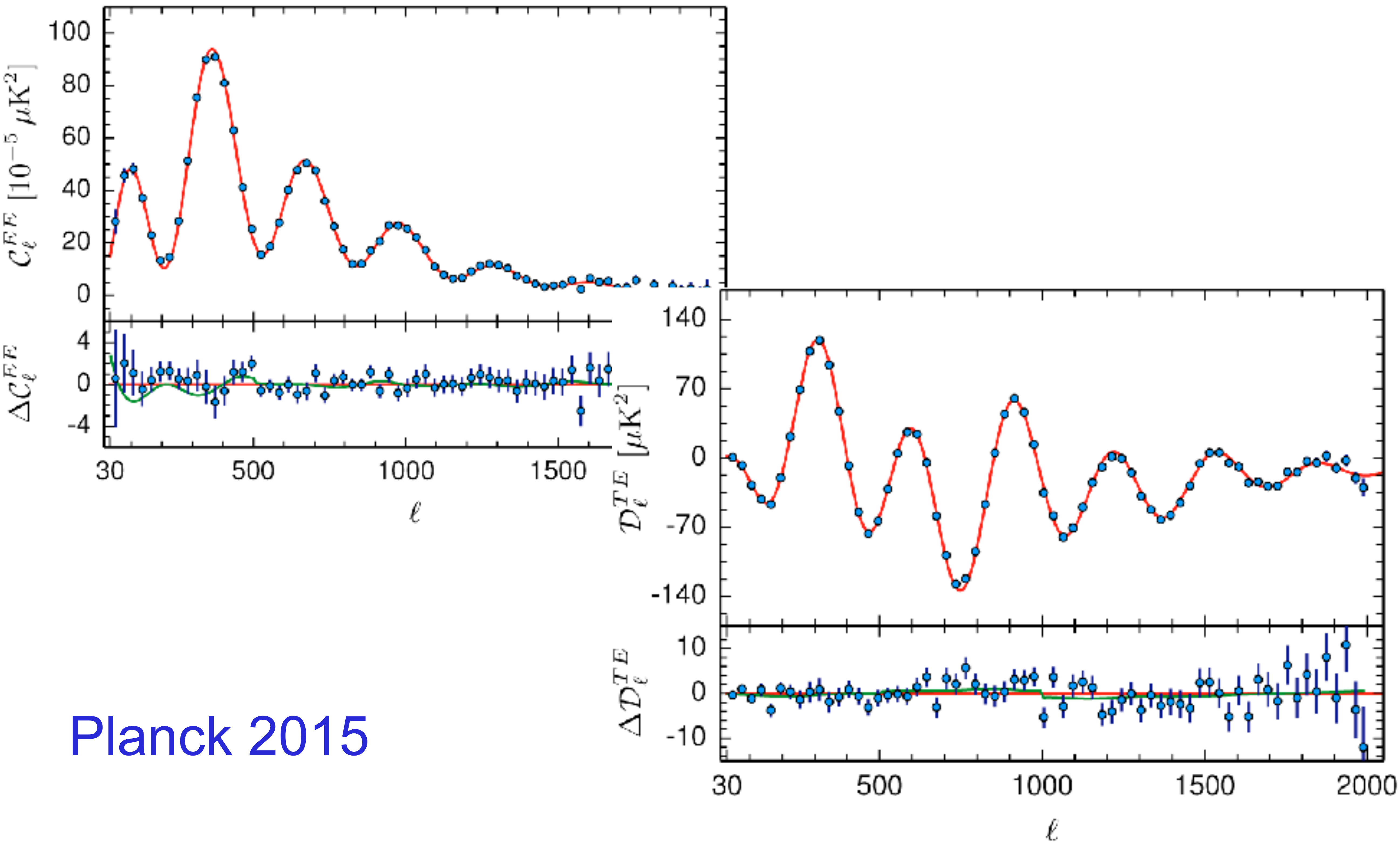

Planck 2015

CMB as a Backlight

- Photons from the CMB are gravitationally deflected by structure

- Can reconstruct maps of the dark matter distribution

- Lensing probes the growth of structure → dark energy, $\sum m_{\nu}$

- Need improved temperature + polarization measurements on small angular scales across large areas of the sky

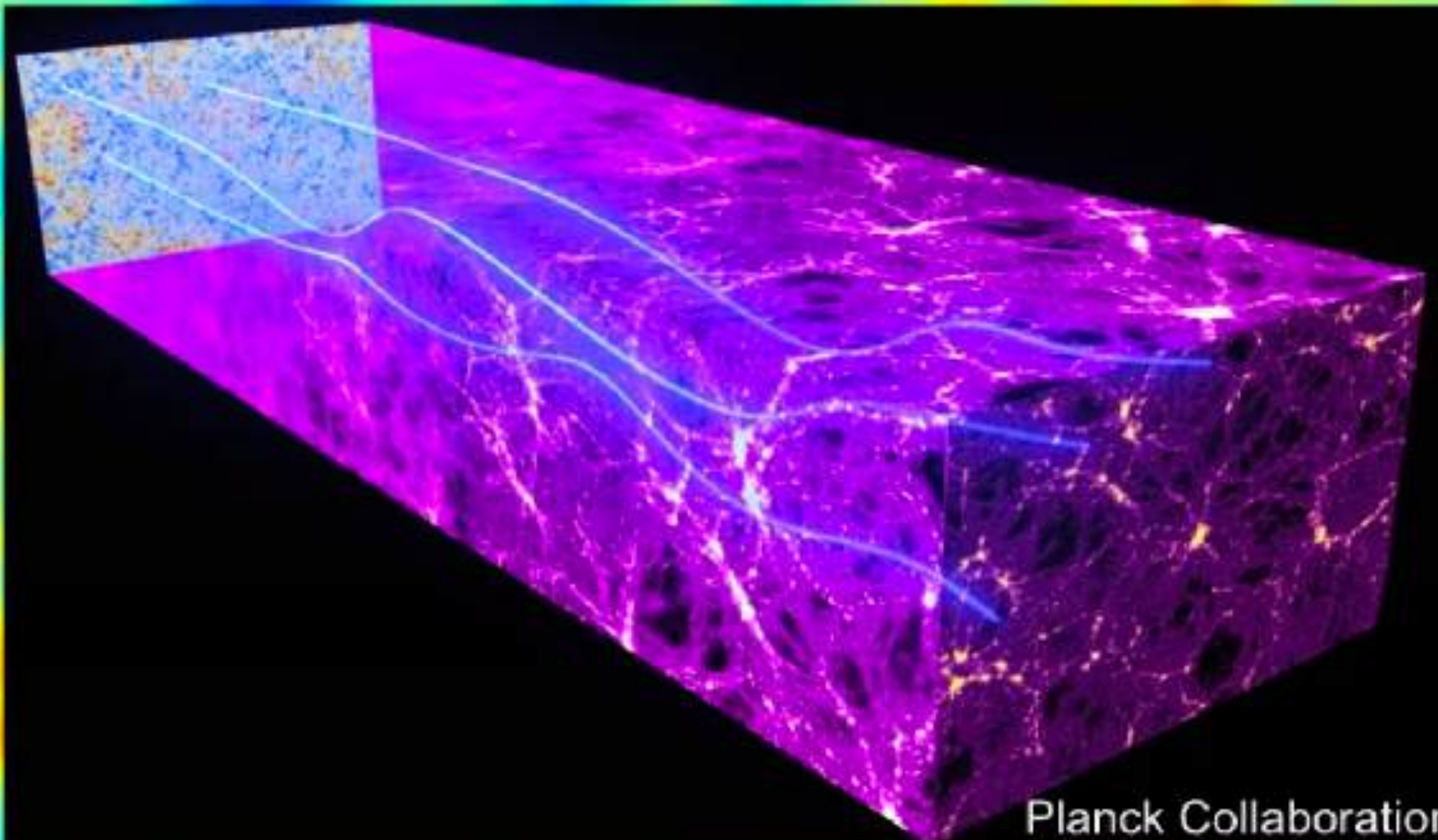

Planck Collaboration

Small scale spectrum

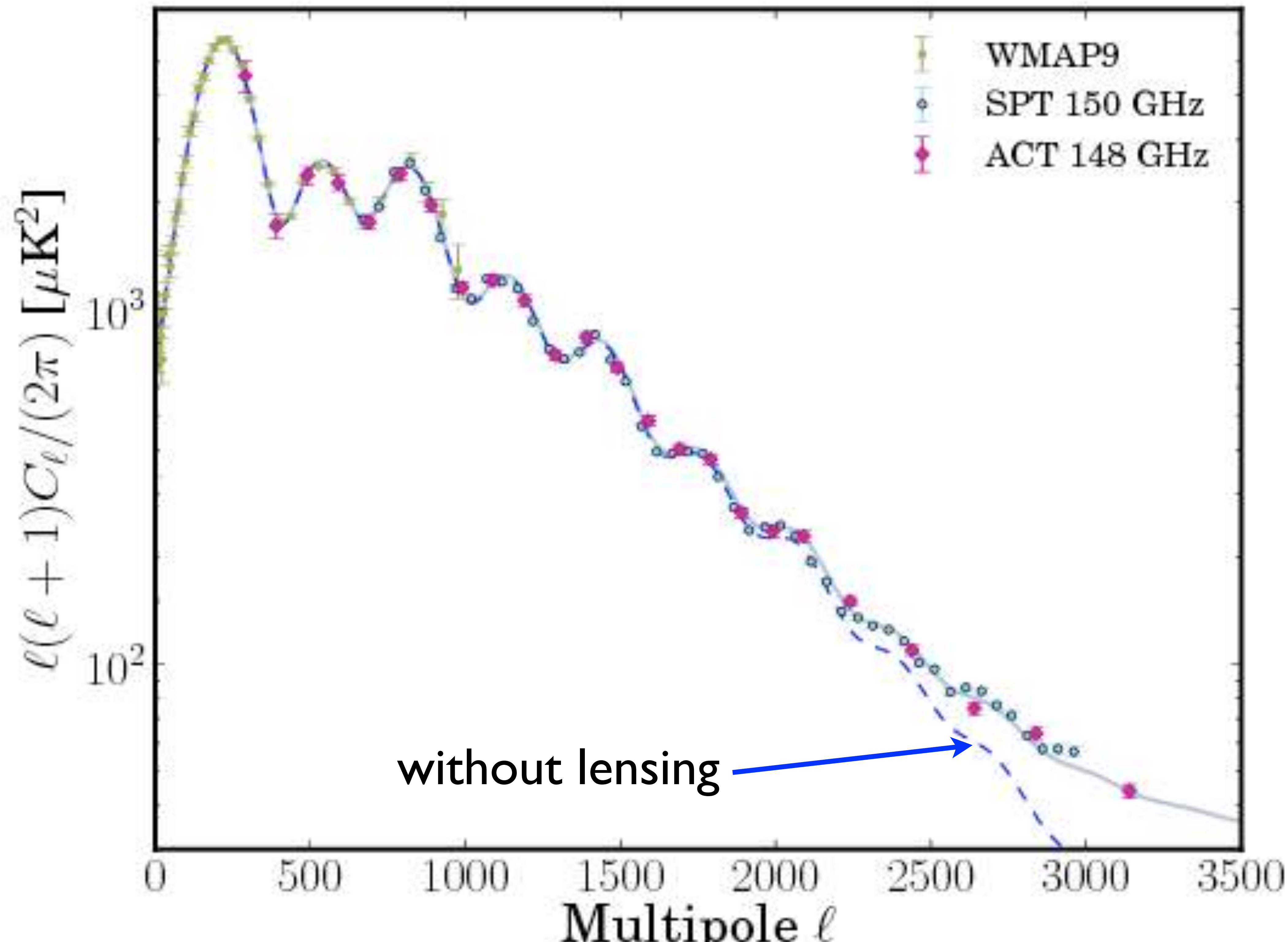

Power spectrum @ 2013

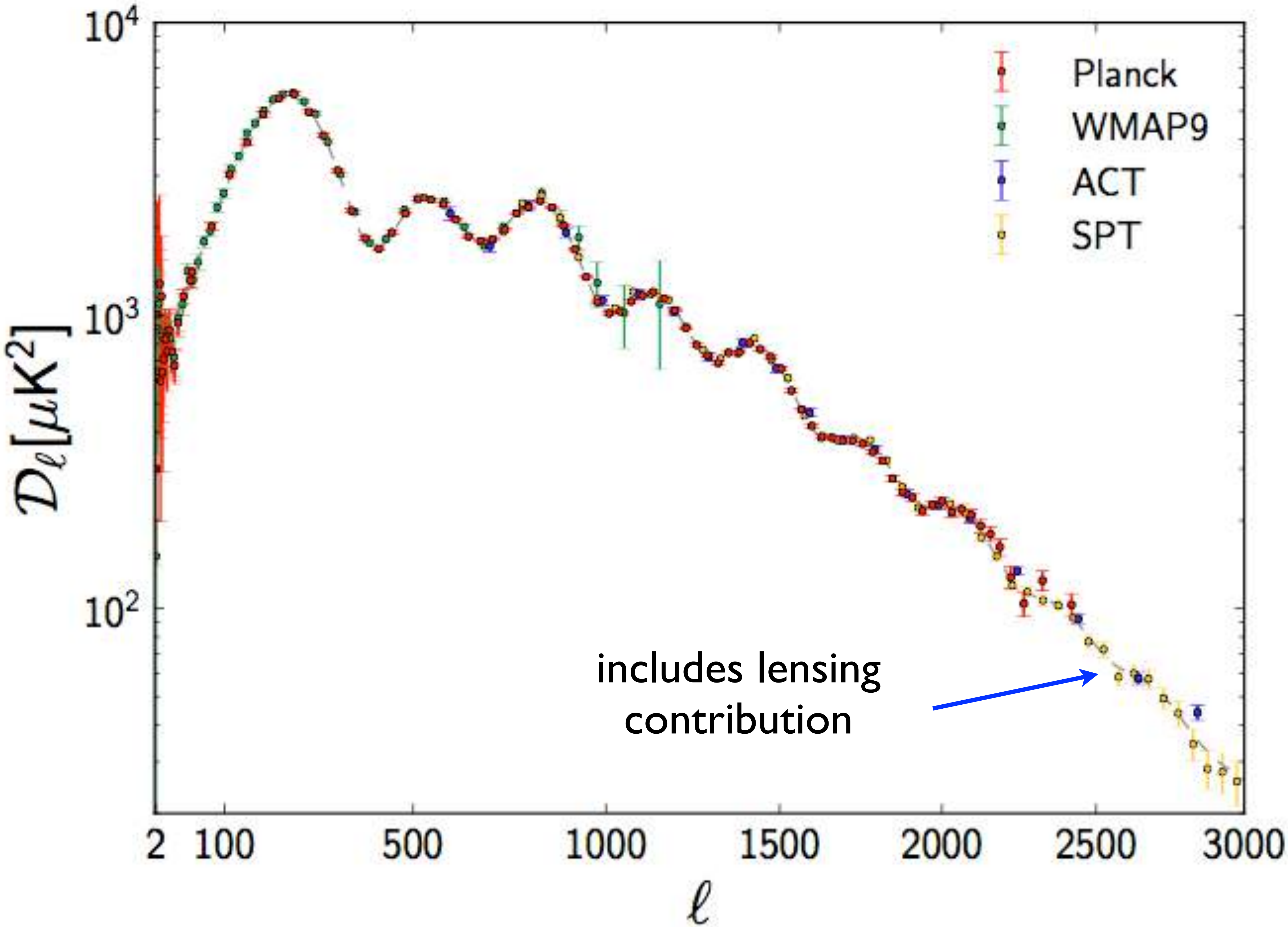

Small scale spectrum

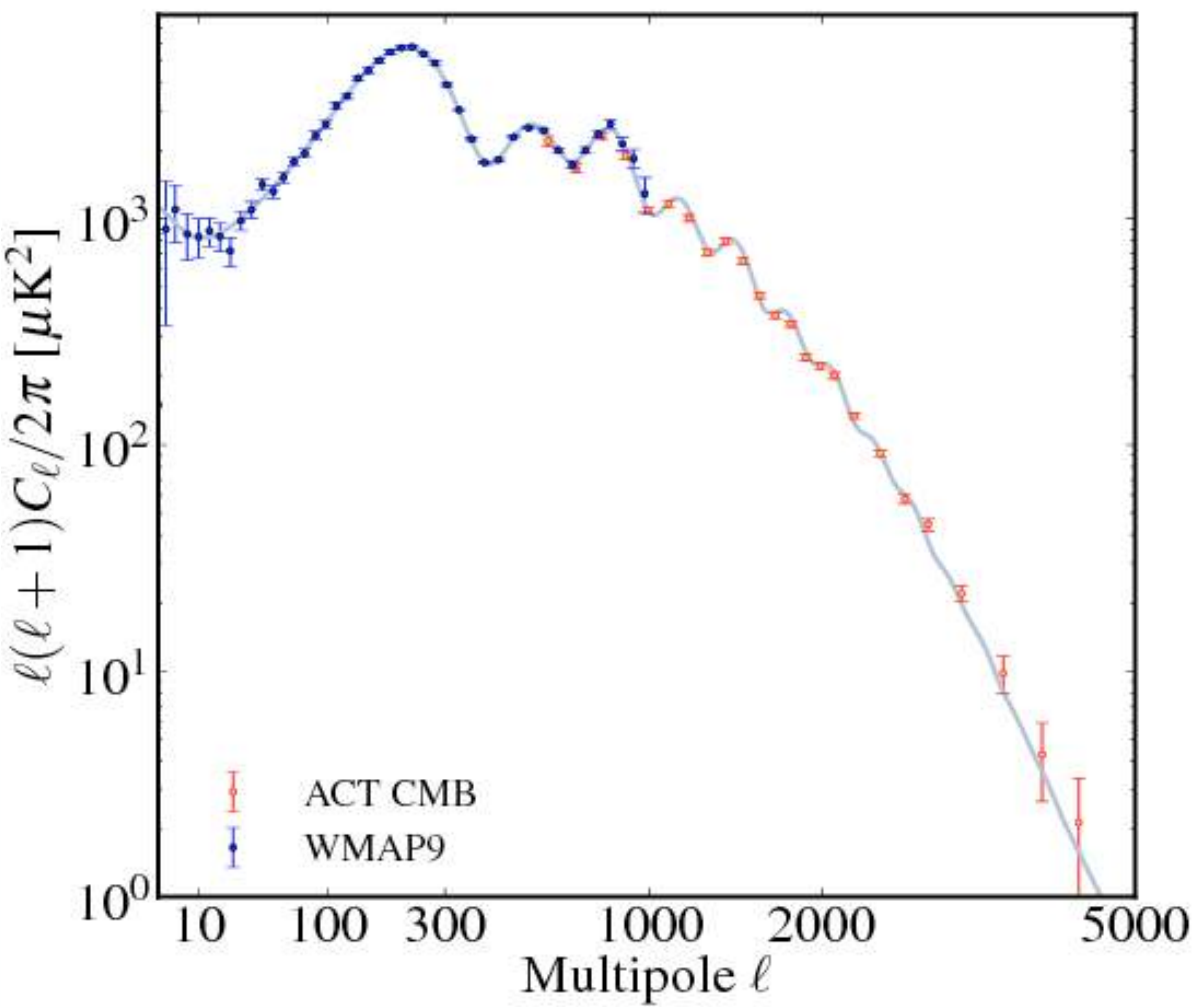

A&A 641, A8 (2020)
https://doi.org/10.1051/0004-6361/201833886

Planck 2018 results

Planck 2018 results

VIII. Gravitational lensing

Astronomy & Astrophysics
Special issue

Lensing power spectrum

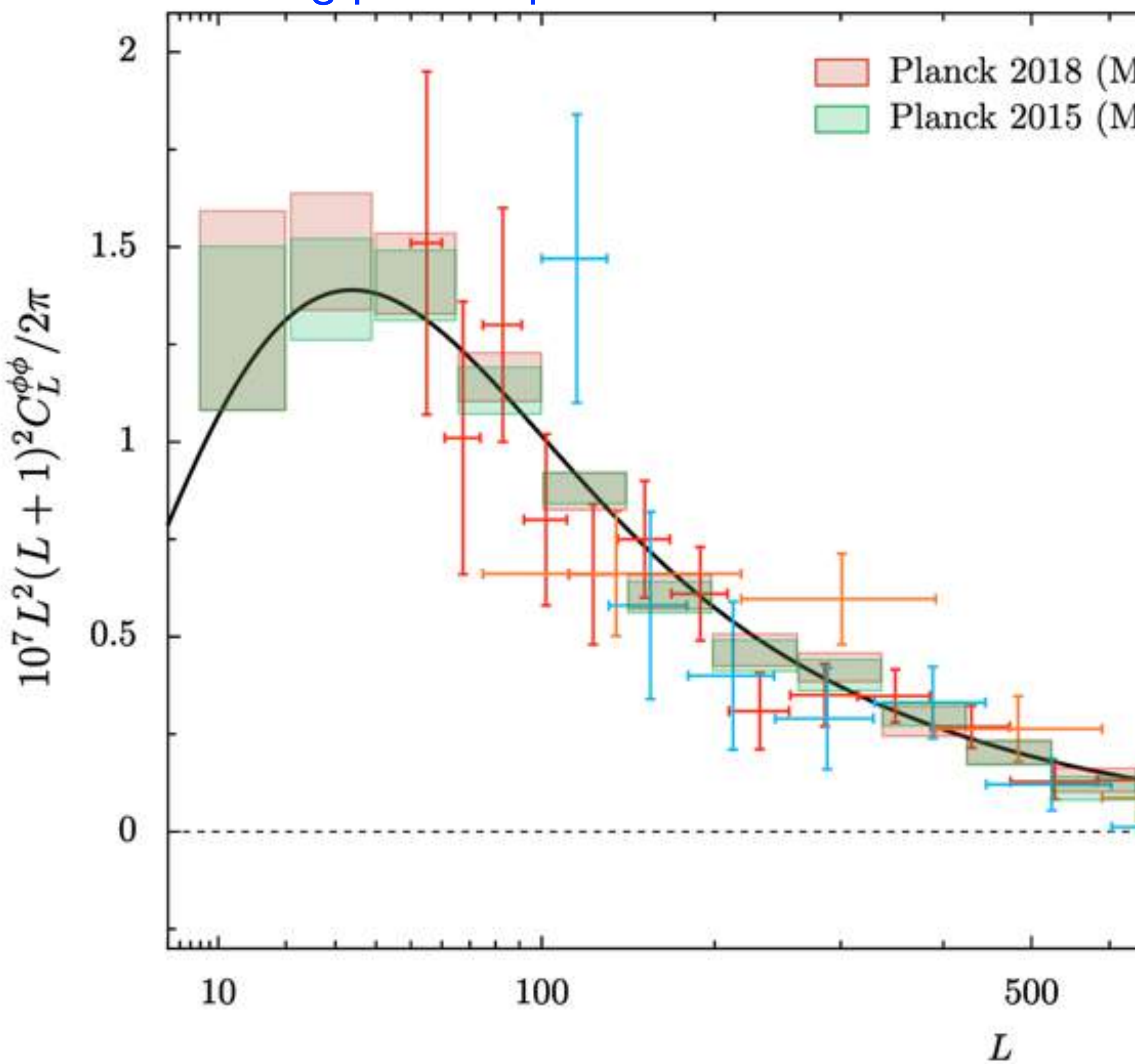

Cosmological parameters

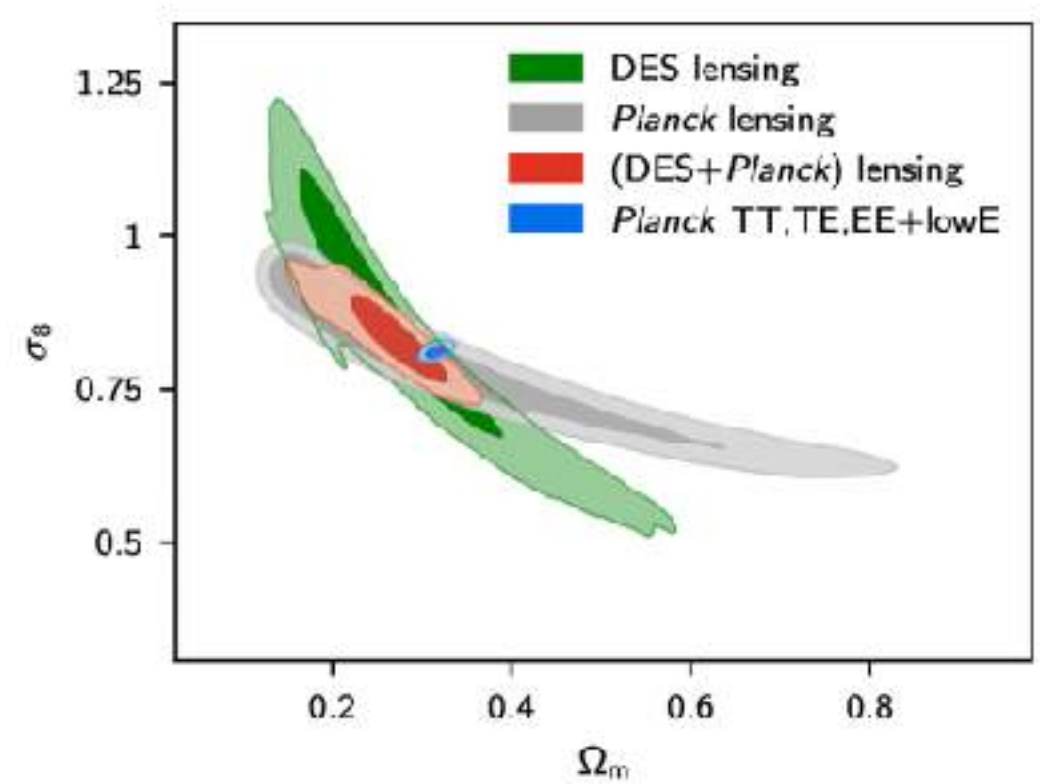

Removiendo la señal de lentes de los espectros de potencias

The Atacama Cosmology Telescope: delensed power spectra and parameters

arXiv:2007.14405

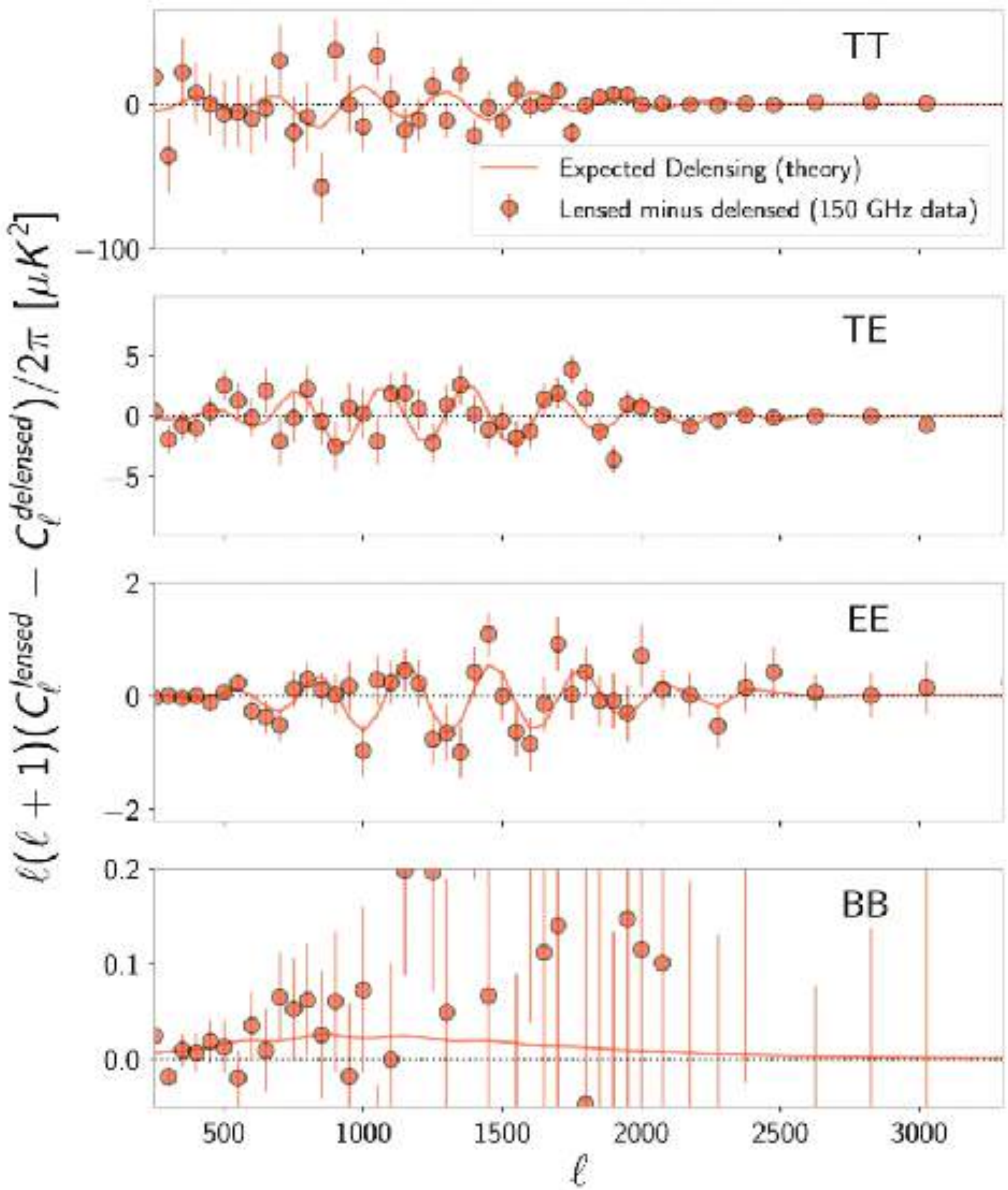

Correlación entre grupos de galaxias y la convergencia medida en la CMB

Monthly Notices of the Royal Astronomical Society

MNRAS 511, 3548–3560 (2022) https://doi.org/10.1093/mnras/stac138
Advance Access publication 2022 February 2

Cross-correlation of Planck cosmic microwave background lensing with DESI galaxy groups

Galaxy/galaxy group overdensity δ_g and CMB lensing convergence κ are both projections of 3D density fields, expressed as line-of-sight integrals over their respective projection kernels. The angular cross-correlation power spectrum, adopting the Limber approximation (Limber 1953), is

$$C_\ell^{\kappa g} = \int \mathrm{d}\chi\, W^\kappa(\chi) W^g(\chi) \frac{1}{\chi^2} P_{\mathrm{mg}} \left(k = \frac{\ell + 1/2}{\chi}; z \right). \quad (1)$$

The Limber approximation is inaccurate for $\ell < 10$, but such very large-scale modes are excluded from our fitting anyway, due to poor S/N. The above expression assumes spatial flatness. Here, W^κ and W^g are the projection kernels for κ and the group number density fields, respectively.

$$W^g(z) = n(z) = \frac{c}{H(z)} W^g(\chi). \quad (2)$$

$$W^\kappa(z) = \frac{3}{2c} \Omega_{\mathrm{m}0} \frac{H_0^2}{H(z)} (1+z) \frac{\chi(\chi_* - \chi)}{\chi_*} = \frac{c}{H(z)} W^\kappa(\chi). \quad (3)$$

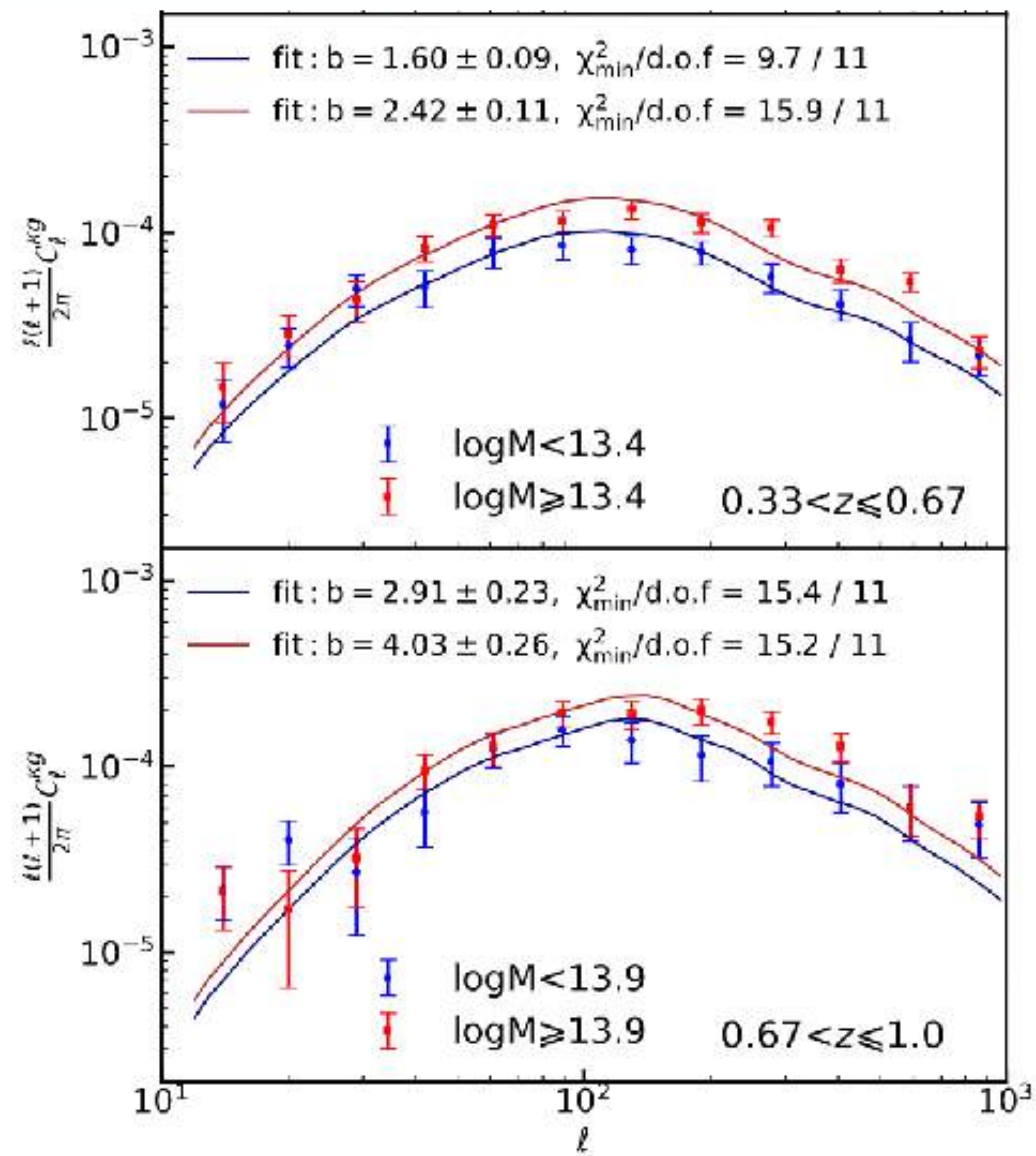

PHYSICAL REVIEW D
particles, fields, gravitation, and cosmology

Correlation of CMB lensing with LSS lensing in CS82

Hand et al. 2015, Phys. Rev. D, 91, 062001

EDITORS' SUGGESTION

First measurement of the cross-correlation of CMB lensing and galaxy lensing

CS82 x ACT

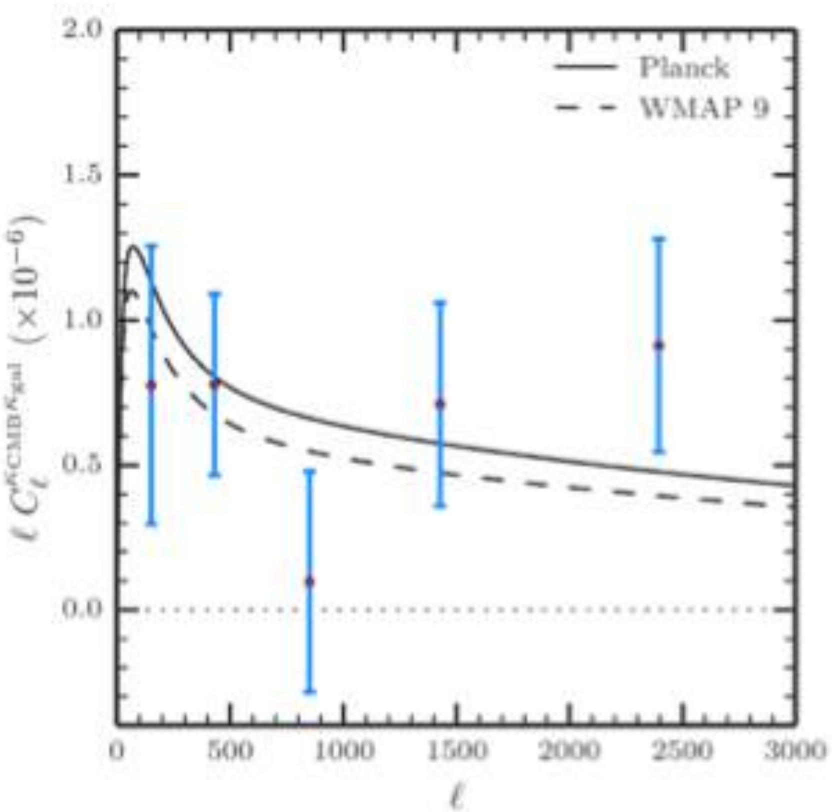

The authors measure for the first time the cross-correlation between CMB lensing and galaxy lensing. This provides a robust test of the ΛCDM model on the largest cosmic scales, and offers powerful constraints on the evolution and nature

$$\kappa(\hat{\mathbf{n}}) = \int_0^\infty dz W^\kappa(z)\delta(\chi(z)\hat{\mathbf{n}}, z)$$

$$W^\kappa(z) = \frac{3}{2}\Omega_m H_\circ^2 \frac{(1+z)}{H(z)}\frac{\chi(z)}{c}\int_z^\infty dz_s p_s(z_s)\frac{\chi(z_s)-\chi(z)}{\chi(z_s)}$$

$$W^{\kappa_{\rm CMB}}(z) = \frac{3}{2}\Omega_m H_\circ^2 \frac{(1+z)}{H(z)}\frac{\chi(z)}{c}\left[\frac{\chi(z_\star)-\chi(z)}{\chi(z_\star)}\right]$$

$$C_\ell^{\kappa_{\rm CMB}\kappa_{\rm gal}} = \int_0^\infty \frac{dz}{c}\frac{H(z)}{\chi(z)^2} W^{\kappa_{\rm CMB}} W^{\kappa_{\rm gal}} P\left(k=\frac{\ell}{\chi}; z\right)$$

A&A 649, A146 (2021)
https://doi.org/10.1051/0004-6361/202039975

Astronomy & Astrophysics

Strong detection of the CMB lensing and galaxy weak lensing cross-correlation from ACT-DR4, *Planck* Legacy, and KiDS-1000

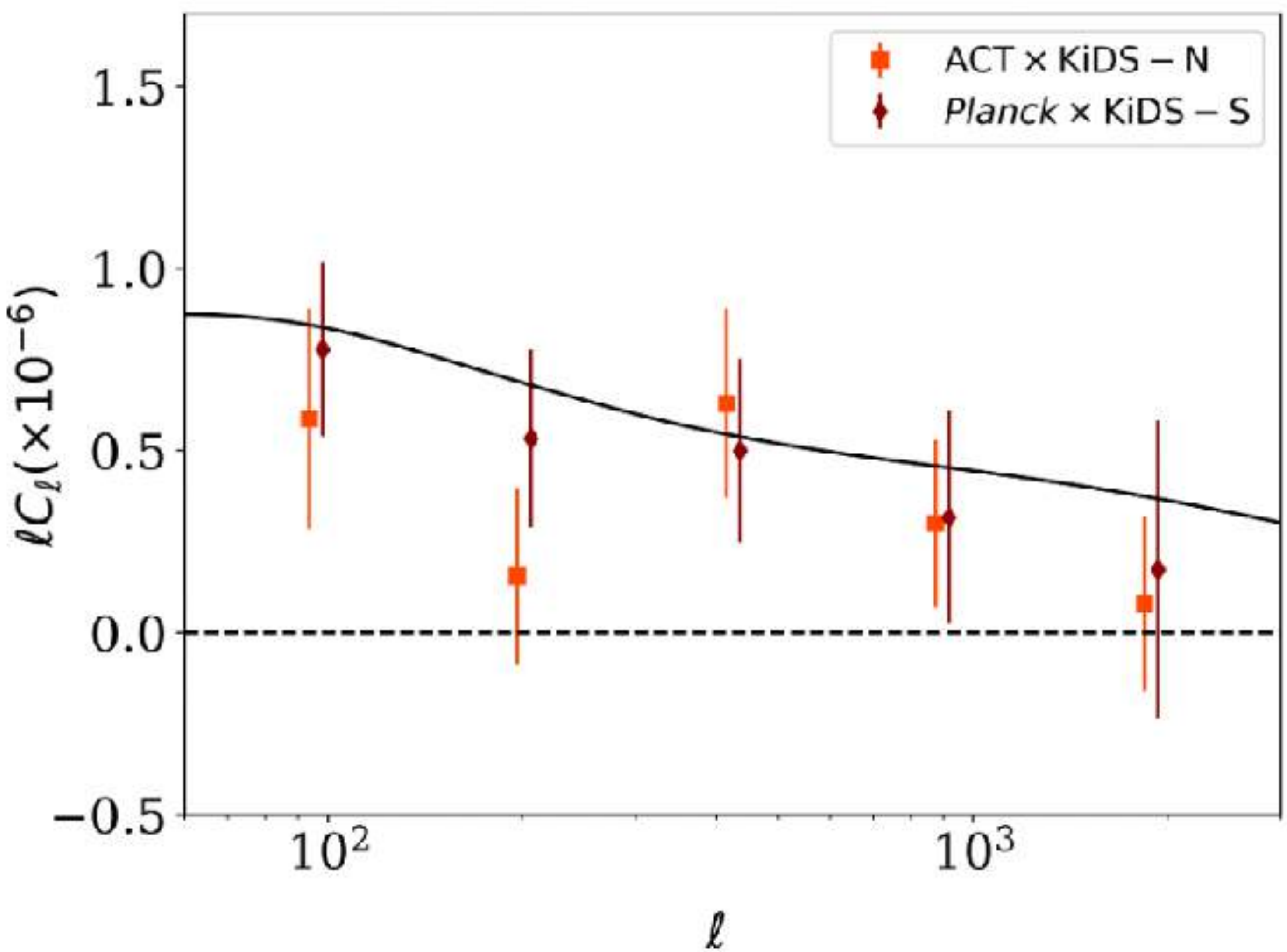

arXiv:2011.11613

Monthly Notices of the ROYAL ASTRONOMICAL SOCIETY

MNRAS **528,** 2112–2135 (2024) https://doi.org/10.1093/mnras/stad3987
Advance Access publication 2024 January 3

Cosmology from cross-correlation of ACT-DR4 CMB lensing and DES-Y3 cosmic shear

$$C_\ell^{\kappa_C\gamma_E} = \int_0^{z_H} dz \frac{H(z)}{\chi^2(z)c} W_\kappa^{\rm CMB}(z) W_\gamma^{\rm g}(z) P_{\delta\delta}\left(k = \frac{\ell+0.5}{\chi(z)}, z\right)$$

$$W_\kappa^{\rm CMB}(z) = \frac{3H_0^2\Omega_{\rm m,0}}{2H(z)c}\frac{\chi(z)}{a(z)}\frac{\chi(z^*)-\chi(z)}{\chi(z^*)}.$$

$$W_\gamma^{\rm g}(z) = \frac{3H_0^2\Omega_{\rm m,0}}{2H(z)c}\frac{\chi(z)}{a(z)}\int_z^{z_H} dz' n(z')\frac{\chi(z')-\chi(z)}{\chi(z')}$$

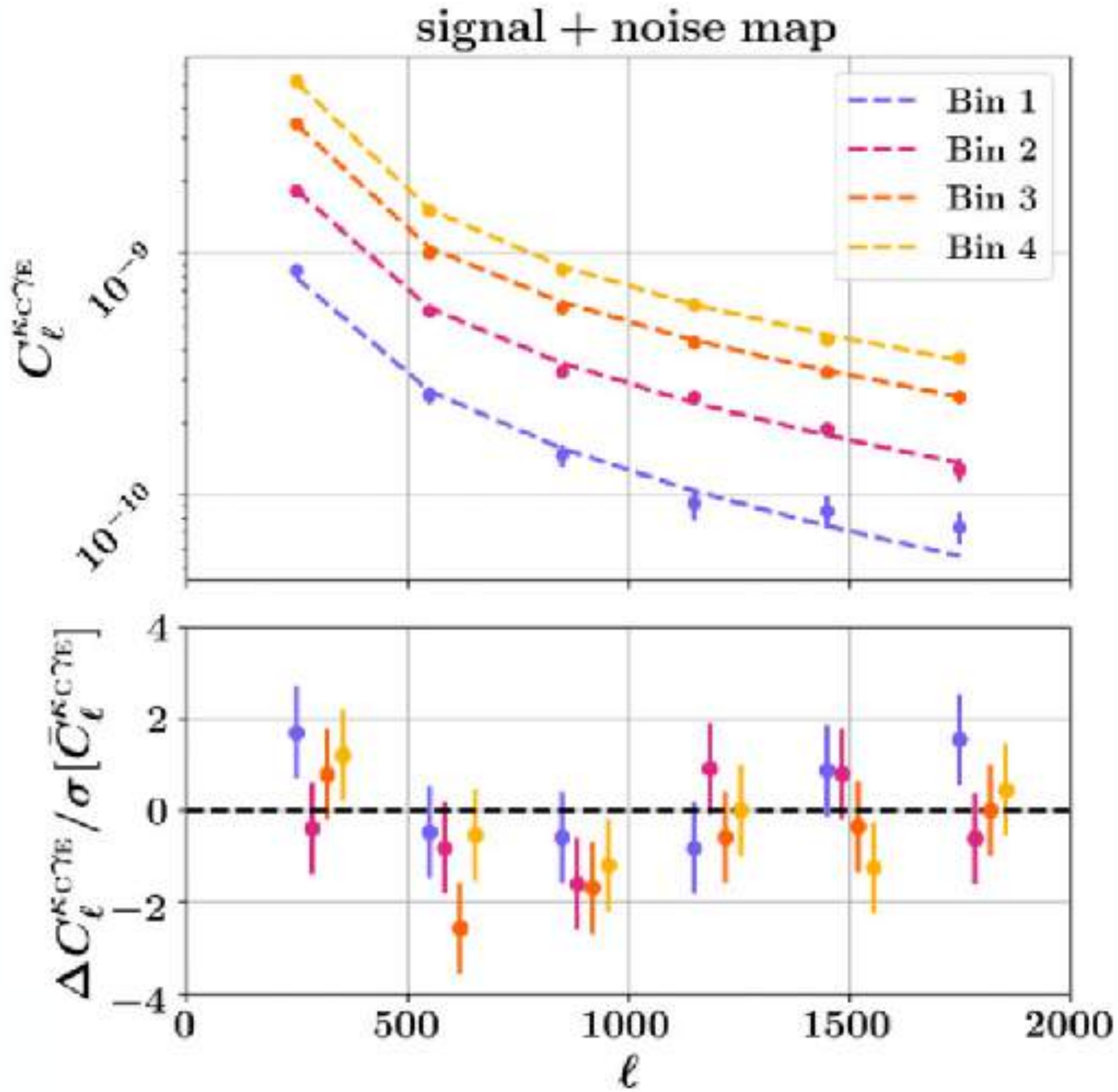

Transformational Lensing Science with Rubin

- ~4 billion galaxies with shape determination and photometric redshifts for weak lensing
- Cross correlation, tomography, ...
- LSST will be the most powerful weak lensing survey ever conducted, thanks to its unique combination of depth, area, cadence, and data quality
- Over ~ 10.000 strong lenses
- Strong Lensing of Transients and variable objects(extragalactic)
  - ~ 400 SGLSNe
  - watchlist for lensed transients (GW, GRB, FRB...)
- Microlensing (stelar)
  - unprecedented combination of sky coverage, depth and cadence (microlensing all over the sky!)
  - overlap with Roman in the bulge

TVSSC SLSC LSST DESC Dark Energy Science Collaboration

VERA C. RUBIN OBSERVATORY

Lentes Gravitacionales y Gravedad Modificada

Modified Gravity

conformal newtonian metric (choices and assumptions):

$$\mathrm{d}s^2 = a^2(\tau)[-(1+2\Phi)\,\mathrm{d}\tau^2 + (1-2\Psi)\gamma_{ij}\,\mathrm{d}x^i\,\mathrm{d}x^j]$$

for General Relativity (for *standard* matter components) in general

$$\Phi = \Psi$$

slip parameter

$$\boxed{\eta = \frac{\Phi}{\Psi}}$$

for $\eta = \mathrm{const.}, \quad \eta = \gamma_{\mathrm{PPN}}$

$\gamma = 1$ compatible with GR

$\gamma \neq 1$ GR ruled out

E.g. DHOST, Beyond Horndeski: F. Araújo, E. Valadão++in prep.

One gravitational potential or two? Forecasts and tests

Phil. Trans. R. Soc. A (2011) **369**, 4947–4961
doi:10.1098/rsta.2011.0369

BY EDMUND BERTSCHINGER*

métrica no calibre newtoniano conforme (premissas):

$$ds^2 = a^2(\tau)[-(1+2\Phi)\,d\tau^2 + (1-2\Psi)\gamma_{ij}\,dx^i\,dx^j]$$

geodésicas

$$\frac{dx^i}{d\tau} = (1+\Phi+\Psi)v^i$$

$$\frac{1}{\gamma a(1-\Psi)}\frac{d}{d\tau}[\gamma a(1-\Psi)v^i] = -\nabla^i(\Phi + v^2\Psi) - (1+\Phi+\Psi)\gamma^i_{jk}v^j v^k$$

One gravitational potential or two? Forecasts and tests

By Edmund Bertschinger*

Phil. Trans. R. Soc. A (2011) **369**, 4947–4961
doi:10.1098/rsta.2011.0369

conformal newtonian metric (choices and assumptions):

$$ds^2 = a^2(\tau)[-(1+2\Phi)\,d\tau^2 + (1-2\Psi)\gamma_{ij}\,dx^i\,dx^j]$$

geodesics

$$\frac{1}{a}\frac{d(a\boldsymbol{v})}{d\tau} = -\boldsymbol{\nabla}\Phi, \quad v^2 \ll 1 \text{ (CDM)} \longrightarrow \text{Jean's equation}$$

$$\frac{d\boldsymbol{v}}{d\tau} = -\boldsymbol{\nabla}_\perp(\Phi + \Psi), \quad v^2 = 1 \text{ (photons)} \longrightarrow \text{lensing}$$

on ~ 100 kpc galaxy scales

kinematics: Φ

from galaxy velocity dispersion

deflection angle: $\Phi + \Psi$

from strong lensing

Ecuaciones de Einstein

Tensor de Einstein descompuesto en escalar-tensorial-vectorial:

$$G^0{}_0: \qquad \left(\nabla^2 + 3K\right)\Phi - 3\frac{\dot a}{a}\left(\dot\Phi + \frac{\dot a}{a}\Psi\right) = 4\pi G a^2 \delta\rho \ ,$$

$$G^0{}_{i,\,\parallel}: \qquad -(\dot\Phi + \frac{\dot a}{a}\Psi)_{;i} = 4\pi G a^2 \left[(\rho+p)(v_i + W_i)\right]_{\parallel} \ ,$$

$$G^0{}_{i,\,\perp}: \qquad \left(\nabla^2 + 2K\right)W_i = 16\pi G a^2 \left[(\rho+p)(v_i + W_i)\right]_{\perp} \ ,$$

$$G^i{}_i: \qquad \ddot\Phi - K\Phi + \frac{\dot a}{a}(\dot\Psi + 2\dot\Phi) + \left[2\frac{\dot a}{a} + \left(\frac{\dot a}{a}\right)^2\right]\Psi - \frac{1}{3}\nabla^2(\Phi - \Psi) = 4\pi G a^2 \delta p$$

$$G^i{}_{j\neq i,\,\parallel}: \qquad \boxed{\left(\Phi - \Psi\right)_{,(i;j)} - \frac{1}{3}\gamma_{ij}\nabla^2\left(\Phi - \Psi\right) = 8\pi G a^2 \Sigma_{ij,\,\parallel}} \ ,$$

Se pueden generar diferencias entre los potenciales en RG (en ese caso, en general, materia oscura)

$$G^i{}_{j,\,\perp}: \qquad \dot W_{(j;i)} + 2\frac{\dot a}{a}W_{(j;i)} = -8\pi G a^2 \Sigma_{ij,\,\perp} \ ,$$

$$G^i{}_{j,\,\mathrm{T}}: \qquad \ddot S_{ij} + 2H\dot S_{ij} - \nabla^2 S_{ij} + 2K S_{ij} = 8\pi G a^2 \Sigma_{ij,\,\mathrm{T}} \ ,$$

obs.: neste módulo $\dot{} = \frac{d}{d\tau}$ e $H = \frac{\dot a}{a}$ $\qquad (\nabla^2 A_{ij} := A_{ij;k}{}^{;k})$

Gravidade Modificada

- teoria de Horndeski (e.g. 1902.06978)

(teoria escalar tensor mais geral que leva a equações de movimento de segunda ordem)

$$S = \int d^4x \sqrt{-g} \sum_{i=2}^{5} \mathcal{L}_i + S_m$$

$$\begin{aligned}
\mathcal{L}_2 =& K(\phi, X)\,, \\
\mathcal{L}_3 =& -G_3(\phi, X)\Box\phi\,, \\
\mathcal{L}_4 =& G_4(\phi, X)R + G_{4,X}\left[(\Box\phi)^2 - (\nabla_\mu\nabla_\nu\phi)^2\right]\,, \\
\mathcal{L}_5 =& G_5(\phi, X)G_{\mu\nu}\nabla^\mu\nabla^\nu\phi - \frac{G_{5,X}}{6}\left[(\Box\phi)^3 - 3\,(\Box\phi)\,(\nabla_\mu\nabla_\nu\phi)^2 + 2\,(\nabla_\mu\nabla_\nu\phi)^3\right]
\end{aligned}$$

Obs.: *hi_class: Horndeski in the Cosmic Linear Anisotropy Solving System*, Zumalacárregui. et al., www.hiclass-code.net

Gravidade Modificada

- Calibre longitudinal

$$ds^2 = -(1+2\Psi)dt^2 + a^2(t)(1+2\Phi)\delta_{ij}dx^i dx^j$$

- Aproximação quase estática (e.g. 1902.06978)

$$k^2\Phi = \frac{1}{2}Y(k,z)\eta(z,k)\rho_m(z)\delta_m(z,k)$$

$$k^2\Psi = -\frac{1}{2}Y(k,z)\rho_m(z)\delta_m(z,k)$$

$$\eta = -\frac{\Phi}{\Psi}$$

parâmetro de *slip*

$$\eta = h_2\left(\frac{1+k^2h_4}{1+k^2h_5}\right), \; Y = h_1\left(\frac{1+k^2h_5}{1+k^2h_3}\right)$$

apenas funções do tempo
Silvestri A, Pogosian L, Buniy RV., PRD87:104015 (2013)

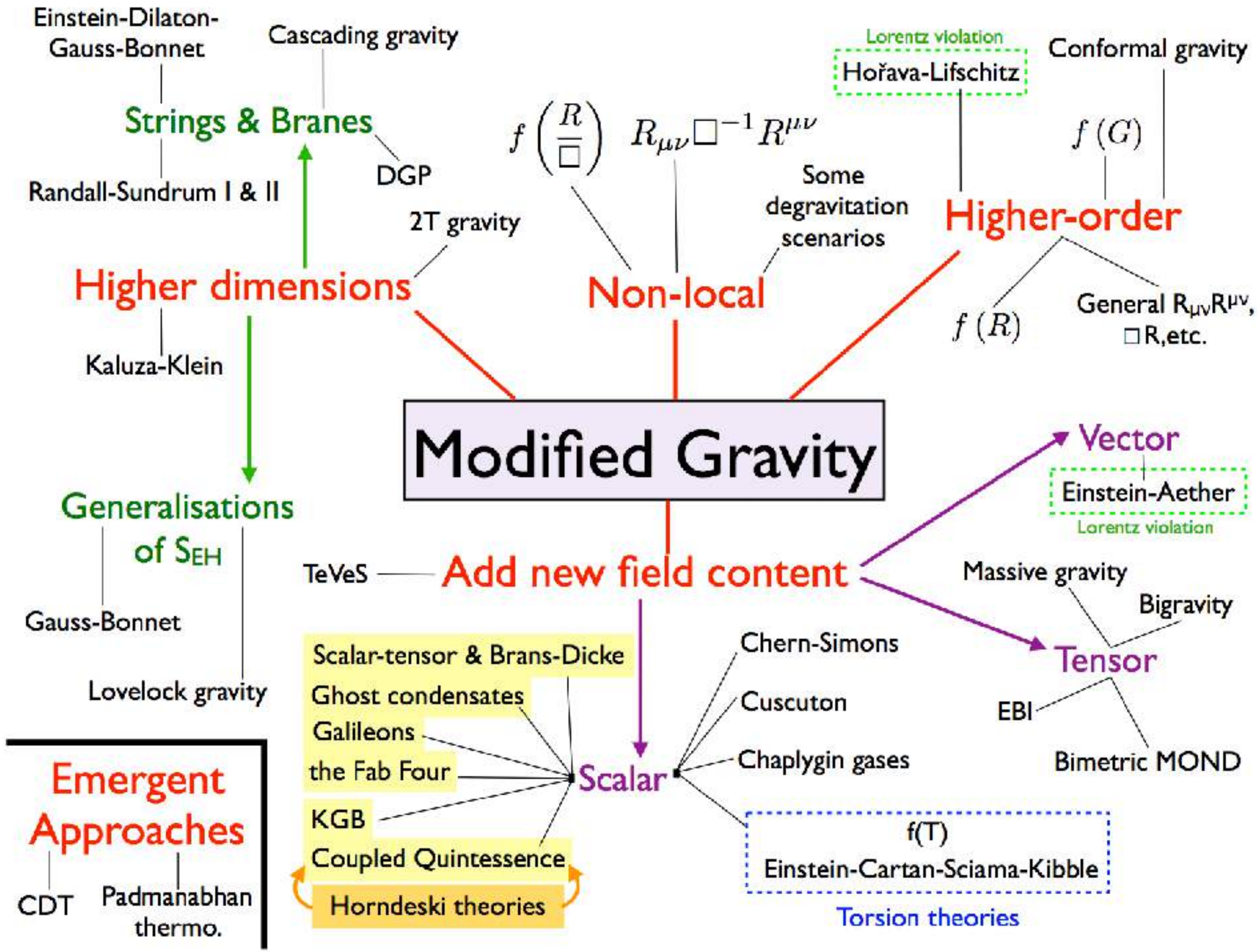

From arXiv:1512.05356

Testing Gravity at Different Scales

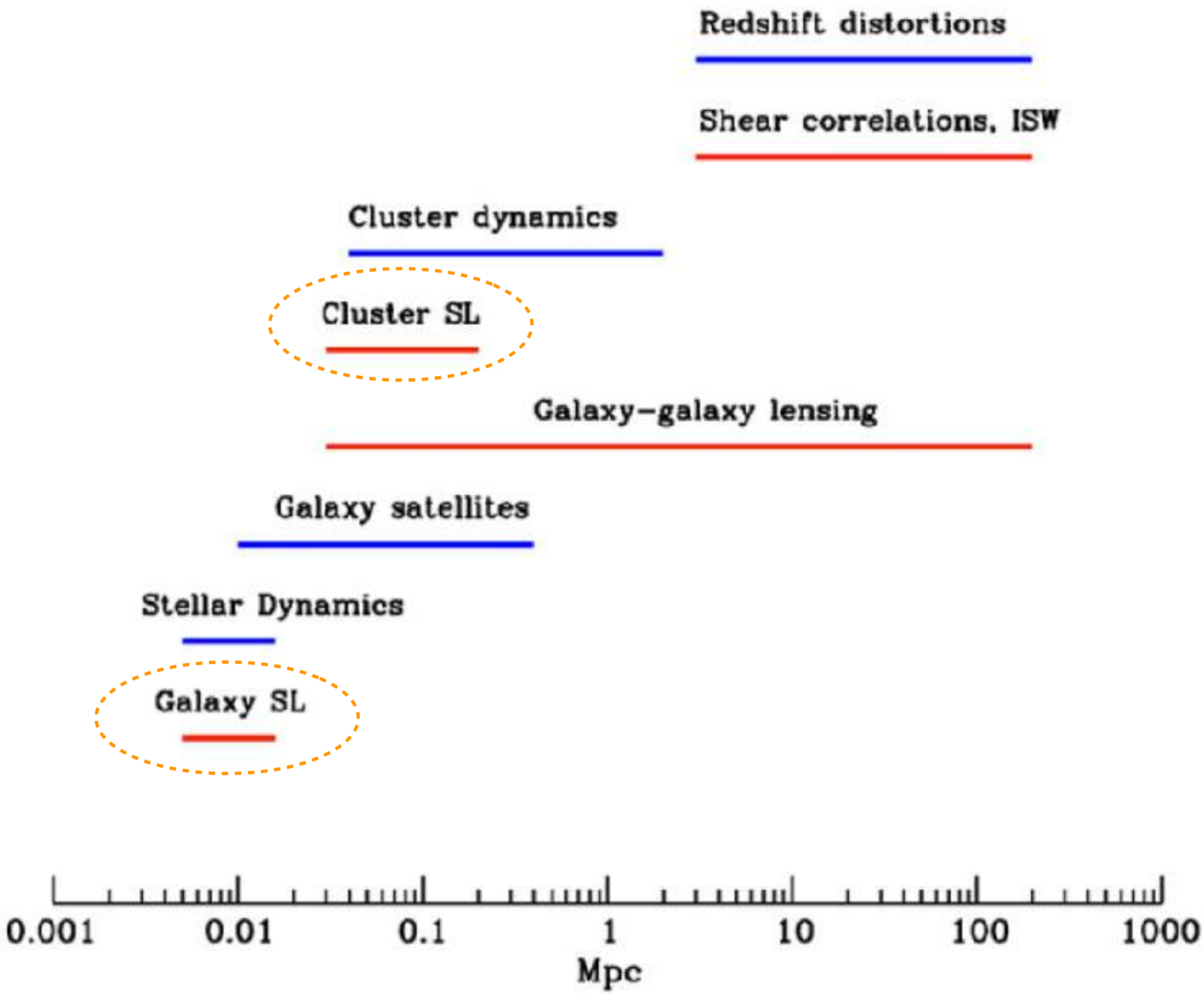

Jain, Bhuvnesh; Khoury, Justin, 2010, *Cosmological tests of gravity*, Annals of Physics, 325, 1479

Testing Gravity at Different Scales

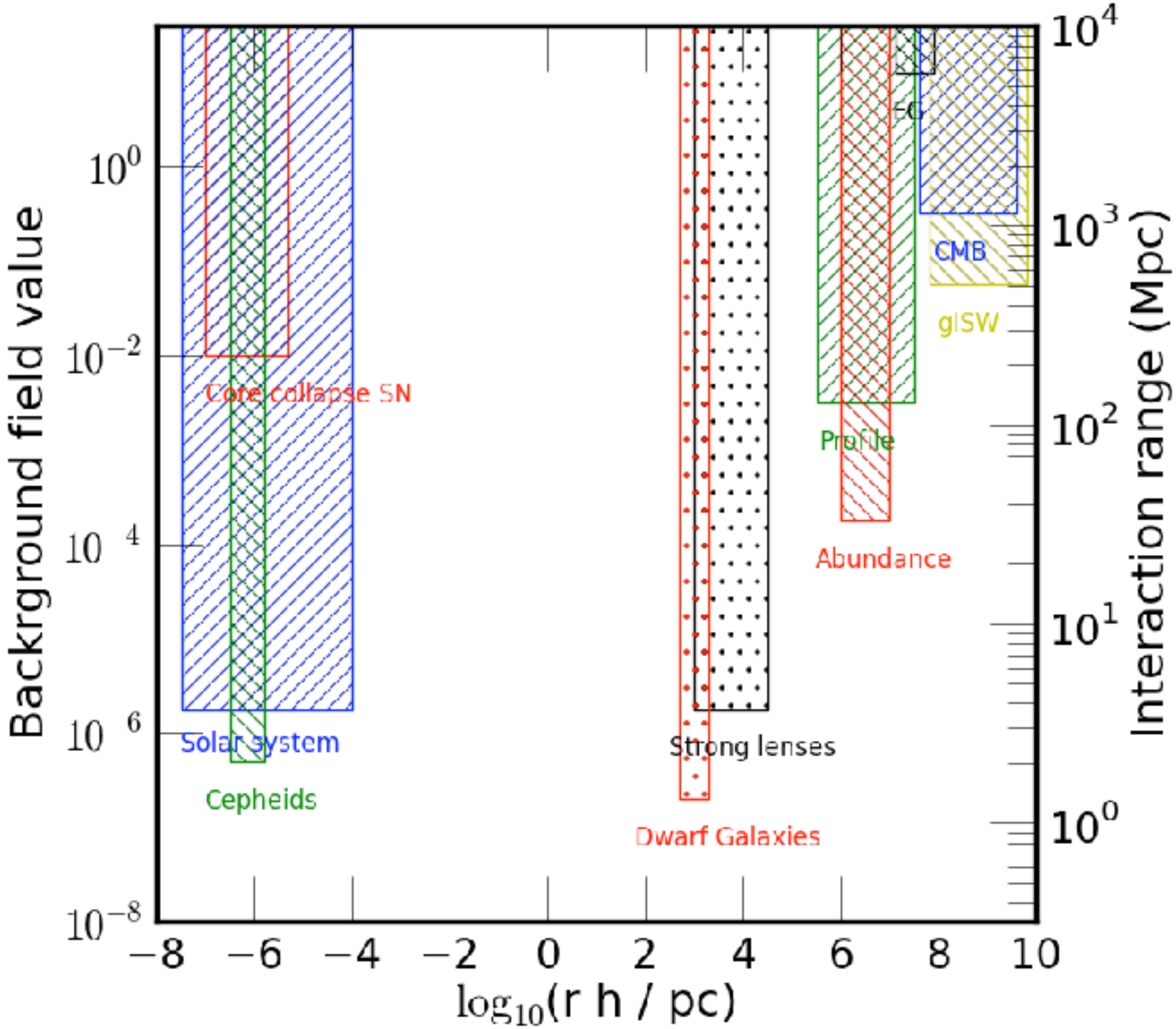

Jain, Bhuvnesh, et al., 2013, *Novel Probes of Gravity and Dark Energy*, arXiv:1309.5389 (adapted from Lombriser et al. 2012, Phys.Rev., D85:102001)

Bending of light by gravity

Null geodesic,
Fermat principle

$$ds^2 = \left(1 + \frac{2\phi}{c^2}\right) c^2 dt^2 - \left(1 - \frac{2\phi}{c^2}\right) d\sigma^2$$

$$\frac{d\sigma}{dt} := c' = \sqrt{\frac{1 + 2\phi/c^2}{1 - 2\phi/c^2}} \simeq c\left(1 + \frac{2\phi}{c^2}\right)$$

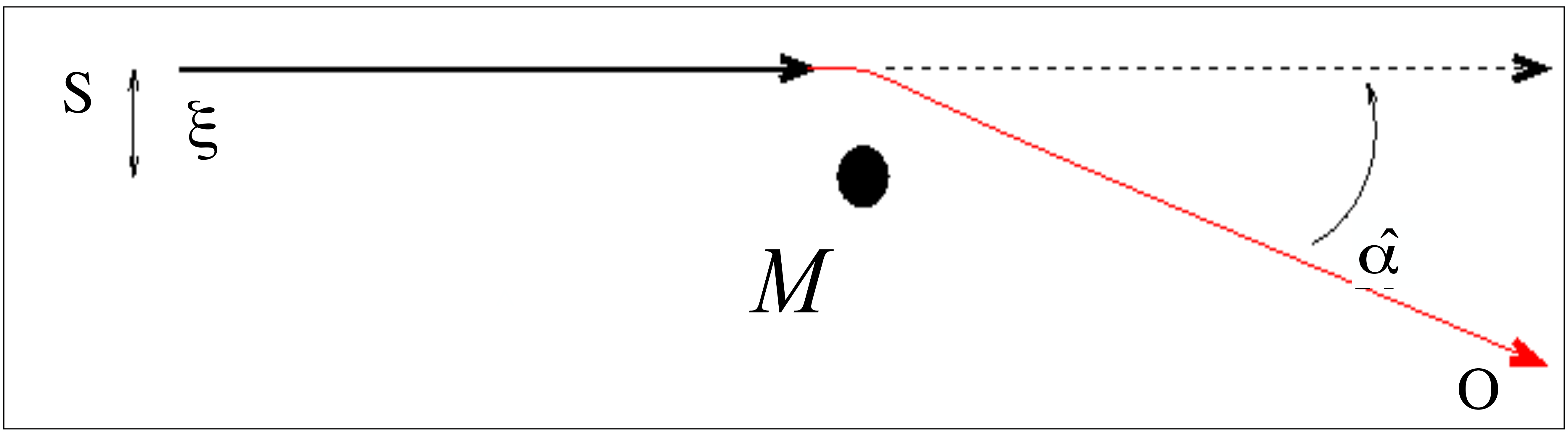

Bending of light by (modified) gravity

Null geodesic,
Fermat principle

$$ds^2 = \left(1 + \frac{2\psi}{c^2}\right) c^2 dt^2 - \left(1 - \frac{2\phi}{c^2}\right) d\sigma^2$$

peculiar gravitational potentials
(in GR $\psi = \phi$)

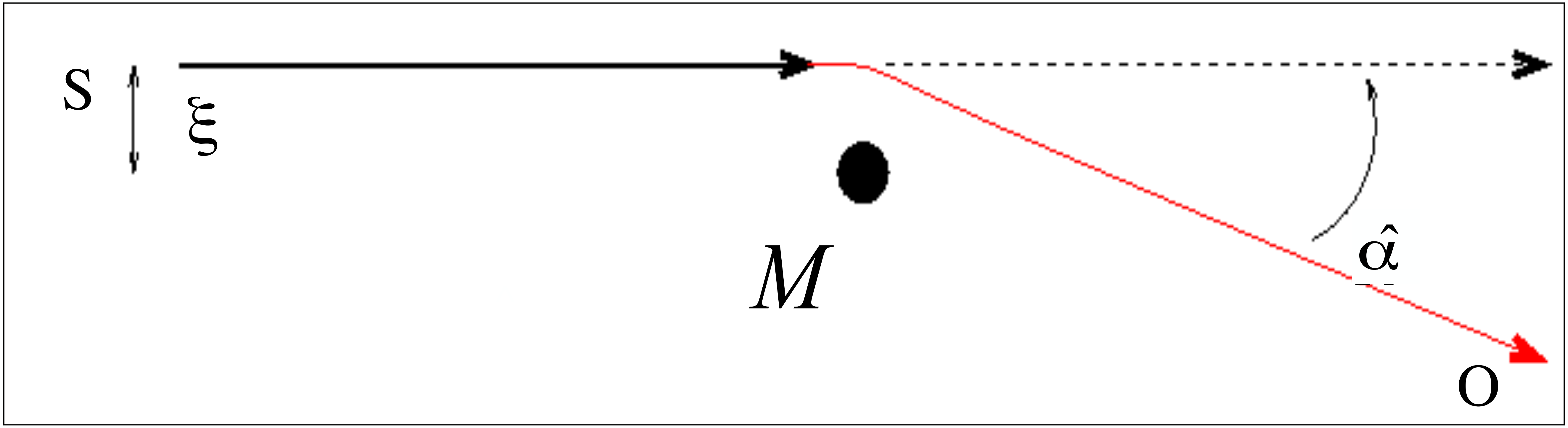

Bending of light by (modified) gravity

Null geodesic,
Fermat principle

$$ds^2 = \left(1 + \frac{2\psi}{c^2}\right) c^2 dt^2 - \left(1 - \frac{2\phi}{c^2}\right) d\sigma^2$$

$$\frac{d\sigma}{dt} = c' = c\sqrt{\frac{1+\frac{2\psi}{c^2}}{1-\frac{2\phi}{c^2}}} \simeq c\left(1 + \frac{\psi+\phi}{c^2}\right) = c\left(1 + \frac{2\phi}{c^2}\left[\frac{1+\gamma}{2}\right]\right)$$

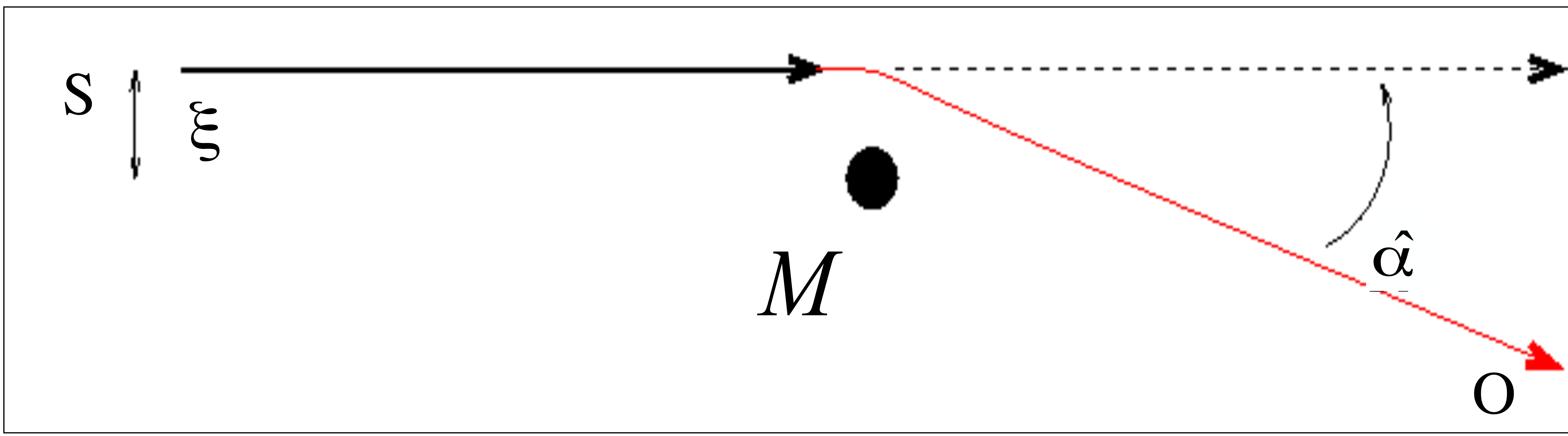

Dynamical mass obtained from

$$\nabla^2\psi = 4\pi G\rho$$

Use combination of lensing + dynamics to test gravity

Galaxy kinematics

The Jeans equation described the motion of a collection of stars. In spherical symmetry,

$$\frac{d}{dr}\left(\nu(r)\sigma_r^2(r)\right) + \frac{2\beta(r)}{r}\nu(r)\sigma_r^2(r) = \nu(r)\frac{d\Phi}{dr},$$

where

$$\frac{d\Phi}{dr} = \frac{GM(r)}{r^2}, \quad \beta(r) := 1 - \frac{\sigma_t^2}{\sigma_r^2},$$

where $M(r)$ is the total mass inside a sphere of radius r.
For $\beta =$ constant,

$$\sigma_r^2(r) = \frac{G}{r^{2\beta}\nu(r)}\int_r^\infty (r')^{2\beta-2}\nu(r')M(r')dr'.$$

The total mass contained within a sphere with radius r is,

$$M(r) = 4\pi\int_0^r (r')^2\rho(r')dr' = 4\pi\frac{r^{(3-\alpha)}}{3-\alpha}\frac{\rho_0}{r_0^{-\alpha}}$$

The actual velocity dispersion measured by observations is given by,

$$\bar{\sigma}_*^2 := \frac{\int_0^\infty dR R w(R) \int_{-\infty}^\infty dz \nu(r) \left(1 - \beta \frac{R^2}{r^2}\right) \sigma_r^2(r)}{\int_0^\infty dR R w(R) \int_{-\infty}^\infty dz \nu(r)},$$

where $w(R)$ is the convolution of the atmospheric seeing σ_{atm} and fiber aperture θ_{ap}.

$$\bar{\sigma}_*^2 = \left[\frac{2}{1+\gamma}\frac{c^2}{4}\frac{D_S}{D_{LS}}\theta_E\right]\frac{2}{\sqrt{\pi}}\frac{(2\tilde{\sigma}_{\mathsf{atm}}^2/\theta_E^2)^{1-\alpha/2}}{\xi - 2\beta} \times \left[\frac{\lambda(\xi) - \beta\lambda(\xi+2)}{\lambda(\alpha)\lambda(\delta)}\right]\frac{\Gamma(\frac{3-\xi}{2})}{\Gamma(\frac{3-\delta}{2})},$$

where

$$\tilde{\sigma}_{\mathsf{atm}} \approx \sigma_{\mathsf{atm}}\sqrt{1 + \chi^2/4 + \chi^4/40}, \quad \chi = \theta_{\mathsf{ap}}/\sigma_{\mathsf{atm}}.$$

Joint Arc sample for Investigations into Relativity (JAIR): Follow-up Observations and Implications (FOI)

SOAR follow-up program focusing on the determination of σ_v

21 systems observed in 2022 (A+B) + 1 Gemini FT (Arg)

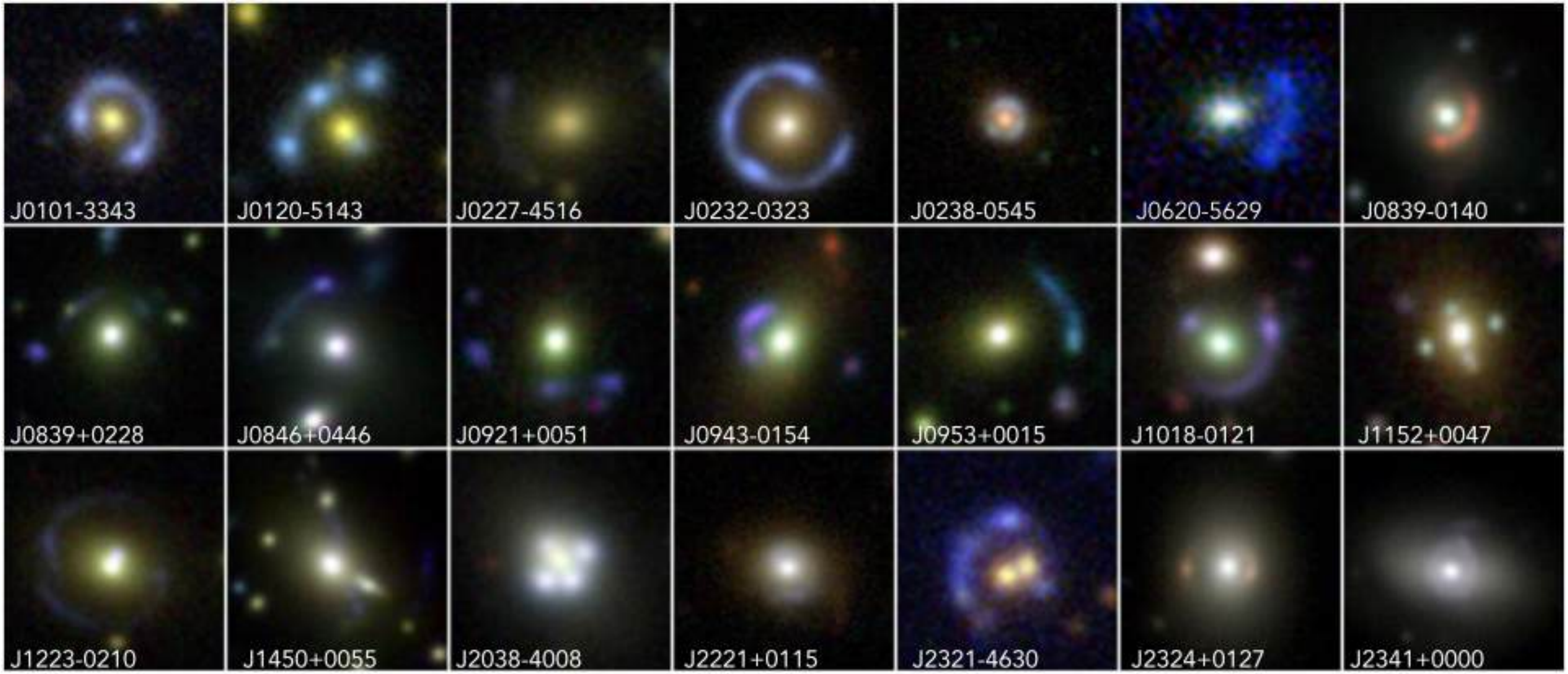

Testing general relativity in galaxies with combined velocity dispersion and gravitational lensing

SOAR program focusing on the determination of σ_v

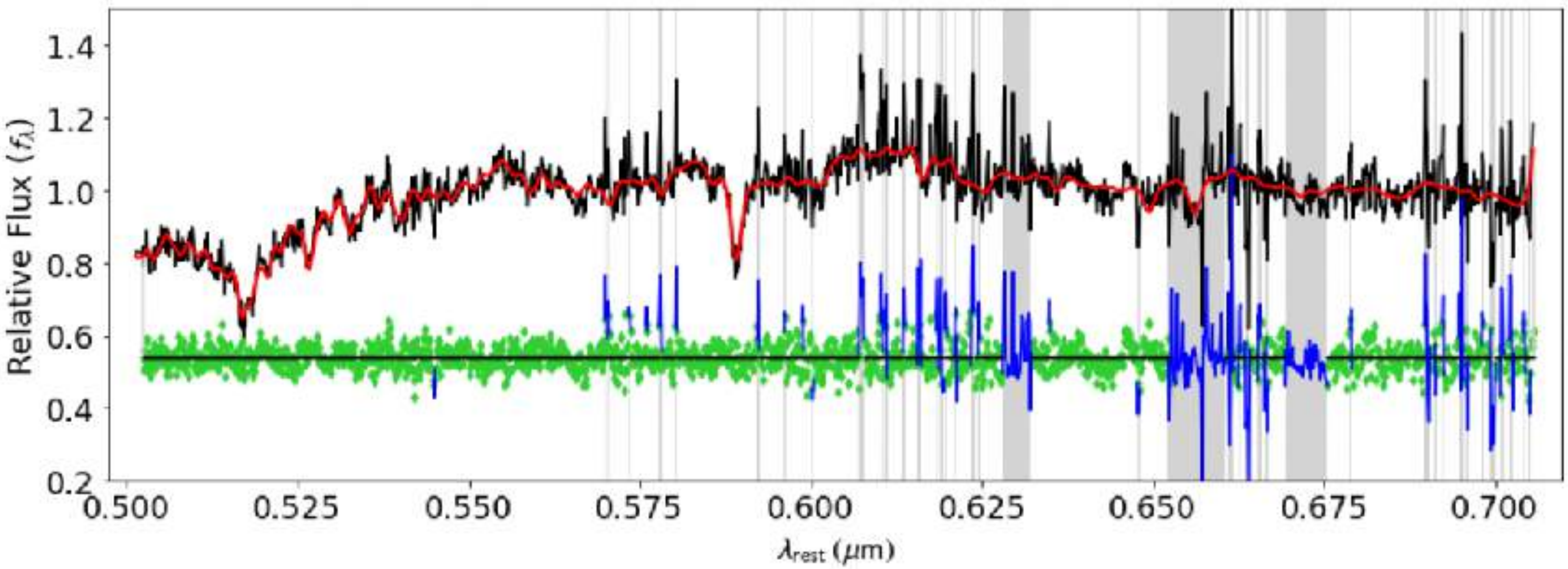

- Highly efficient/successful (know z_L, z_S in advance)
- 2022A: 10 (out of 13) systems with velocity dispersion (and z_L) measurements
- 9 with S/N > 10, 5 with S/N > 15, 3 with S/N > 20 (new strategy for 2022B)
- spectra modeled with (pPXF: Penalized PiXel-*Fitting)*

  7 systems with $\frac{\Delta\sigma_v}{\sigma_v} < 10\%$

(not all systems are suitable for testing MoG)

Joint Arc sample for Investigations into Relativity (JAIR): Follow-up Observations and Implications (FOI)

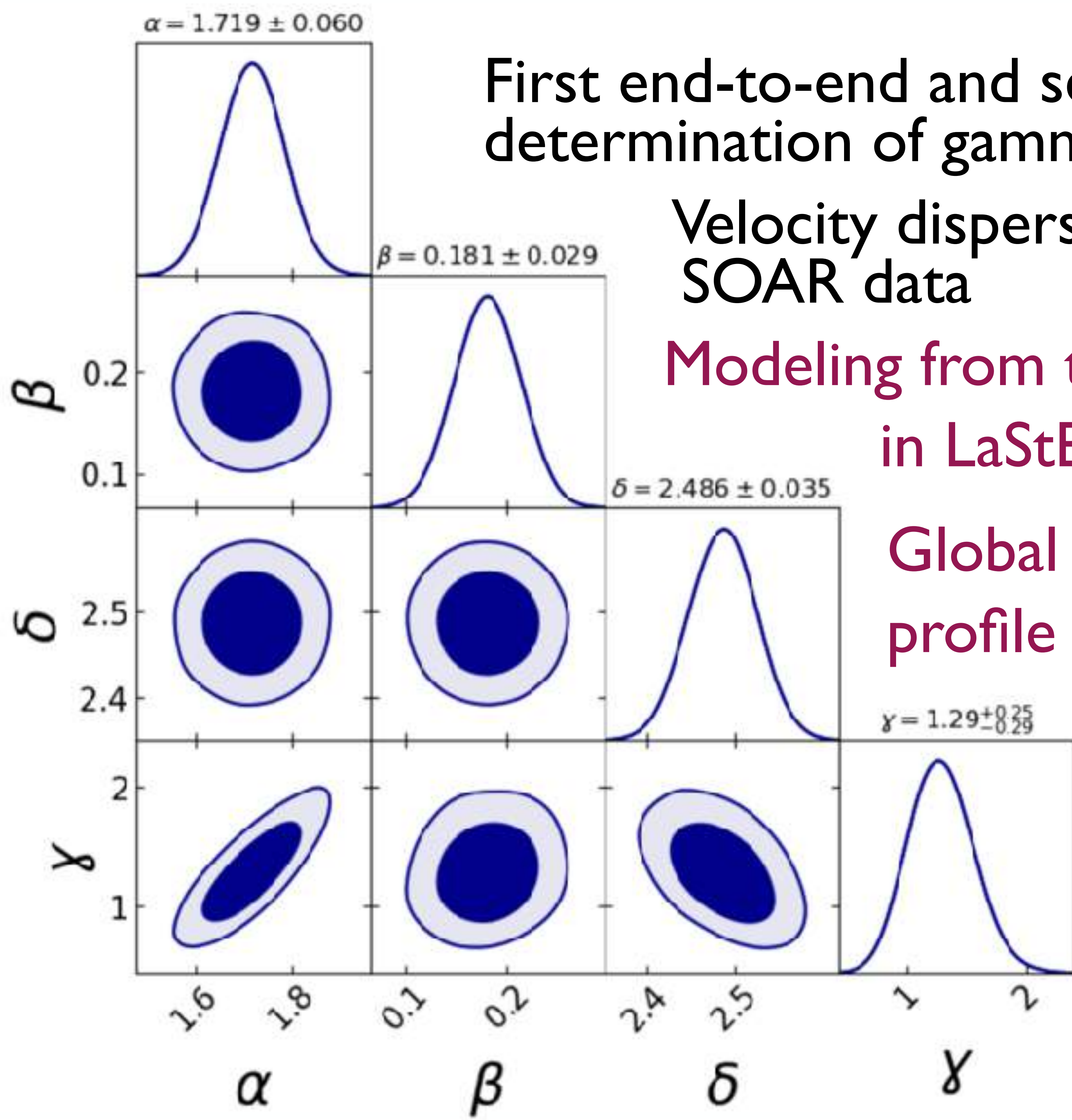

First end-to-end and self-consistent determination of gamma

Velocity dispersions for 21 systems from SOAR data

Modeling from the ground based images in LaStBeRu

Global priors in the density profile and the light distribution from the ground based modeling

Modified gravity tests with JAIR-FOI

J. França, M. Makler ++ (In prep)


João Paulo França

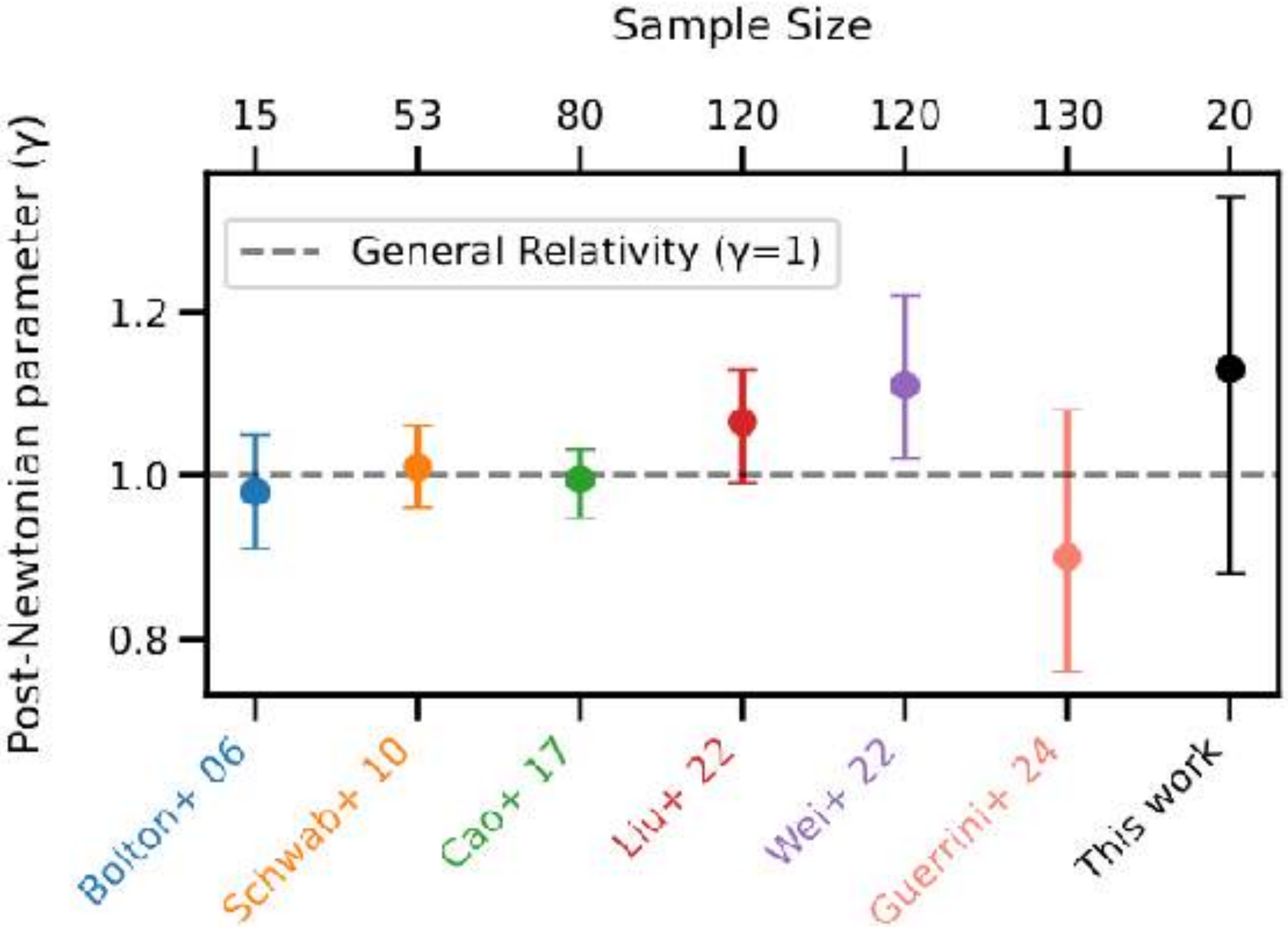

First end-to-end and self-consistent determination of γ_{PPN}

Velocity dispersions for 20 systems from SOAR data

Aperture correction accounting for the seeing in each observation

Light profile directly measured on the images

Uniform lens modeling from the ground

Prior on the lens and light profiles from the data

Motivation to test modified gravity from the ground: larger samples!

베르

LaStBeRu_cosmo_ground sample

- Visual inspection of all cutouts:
  - clear SL morphology, modelable systems
  - isolated
- SDSS velocity dispersion
- Largest, complementary sample for many applications
- Application to test modified gravity

Application: modified gravity

- queried the database for systems containing $z_L, z_S, \sigma_v, \delta\sigma_v,$ and $\theta_{\rm E}$: 409 systems
- 352 with SDSS spectroscopy (+ seeing, light profile fitting)
- 249 good data, galaxy-galaxy
- Visual inspection to select good systems: **206**
  - Final sample of 206, of which 103 not in Chen et al.
- Use for "gammology"

베르

LaStBeRu_cosmo_ground sample

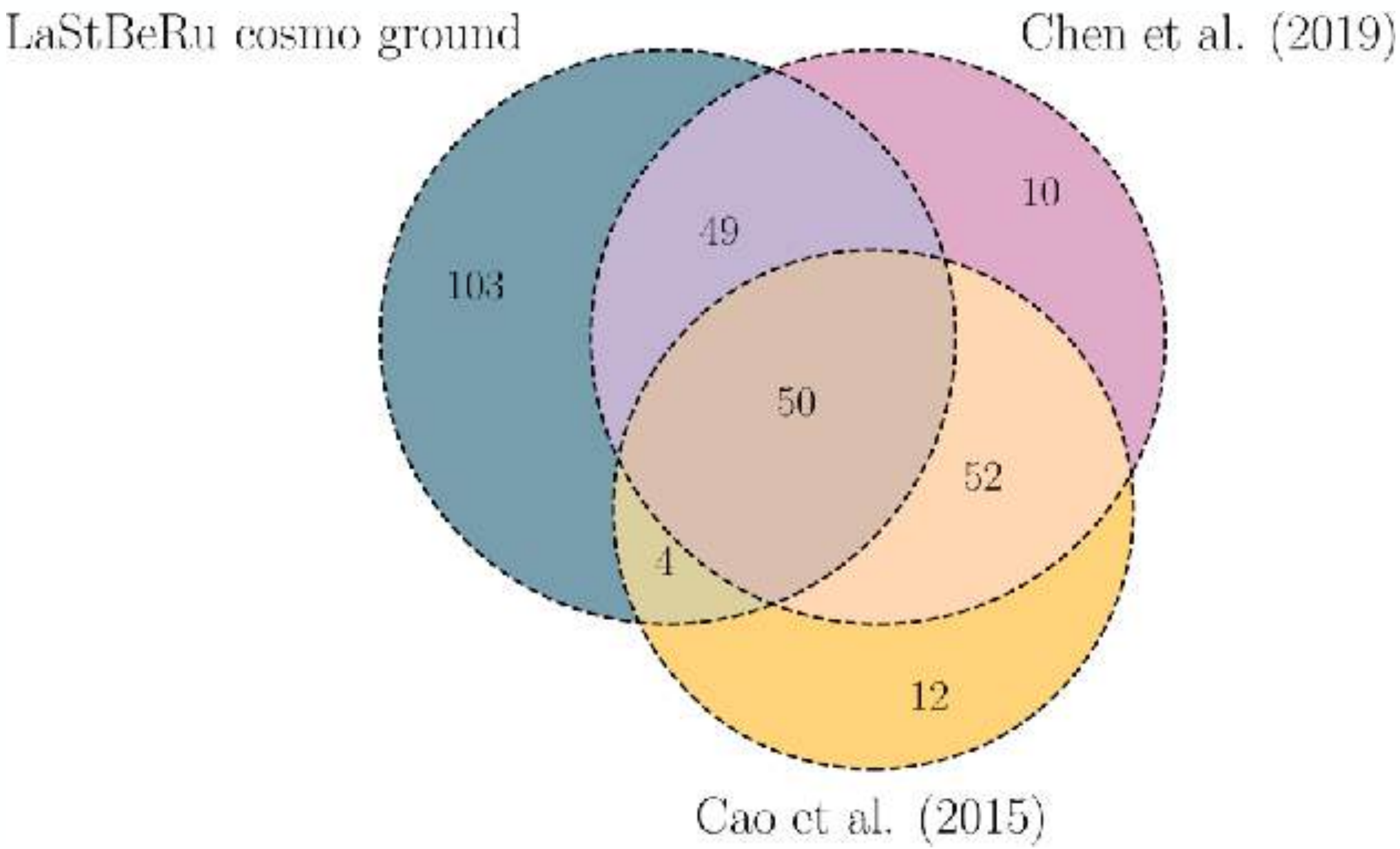

- Largest, complementary sample for many applications
- Uniform velocity dispersion measurements from SDSS
- Example application from purely archival data:
  test of modified gravity

Gamma from LaStBeRu_cosmo_ground

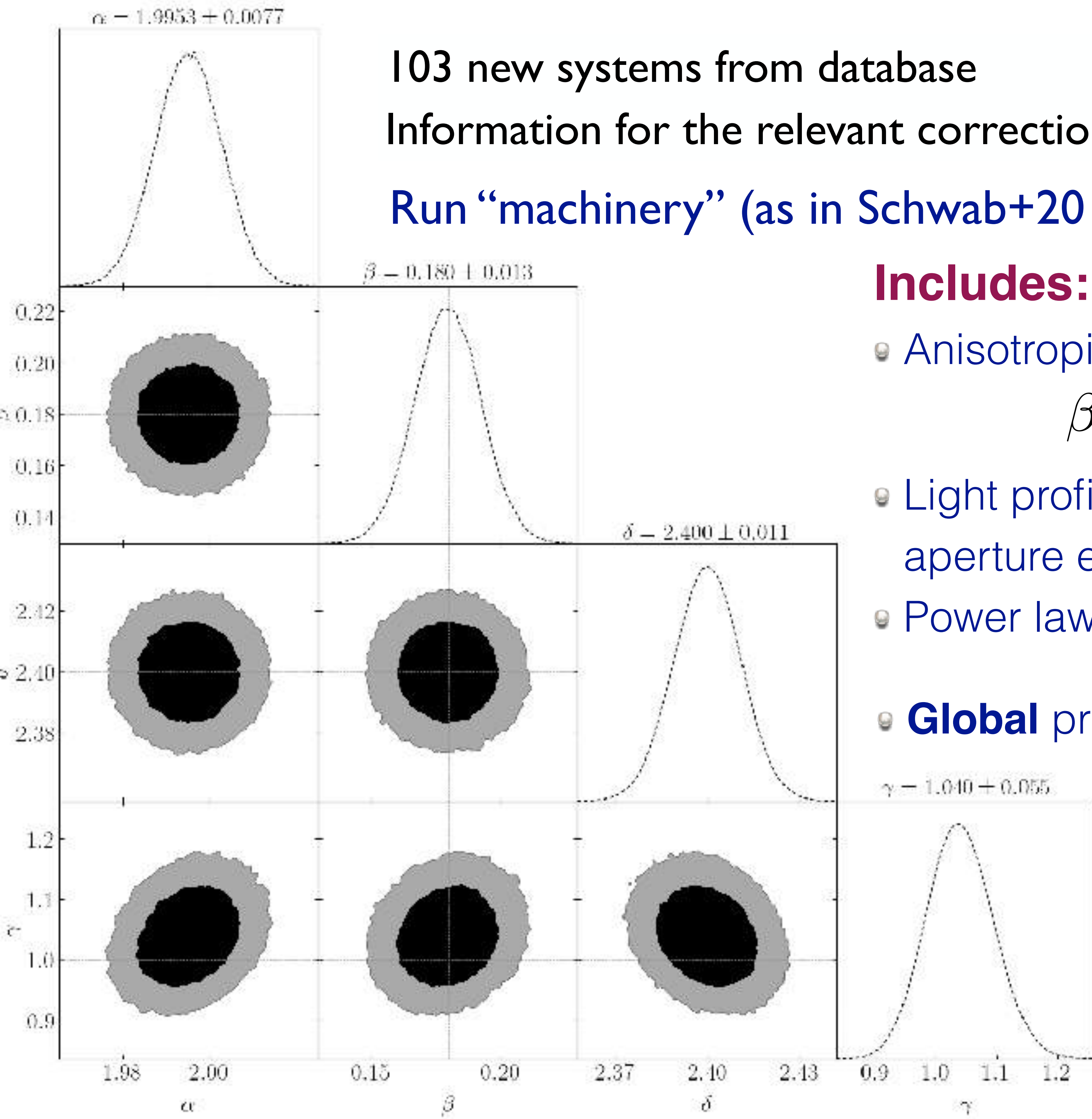

103 new systems from database

Information for the relevant corrections from the database!

Run “machinery” (as in Schwab+2010, Cao+2017, Chen+2022)

Includes:

- Anisotropic velocity dispersion

$$\beta = 1 - \sigma_t^2/\sigma_r^2$$

- Light profiles, seeing and fiber/slit aperture effects
- Power law density profile $\rho(r) \propto r^{-\alpha}$
- **Global** priors on $\beta = 0.180^{+0.014}_{-0.014}$, $\alpha = 1.995^{+0.009}_{-0.009}$

$$\gamma = 1.04 \pm 0.05$$

First constraint from “ground based” systems

베르

LaStBeRu_cosmo_ground sample

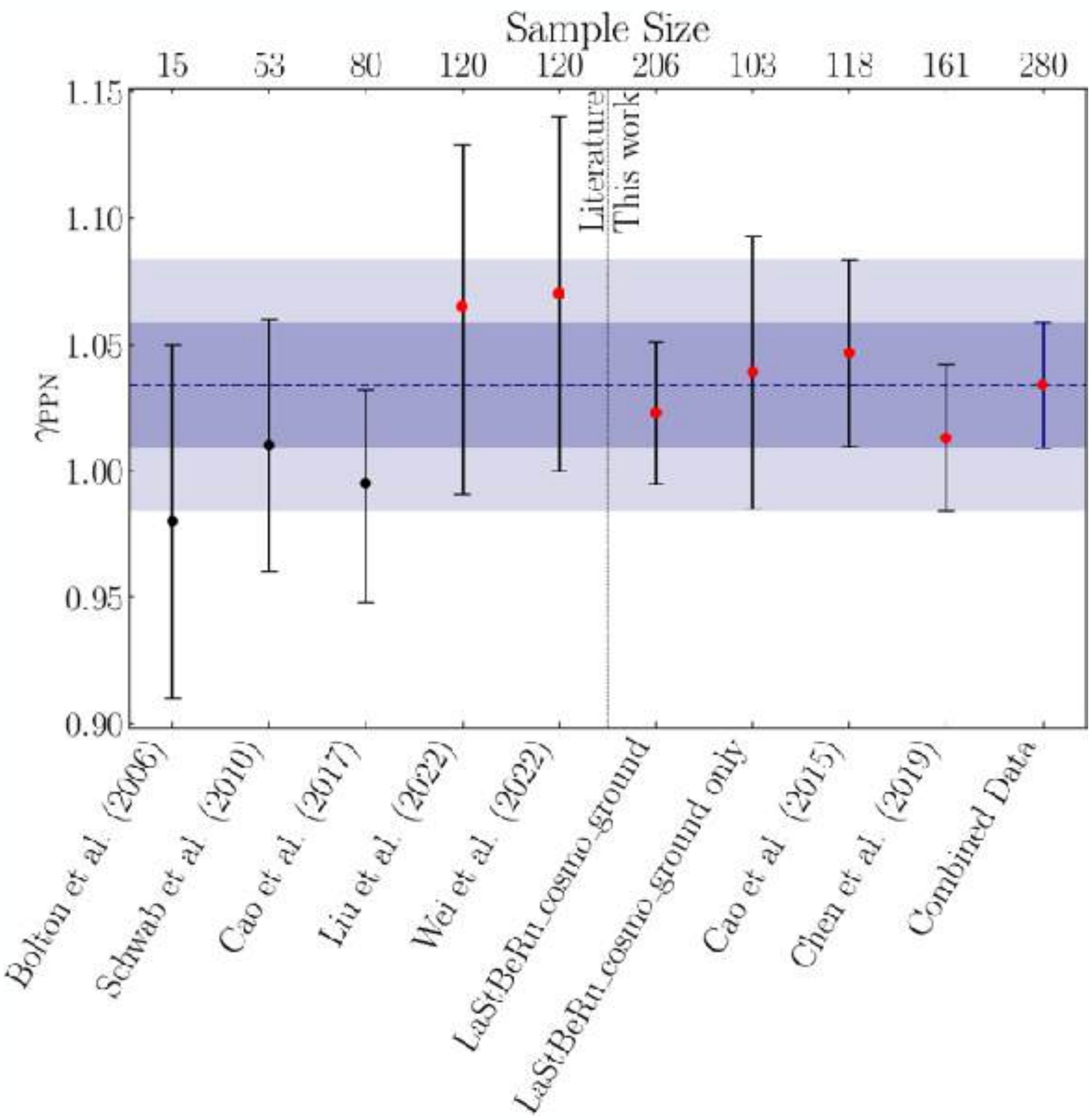

- First constraint on γ_{PPN} from purely ground based systems
- Totally independent sample from previous studies
- Most stringent constraints on γ_{PPN} when combined with other data

LaStBeRu

meets

JAIR

DHOST in EFTDE

la solution

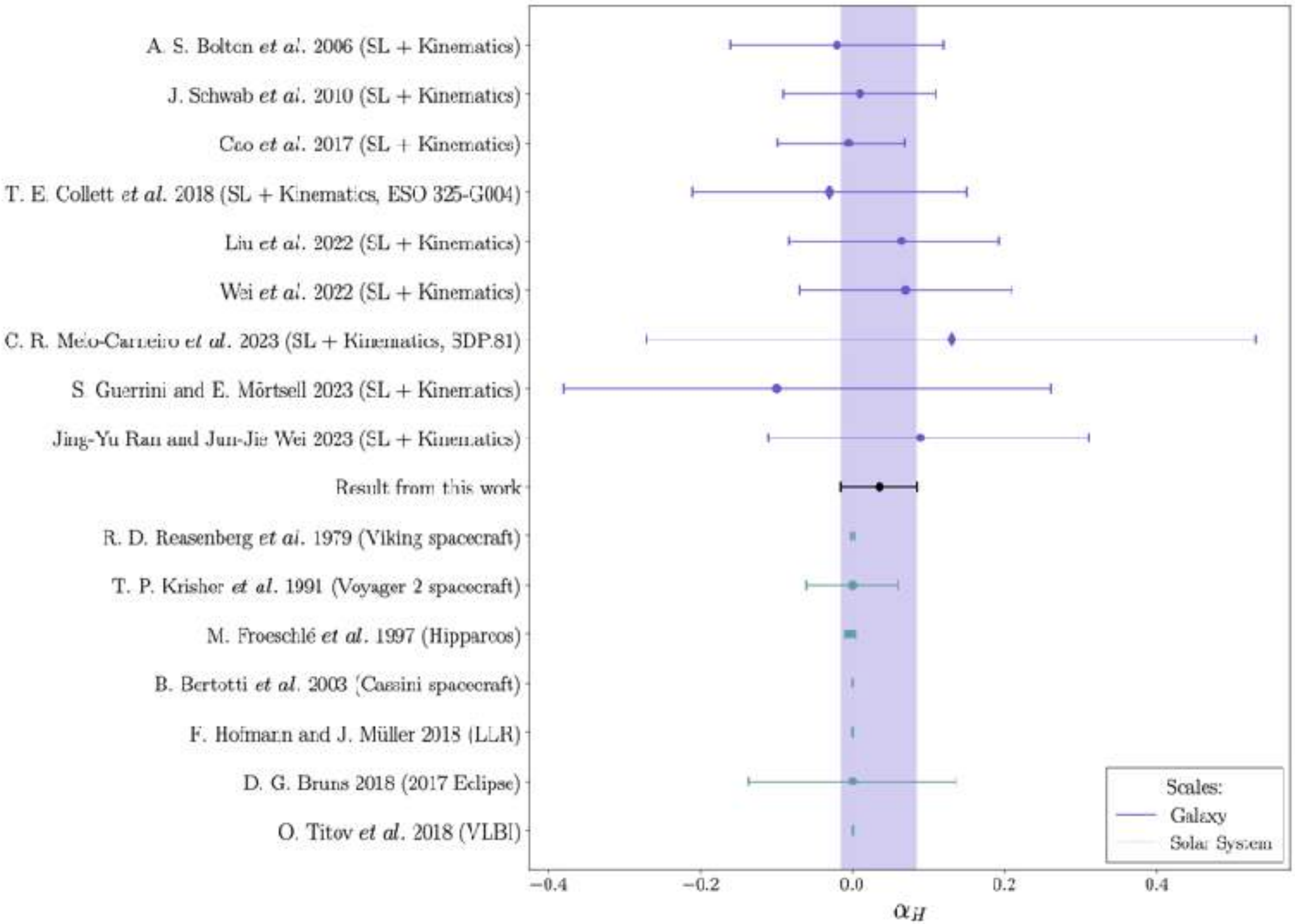

Beyond-Horndeski theories

aka Gleyzes-Langlois-Piazza-Vernizzi (GLPV)

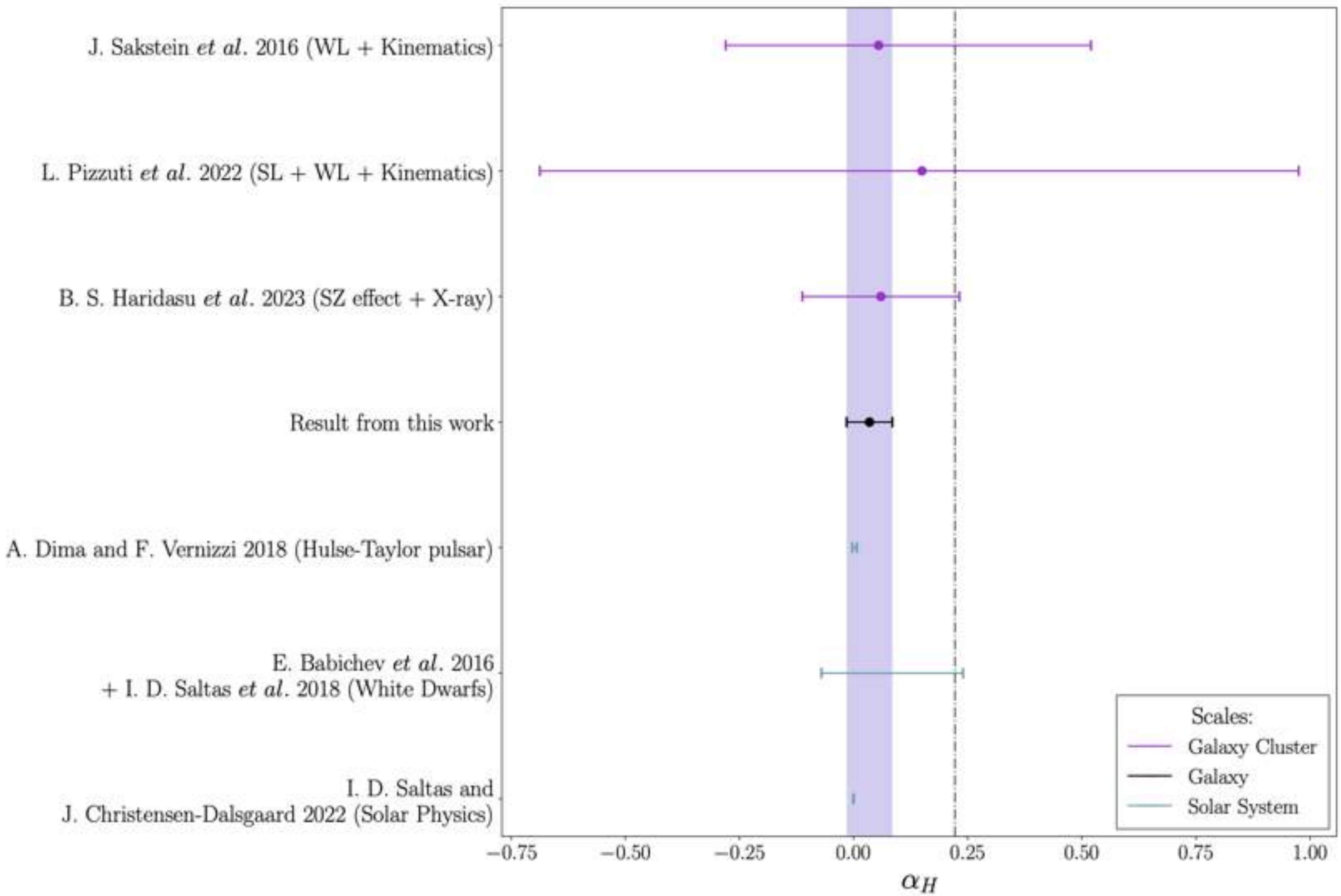

Lensing + Dynamics

- In general, powerful cosmological probe:
  DE models, space-time curvature, etc.

CLASH-VLT: testing the nature of gravity with galaxy cluster mass profiles

To cite this article: L. Pizzuti *et al* JCAP04(2016)023

The first simultaneous measurement of Hubble constant and post-Newtonian parameter from time-delay strong lensing

Tao Yang,[1,2] Simon Birrer[3] and Bin Hu[1]★

[1] *Department of Astronomy, Beijing Normal University, Beijing 100875, China*
[2] *Asia Pacific Center for Theoretical Physics, Pohang 37673, South Korea*
[3] *Kavli Institute for Particle Astrophysics and Cosmology and Department of Physics, Stanford University, Stanford, CA 94305, USA*

MG-MAMPOSST: a code to test modifications of gravity with internal kinematics and lensing analyses of galaxy clusters

Lorenzo Pizzuti,[1]★ Ippocratis D. Saltas[2] and Luca Amendola[3]

[1] *Osservatorio Astronomico della Regione Autonoma Valle d'Aosta, Loc. Lignan 39, I-11020 Nus, Italy*
[2] *CEICO, Institute of Physics of the Czech Academy of Sciences, Na Slovance 2, 182 21 Praha 8, Czechia*
[3] *Institute of Theoretical Physics, Heidelberg University, Philosophenweg 16, D-69120 Heidelberg, Germany*

Strong Lensing in Strong Gravity

La “sombra” de un Agujero Negro

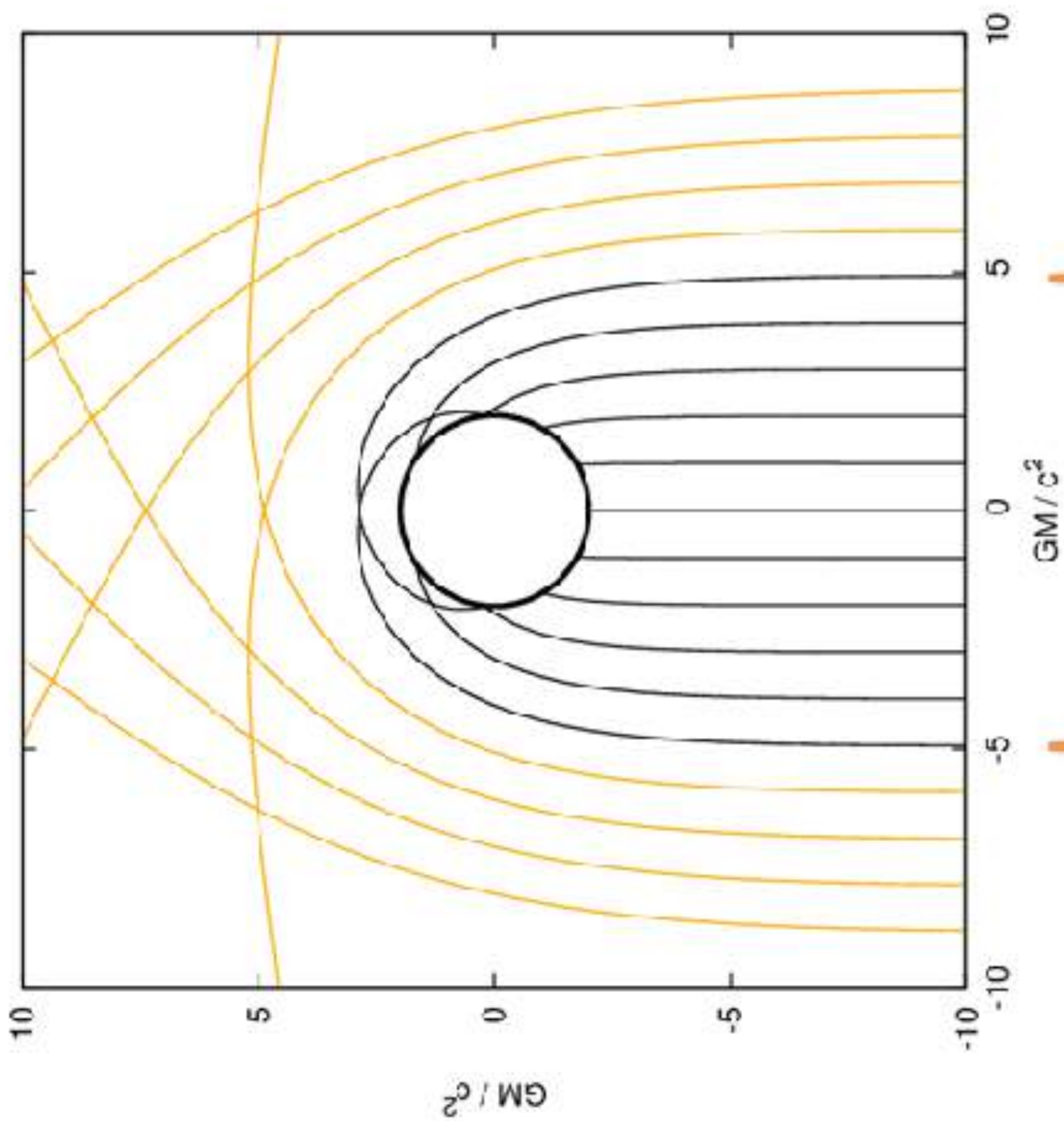

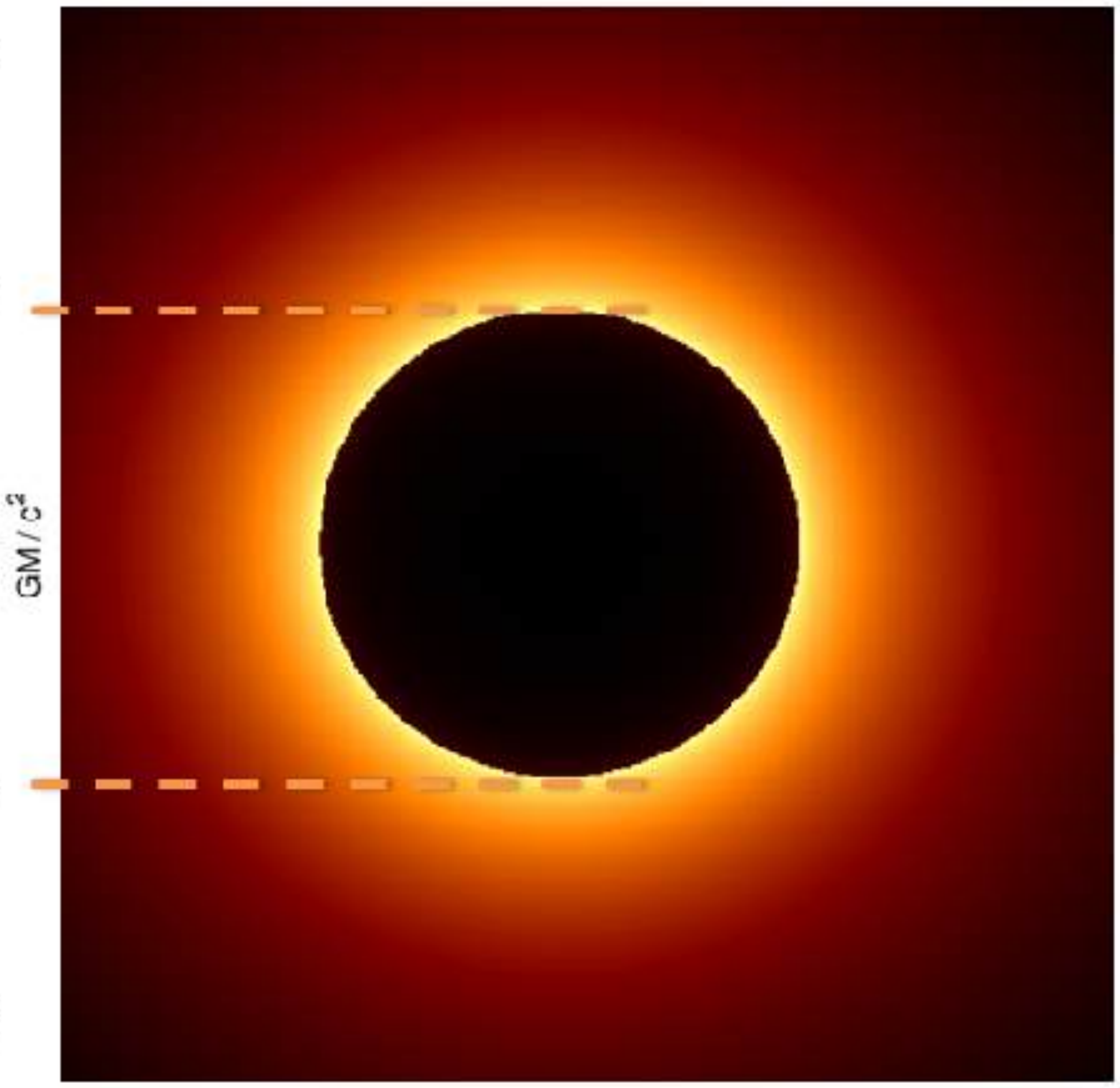

“solo tengo adentro, soy un pobre agujero”

León Gieco

Agujero negro estático (sin rotación)

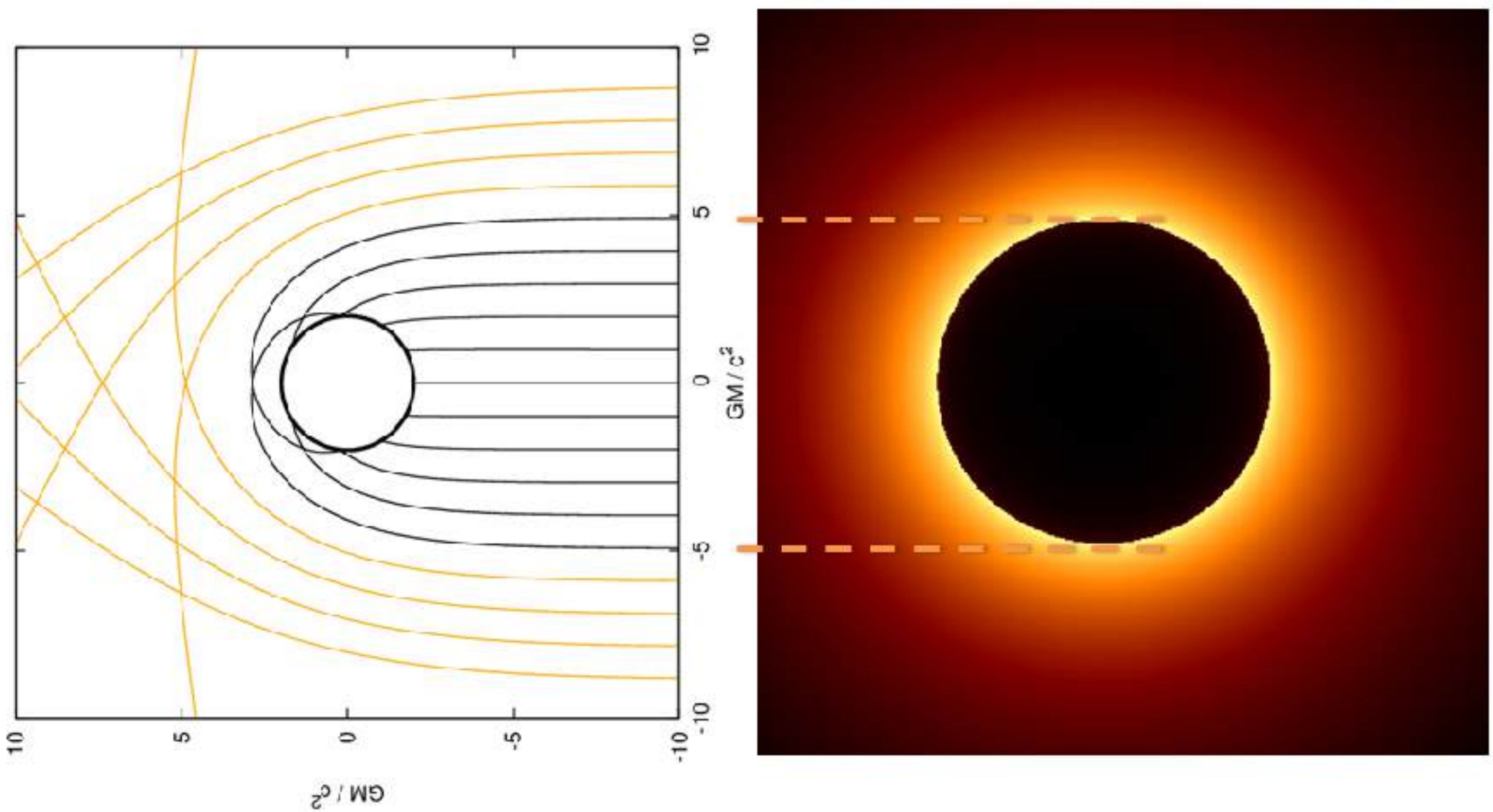

Agujero negro en rotación

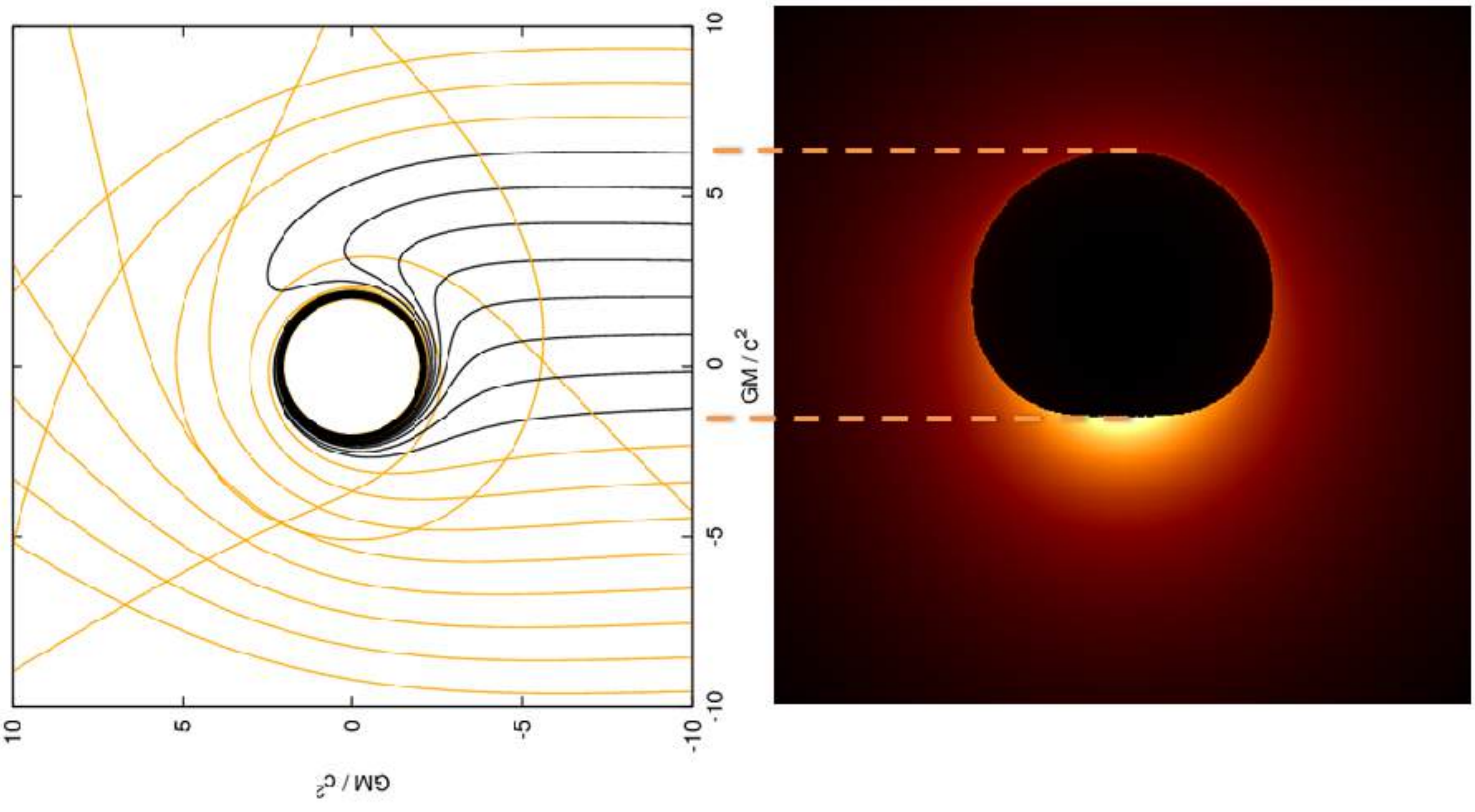

La sombra del Agujero Negro

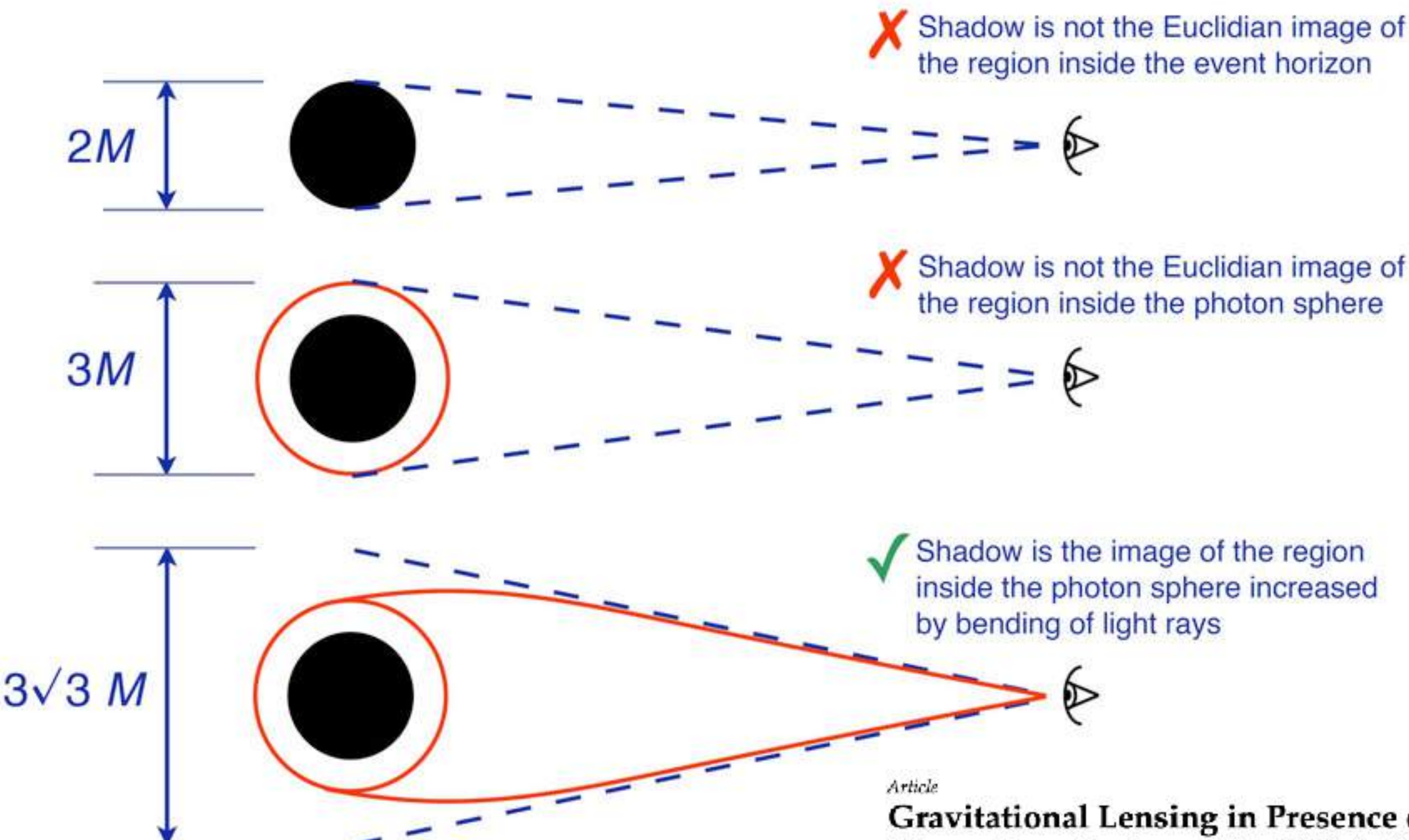

Article

Gravitational Lensing in Presence of Plasma: Strong Lens Systems, Black Hole Lensing and Shadow

Gennady S. Bisnovatyi-Kogan [1,2] and Oleg Yu. Tsupko [1,*]

Gargantua (filme interstellar)

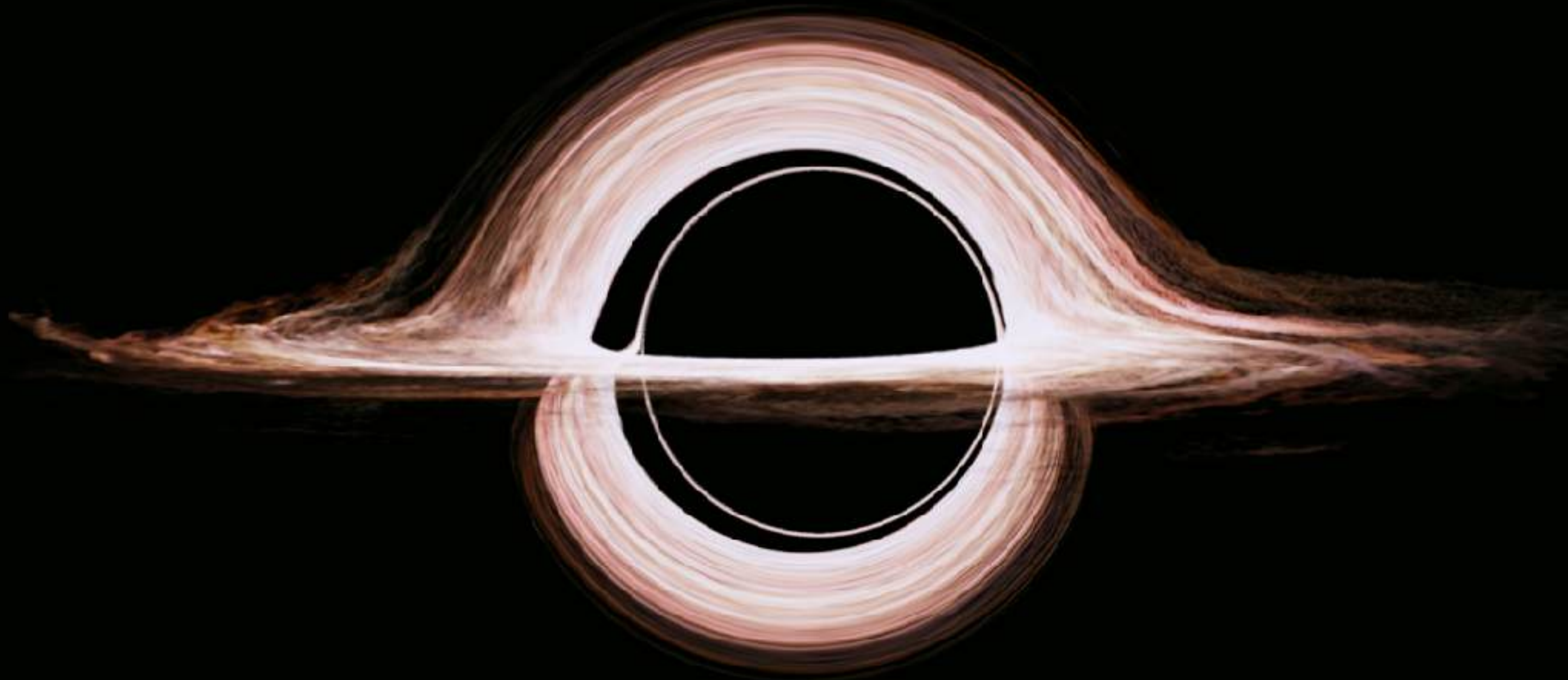

Gravitational lensing by spinning black holes in astrophysics, and in the movie Interstellar, Oliver James et al 2015 Class. Quantum Grav. 32 065001

Class. Quantum Grav. **32** (2015) 065001 (41pp) doi:10.1088/0264-9381/32/6/065001

Gravitational lensing by spinning black holes in astrophysics, and in the movie *Interstellar*

Oliver James[1,*], Eugénie von Tunzelmann[1], Paul Franklin[1] and Kip S Thorne[2]

[1] Double Negative Ltd., 160 Great Portland Street, London W1W 5QA, UK
[2] Walter Burke Institute for Theoretical Physics, California Institute of Technology, Pasadena, California 91125, USA

E-mail: oj@dneg.com, evt@dneg.com, paul@dneg.com and kip@caltech.edu

Received 27 November 2014, revised 12 January 2015
Accepted for publication 13 January 2015
Published 13 February 2015

CrossMark

Abstract

Interstellar is the first Hollywood movie to attempt depicting a black hole as it would actually be seen by somebody nearby. For this, our team at *Double Negative Visual Effects*, in collaboration with physicist Kip Thorne, developed a code called Double Negative Gravitational Renderer (DNGR) to solve the equations for ray-bundle (light-beam) propagation through the curved space-time of a spinning (Kerr) black hole, and to render IMAX-quality, rapidly changing images. Our ray-bundle techniques were crucial for achieving IMAX-quality smoothness without flickering; and they differ from physicists' image-generation techniques (which generally rely on individual light rays rather than ray bundles), and also differ from techniques previously used in the film industry's CGI community. This paper has four purposes: (i) to describe

A sombra do Buraco Negro

Esta es una imagem gravitacionalmente lenteada!

Event Horizon Telescope

Este no es el horizonte de eventos
de agujero negro

Diffractive Gravitational Lensing

Ecuaciones de Maxwell en el espacio-tiempo curvo

$$\begin{aligned} F_{\alpha\beta,\gamma} + F_{\beta\gamma,\alpha} + F_{\gamma\alpha,\beta} &= 0 \\ F^{\alpha\beta}_{;\gamma} &= 0 \end{aligned}$$

Perturbación escalar, expansión lineal:

$$\nabla^2 \vec{E} = (1 + 2U) \frac{\partial^2 \vec{E}}{\partial t^2}$$

Onda estacionaria: $\vec{E}(\vec{r}, t) = \phi(\vec{r}) e^{i\omega t}$

Amplitud de la onda en la presencia del campo gravitacional

$$\left(\nabla^2 + \omega^2\right) \phi = 4\omega^2 U \phi$$

Wave optics effects

- Maxwell's equations on a curved background
  Solution for the amplitude ratio of the field:

$$F(\omega, \vec{\eta}) = \frac{D_{\rm S}}{D_{\rm L} D_{\rm LS}} \frac{\omega}{2\pi i} \int d^2\xi \exp\left[i\omega t'(\vec{\xi}, \vec{\eta})\right]$$

Where $F = \phi/\phi_0$ and *t'* is the time delay function

$$t'(\vec{\xi}, \vec{\eta}) = \frac{D_L D_S}{2D_{LS}} \left(\frac{\vec{\xi}}{D_L} - \frac{\vec{\eta}}{D_S} \right)^2 - \hat{\psi}(\vec{\xi})$$

with $\nabla_\xi^2 \hat{\psi} = 8\pi\Sigma$

Wave optics effects

- Maxwell's equations on a curved background
  Solution for a **point lens**

$$F(w,u) = e^{\frac{i}{2}(u^2 - \ln(w/2))} e^{\frac{\pi}{4}w} \Gamma\left(1 - \frac{i}{2}w\right) {}_1F_1\left(1 - \frac{i}{2}w, 1; -\frac{i}{2}wu^2\right)$$

The magnification is therefore: $\mu = |F|^2$

$$\mu_{\text{ond}}^{\text{inf}}(w,u) = \frac{\pi w}{1 - e^{\pi w}} \left| {}_1F_1\left(\frac{i}{2}w, 1; \frac{i}{2}wu^2\right)\right|^2$$

Dimensionless, characteristic frequency:

$$w = \frac{4GM}{c^2}\omega(1 + z_L) = 4\pi(1 + z_{\text{L}})\frac{r_{\text{sch}}(M)}{\lambda}$$

- If the wavelength is comparable to the Schwarzschild radius, one has to account for wave optics!

Wave optics effects in gravitational lensing

- Maxwell's equations on a curved background
  Solution for a point lens:

$$\mu^{\rm inf}_{\rm ond}(w,u) = \frac{\pi w}{1-e^{\pi w}}\left|{}_1F_1\left(\frac{i}{2}w, 1; \frac{i}{2}wu^2\right)\right|^2$$

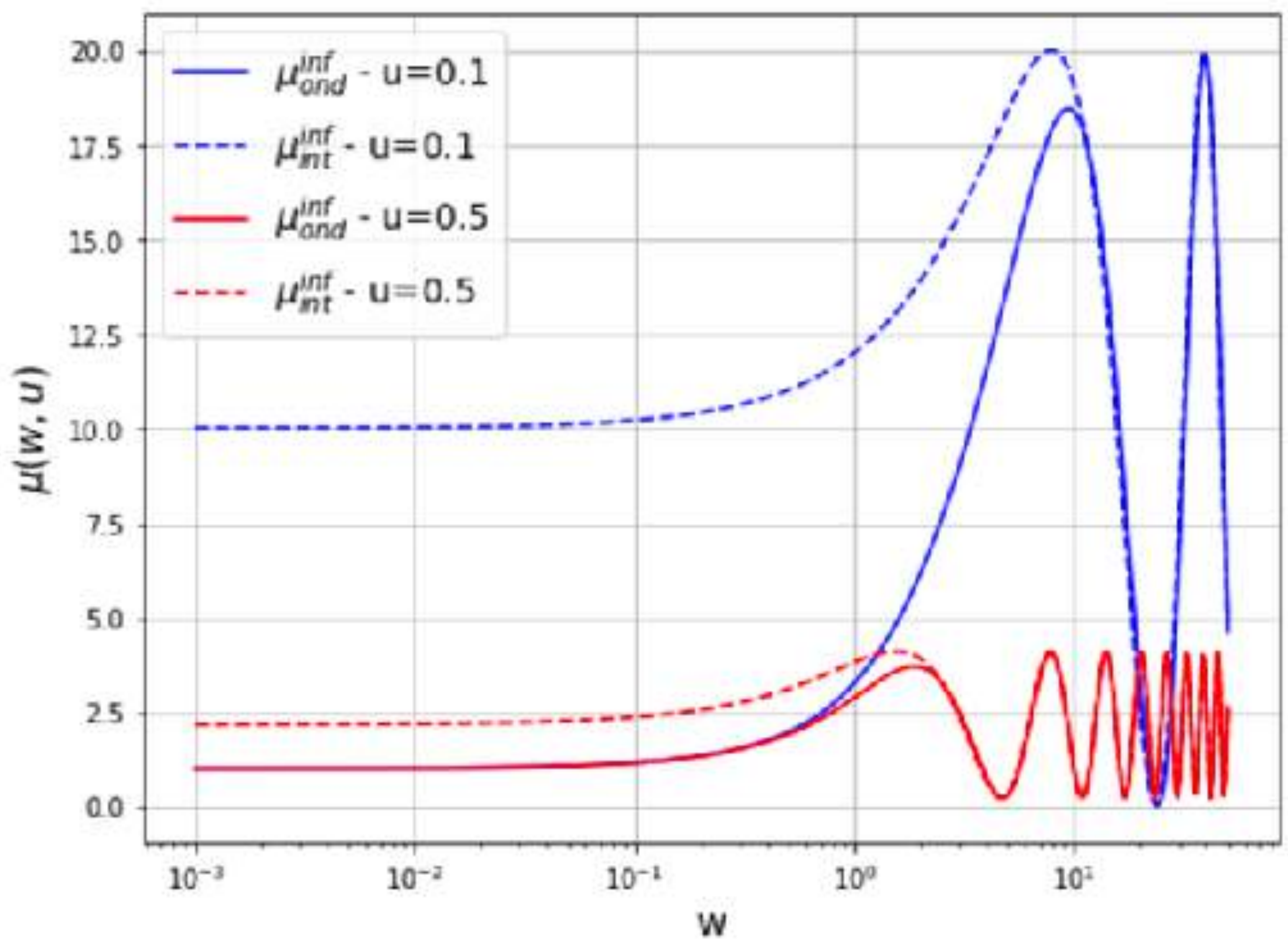

Arthur Mesquita, CBPF

Effect on a spectrum

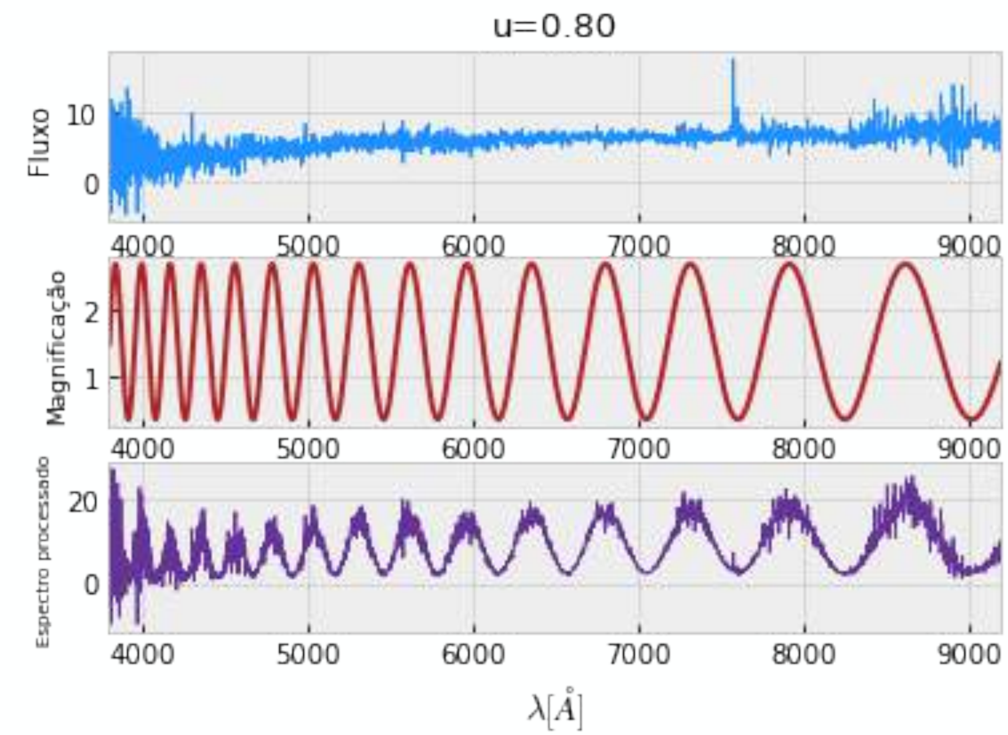

Wavelensing!

wave optics kills microlensing at the refractive limit

$$w = \frac{4GM}{c^2}\omega(1+z_L) = 4\pi(1+z_{\rm L})\frac{r_{\rm sch}(M)}{\lambda}$$

Wave optics effects

- For high frequencies (eikonal limit)

$$\mu_{\text{int}}^{\text{inf}}(w,u) = \frac{u^2+2}{u\sqrt{u^2+4}} + \frac{2}{u\sqrt{u^2+4}}\sin\left\{w\left[\frac{1}{2}u\sqrt{u^2+4} + \ln\left(\frac{\sqrt{u^2+4}+u}{u-\sqrt{u^2+4}}\right)\right]\right\}$$

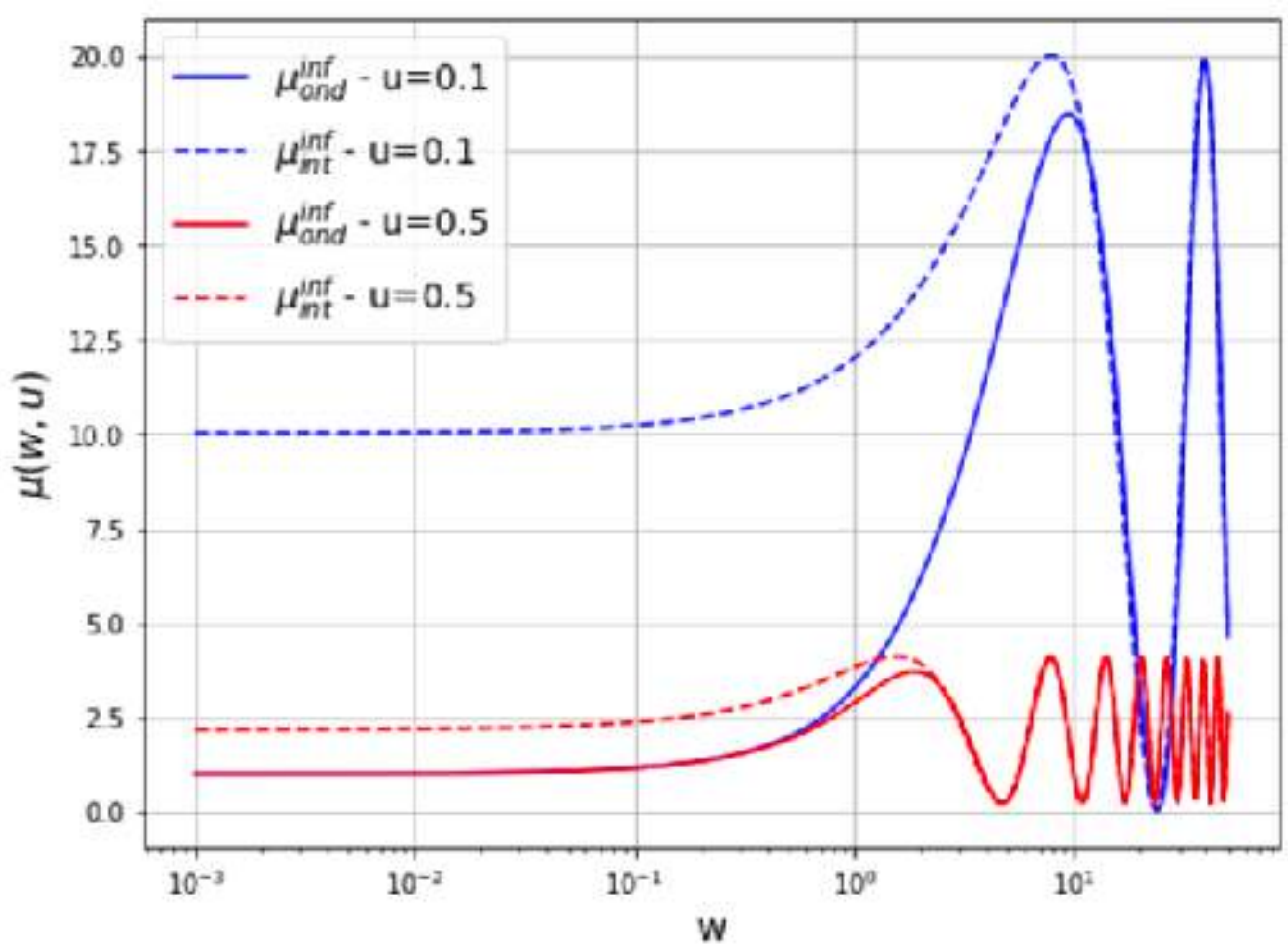

Effect on a spectrum

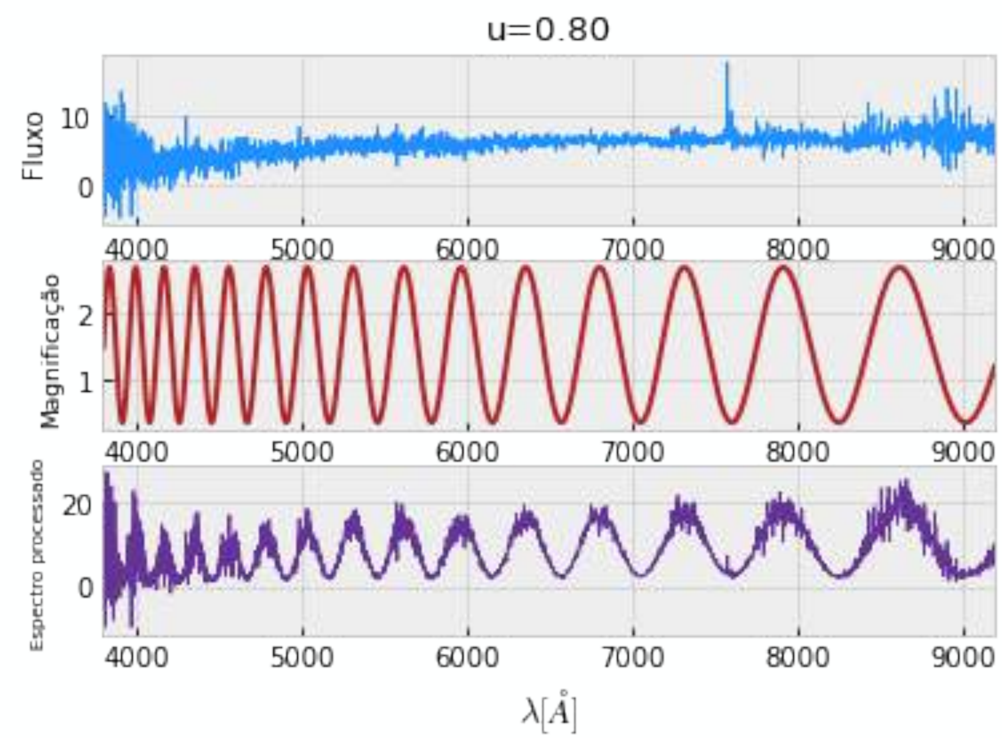

Femtolensing!

$$w = \frac{4GM}{c^2}\omega(1+z_L) = 4\pi(1+z_{\text{L}})\frac{r_{\text{sch}}(M)}{\lambda}$$

Finite source size

- Fuente incoerente: $$\mu = \frac{\int_{-\infty}^{+\infty} W(\vec{u})\mu(w,u)d^2u}{\int_{-\infty}^{+\infty} W(\vec{u})d^2u}$$

- Fuente uniforme circular: $$\mu(w,r,u) = \frac{1}{\pi r^2}\int_0^r \int_0^{2\pi} \mu(w,\nu)\, \chi d\alpha d\chi$$

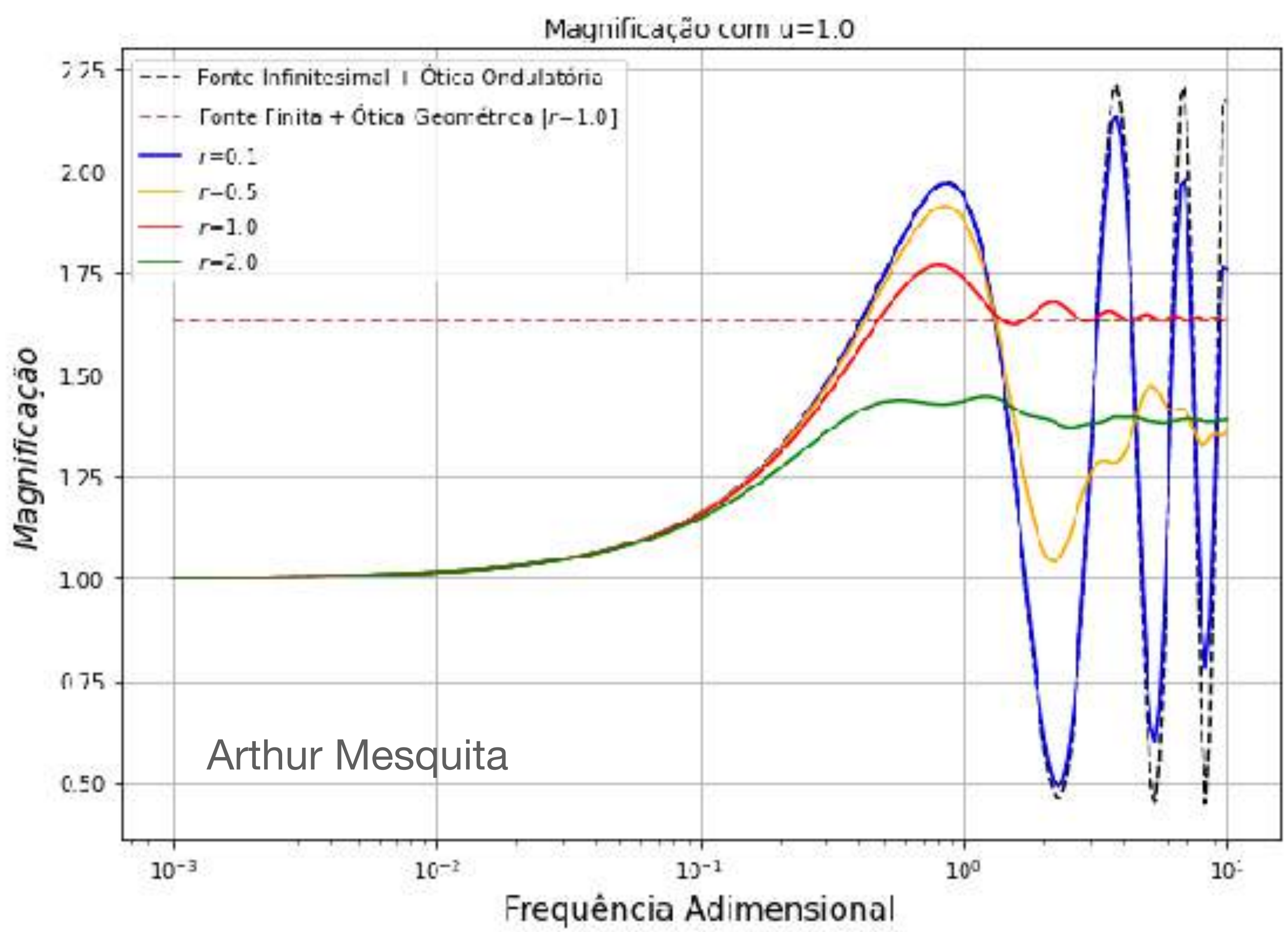

Femtolensing: wave optics

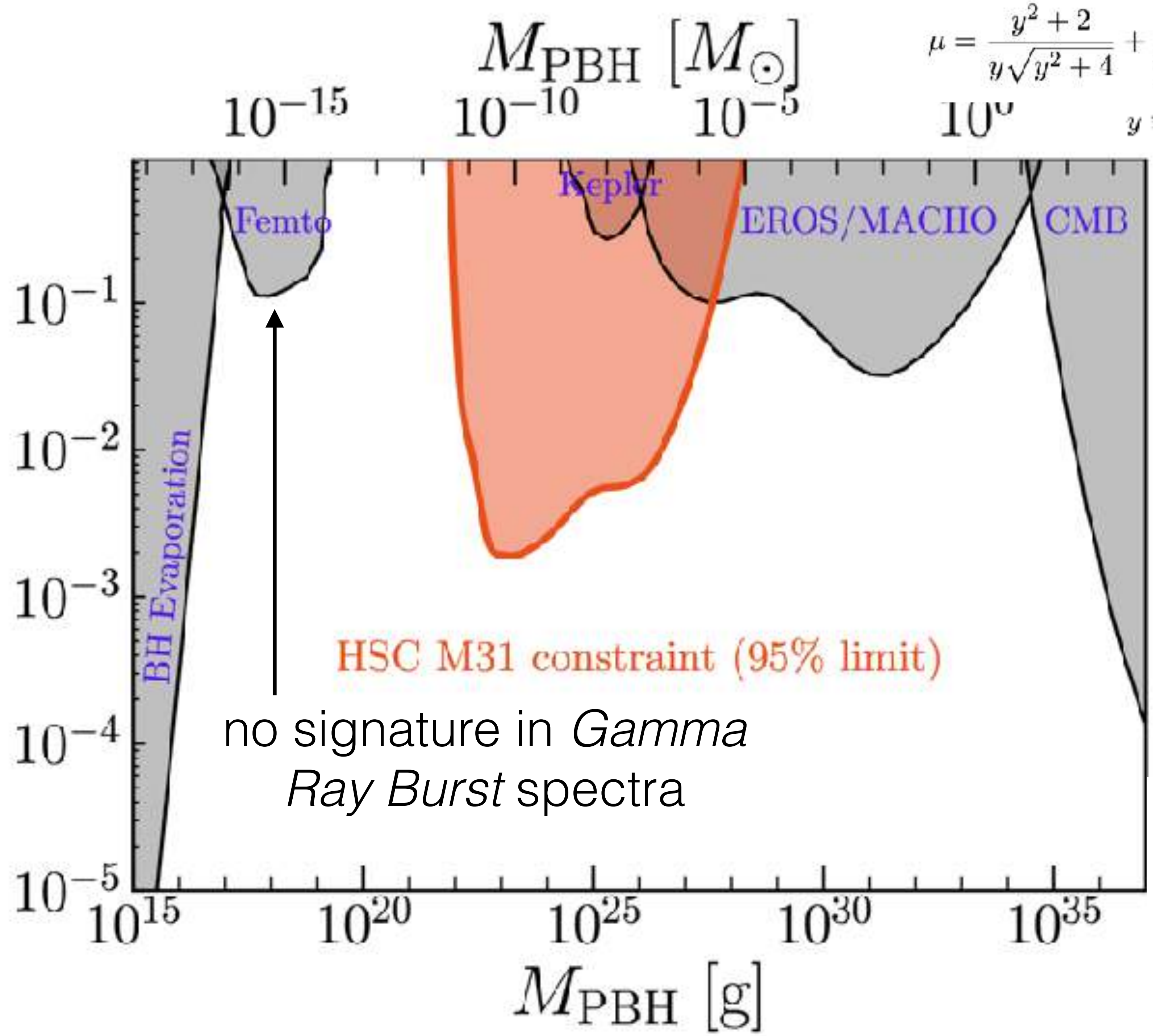

no signature in *Gamma Ray Burst* spectra

$$\mu = \frac{y^2+2}{y\sqrt{y^2+4}} + \frac{2}{y\sqrt{y^2+4}} \sin\left(\Omega\left[\frac{y\sqrt{y^2+4}}{2} + \log\left|\frac{y+\sqrt{y^2+4}}{y-\sqrt{y^2+4}}\right|\right]\right)$$

$$y = \beta/\theta_E$$

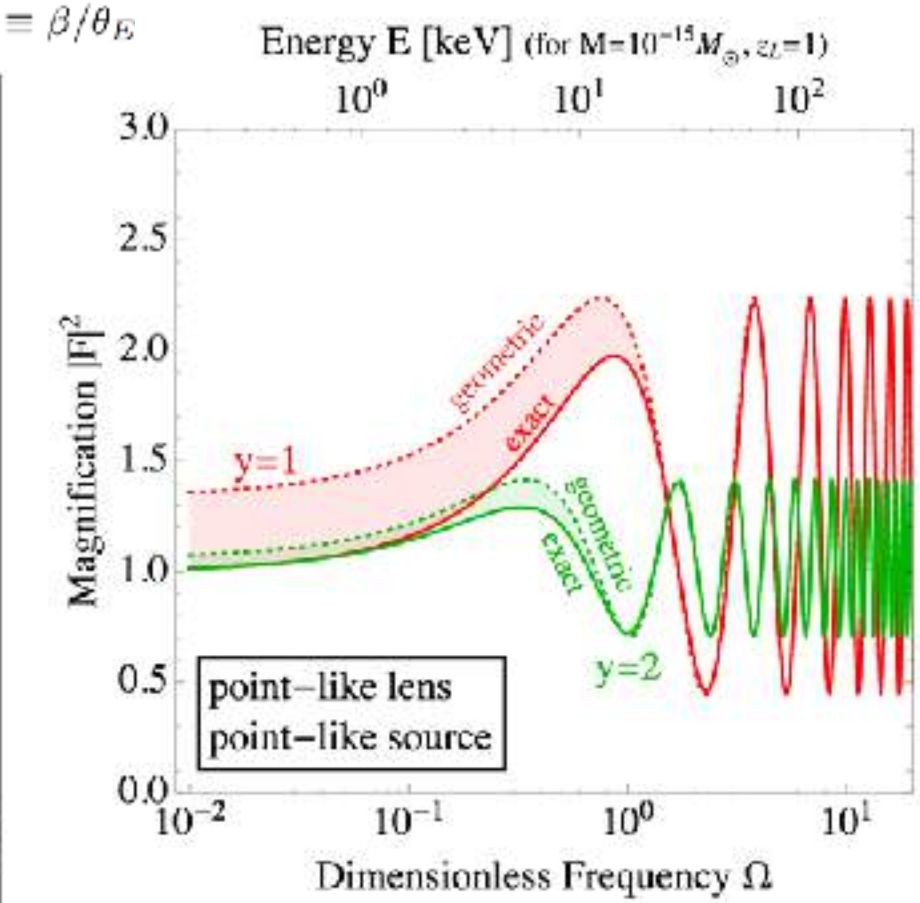

$$\Omega \equiv \frac{1}{c}\frac{D_S D_L}{D_{LS}}\theta_0^2(1+z_L)\,\omega \equiv \Delta t_0\,\omega\,.$$

arXiv:1701.02151v3

Femtolensing: wave optics

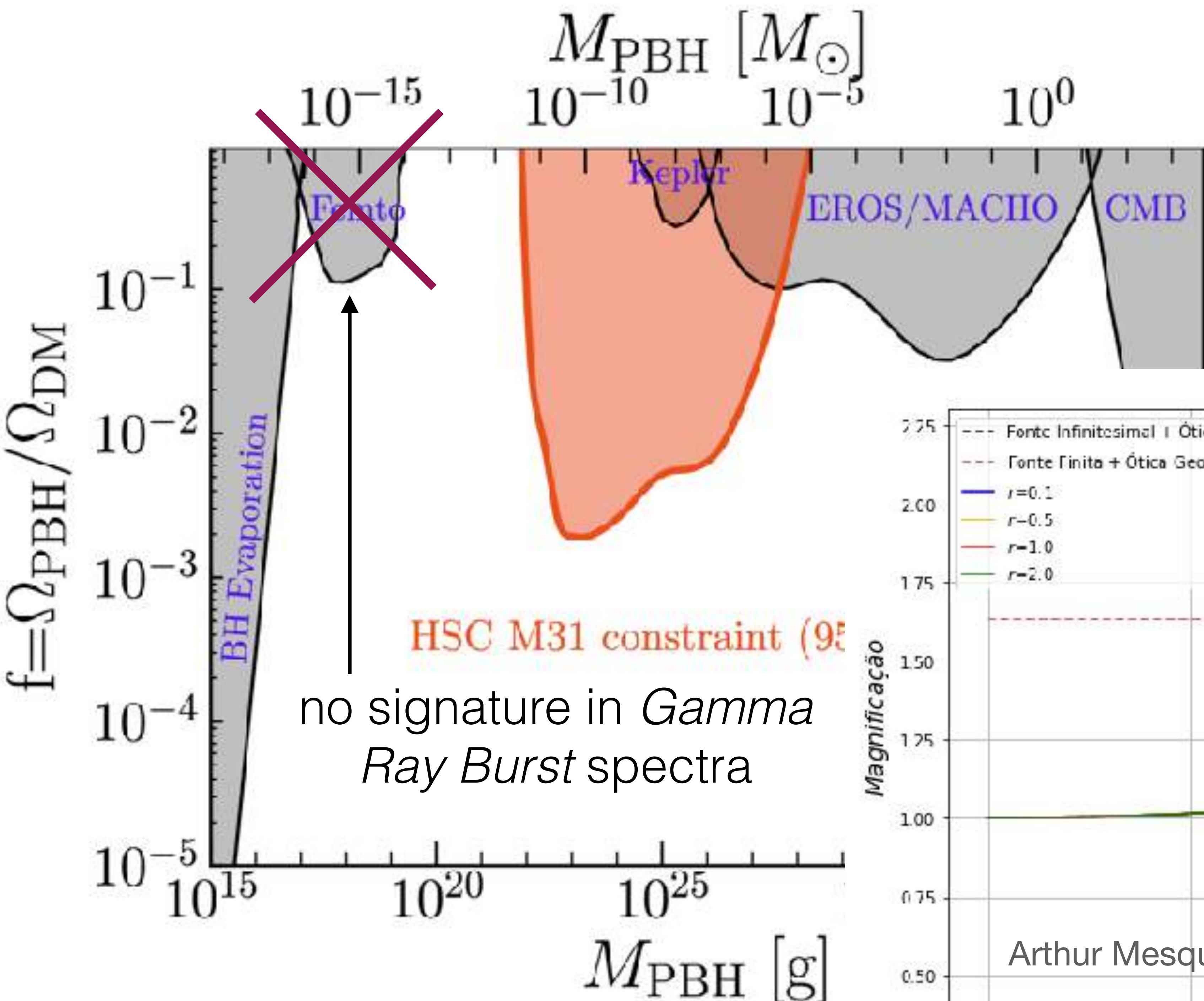

no signature in *Gamma Ray Burst* spectra

arXiv:1701.02151v3

Finite size effects destroy the signal!

arXiv:1807.11495

Projections for femtolensing of GRB: arXiv:1807.11495

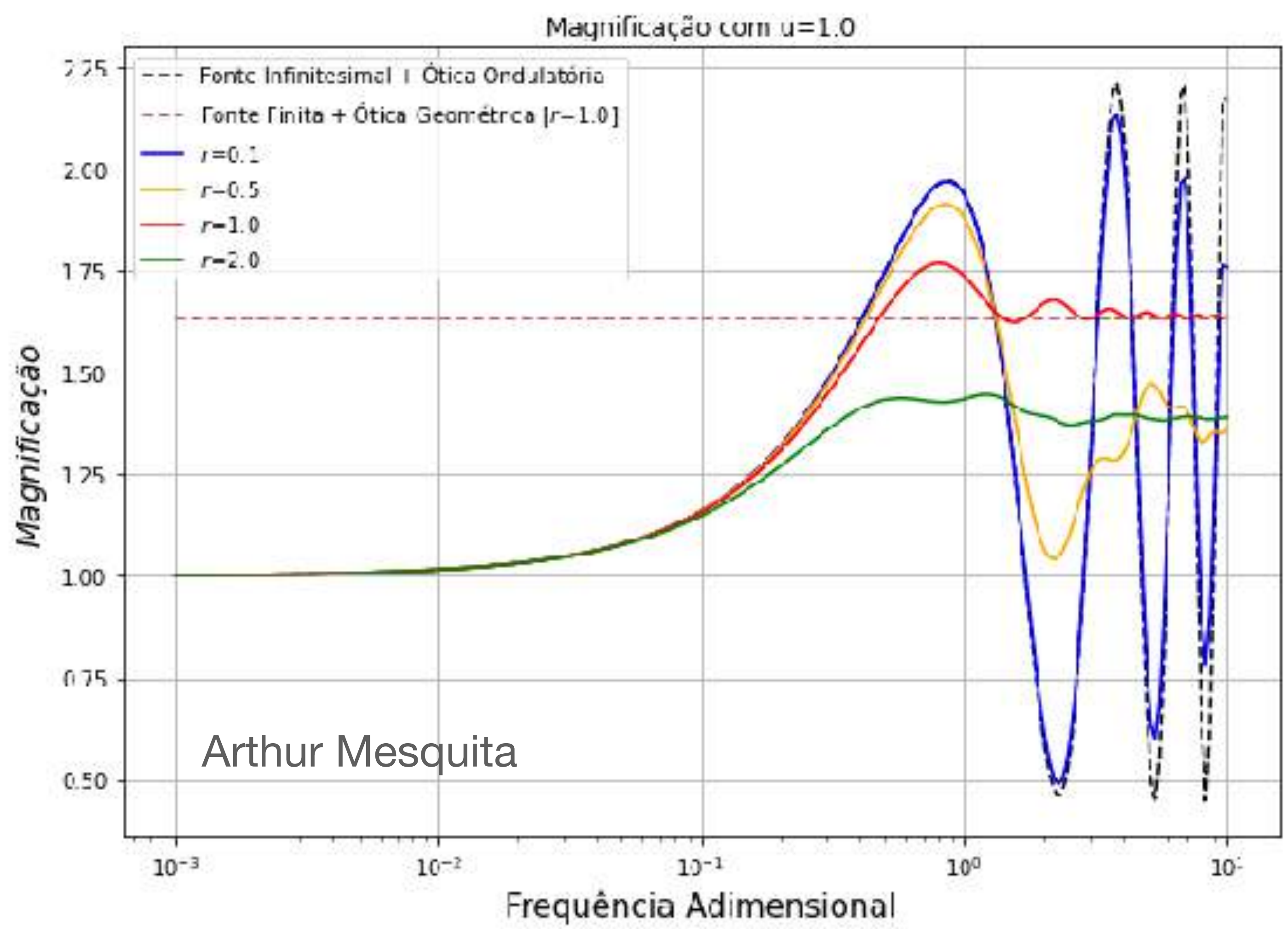

Limits on the fraction of Dark Matter in condensed objects

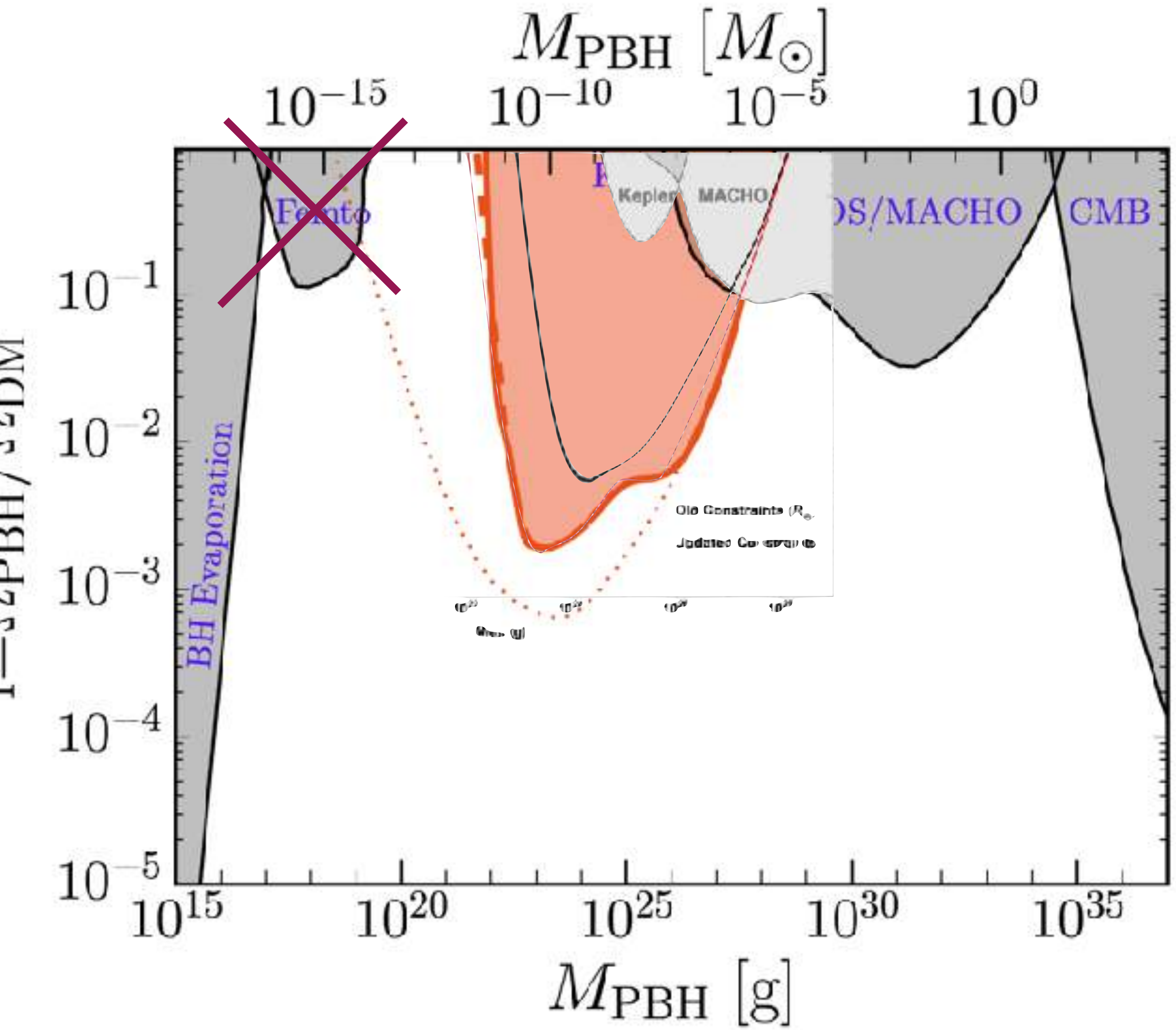

Can we improve over the low mass limits with higher cadence observations of M31?

Rubin micro-survey?

(Anibal Varela, Arthur Mesquita)

Original femtolensing limits destroyed by finite source effects

Femtolensing

Wave-optics effects in gravitational lensing

- Oscillations on the magnification induce oscillations in the spectrum

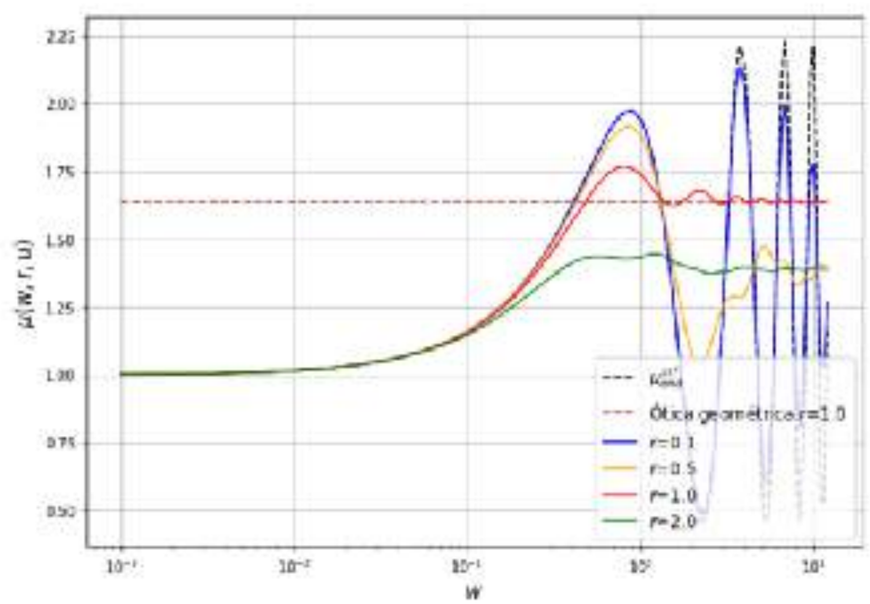

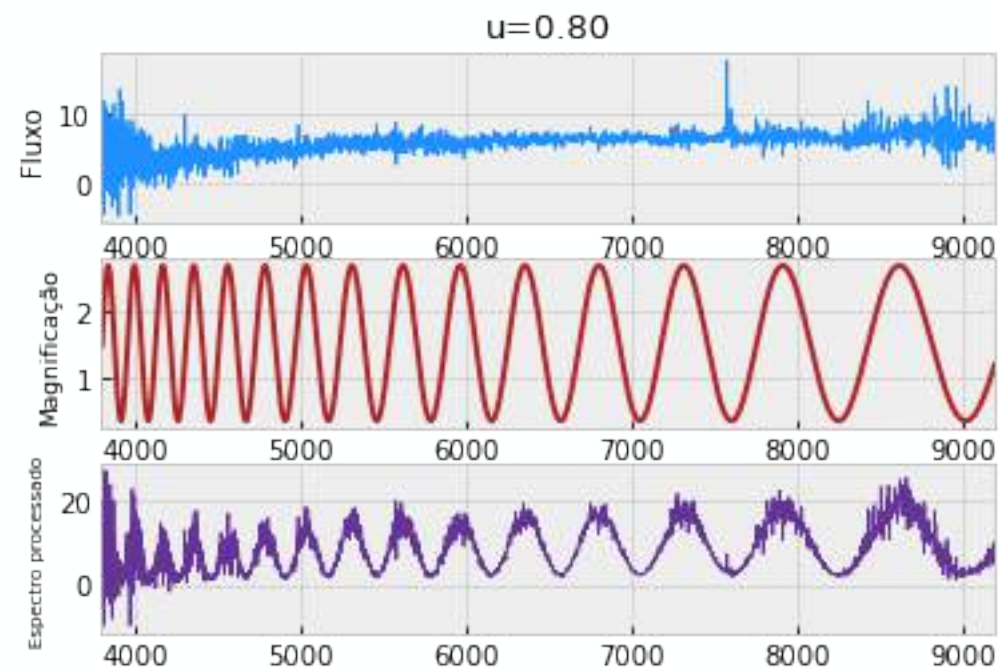

- Schwarzschild radius comparable to wavelength
- Finite source size breaks effect
- **Exploring observability for DM and lensing by exoplanets and extragalactic sources!**

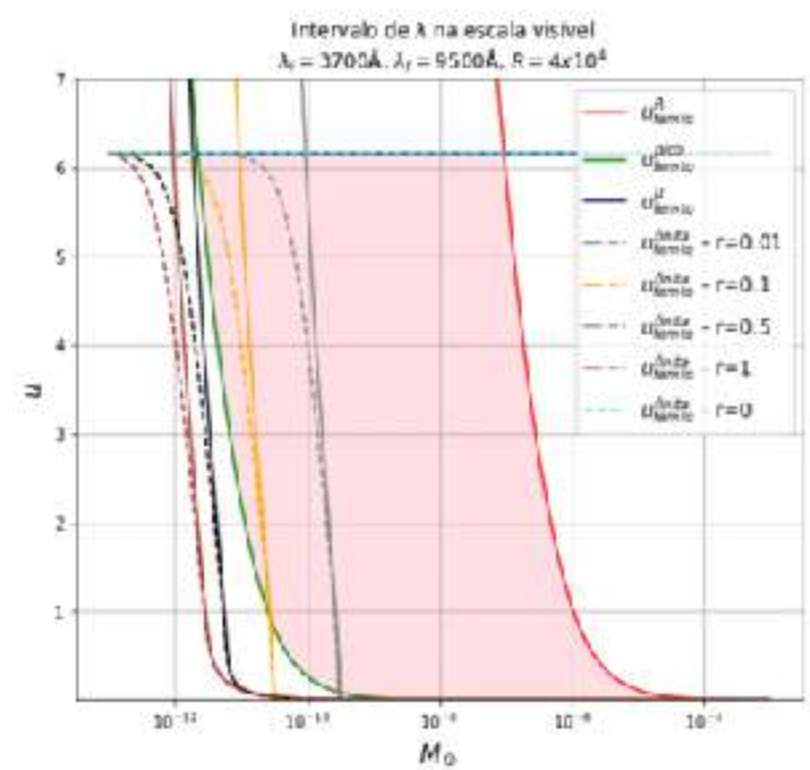

Detectability conditions

Presence of clear oscillatory patters sets constraints on the *u* x lens mass parameter space

- Depends on the wavelength and resolution of the instrument

SETI	Radio	$[3 - 30]\times10^8$	5×10^8
ALMA	Submm	$[3 - 35]\times10^6$	3×10^7
VLT (CRIRES)	IR	$[1 - 5]\times10^4$	1×10^5
VLT (FLAMES)	Optical	3700 - 9500	4×10^4
HST (GHRS)	UV	1150 - 3200	1×10^5
Chandra X-Ray (LETG)	X-ray	50 - 160	1×10^3
INTEGRAL (SPI)	γ-ray	10^{-3} - 0.1	5×10^2

Arthur Mesquita, CBPF

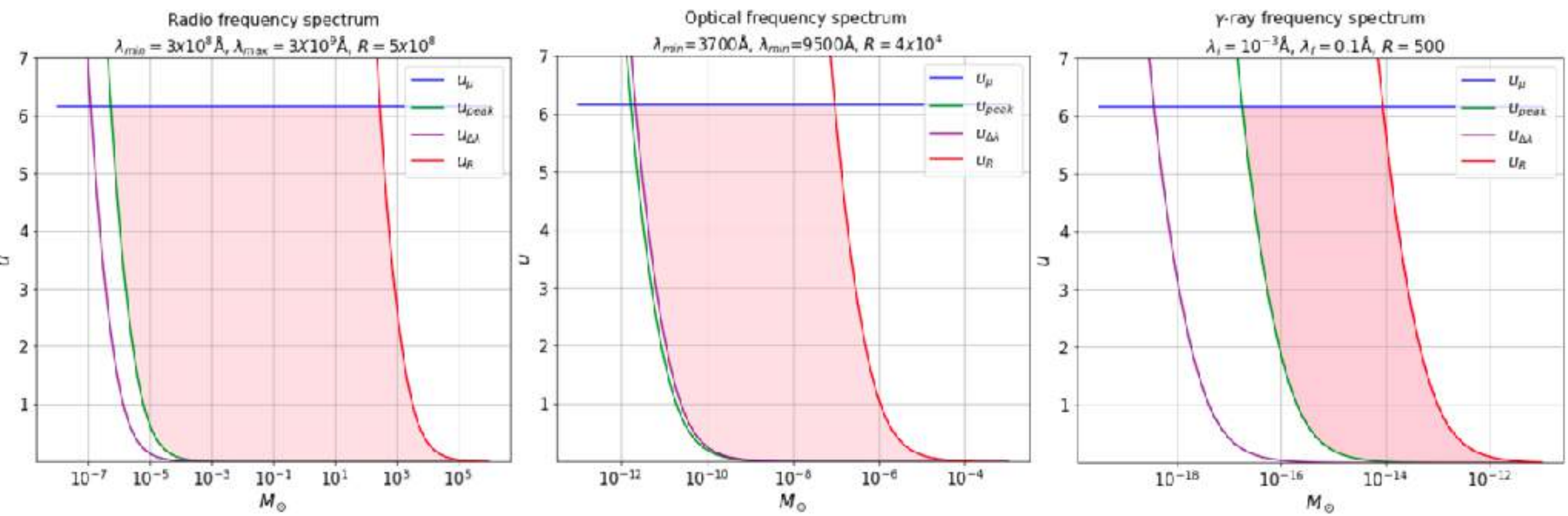

Arthur Mesquita, CBPF

Finite sources

Finite size effects destroy the signal for incoherent sources

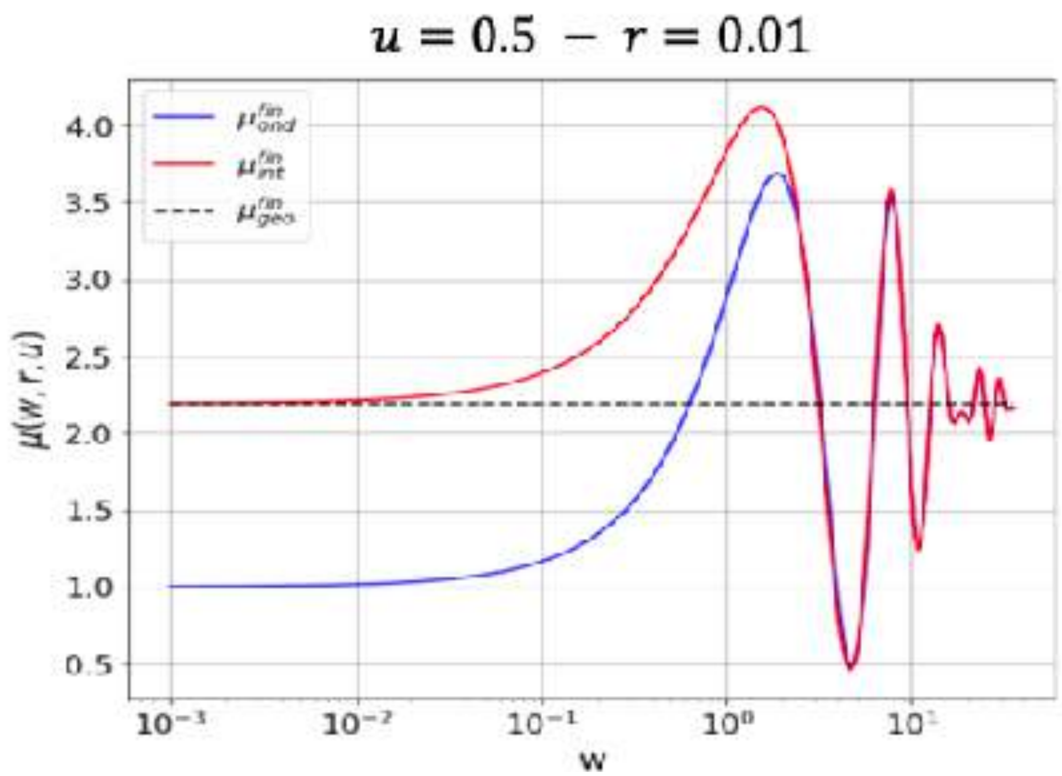

Source	r_S	
Neutron Star	$\sim 10^4$m	Local Universe
White Dwarf	$\sim 10^6$m	
Main Sequence Star	$\sim R_\odot$	
Kilonova	$\sim 10^5$m	Cosmological Universe
sGRB e GRB (short/large γ-ray burst)	$\sim [10^8, 10^9]$m	
Supernova	$\sim 10^{12}$m	

Sources in the local Universe

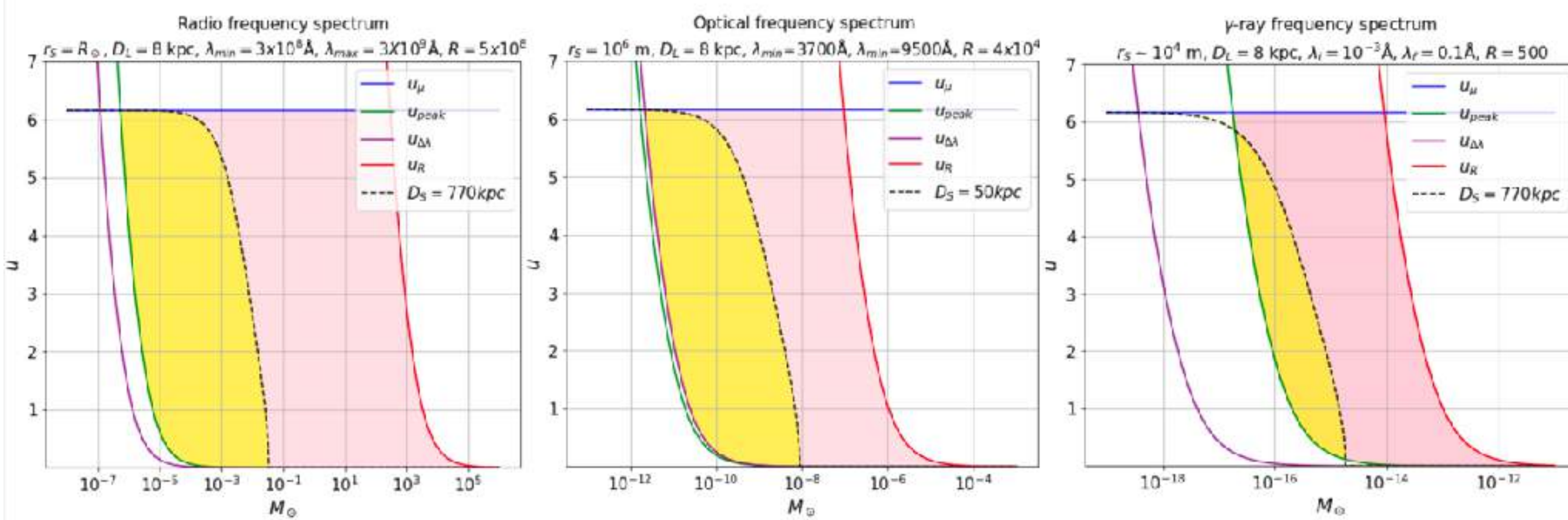

Gravitational Waves

Ondas gravitacionais

Relatividade geral: métrica $$ds^2 = g_{\mu\nu} dx^\mu dx^\nu$$

Perturbação do espaço plano: $$g_{\mu\nu} = \eta_{\mu\nu} + h_{\mu\nu}$$

Equações de Einstein $$G_{\mu\nu} = \frac{8\pi G}{c^4} T_{\mu\nu}$$

No regime linear: $$\Box h_{\mu\nu} = -16\pi T_{\mu\nu}$$

Coalescência de buracos negros

"solo tengo adentro, soy un pobre agujero"
León Gieco

- Intenso (objetos massivos, altas velocidades)
- Sinal muito característico em frequência e amplitude (simulações computacionais + teoria)
- Independente de qualquer outra física

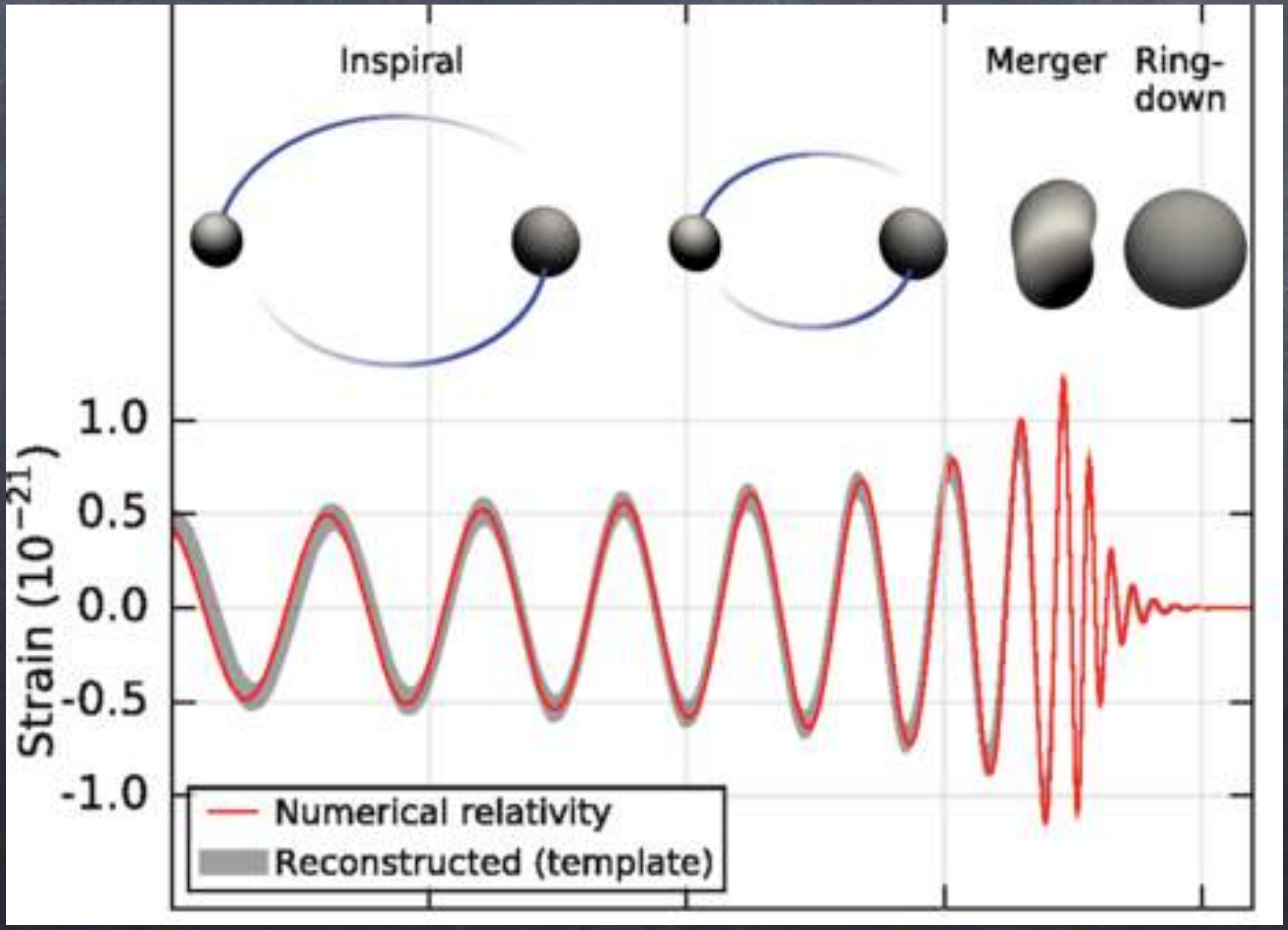

Coalescência de buracos negros

“solo tengo adentro, soy un pobre agujero”
León Gieco

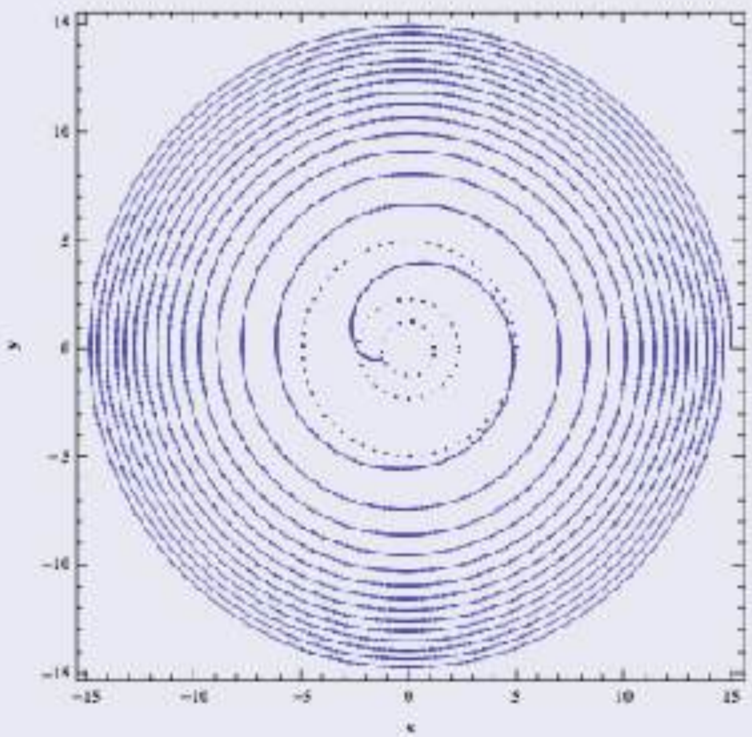

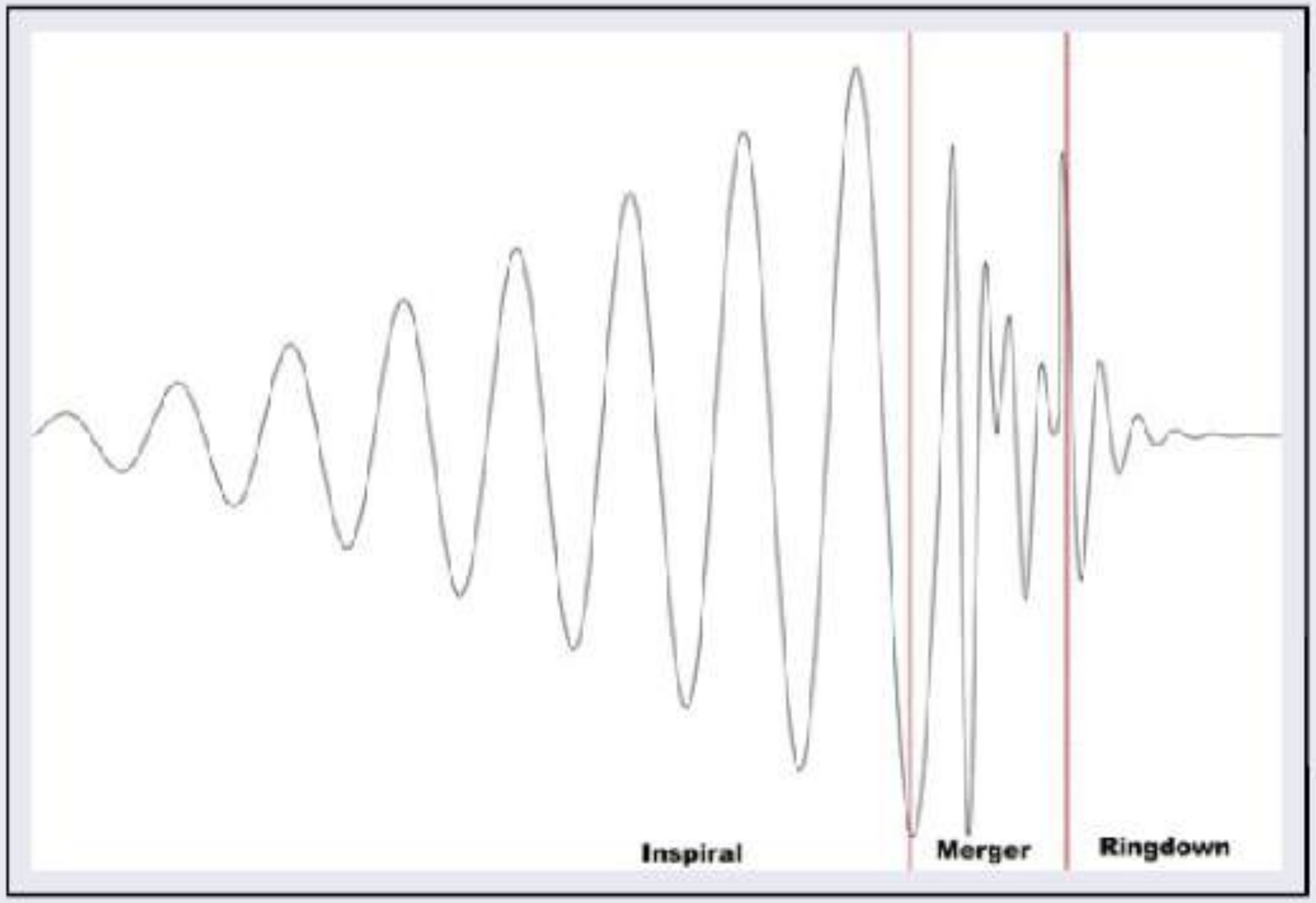

- Assinatura clara e característica
- Templates de relatividade numérica
- Numérico + métodos perturbativos

Prêmio Nobel de 2017!

"for decisive contributions to the LIGO detector and the observation of gravitational waves"

© Nobel Media AB. Photo: A.Mahmoud	© Nobel Media AB. Photo: A.Mahmoud	© Nobel Media AB. Photo: A.Mahmoud
Rainer Weiss	Barry C. Barish	Kip S. Thorne
Prize share: 1/2	Prize share: 1/4	Prize share: 1/4

O evento de 17/08/2017

- Busca de contrapartidas óticas, com telescópios
- Virgo em ação: localização da fonte e imagens, inclusive DECam
- Confirmação das ondas gravitacionais
- Fusão de duas estrelas de nêutrons **formando** um buraco negro

  M_1 = 1.4-2.3 M_{sol}, M_2 = 0.9-1.4 M_{sol}
- Formação de elementos pesados

  16.000 a massa da Terra!

  10x em ouro e platina

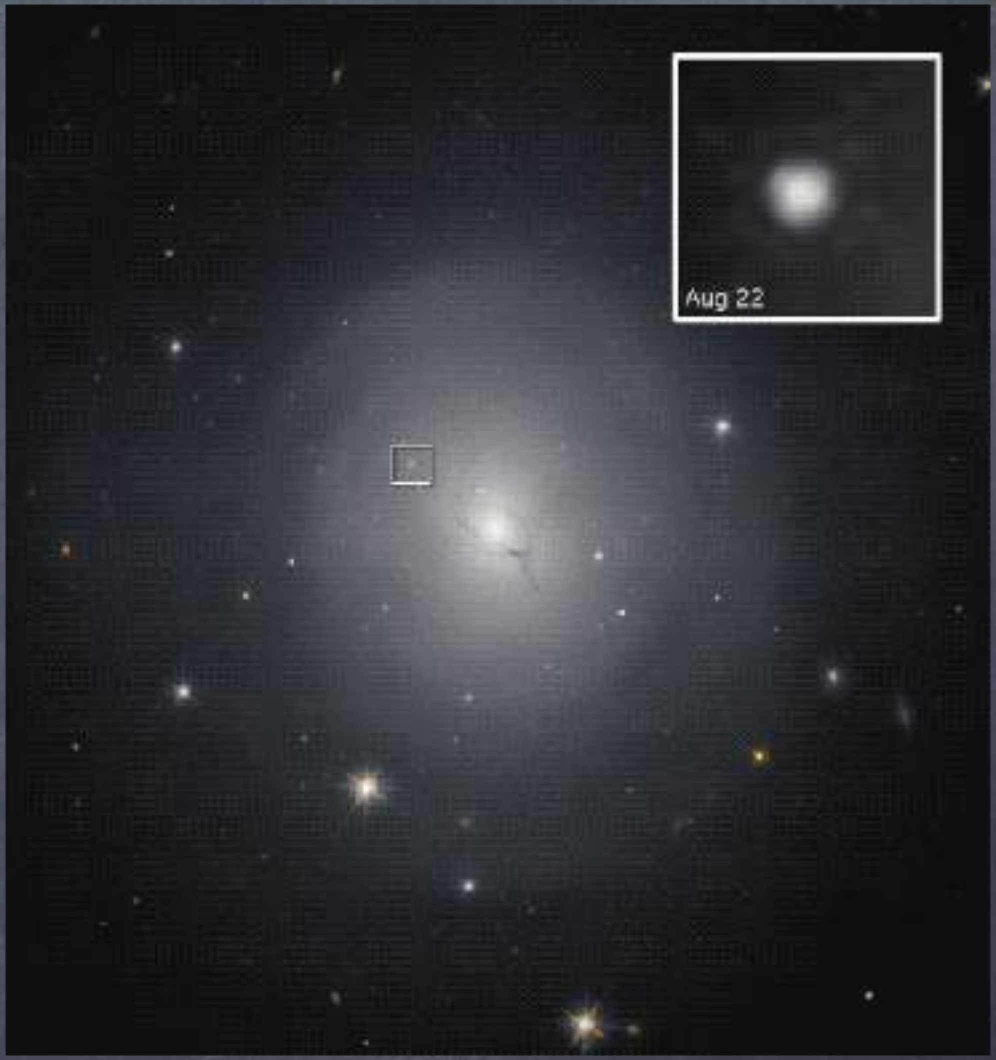

Contrapartidas óticas: kilonovae!

Lensing of Gravitational Waves

Lensing of Gravitational Waves

- GW are tensor waves but strain (amplitude) follows same lensing equations
- Detected in interferometers
- Regimes of GW lensing
    - **Magnification:** statistical or individual

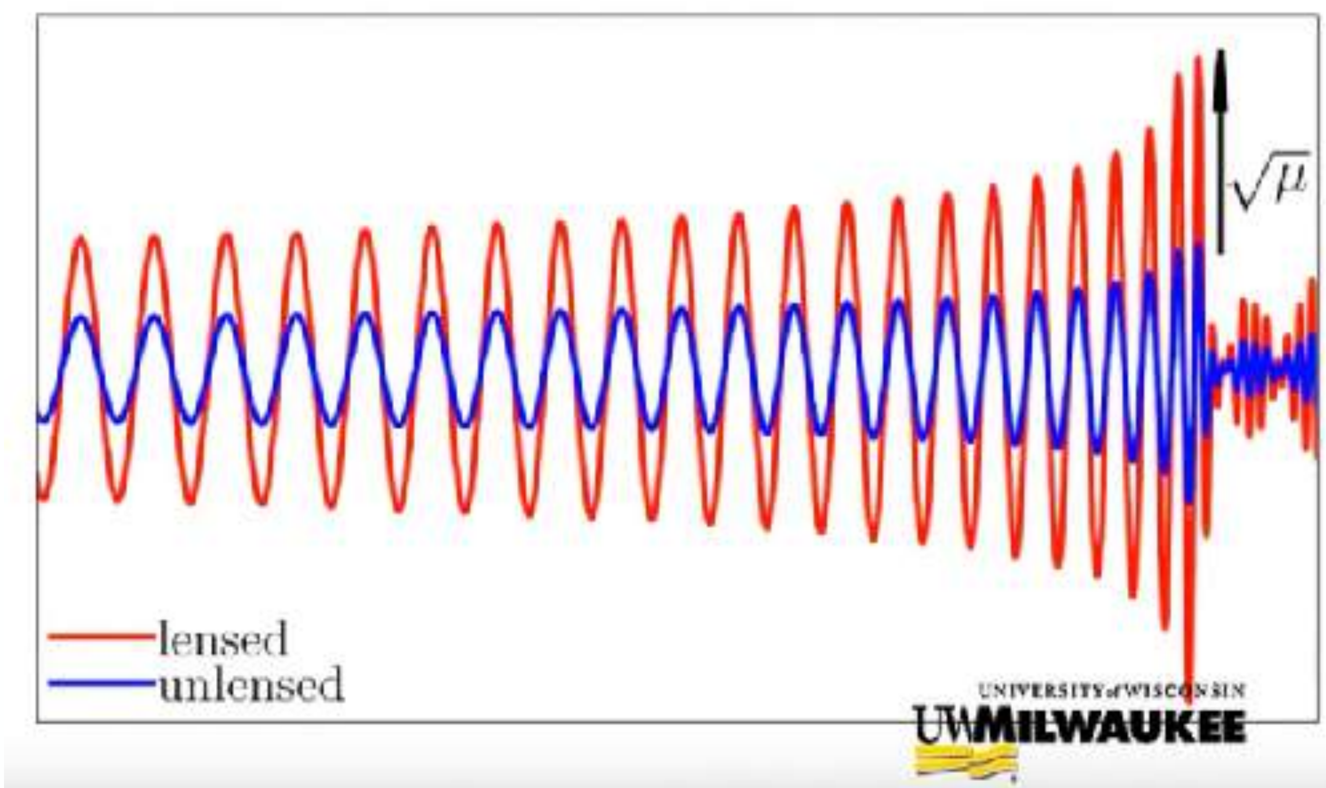

- could explain mass gap events?

Regimes of GW lensing

- Magnification: statistical or individual
  - could explain mass gap events?
- Strong Lensing (lens is galaxy or cluster): multiple images
  - different arrival times and different magnifications

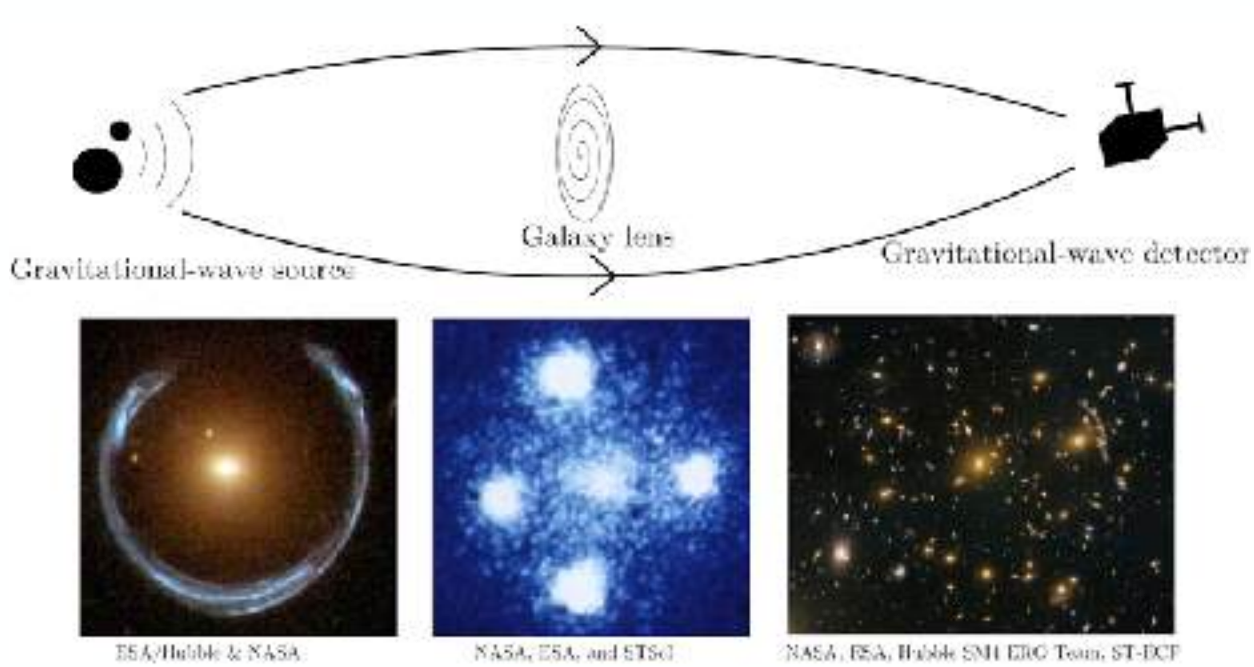

https://www.ligo.org/science/Publication-O3aLensing/images/O3aLensing-Fig1.png

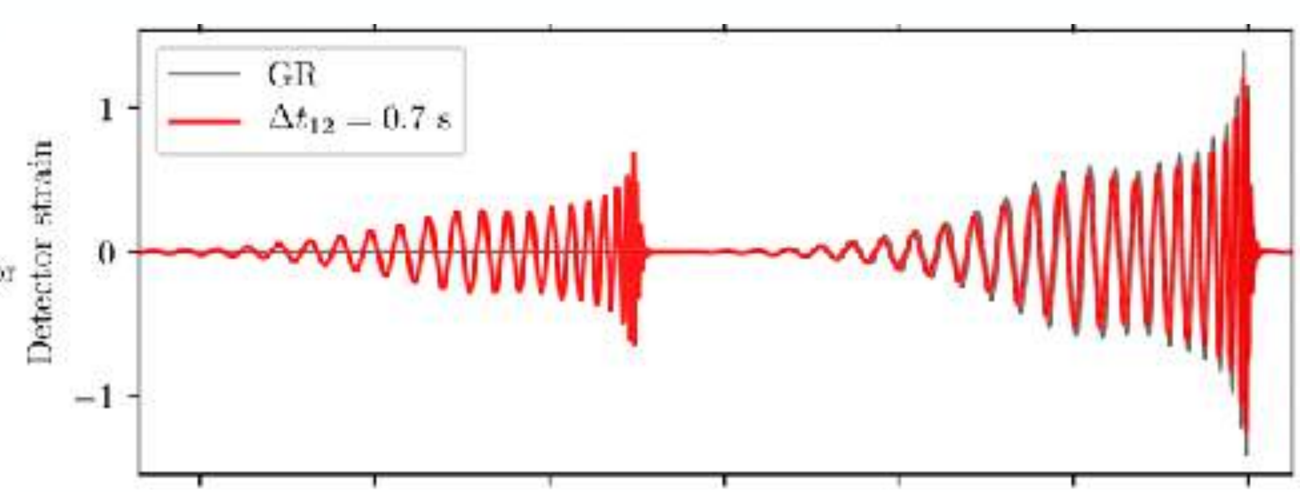

Ezquiaga & Zumalacárregui, PRD 102, 124048 (2020)

typical time delays from minutes to months

Regimes of GW lensing

- Magnification: statistical or individual
  - could explain mass gap events?
- Strong Lensing (lens is galaxy or cluster): multiple images
  - different arrival times and different magnifications
- Microlensing (lens is a massive BH):
  - frequency dependent magnification: beating pattern

$$h_{\mathrm{ML}}(f, \theta_{\mathrm{s}}, \theta_{\mathrm{ML}}) = F(f, M_{\mathrm{ML}}^{z}, y) \times h_{\mathrm{U}} \quad (f, \theta_{\mathrm{s}})$$

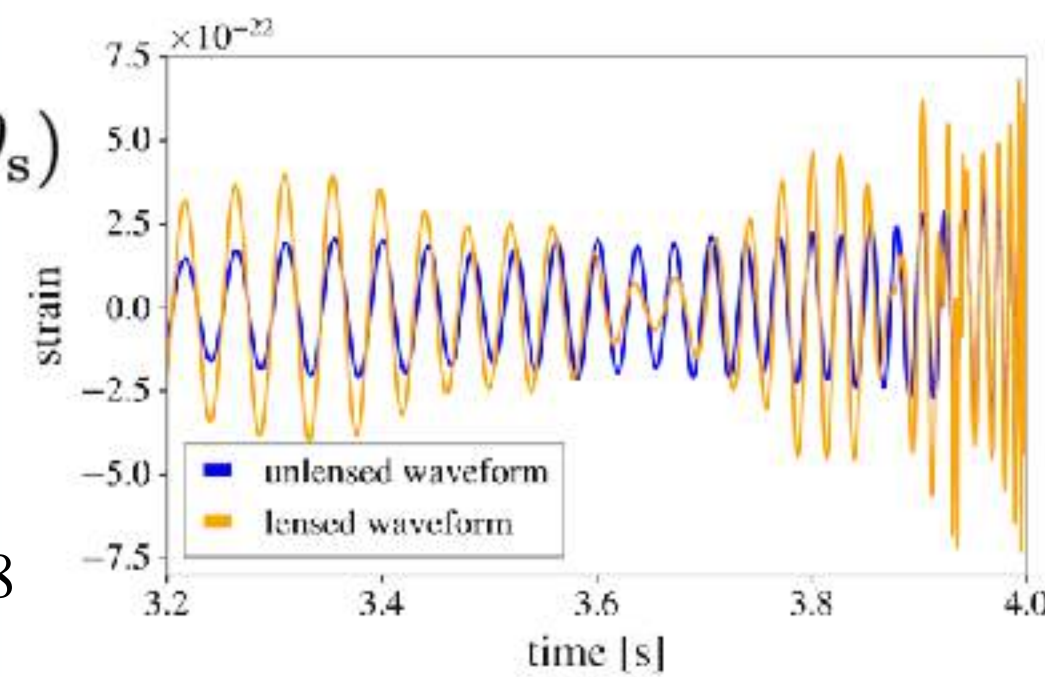

arXiv:2110.03308

Strong Lensing of Gravitational Waves

- Expected numbers
  - LIGO design sensitivity: 1/year
  - Einstein Telescope: ~ 100/year (out of 10^4-10^5 GWs)
- Excellent time delay determination
- Absolute (waveform reconstruction) + Relative strains
- No spatial resolution

Lensed GW with EM counterpart: prospects for cosmology

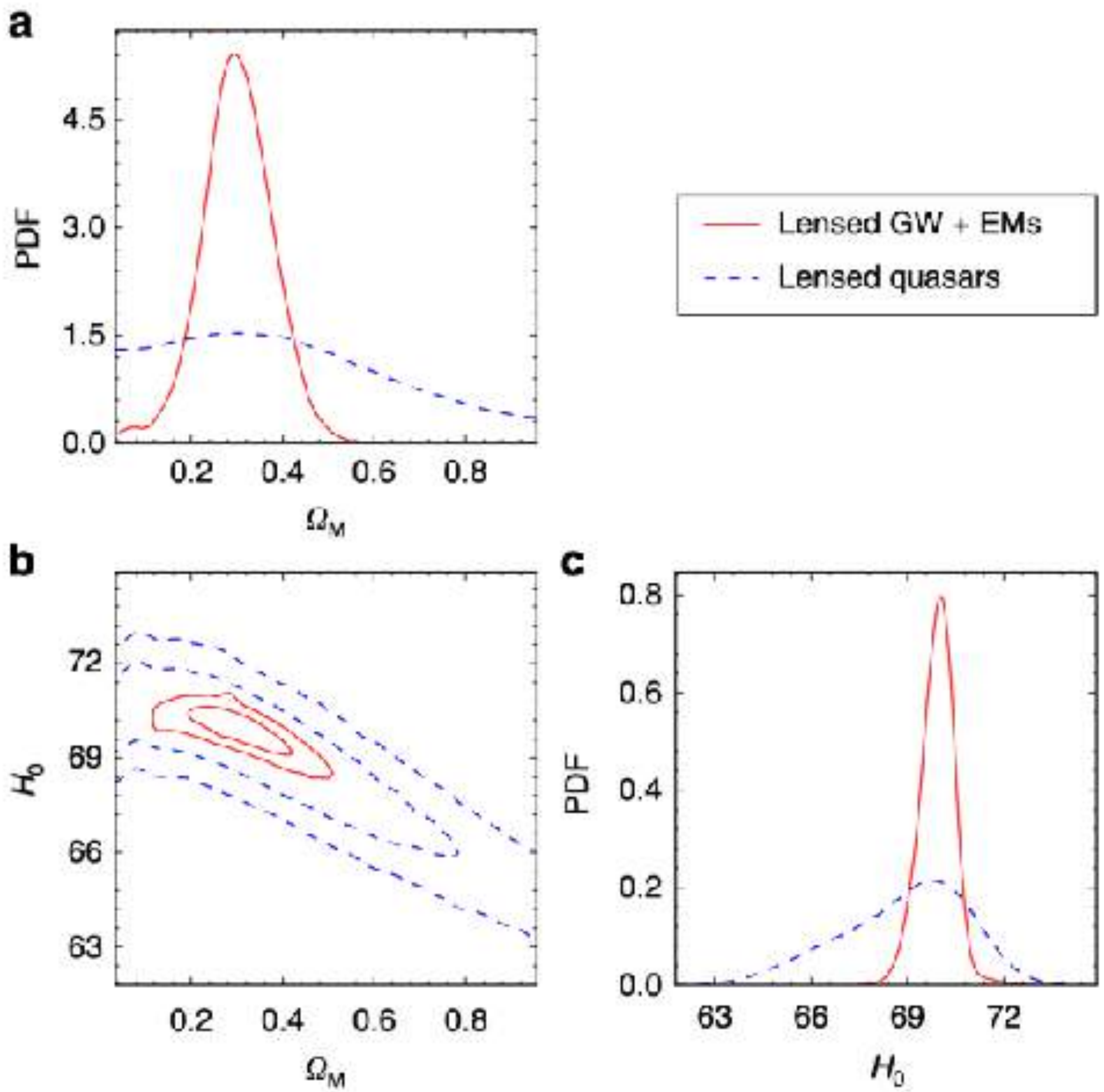

- Typically optical counterparts (MMA)
- Extremely valuable
- Extensive follow-up program
- Only GW170817 for now
- Example not using standard siren:
  - Waveform independent
  - Better reconstruction (transient goes away)
  - < 0.7% determination of H_0 from 10 Strongly Lensed BBH!

Liao et al., Nature Communications, 8, 1148 (2017)

Lensed GW with EM counterpart: prospects for cosmology

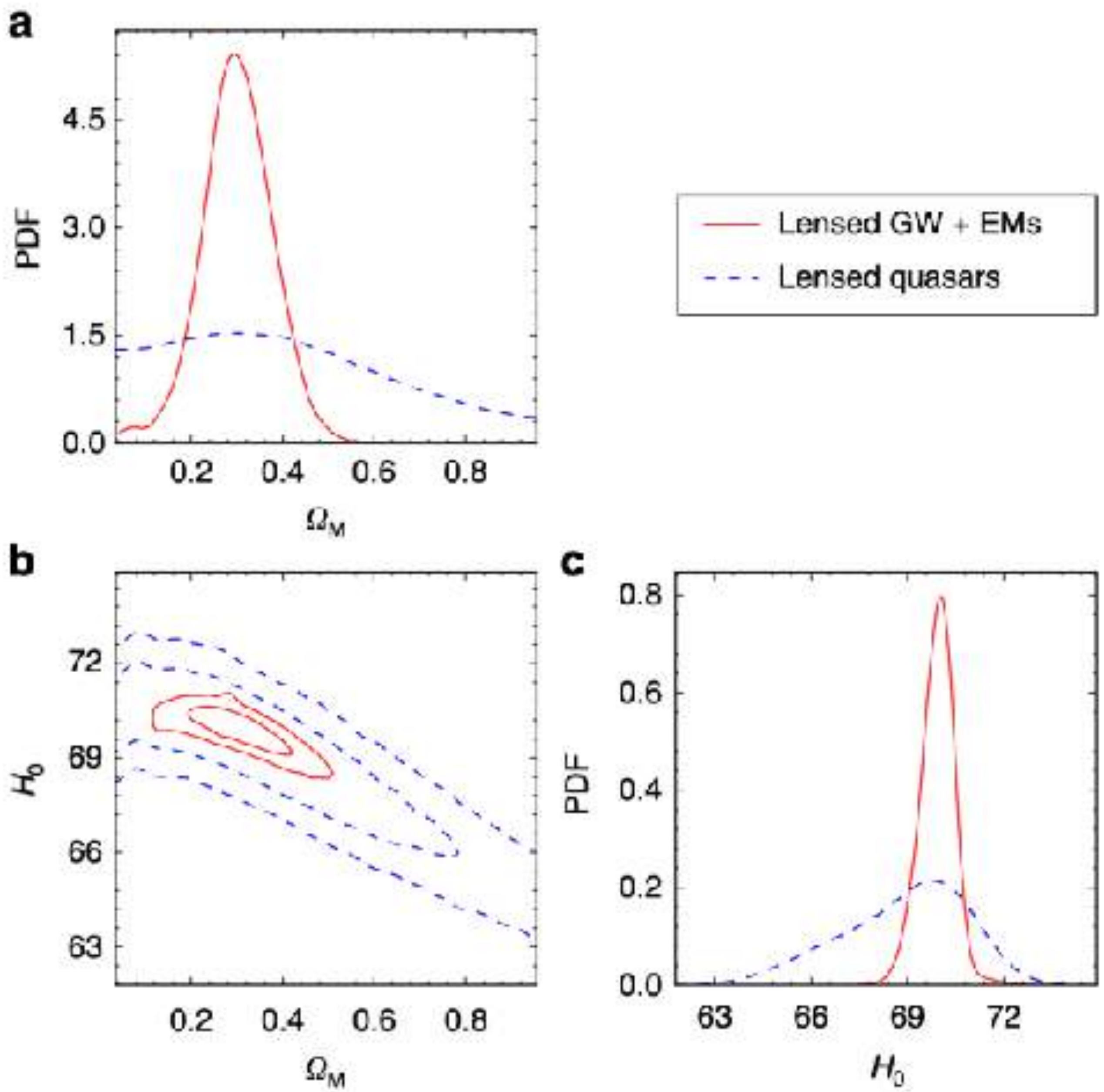

Liao et al., Nature Communications, 8, 1148 (2017)

- Compare to GW170817 standard siren (complementary to)

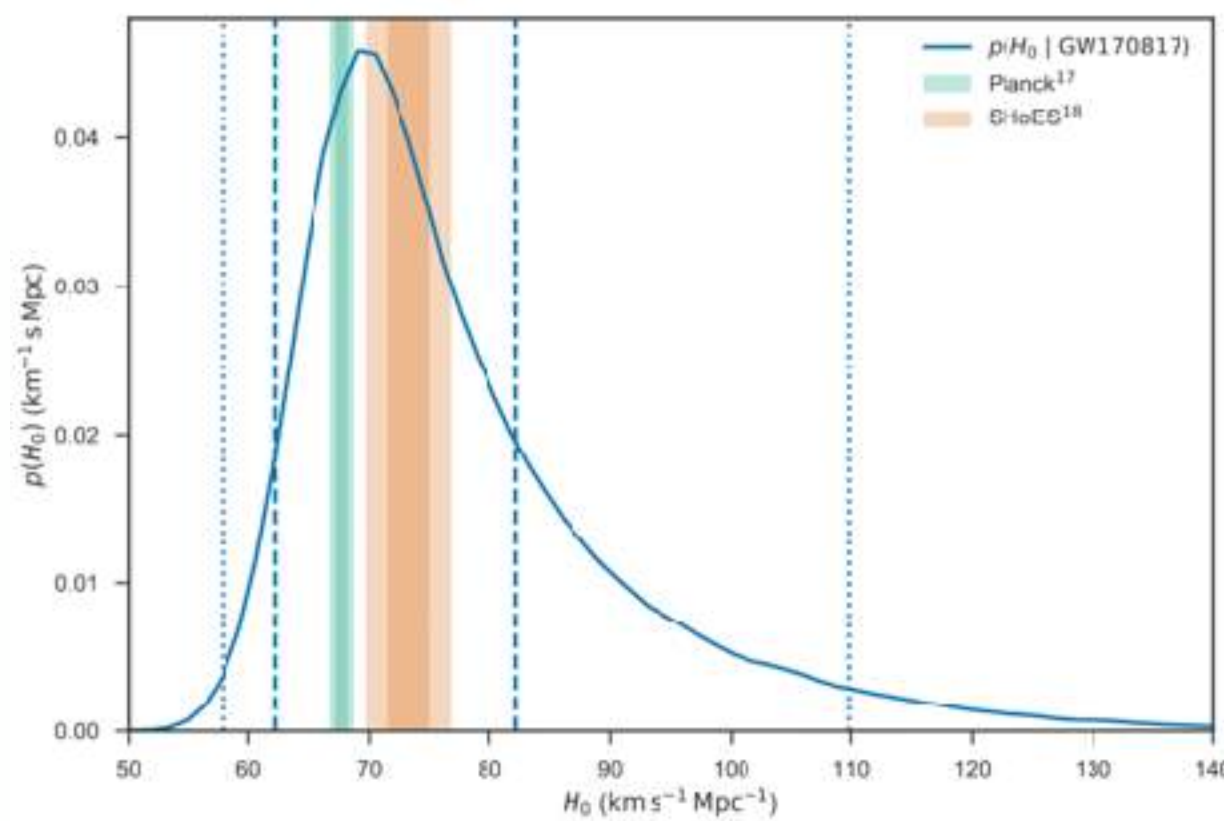

LIGO, Nature 551, 85 (2017); arXiv:1710.05835

Lensed GW with no EM counterpart

- BBH much more frequent than Kilonovae
- Localization is bad

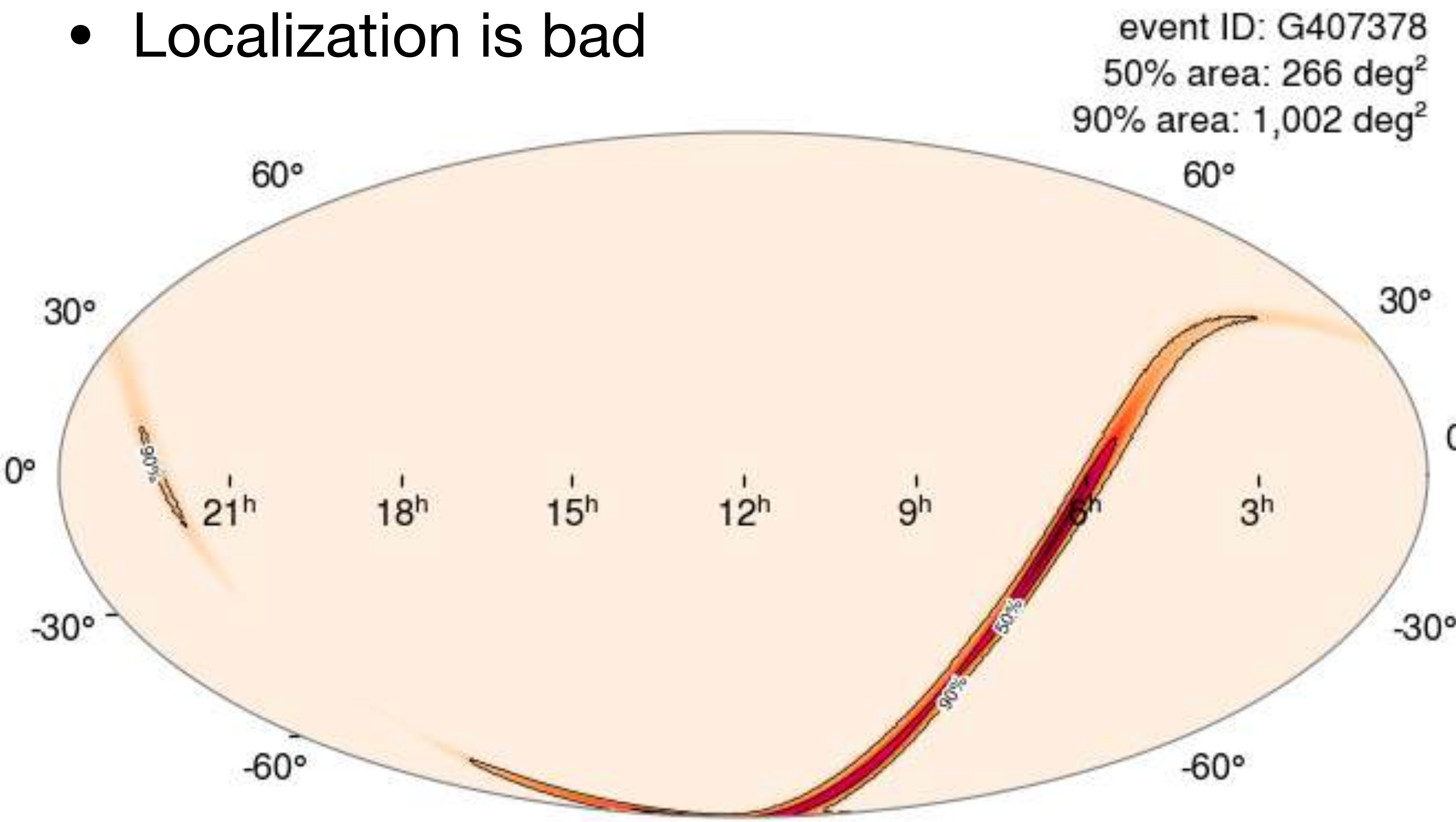

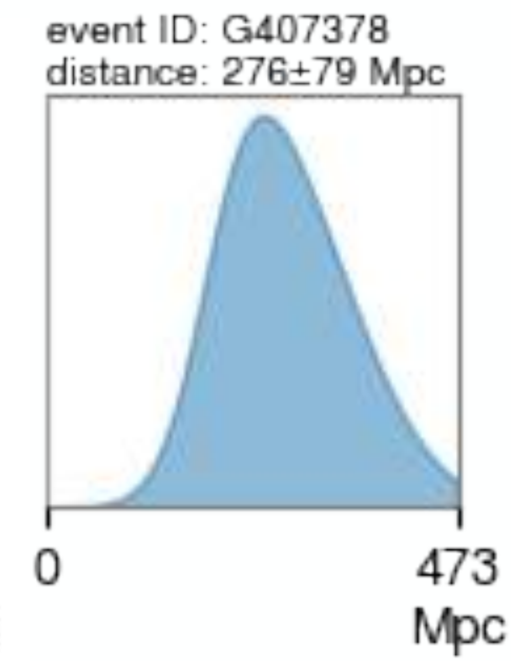

https://gracedb.ligo.org/superevents/S230518h/

Localization

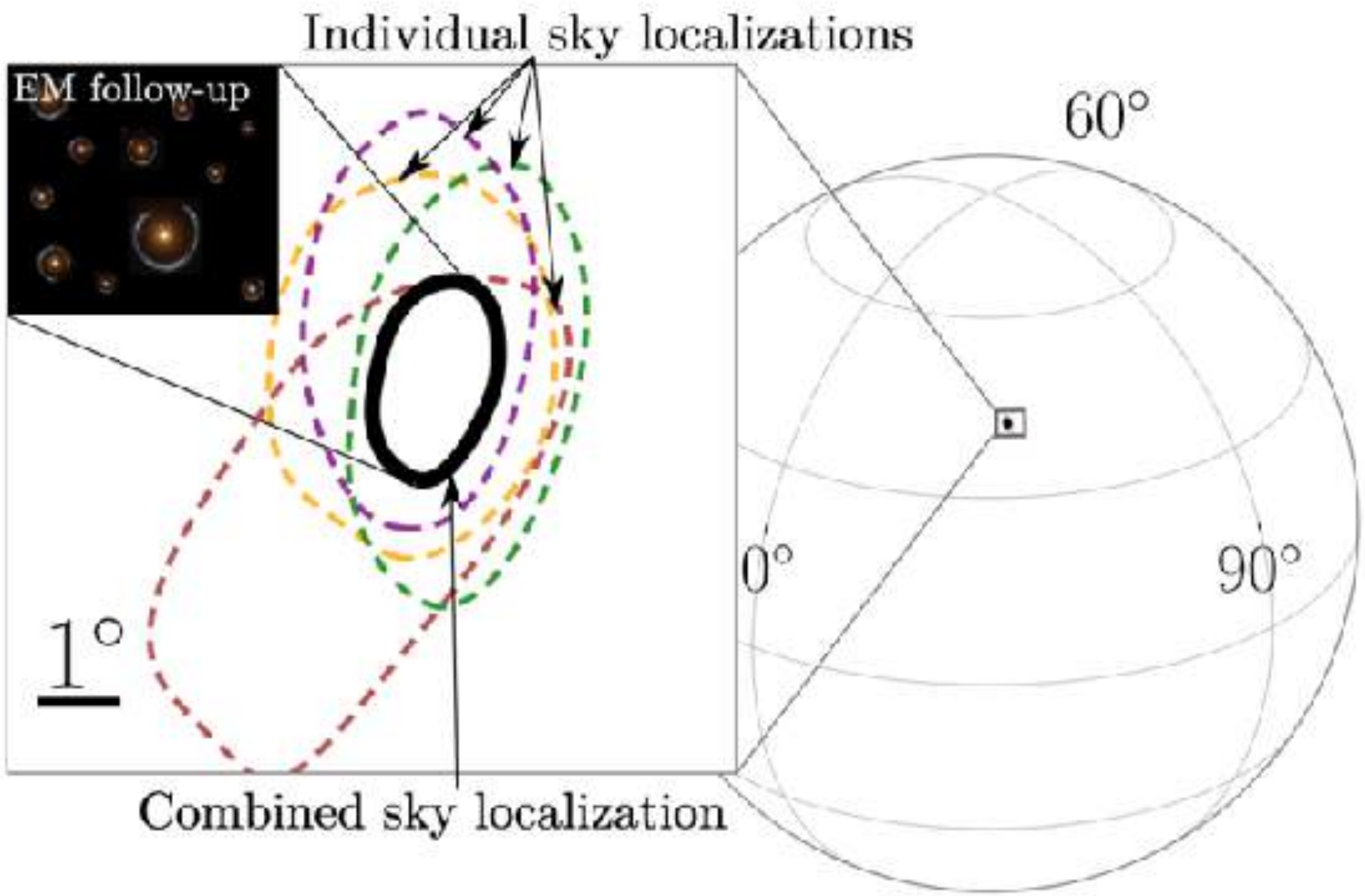

arXiv:2004.13811

- Needs spectroscopic data of both lens and source galaxies
- High resolution imaging of candidate(s)
- Important optical follow-up program (MMA)

- If GW is strongly lensed, its host galaxy should be too!
- Strong Lenses are rare, yet, still ~ 100/sq-deg
- Use relative time-delays and strains to pin-point the right system!
- Use quadruply imaged systems
- Relies on detection of all strongly lensed galaxies to required depth

Lensed Binary Black-Holes

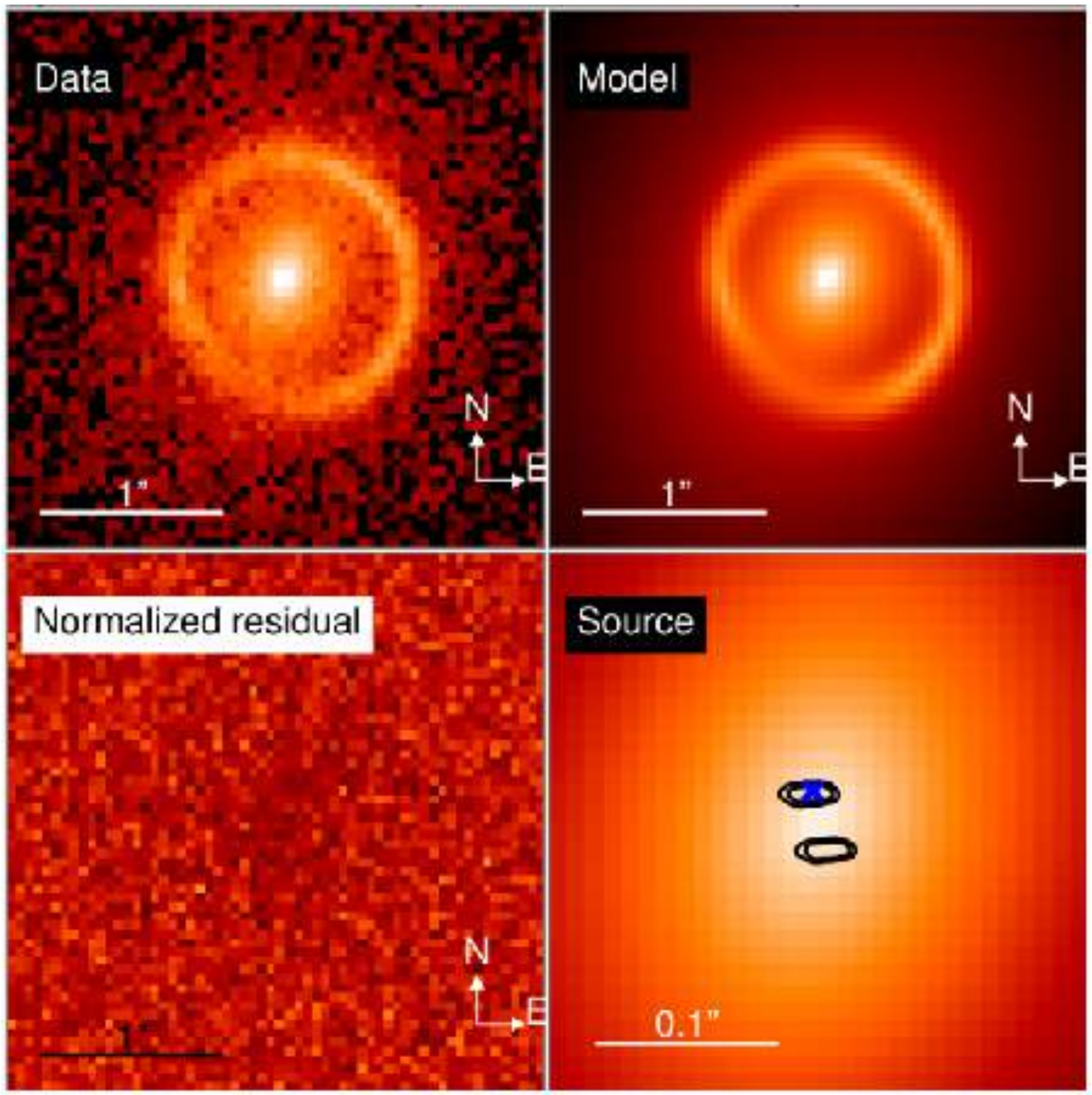

arXiv:2004.13811

- Source and lens potential reconstruction from high resolution imaging
- Extra constraints from relative magnifications and time-delays
- BBH localization within the host galaxy!
- 10% determination of H_0 from a single Strongly Lensed BBH!

Lensed Binary Black-Holes

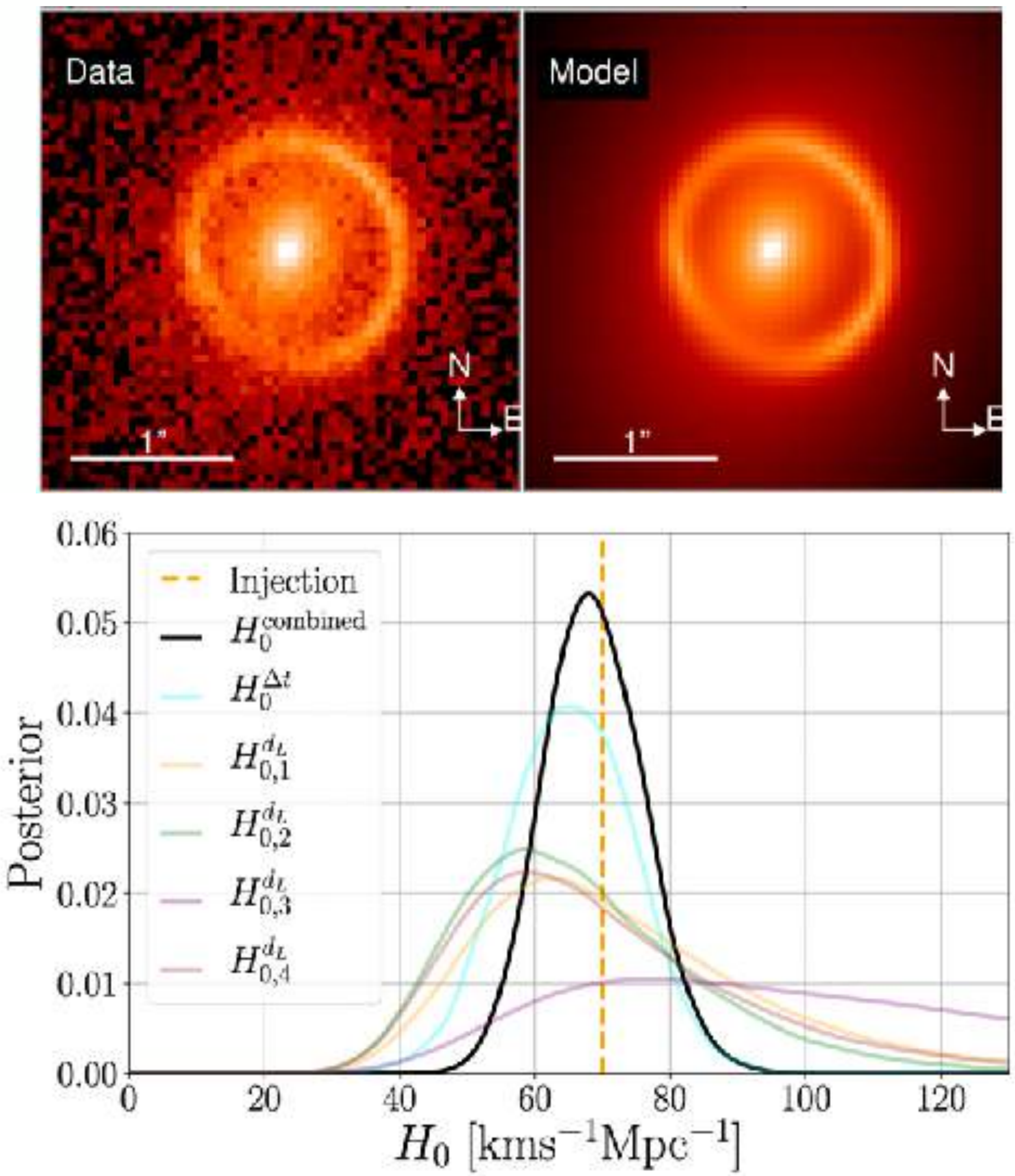

arXiv:2004.13811

- Source and lens potential reconstruction from high resolution imaging
- Extra constraints from relative magnifications and time-delays
- BBH localization within the host galaxy!
- 10% determination of H_0 from a single Strongly Lensed BBH!

Multi-messenger

- Kilonovae and dark sirens
  - look for repeating pattern in the strain data
  - Localization of Strongly Lensed transients (even without light!)
  - SL Gravitational Waves: ~ 1 in A+, ~ 100 in ET

Multi-wavelength

- Towards *wavelensing* detection!
- From microlensing LC, estimate physical parameters capable of producing wavelensing and choose follow-up accordingly
- Trigger from galactic and extragalactic microlensing events at the suitable wavelengths

Lensing with no images

- Transients offer a unique opportunity to discover invisible strongly lensed systems
- Distinct signal, the simplest being a repeating transient
- Localization region is usually much larger than optical
- But strong lenses are rare!
- Look up tables to identify the invisible lensed sources
- Key to model/predict time delay distributions
- Detailed modeling, precise time delay: improve localization
- Localization of the source even for dark sirens!
- Other possibly repeating signals: GRB, FRB…

Look-up table for lensing of transients

- Optical transients
  - Example Rubin transients prior to Strong Lensing finding (only need position)
  - Nonresolved observations (e.g. SN@ZTF, ongoing work)
  - System confirmation: prediction of time-delays from modeling
- Repeating signals
  - GRB, FRB, gravitational waves…
  - Does not need precise position
  - Predicted time delay distribution!
- Localization of the source even for dark sirens!

Summary

Strong Lensing:

Joint Arc sample for Investigations into Relativity:
Follow-up Observations and Implications
JAIR FOI

Microlensing:

Adding microlensing events to DP0 images:
MIcroLEnsIng Injection and Recovery Analysis
MILEI IRA

Comentarios Finales

- Durante el siglo XXI las lentes gravitacionales se han transformado de una curiosidad a promesa interesante y después a una herramienta fundamental en astrofísica
  - Los observables son deformaciones, imágenes múltiples, arcos gravitacionales, magnificación y desvíos temporales
  - Permiten estudiar las lentes, las fuentes y la geometría del Universo a grandes escalas
  - En particular, es un observable único para testear la gravedad modificada y la distribución de la matéria oscura en todas las escalas
- Es un área interdisciplinar, involucrando desde física fundamental hasta análisis de datos, incluyendo procesamiento de imágenes, estadística, simulaciones, *deep learning*, etc.
- Una miríada de fenómenos medidos y aún muchos por descubrir
- Muchísimos datos de alta calidad en la actualidad (e.g. LaStBeRu) y en un futuro próximo (Rubin/LSST, Euclid, Roman, DESI, 4MOST, MSE…)

Gracias!


Vamos a sonreir ¡Sonrian!